2010

Mechanisms of Controlled Proteolysis during Drosophila Spermatogenesis: Coordinate Action of Apoptotic Caspases and the Ubiquitin-Proteasome System

Maya Bader

Mechanisms of controlled proteolysis during *Drosophila* spermatogenesis: coordinate action of apoptotic caspases and the Ubiquitin-Proteasome System

A Thesis Presented to the Faculty of

The Rockefeller University

In Partial Fulfillment of the Requirements for

The degree of Doctor of Philosophy

by

Maya Bader

June 2010

Mechanisms of controlled proteolysis during *Drosophila* spermatogenesis: coordinate action of apoptotic caspases and the ubiquitin-proteasome system

Maya Bader, PhD
The Rockefeller University 2010

Summary

The regulation of apoptosis, or programmed cell death has been the subject of a vast body of research because of its implication in normal development, tissue homeostasis and a wide range of diseases. The major point of focus for understanding apoptosis regulation is the activation of its primary executioner: the caspase. This family of proteolytic enzymes has been shown to be tightly controlled, as many different proteins govern their transcription, stability, activation, and activity. Consequently, caspase regulation is extremely complex, and is further complicated by a discrepancy between different cell types and paradigms. Caspases have also been shown to have non-apoptotic roles in many vital cellular processes, heightening the need for specific modulators. Therefore, exactly how caspases are regulated is still being worked out, and new factors are still being discovered.

In this thesis, I describe the isolation of new caspase regulators. From a genetic screen for mutants that abrogate caspase activity during terminal spermatid differentiation, we isolated several mutants that have unique roles in caspase activation. The screen revealed 33 mutants that complement into 22 genetic groups. Although they all share a deficiency in caspase activation, these mutants were further sub-divided into groups with distinct

morphological phenotypes. One group mapped to *cytochrome-c-d,* previously shown to be required for caspase activation in this system. We also isolated two members of a Cullin-3-based ubiquitin ligase complex, Cullin-3T and KLHL10. The mutations in *cullin-3* were in a specialized intron that splices into a testis-specific isoform, the first characterization of a tissue-specific isoform of this gene. It was the first report describing the function of this type of ubiquitin ligase in caspase regulation. Another isolated mutant was in a yet uncharacterized F-box protein we termed Nutcracker. F-box proteins are the substrate-binding units of SCF ubiquitin ligases, and we showed that Nutcracker is indeed part of such a complex. From a proteomics screen for Nutcracker physical interactors, we isolated DmPI31. Nutcracker promotes DmPI31 stability, and a complex between these proteins is essential for both caspase activation and sperm differentiation. DmPI31 is conserved with the mammalian PI31 proteins, initially described as proteasome inhibitors. By contrast, we show that DmPI31 is a proteasome activator both *in vitro* and *in vivo*. Generation of *dmPI31* mutants by homologous recombination revealed that *dmPI31* is required for viability and fertility, as the targeted depletion of *dmPI31* resulted in sterility due to meiotic cell-cycle abnormalities. These results define a new mechanism for the regulation of proteasome function. The overall findings demonstrate that cellular remodeling during spermatid differentiation requires the coordinate action of two major proteolytic entities: caspase and ubiquitin-proteasome systems.

Dedicated to my family

In loving memory of my grandfather, Norman Edelshain

Acknowledgements

First and foremost, I would like to thank my advisor, Hermann Steller, for his mentorship and support. His enthusiasm for science, and the intellectual freedom he permitted was an inspiration and motivation to conduct rigorous, creative research. I will always credit him with my development as a scientist, as he encouraged my confidence and taught me how to communicate my work to others.

Thank you past and present Steller lab members for being such helpful, courteous and supportive fellow researchers. I appreciate the time people took to teach, read, advise, discuss and consult. I especially want to thank Eli Arama, for teaching me everything there was to know about spermatogenesis specifically and fly genetics in general, and for originating the fruitful genetic screen. Joe Rodriguez was my chief moral supporter, and gave me very useful scientific ideas along the way. It would not be the same without the friendship and scientific collaboration of Sigi Benjamin, who came just at the right time. Samara Brown's language skills helped me sound good. Alana, Travis, Gabrielle and the rest of the technical staff, thanks for making the lab work so well. Chris, Ann, Andy, Brie, Magali, Maria, Ainoha, Julie - the past six years were a blast.

I am grateful to my committee members, Drs. Cori Bargmann and Shai Shaham, for their time, encouragement and interest in my research and career. Dr. Margaret Fuller made the long journey from California to be my outside committee member, and also wrote the chapter on *Drosophila* spermatogenesis on which my work heavily relies. Thank you Matt Sekedat and Dr. Brian Chait for teaching me the wonders of proteaomics and Drs.

Fred Goldberg and David Smith, for introducing me to proteasome science (while hosting me twice!).

My New-York friends were a home away from home. I credit Howard Hang with my heightened appreciation for ethnic food and superior science. My parents, siblings, grandparents, Ilana and Orna, thanks for your unlimited love and putting up with my absence. Eitan, Elka and the girls - I loved having you so close. Lastly, I would like to thank my husband, the infamous Matt Pratt, whose steady temperament helped me enjoy science more and freak out about it less.

Table of Contents

List of Figures and Illustrations

List of Tables

1. Introduction

1.1 Caspases

Caspases are a family of cysteine proteases that are responsible for executing apoptosis, a form of programmed cell death that is essential for metazoan development and organismal homeostasis (Abraham and Shaham, 2004; Steller, 1995; Steller, 2008). The role of these proteases in programmed cell death was unveiled in an innovative study seeking the genetic basis for the stereotypic elimination of 131 cells in the nematode *C. elegans* (Sulston and Horvitz, 1977). A screen for mutants that abrogate the death of these cells uncovered several genes involved in this cell death pathway, among them *ced-3*, encoding this unique protease (Cerretti et al., 1992; Yuan et al., 1993). This study was fundamental to understanding the molecular basis of apoptosis, and impelled the discovery of orthologous caspases in other organisms, as well as their regulators (Conradt and Horvitz, 1998; Ellis and Horvitz, 1986; Hengartner et al., 1992; Shaham and Horvitz, 1996) (Danial and Korsmeyer, 2004; Vaux and Korsmeyer, 1999) (Hay and Guo, 2006).

Caspases are highly conserved among metazoans, but the number of caspase genes in an organism tends to increase over phylogenetic time; four in *C. elegans*, seven in *Drosophila*, ten in mice and twelve distinct caspases in humans (Lamkanfi et al., 2002; Shaham, 1998). Caspases are broadly classified into two main groups based on their domain architecture and physiologic function: initiator (apical) and executioner (effector). Initiator caspases are thought to auto-activate and, in turn activate executioner caspases, their proteolytic activity resulting in apoptosis.

Caspases are initially transcribed as weakly active zymogens, which upon proper stimulation are cleaved to form the active enzyme. Most caspase molecules consist of a

N-terminus pro-domain and a large and small subunit; cleavage between the subunits at specific aspartate residues determined by a four-amino acid recognition motif results in the formation of an active heterodimer. Two heterodimers then form a heterotetramer. The resulting active site of these enzymes is highly conserved, and contains a cysteine residue that proteolyzes after an aspartic acid residue (Thornberry and Lazebnik, 1998). The long pro-domains of initiator caspases encode related homeotypic protein-protein interaction domains, such as the caspase recruitment domain (CARD) or the death effector domain (DED). These domains allow for interaction with regulatory proteins that carry a similar sequences, most likely as a means of controlling their auto-activation (Degterev et al., 2003). In contrast, the effector caspase pro-domain is short and does not contain a regulatory region.

1.1.1 Regulation of caspases

The characteristic morphology of apoptosis is thought to result from caspase cleavage of hundreds of specific cellular substrates. Because of the inherently destructive nature of these proteases, caspase activity is tightly regulated by both activators and inhibitors. In the same screen that discovered *ced-3*, researchers identified *ced-4* as a caspase activator (Ellis and Horvitz, 1986) (Shaham and Horvitz, 1996; Yuan and Horvitz, 1990). Subsequent biochemical studies led to the discovery of its mammalian homologue, **A**poptotic **P**rotease **A**ctivating **F**actor-**1** (Apaf-1), which forms the "apoptosome" complex with the initiator caspase, Caspase-9, and Cytochrome-c. This complex is sufficient to activate the effector caspase, Caspase-3, in an ATP-dependent manner (Li et al., 1997; Zou et al., 1997; Zou et al., 1999). Homologous complexes are

found in other organisms, including *Drosophila*, where the Apaf-1 homologue Dark interacts with the initiator caspase, Dronc. In some cell types caspase activity requires Cytochrome-c as well (Zhou et al., 1999) (Kanuka et al., 1999)1999;(Rodriguez et al., 1999) (Arama et al., 2003; Arama et al., 2006; Mendes et al., 2006; Rodriguez and Lazebnik, 1999).

The requirement of Cytochrome-c, a mitochondrial resident protein, to facilitate caspase activation exemplifies the role the mitchondria play in caspase regulation. In *C. elegans*, CED-4 is sequestered to the mitochondria through its interaction with the anti-apoptotic CED-9, which is bound to the outer mitochondrial membrane (James et al., 1997; Spector et al., 1997; Wu et al., 1997; Wu et al., 2000). When an apoptotic signal is sensed, the pro-apoptotic EGL-1 binds to CED-9 and causes the release of CED-4 from the mitochondrial membrane, allowing it to activate CED-3 (Chen et al., 2000; Conradt and Horvitz, 1998; del Peso et al., 2000; del Peso et al., 1998; Seshagiri and Miller, 1997; Yang et al., 1998). CED-9 and EGL-1 are conserved to the mammalian *bcl-2* family of apoptotic regulators (Vaux et al., 1988). This family of proteins regulates both pro- and anti- apoptotic activities, and the balance between them determines the fate of the cell. Some studies suggest that *bcl-2* proteins regulate apoptosis by altering the architecture of the outer-mitochondrial membrane (Chipuk et al., 2008; Danial and Korsmeyer, 2004), thus allowing the release of caspase regulators, such as Cytochrome-c, Smac/Diablo, Omi/HtrA2 and ARTS (Green and Kroemer, 2004; Larisch et al., 2000; Wang, 2001). Evidence also shows that the *Drosophila* cell death inducers Reaper, Hid and Grim are required at the mitochondria for full apoptotic activity, and contain an essential mitochondrial targeting sequence referred to as the GH3 domain (Abdelwahid et al.,

2007; Freel et al., 2008) (Haining et al., 1999).

In *Drosophila*, there is some debate on the role of Cytochrome-c in caspase activation (Kornbluth and White, 2005). Although RNAi experiments in S2 cells suggest that Cytochrome-c is not required for apoptosis (Zimmermann et al., 2000), other experiments show that Cytochrome-c is released from mitochondria in cells destined to die (Varkey et al., 1999). Furthermore, one of the *Drosophila* Apaf-1 isoforms binds Cytochrome-c and promotes Cytochrome-c-dependent caspase activation in embryo lysates (Kanuka et al., 1999). Recent *in vivo* studies implicate Cytochrome-c in caspase activation. Mutations in one of the two *Drosophila* Cytochrome-c isoforms, *cytochrome-c-d*, disrupt caspase activation in an apoptosis-like mechanism during spermatogenesis (Arama et al., 2003) (Arama et al., 2006) (see also Chapter 2). This gene also appears to accelerate normal developmental cell death in the *Drosophila* retina (Mendes et al., 2006).

1.1.2 IAPs

Another level of caspase regulation is achieved through inhibitors, namely by a family of proteins called **I**nhibitor of **A**poptosis **P**roteins (IAPs) (Clem and Miller, 1994) (LaCasse et al., 2008; Steller, 2008) (Broemer and Meier, 2009; Deveraux and Reed, 1999; Salvesen and Duckett, 2002). Members of this conserved protein family, the first identified being baculovirus *Op-iap* (Crook et al., 1993), bind the active site of caspases through 1-3 copies of their Baculovirus inhibitory repeat (BIR) domain, and only when they are removed can caspase substrates gain access to the protease (Hinds et al., 1999) (Chai et al., 2001; Huang et al., 2001; Riedl et al., 2001; Shiozaki et al., 2003). The

Drosophila genome encodes four IAPs of which Diap1 appears to be the most important. Genetic loss of *diap1* (*th*) leads to uncontrolled caspase activation causing premature and widespread apoptosis, and resulting in embryonic lethality (Goyal et al., 2000; Hawkins et al., 1999). This suggests that *diap1* is strictly required for the inhibition of apoptosis and is consistent with the fact that *diap1* had been shown to directly interact with at least three *Drosophila* caspases, the apical caspase Dronc and the effector caspases Drice and Dcp-1 (Ditzel et al., 2003; Hawkins et al., 1999; Kaiser et al., 1998; Meier et al., 2000) (Wang et al., 1999) (Chai et al., 2003) (Tenev et al., 2005; Yan et al., 2004a). Similarly, mammalian XIAP, cIAP1, and cIAP2 had also been shown to directly inhibit effector Caspase-3 and -7 and initiator Caspase-9 (Deveraux et al., 1997) (Roy et al., 1997) (Chai et al., 2001; Harlin et al., 2001; Riedl et al., 2001; Scott et al., 2005; Shiozaki et al., 2003; Sun et al., 1999; Takahashi et al., 1998). However, much remains to be learned about the physiological function of mammalian IAPs *in vivo*, as the apparent redundancy of IAP family member function has confounded genetic analysis (Steller, 2008). Targeted gene disruption of several IAPs, including XIAP, cIAP1, and cIAP2, had no significant apoptotic phenotypes (Conte et al., 2001; Conze et al., 2005; Harlin et al., 2001). Although *XIAP* deficiency sensitizes sympathetic neurons to Cytochrome-c-induced apoptosis (Potts et al., 2003), mutant mice are viable and appear phenotypically normal (Harlin et al., 2001; Schile et al., 2008). Nonetheless, a recent in depth analysis demonstrated a direct *in vivo* role of XIAP in Caspase-3 regulation (see below).

Another BIR containing protein is Bruce/Apollon, a large (~500kd) protein that also contains a **Ub**iquitin **C**onjugating (UBC) domain, which is found in E2 conjugating enzymes. Although a direct role in inhibiting caspases has yet to be shown,

Bruce/Apollon is upregulated in several types of cancer (Chen et al., 1999), and its removal or dowregulation cause defects associated with excess cell death (Bartke et al., 2004; Hao et al., 2004; Lotz et al., 2004). In *Drosophila, dbruce* was originally characterized as an enhancer of cell death induced by Reaper and Grim (Agapite, 2002) (Vernooy et al., 2002). Furthermore, mutants of *dbruce* are male sterile, a result of nuclear degeneration, presumably because of excess caspase activation (Arama et al., 2003). These studies suggest that Bruce regulates apoptosis in a manner similar to other IAPs, and investigations on the molecular mechanism of its role are ongoing (Arama et al., 2007) (see also chapters 3 and 4).

In cells that are destined to die, IAPs are inactivated by pro-apoptotic IAP-antagonists, which bind to BIR-domains with higher affinity than caspases (Kornbluth and White, 2005) (Steller, 2008). These antagonists, such as Reaper, Hid and Grim (RHG), were initially identified in *Drosophila* based on their essential role for the initiation of apoptosis (White et al., 1994) (Steller, 2008). RHG proteins contain a short N-terminal motif, termed **I**AP-**B**inding-**M**otif (IBM), which is required for IAP-binding and cell killing (Steller, 2008). In mammals, IBM-domain proteins like Smac/DIABLO and Omi/HtrA2 have been identified as well (Salvesen and Duckett, 2002; Vaux and Silke, 2005). Like in *Drosophila*, these proteins use their N-terminal IBM for IAP-binding and inhibition. However, the targeted gene disruption of either Smac/DIABLO, Omi/HtrA2, or both together in double-mutant mice did not cause an increased resistance toward apoptosis (Jones et al., 2003; Martins et al., 2004; Okada et al., 2002). Therefore, a physiological role of these proteins for regulating IAPs remains to be established, and it is likely that additional IAP-regulators remain to be discovered in mammals. One

example is ARTS, which binds to mammalian IAPs, such as XIAP, and inhibits their anti-apoptotic activity (Gottfried et al., 2004). However, ARTS contains no detectable IBM motif and appears to use a distinct mechanism for IAP-binding and inhibition. Finally, cleaved caspases also contain an IBM, although it has been shown that the monomeric Caspase-9 and its *Drosophila* homologue Dronc are also able to bind IAPs (Chai et al., 2003; Meier et al., 2000; Shiozaki et al., 2003) (Broemer and Meier, 2009).

Figure 1.1: Core pathways of caspase activation in fly, worm and mammal

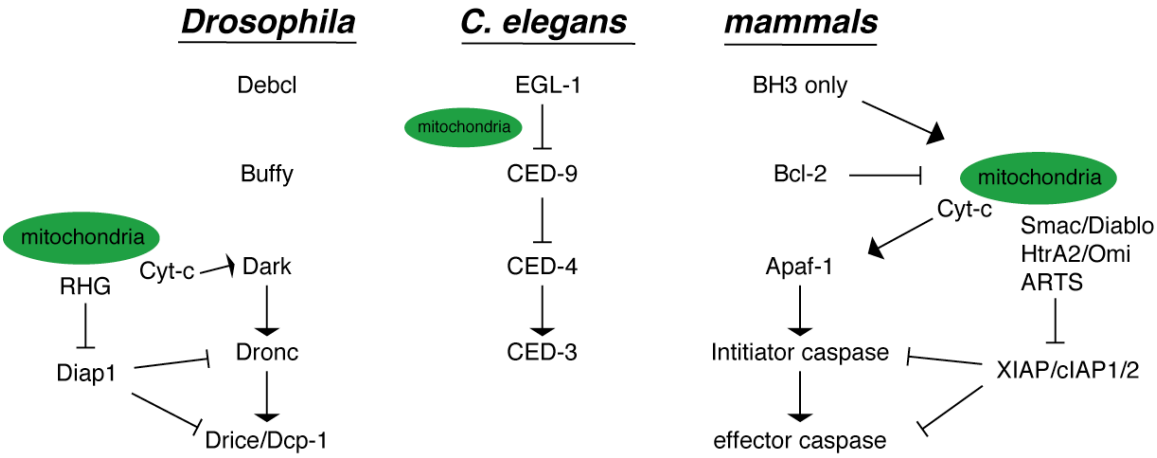

Figure 1.1 The integration of multiple activation and inhibition signals is sometimes referred to as the "gas and break" model for capsase activation. Apoptotic stimulation promotes the assembly of the 'apoptosome', made up of Dark/CED-4/Apaf-1 and the initiator caspase Dronc/Caspase-9 (or CED-3 in worms), and in some cases, Cytochrome-c. The formation of this complex allows the caspase to autoactivate by cleavage. The initiator caspase can now activate effector caspases that cause the stereotypical morphology of apoptosis. To prevent unwanted caspase activation in worms, CED-9 sequesters CED-4 to the mitochondria, thus preventing the interaction with CED-3. Similarly, multiple pro- and anti- apoptotic signals by the bcl-2 family of proteins in mammals are balanced at the mitochondria to prevent or promote the release of Cytochrome-c or pro-apoptotic factors. The binding of Cytochrome-c to Apaf-1 releases the inhibition that is otherwise placed on it. Once caspases are activated, their activity is held in check by IAPs. IAPs inhibit caspases through both physical binding and RING-mediated ubiquitination (see Figure 1.2). When IAP antagonists, namely RHG proteins in *Drosophila,* or Smac/Diablo, Omi-HtrA2 or ARTS in mammals, are upregulated, they release the IAP inhibition from caspases, by either physical binding through the IBM motif, or by ubiquitination. Not portrayed is caspase activation through the extrinsic pathway.

1.1.3 The Ubiquitin-Proteasome System in Caspase regulation

The Ubiquitin-Proteasome System (UPS) is the major system for selective degradation of proteins in eukaryotic cells, and is implicated in the regulation of most cellular processes, including cell-cycle control, transcription, signal transduction, inflammation and cell viability (Glickman and Ciechanover, 2002) (Finley, 2009). In the UPS, protein substrates are targeted for degradation by a set of enzymes that attach multiple molecules of the small protein Ubiquitin (Ub) to them. These include the Ub-activating enzymes (E1s), Ub-conjugating enzymes (E2s) that catalyze the transfer of Ub, and a large variety of Ub-protein ligases (E3s), which are responsible for substrate recognition and specificity (Glickman and Ciechanover, 2002).

In addition to BIR domains, some IAPs also harbor a second highly conserved zinc-binding motif at their carboxyl terminus called the **R**eally **I**nteresting **N**ew **G**ene domain (RING). The RING domain can behave as an E3 ubiquitin ligase by recruiting E2 ubiquitin-conjugating enzymes (Joazeiro and Weissman, 2000). By combining a substrate-binding domain (the BIRs) and a RING domain in the same protein, IAPs can behave like a multi-subunit E3 ligase.

Studies in both mammalian systems and *Drosophila* revealed that the RING domain catalyzes many of the ubiquitination events associated with regulating apoptosis (Yang Y 2002), and its activity has been implicated in both promoting and inhibiting apoptosis. RHG proteins can induce IAP auto-ubiquitination and degradation, thus removing caspase inhibition (Ryoo et al., 2002) (Wilson et al., 2002). Furthermore, this degradation is mediated by other ubiquitination machinery proteins, such as the E1 Ub-activating enzyme Uba1, (Lee et al., 2008) and the E2 Ub-conjugase *Effete* (Ubcd1)

(Ryoo et al., 2002), which are needed for the efficient removal of Diap1. Apoptosis has also been shown to be stimulated by the de-ubiquitinase (DUb) *fat-facet,* which enhances RHG-induced cell death phenotypes (Wing et al., 2002), and *emperor's thumb* (Ribaya et al., 2009), which causes cell-death when over-expressed. In mammals, the IAP antagonist ARTS has also been shown to bind and stimulate XIAP ubiquitination (Gottfried et al., 2004), and the SMAC/DIABLO peptide can induce cIAP1 or cIAP2 ubiquitination and degradation (Varfolomeev et al., 2007) (Vince et al., 2007). Furthermore, Caspase-8 can be directly activated by Cullin-3-mediated ubiquitination, which enables the binding of proteins that facilitate caspase oligomerization and auto-activation (Jin et al., 2009).

In the above-mentioned examples, ubiquitination promotes caspase activation and apoptosis. However, ubiquitination can also play an anti-apoptotic role, which appears to be the dominant function in most cases studied. The physical interaction between IAPs and caspases is insufficient to block apoptosis, and mutations in *diap1* that eliminate or disrupt the RING motif behave as loss-of-function alleles and die as embryos due to massive cell death (Lisi et al., 2000), (Wilson et al., 2002). Furthermore, loss of *diap1* RING function in mutant clones leads to rapid caspase activation and apoptosis, but mutant cells can be permanently rescued by expressing the caspase inhibitor protein p35 (Ryoo et al., 2004). Significantly, these "undead cells" survive for extended periods of time and differentiate into adult structures. This indicates that the primary function of the Diap1 RING is to inhibit caspases, and that Diap1 RING function is not essential for many basic cellular functions as long as caspases are kept inactive.

It was shown that IAPs can directly ubiquitinate and inactivate caspases. For instance, the *Drosophila* Caspase-9 homologue Dronc is inactivated by Diap1 ubiquitination, and Caspase-3 has been reported to be both poly- and mono-ubiquitinated by both XIAP1 and cIAP1 respectively (Broemer and Meier, 2009). However, much remains to be learned about the precise mechanism by which caspase inactivation occurs. In particular, in many cases it is not clear to what extent the ubiquitination of caspases leads to their degradation, or their inhibition by other mechanisms. A recent study aimed at elucidating the effect of caspase ubiquitination showed that the *Drosophila* caspase Drice is ubiquitinated, and that this event is important for its inhibition by Diap1 (Ditzel et al., 2008). In this case, ubiquitination does not target Drice for degradation, because the addition of a proteasome inhibitor did not change its steady-state levels, nor did over-expression of Diap1 alter Drice stability.

Another indicator that caspases are controlled by IAP-mediated ubiquitination came from targeted disruption of the XIAP gene in the mouse (Schile et al., 2008). Targeted deletion of the XIAP RING ("ΔRING") mutant mice led, as expected, to increased stability of the truncated XIAP protein. However, contrary to predications based on biochemical studies suggesting that caspase inhibition is only mediated by the BIR domains, ΔRING MEFs display elevated Caspase-3 activity in response to different apoptotic stimuli. This elevated activity was associated with less Caspase-3 ubiquitination, but like in the case of Drice, this ubiquitination did not influence steady-state protein levels. ΔRING mice also displayed more apoptosis and suppressed Eμ-myc-induced lymphomas. Taken together, these results reveal a physiological requirement of XIAP ubiquitin-ligase activity for the inhibition of mammalian caspases and for tumor

suppression *in vivo*. The general picture that emerges is that while IAP-RING function serves opposing roles in cell death, the net effect of eliminating RING function for most cases studied so far appears to favor caspase activation and apoptosis. Based on biochemical and structural studies it was suggested that XIAP is the only *bona fide* mammalian caspase inhibitor (Eckelman et al., 2006). However, these conclusions were based on simplified *in vitro* assays with individual domains of IAPs that ignore their E3-ligase activity. Furthermore, because different IAPs can form heteromeric complexes, it is possible that IAPs that do not have the ability to inhibit caspases *in vitro* may regulate caspases *in vivo*.

Protein stability controlled by ubiquitination can also be used to regulate pre-activated caspases, as a way of maintaining continuous low levels of the apoptotic machinery and creating a negative feedback loop for preventing unwanted death. A recent study showed that *Drosophila* apoptosome components Dark and Dronc reciprocally control each other's protein level (Shapiro et al., 2008). Inactive full-length Dronc levels are reduced by over-expressing Dark, and are elevated in mutant *dark* tissue-clones. Similarly, Dark levels were increased in *dronc* mutant clones. This interaction is mediated by active Dronc, since Dark cleavage-resistant constructs were no longer able to change full-length Dronc levels. The Diap1 RING domain also plays a role in this system, by possibly mediating the ubiquitin-dependent degradation of both Dronc and Dark. These findings support the idea that low levels of caspase activation can induce the ubiquitination and degradation of pro-apoptotic factors, so as to create a barrier against a "run-away" proteolytic cascade.

IAP antagonists are also subject to ubiquitination, presumably as another means of preventing unwanted death. *Drosophila* Reaper is ubiquitinated by Diap1, which promotes its degradation, while constructs of *reaper* that cannot be ubiquitinated are more potent killers (Olson et al., 2003). Likewise, the mammalian IAP-antagonist ARTS is kept in check by ubiquitin-dependent degradation, which is overcome when apoptosis is induced (Lotan et al., 2005). Taken together, these examples of the anti-apoptotic role of IAP-induced ubiquitination demonstrate ways for a cell to maintain viability while keeping a "finger on the trigger" to enable apoptosis when appropriate.

Further work in this area is likely to advance our understanding of both the regulation of normal cell death, and also provide insight into the mechanisms of de-regulated cell death in human diseases. In particular, IAPs are commonly over-expressed in human tumors and have become prominent targets for the development of novel anti-cancer drugs (LaCasse et al., 2008). Initially, small IBM-motif peptides and small molecule derivatives that mimic the physical interaction between IAPs and their antagonist were designed to compete with IAP-caspase binding, thus removing their inhibition and allowing death to occur. However, it turns out that these molecules can also target certain IAPs for ubiquitination and degradation (Vince et al., 2007) (Varfolomeev et al., 2007). Therefore, the ability to modulate IAP-mediated ubiqutination is expected to have profound implications for the development of novel anti-cancer therapies.

Fig. 1.2: Role of Ubiquitin in the regulation of apoptosis

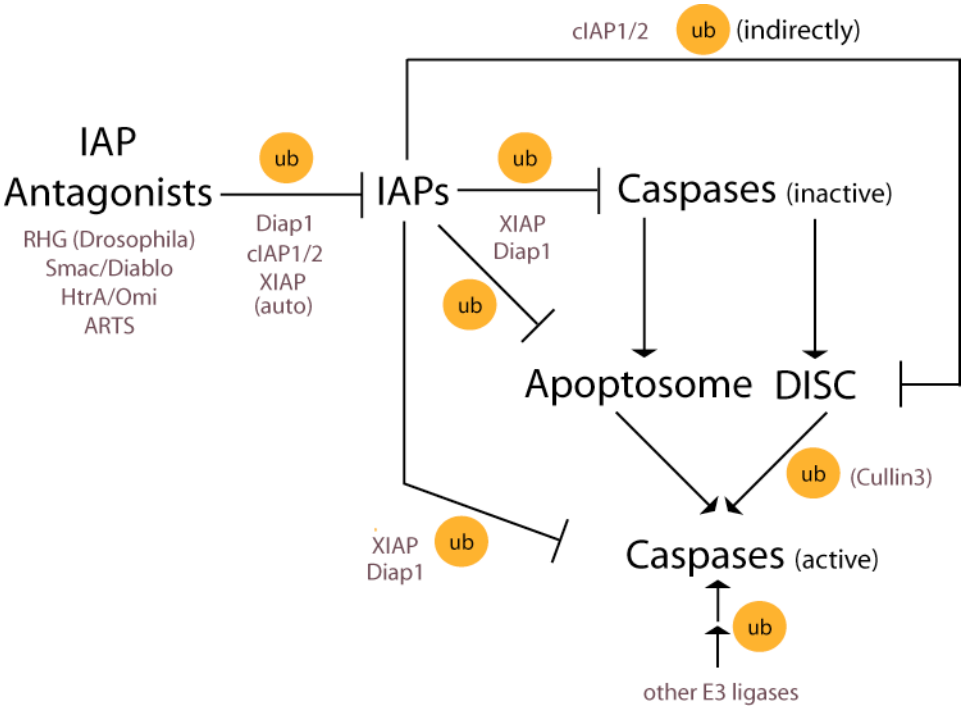

Figure 1.2 Ubiquitination plays opposing roles at different stages during the life-death decision in a cell. In cells that live, IAP-mediarted ubiquitination serves to inhibit unwanted caspase activity. IAP-dependant ubiquitination of caspases leads to inhibition of apoptosis through both proteasomal degradation and a non-degradative pathway. In addition, it can also be used to eliminate caspase activators, like apoptosome subunits. Upon induction of apoptosis, IAP-RING function promotes self-conjugation and UPS-mediated degradation of IAP-proteins, thereby removing the "brakes on death" and facilitating the execution of apoptosis. Non-degradative ubiquitination can also directly activate caspases, by mediating self-cleavage through the induction of specific protein-protein interactions. Besides IAPS, other E3's, such as cullin-based E3 ligases, have also been shown to regulate caspase activation, as in sperm differentiation.

1.2 The non-apoptotic role of caspases

CED-3 was discovered based on its homology to ICE, a non-apoptotic caspase, and is therefore a fitting example that although the primary role for caspases is to promote cell death, this family of enzymes is also utilized in a variety of vital cellular pathways. These include immunity, cell-fate specification, cell survival, cell cycle regulation, cell proliferation and cell migration (Feinstein-Rotkopf and Arama, 2009; Kuranaga and Miura, 2007; Yi and Yuan, 2009). Within these non-lethal roles, there is a general distinction between processes that involve caspases as part of signaling pathways and those that result in partial degeneration of the cell (closely related to the apoptotic program). Several studies have started to elucidate this broad role of caspases, but the precise mechanisms by which their activity is restricted to a sub-cellular space, or to the cleavage of only a subset of substrates, is largely unknown.

1.2.1 Role in immunity

Caspases have an extensive role in regulating and executing immunological responses. For example, the *Drosophila* caspase Dredd functions in the **IM**mune **D**eficiency (IMD) pathway against Gram-negative bacteria, as *dredd* mutants are highly susceptible to infection (Leulier et al., 2000). Stimulating this pathway leads to the activation of Relish, an Nf-kappaB transcription factor, and it is thought that Dredd binds and processes Relish (Stoven et al., 2003). Interestingly, a recent study showed that a Gram-negative-like infection causes Dredd-mediated cleavage of IMD, which exposes an IBM motif in this protein (Paquette et al.). This motif is important for the association with Diap2, a BIR and RING containing protein, which attaches non-degradative

ubiquitin chains to it. This study demonstrated a clear link between caspase-mediated cleavage and signaling through the Nf-kappaB pathway.

Dredd promotes the expression of anti-microbial peptides upon bacterial infection, in a role similar to that of its mammalian ortholog, Caspase-8. Caspase-8 deficient mice are unable to clear a viral infection compared to control mice (Salmena 2003), and were more susceptible to bacterial colonization in the liver (Ben-Moshe 2008). Like Dredd, Caspase-8 is associated with Nf-kappaB pathway proteins, such as IkappaB-kinase (IKK), which promotes Nf-kappaB activation (Lemmers et al., 2007).

An additional branch of caspase-mediated immune response are "inflammasomes", which regulate the activation of Caspase-1 (ICE). These include other caspases like human Caspase – 4 and -5, and mouse Caspase – 11 and 12, and regulatory proteins such as NALP1, NALP3, and Ipaf (Mariathasan et al., 2004; Mariathasan et al., 2006; Martinon et al., 2006; Sutterwala et al., 2006). Caspase-1 processes pro-IL-1ß into IL-1ß, and also cleaves IL-18 and IL-33, in response to various bacteria, toxins or "danger signals", which lead to the inflammatory and immune responses.

1.2.2 Role in cell differentiation

The observation that *Drosophila dark*, *dronc* or *cytochrome-c* mutants exhibit extra external sensory organs (macrochaetae) on their notum guided the discovery of the role of non-apoptotic caspase activation in differentiation of sensory organ precursor (SOP) cells (Chew et al., 2004; Kanuka et al., 1999; Mendes et al., 2006; Rodriguez et al., 1999). The increased number of SOP cells in these mutants is not due to their

artificial survival, because transient inhibition of caspase activity by p35 at a stage prior to SOP specification still resulted in extra macrochaetae, and caspase staining was only detected at an early stage. This implies that caspase activity in the system prevents differentiation of SOP cells. One way that this differentiation is regulated is through the *Wingless* (Wnt) pathway (Kanuka et al., 2005). A screen for genes that regulate macrochaetae number uncovered an antagonist of the Wnt pathway, *Sgg46*, a potential Dronc substrate. Furthermore, it was also demonstrated that knockdown of the IKK-related kinase gene, *dmIKKε* in the notum resulted in extra SOP cells and macrochaetae, and suppression of caspase activity (Kuranaga et al., 2006). Importantly, DmIKKε can phosphorylate and inhibit Diap1 in a Repear-independent manner which does not lead to cell death, suggesting that DmIKKε may control Diap1 to induce a certain threshold of caspase activity that is still compatible with cell-survival. Curiously, the mammalian DmIKKε homologue, NAK, was also shown to mediate the phosphorylation-dependent degradation of XIAP (Kuranaga et al., 2006). This similarity to the differentiation program of neuronal SOP cells might help explain the increased Caspase-3 activity observed during the differentiation of embryonic neuronal progenitor cells (Fernando et al., 2005).

The role of non-apoptotic caspase activation in differentiation is not limited to neuronal cells, and has been observed in a variety of other cell types, although the mechanisms by which they are regulated is the subject of ongoing research. For instance, the differentiation of monocytes into macrophages relies on Caspase-3 and Caspase-9 activation and Cytochrome-c release (Netea et al., 2008; Secchiero et al., 2002; Sordet et al., 2002). Furthermore, conditional deletion of Caspase-8 in bone marrow prevents

differentiation of the myelomonocytic lineage into macrophages. This is thought to involve the Caspase-8-dependent cleavage of RIP, a kinase in the NF-kappaB pathway, along with several other proteins (Kang et al., 2008) (Cathelin et al., 2006). In another type of blood-cell differentiation program, Caspase-3 has been shown to cleave GATA-1, a transcription factor that performs an essential function in differentiation (De Maria et al., 1999). It was demonstrated that GATA-1 is cleaved when these cells are induced to die, but is protected by Hsp70 when they differentiate (Ribeil et al., 2007). This study provided a clear example of the mechanisms by which caspase activity leads to two different outcomes, differentiation vs. death.

Another cell type that depends on caspases for differentiation are skeletal muscle cells, where sterile-twenty-like-kinase (MST1) is cleaved by Caspase-3 to promote differentiation into myoblasts and myotubes (Fernando et al., 2002). Osteoblasts, embryonic keratinocytes and Bergmann glial cells are also differentiated in Caspase-3 dependent manner (Miura et al., 2004; Okuyama et al., 2004; Oomman et al., 2006). Caspase mediated involvement is not limited to terminal differentiation, but also affects pluripotency of stem cells. For example, Caspase-3 upregulation and cleavage of Nanog, one of the four transcription factors that control the self-renewing state of embryonic stem cells is associated with the exit from their pluripotent state (Fujita et al., 2008). Moreover, loss of Caspase-3 leads to increased proliferation of long-term repopulating hematopoietic stem cells and was shown to maintain their quiescent state (Janzen et al., 2008). These results suggest that Caspase-3 activity might also be responsible for blocking self-renewal, and together with the above examples, it is clear that caspases are used in diverse ways in signaling pathways that lead to differentiation.

1.2.3 Role in actin dynamics

During the normal apoptotic program, the cytoskeleton is extensively reorganized. Williams and colleagues showed that reorganization is brought about in part by a Caspase-3 dependent depolymerization of F-actin filaments (Kothakota et al., 1997). By cleaving Gelsolin, Caspase-3 mediates the actin severing process, resulting in the characteristic apoptotic morphology. Rac, a GTPase involved in actin-dynamics, is also cleaved after drug-induced apoptosis of lymphoma cells (Zhang et al., 2003). In later works, it was shown that caspases are critical elements in actin-based cellular morphogenesis and motility. In mammals, Caspase-11 regulates actin dynamics in macrophages during inflammation in a process involving a gelsolin-type protein (Li et al., 2008). Furthermore, disruption of Caspase-8 in mouse embryonic fibroblasts results in disrupted motility and defective lamellipodia, which might be caused by the need for Caspase-8 in Calpain and Rac activation (Helfer et al., 2006).

During *Drosophila* oogenesis, border follicle cells migrate to the center of the developing egg chamber. This developmental process is used as a tractable system to study migration *in vivo*. In a screen aimed at understanding the role of Rac in migration, researchers found that expressing both Diap1 and Actin5A can rescue migration defects caused by a Rac dominant-negative allele (Geisbrecht and Montell, 2004). Mutations in *dronc* and *dark* where also able to inhibit the defect, but not the expression of p35, demonstrating that this process is effector-caspase independent. In another actin-dependent paradigm in *Drosophila*, correct branching of tracheal terminal cells, bristles and arista laterals are affected by mutations in *dmIKKε* (Kuranaga and Miura, 2007; Oshima et al., 2006). Similar to SOP cell differentiation, this effect is also sensitive to

the dosage of Diap1, Dronc and Dark, but not to p35. In these systems, caspase staining is widespread, but only a small portion of cells are undergoing death, implying that some of the non-apoptotic roles of Dronc do not involve the activation of effector caspases, and are controlled by sensitively modulating the levels of Diap1 (Cullen and McCall, 2004; Kuranaga and Miura, 2007; Oshima et al., 2006). Although there is no direct evidence, an interesting model emerges by which Rac and DmIKKe coordinate the stability of Diap1, which in turn specifically regulates non-apoptotic Dronc activity in actin dynamics.

1.2.4 Role in cellular remodeling

During differentiation and development, certain cells undergo major re-structuring and remodeling. This often involves compartmentalized degradation of portions of a cell, such as branched regions and/or elimination of organelles, and can be viewed as 'partial death'. Given the similarity to apoptosis, caspases, with their ability to cleave specific substrates in a finely controlled manner, are good candidates of mediating these processes. Indeed, several published works have implicated caspases in a variety of cellular remodeling programs, including neuronal pruning, spermatogenesis and enucleation of lens fiber cells and erythrocytes.

1.2.4.1 Role in neuronal pruning

Neuronal pruning is the process by which excess or inaccurate projections are eliminated. It is believed that this is achieved by local degeneration, characterized by cytoskeleton destabilization, fragmentation and clearance (Grueber and Jan, 2004; Luo

and O'Leary, 2005; Williams and Truman, 2005). An example that this process is reminiscent of apoptosis came from studying the clearance of the dying fragments during pruning of *Drosophila* mushroom body γ neurons. It was shown that clearance involves engulfment by glial cells and requires *Draper*, a conserved cell death gene. Mutations in *draper* suppress glial engulfment, resulting in the inhibition of axon pruning (Watts et al., 2004) (Awasaki and Ito, 2004; Awasaki et al., 2006) (MacDonald et al., 2006). However, it is still unclear whether caspases are involved in this specific pruning process; pruning is not blocked by the removal of cell death inducers or the expression of cell death inhibitors, nor was caspase staining detected in these cells (Watts et al., 2003) (Feinstein-Rotkopf and Arama, 2009).

Pruning of class IV dendritic arborization sensory neurons (C4da) in *Drosophila* does require local caspase activity (Kuo et al., 2006; Williams et al., 2006). This activity can be detected by restricted caspase staining in degenerating dendrites. Moreover, mutations in *dronc*, *dark* or *draper* suppress branch removal as do Diap1 or p35 over-expression (Williams et al., 2006). Further work demonstrated that the UPS is also involved in this process (Kuo et al., 2005). Proteasome subunits, the E1 Uba1 and the E2 Ubcd1 are necessary for proper dendrite severing as well as the ubiquitin-mediated degradation of Diap1 (Kuo et al., 2006).

Compelling evidence suggest the involvement of Caspase-6 during normal developmental and trophic-factor withdrawal pruning in the mouse (Nikolaev et al., 2009). Local activation of Death-Receptor-6 (DR6) with an activated APP ligand is required for local degeneration of axons, which strongly correlate with punctate active-Caspase-6 staining. Whereas Caspase-3 is involved in executing death of the whole

neuron, Caspase-6 is required for the exclusive elimination of axons in this system. This was not only the first *in vivo* demonstration that mammalian pruning is mediated by caspases, but also provided an interesting hypothesis on the role this pathway plays during Alzheimer's disease (Nikolaev et al., 2009), which involves the abundance of APP ligand.

1.2.4.2 Role in enucleation

Enucleation is the process by which a cell loses its nucleus when becoming a highly specialized cell. This happens in various cell types, as in lens fiber cells, erythroblasts, megakaryocytes and keratinocytes. In some cases, enucleation requires caspases and the apoptotic cascade, but does not lead to death, as these cells continue to metabolize, and are not cleared from the organism (Bassnett, 2002; De Botton et al., 2002; Denecker et al., 2007; Lippens et al., 2000).

During enucleation of the lens fiber cell, morphological and cytological events similar to apoptosis are evident; extensive nuclear DNA fragmentation, disintegration of the golgi and endoplasmic-reticulum, and mitochondrial fragmentation and permeabilization (Appleby and Modak, 1977; Bassnett and Mataic, 1997; Dahm et al., 1998) (Bassnett, 1992; Bassnett, 1995; Bassnett and Beebe, 1992). Marked cleavage of known caspase substrates, such as PARP, Lamin A/C and Lamin B are also detected (Bassnett and Mataic, 1997; Dahm et al., 1998; Ishizaki et al., 1998; Lee et al., 2001). In culture, enucleation is prevented by the addition of caspase inhibitors (Ishizaki et al., 1998; Wride et al., 1999). Nonetheless, it is worth noting that no significant alteration in enucleation is detected in mice deficient for Caspases -3, -6 or -7 or the double mutant -3

and -6, and thus the extent of protease involvement in this process remains to be fully defined (Zandy et al., 2005). Similarly, enucleation of erythrocytes displays some apoptotic features, including DNA fragmentation and staining positively for apoptosis markers and substrate cleavage (Morioka et al., 1998). Although a need for various caspases to proceed in the differentiation program has been demonstrated, it is still unclear whether capsases are used directly for enucleation, or are used in the signaling pathways that lead up to it (Zermati et al., 2001) (Kolbus et al., 2002) (Carlile et al., 2004) (Droin et al., 2008).

1.2.4.3 Role in spermatogenesis

During terminal differentiation of *Drosophila* spermatids, almost all the cytoplasm and excess organelles are removed to create highly motile sperm (Fuller, 1993; Tokuyasu et al., 1972) (see chapter 2). This process was shown to require caspase activation and known apoptosis regulators, including Cytochrome-c, Dark, and dFAdd (Arama et al., 2003) (Arama et al., 2006) (Huh et al., 2004) (Muro et al., 2006) (see chapter 2). Diap1, which is required to prevent unwanted caspase activation and death in most somatic cells, does not appear to play a dominant role for caspase regulation in this system. From a genetic screen, it was discovered that components of a cullin-3 based E3 ubiquitin-ligase are required for caspase activation and sperm differentiation (Arama et al., 2007) (see chapter 3). Mutations in each of the three components of the complex, a testis specific Cullin-3 isoform, the RING protein Roc1B and the substrate binding BTB protein Klhl10, cause male sterility and abolish active-caspase-3 staining from differentiating spermatids. In this regard, mammalian spermatogenesis displays similarities to

Drosophila spermatogenesis, in that the removal of organelles and cytoplasm involves apoptotic proteins and the cells display Caspase-3 staining (Feinstein-Rotkopf and Arama, 2009). Furthermore, targeted deletion of the ARTS gene causes sterility as a result of defects in the elimination of residual cytoplasm and the accumulation of XIAP (Kissel et al., 2005). Interestingly, it was recently reported that mutations in the human form of Klhl10 are associated with male infertility and low sperm count (Yatsenko et al., 2006), indicating that caspase activation controlled by ubiquitination may be used in a similar fashion for cell sculpting in mammals.

Localized degeneration in these systems can be viewed as "controlled atrophy", which requires the coupling of both caspases and proteasome protease activity. The emerging duel role of these regulation pathways could represent a way of controlling macro-proteolysis of organelles and massive protein turnover and destruction. Caspase activation in the testis, for instance, occurs in parallel to the re-organization of the proteasome with specialized catalytic subunits, which, when mutated, affect caspase activity (Zhong and Belote, 2007). Changing the proteolytic profile of the cell (or sub-compartment) may be a way of controlling large-scale morphological changes. Therefore, it would be interesting to investigate whether the activity of proteasomes themselves can be regulated at the sub-cellular level to control these changes.

1.3 Regulation of proteasome activity

The Ubiquitin-Proteasome System (UPS) is made up of two main components: 'Ubiquitin', representing the regulatory module; the targeted degradation of substrates by E1s, E2s and E3s, and 'Proteasome', the executioner module. The proteasome is a large

(2.5 MDa) protease complex composed of two major assemblies; the **C**ore or **C**atalytic **P**article (CP or 20S), a cylindrical structure within which polypeptides are hydrolyzed to small peptides, and the **R**egulatory **P**article (RP or 19S), one or two of which are associated with the CP. The RP is responsible for binding the ubiquitinated substrate, unfolding it, and translocating the extended polypeptide through the narrow entry channel of the CP (Coux et al., 1996; Demartino and Gillette, 2007; Finley, 2009). Recent studies have also identified many proteins which are loosely associated with the proteasome, and may function as regulators or co-factors, but the precise activities of most of these proteins remains elusive (Besche et al., 2009; Finley, 2009).

An added level of proteasomal regulation is the replacement of the 19S RP with alternative activator complexes, which bind to either or both ends of the 20S particle, and enhance the entry and degradation of small peptide substrates (Whitby et al., 2000). Furthermore, CP subunits are sometimes replaced in a tissue or context dependent manner to process differential substrates or modulate activity rates (Finley, 2009). Proteasomes are also regulated by transcription, localization and post-translational modifications. Given the variety and complexity of these regulatory components, and the growing number of proteasome associated proteins being identified, it is clear that proteasomes are much more complicated, more diverse and highly regulated structures than previously thought (Demartino and Gillette, 2007).

1.3.1 Proteasome composition

The CP is made of 28 subunits, arranged in 4 heptameric rings that create a barrel-like structure, defining an interior space in which proteolysis occurs (Borissenko and Groll, 2007) (Groll et al., 1997). The rings are made of 14 gene products, corresponding to seven unique alpha and seven unique beta subunits. Each CP is composed of two identical alpha-type rings and two beta-type rings. The beta-type rings are stacked interiorly, and contain the proteolytic active site in three of the subunits, β1, β2 and β5. Each of these subunits convey site specificity to a broad range of peptide sequences, but are different from each other in their preferred site. The different specificities are generally classified as caspase-like (β1), trypsin-like (β2) and chymotrypsin-like (β5).

Since the active sites are located within the structure, proteins must unfold to enter the proteolytic space (Groll et al., 2000). This is thought to be a highly regulated event, and involves a gate that is made up of the N-termini of the alpha subunits. Additionally, the alpha-type subunits also contain seven pockets on the interface between the alpha-ring and the RP. Binding between the RP to the CP opens the alpha channel, which leaves it in alignment with a second channel within the RP itself (Forster et al., 2005) (Rabl et al., 2008; Smith et al., 2007).

The RP was first thought to contain nineteen subunits, but the exact number is still being worked out. The subunits are divided into the base and the lid. The base is made of six ATPases (Rpt1-6) forming a ring that sits on top of the CP, and three other proteins, Rpn1, Rpn2 and Rpn13. The C-termini of all the Rpts insert into the alpha pockets of the CP, thus facilitating gate opening (Forster et al., 2005; Rabl et al., 2008; Smith et al., 2007). Indeed, it was found that some of these subunits contain a unique

motif at their very C-terminus, termed the HbYX (Hydrophobic-tyrosine-X) motif, which directly binds to the alpha pocket, and mediates the structural maneuvering of gate opening (Smith et al., 2007). The ATPase activity of the base is required for deubiquitination of substrates, their unfolding and translocation down the channel of the CP (Smith et al., 2005) (Benaroudj et al., 2003; Kleijnen et al., 2007; Liu et al., 2006; Rubin et al., 1998; Verma et al., 2002; Yao and Cohen, 2002). Of the nine lid subunits, only Rpn11 has a known function, a **D**e**UB**iquitinating enzyme (DUB), but it is speculated that the other subunits mediate the identification of ubiquitinated substrates and their processing (Sharon et al., 2006; Verma et al., 2002; Yao and Cohen, 2002).

1.3.2 Alternative activators

The RP, with its ability to control and enhance the degradation of ubiquitinated substrates, is considered the most common proteasome activator, and is sometime referred to as the "housekeeping" form of the proteasome (Glickman and Ciechanover, 2002). CP activity controlled by this type of activator, also called the 26S proteasome, is ATP dependent, and mostly mediates the degradation of proteins that have been targeted by ubiquitination (DeMartino and Slaughter, 1999). Being the most common proteasome, protein degradation is mostly controlled by the ubiquitin modification step, and less so from controlling proteasome activity.

Figure 1.3 The proteasome is a large, multi-subunit protease complex. The 20S core complex is composed of four heptameric rings of distinct α subunits (α1–7) and distinct β subunits (β1–7) subunits. The proteolytic activities are conferred by three of the β subunits, β1, β2, β5, in the interior of the barrel. These subunits are sometimes replaced in a tissue-or signal- dependent manner. The 19S regulatory complex (also called PA700), contains a hexameric ring of AAA-ATPase subunits (Rpt1-6) and 12 non-ATPase (Rpn) subunits. The 19S complex contains ubiquitin receptors that recognize polyubiquitylated substrates, DUBs that remove the ubiquitin tag and other subunits that unfold the protein for translocation into the 20S chamber in an ATP-dependant manner. The interaction and/or cooperation between 19S lid Rpn subunits and other proteasome-associated proteins convey a complex proteolytic regulation network. Alternative activator complexes, such as PA28/11S, REGγ or PA200/Blm10 can change the proteolytic complexity of the 20S, or the way substrates are recognized and processed by the 20S. The cartoon depicts these alternative activators as 'hybrid proteasomes' containing the RP on one side and the alternative activator on the other, but it is still not clear whether this structure is the active form *in vivo*, or one that contains the alternative activator alone. It is worth noting that both signally and doubly capped 20S can degrade ubiquitinated substrates. PI31, originally identified as an inhibitor of the 20S proteasome, acts as an activator of 26S proteasomes, thus behaves as a novel type of regulator through a yet unknown mechanism. Proteasome activity can also be regulated by post-translational modifications, such as phosphorylation, glycosylation and caspase-cleavage. Furthermore, proteasome abundance can be upregulated by transcriptional control. Proteasome distribution is another way its activity is restricted, as proteasomes are found to be preferentially localized in the nucleus, on DNA, on membranes and in distinct sub-cellular areas such as dendrites.

Figure 1.3 Regulation of the proteasome

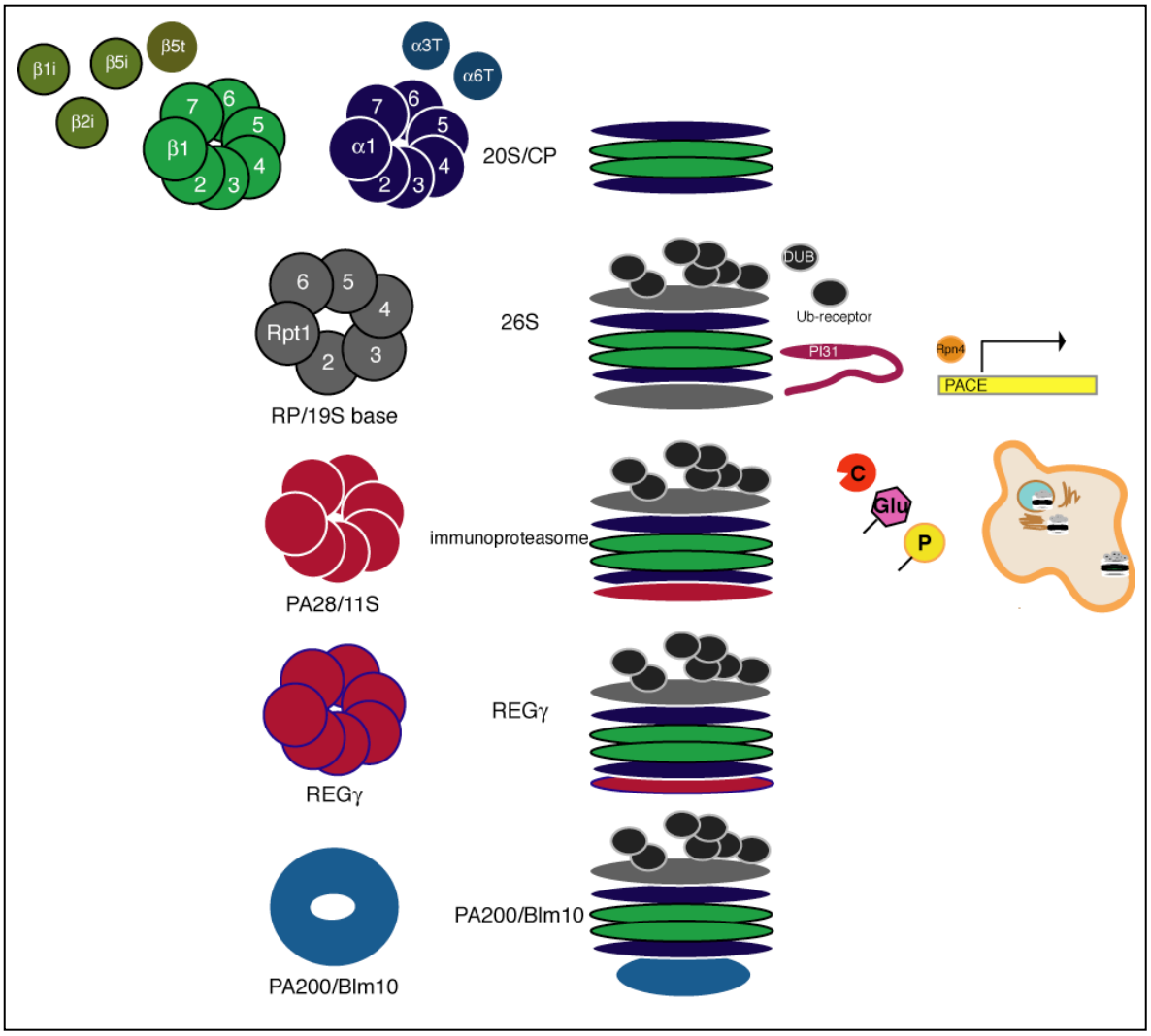

However, proteasome activity is also controlled, through several mechanisms. First, the genome of most organisms encodes alternative activator complexes that act instead of, or together with the RP (the symmetric cylindrical shape of the CP allows binding to both of its ends) (Finley, 2009). Three are known: PA28 (also known as REGα,β or 11S), REGγ and PA200/Blm10 (Ustrell et al., 2002) (Masson et al., 2001; Tanahashi et al., 1997) (Bassnett, 1992). PA28 is upregulated in response to interferon-gamma stimulation, and is situated within the MHC locus. It is believed that this proteasome activator acts to optimize MHC class I presentation, presumably by enhancing the cleavage specificity of certain antigens (Goldberg et al., 2002) (Groettrup et al., 1996) (Strehl et al., 2005) (Cascio et al., 2002). REGγ is similar in size to PA28, but is present in more organisms. REGγ is not inducible, and seems to localize to the cell nucleus. This alternative activator probably mediates the degradation of non-ubiquitinated targets, since it has no ATPase activity to support unfolding, nor does it contain ubiquitin-sensing receptors (Masson et al., 2001). For instance, it was demonstrated that the substrate SRC-3 is degraded in a REGγ-dependent manner, in a mechanism that involves the loosely structured segments of SRC-3. REGγ binds both SRC-3 and the CP, so as to mediate gate opening and degradation (Li et al., 2006). The third proteasome activator, PA200/Blm10 (hence Blm10), is the most conserved (Ustrell et al., 2002). It differs from PA28 and REGγ in that it binds the CP as a monomer, as opposed to the heptameric assemblies of the other two (Iwanczyk et al., 2006). Blm10 is a large protein that includes internal HEAT repeats, conferring a near circular structure that can be placed on the CP like a turban (Schmidt et al., 2005a). Blm10 enhances proteasome activity and is required during spermatogenesis, but its physiological role has

yet to be completely revealed (Khor et al., 2006). Although the mechanisms by which these alternative activators function in regulating proteasome activity is still being investigated, it is clear that they affect proteasome function and cellular degradation.

The proteasome has been shown to be negatively regulated by PI31 (Proteasome Inhibitor 31kd), originally identified in an *in vitro* based screen for proteasome regulators (Chu-Ping et al., 1992). This protein inhibits the hydrolysis of small synthetic substrates and large unfolded proteins by the 20S proteasome (CP) (McCutchen-Maloney et al., 2000; Zaiss et al., 1999). Because this protein competes with the RP (PA700) and PA28 for binding the proteasome, it is assumed that it disrupts the formation of an intact proteasome (McCutchen-Maloney et al., 2000; Zaiss et al., 1999). PI31 harbors a proline-rich domain, which encompasses a third of the protein at its C- terminus, and is important for its inhibitory activity (McCutchen-Maloney et al., 2000). Interestingly, similar to Rpt subunits of the RP base, PI31 proteins contain a HYbX motif, which suggests that it is acting by threading its unfolded C-terminus into the CP channel. When over-expressed in cell-culture, PI31 has no direct effect on proteasome function in the cell-cycle, but was found to disrupt the formation of the immunoproteasome under immunological conditions (Zaiss et al., 2002). Nonetheless, the biological function of this protein has yet to be fully revealed. As described in Chapter 5 of this thesis, this protein can also act as an activator of 26S proteasomes, and has a role in caspase activation and spermatid differentiation, as well as the meiotic cell cycle.

1.3.3 Tissue or context specific catalytic subunits

A second way the proteasome is regulated is by alternative catalytic subunits. In response to interferon-gamma, the three proteolytic subunits of the beta-type ring are replaced by the inducible subunits β1i, β2i and β5i (Goldberg et al., 2002). These subunits have altered cleavage specificity that generate specific antigenic peptides. Therefore, this alternative CP is also called the immunoproteasome. Another example in which regular subunits are replaced by more specialized subunits is in the thymus. This organ is responsible for training the immune system to discriminate between self and non-self immature T cells. It was recently shown that a different β5 subunit, β5t, is upregulated in the thymus (Murata et al., 2007). Together with β1i and β2i, this 'thymoproteasome' is required for the generation of mature CD8+ T cells, suggesting that it has a role in thymic education. Lastly, duplication of CP subunits is observed in the *Drosophila* testis, where testis-specific heterogeneous proteasomes have been described, and in some cases subunits are functionally distinct (Belote et al., 1998; Ma et al., 2002; Zhong and Belote, 2007). In this system, 13 of the 28 CP genes have testis-specific paralogs that are only expressed in this tissue, which suggests the existence of a specialization of proteasome function during spermatogenesis. Differential expression patterns during spermatogenesis have been observed for *alpha3* and *alpha6* with their paralogous genes, *alpha3T* and *alpha6T,* respectively. *alpha6T* mutants are viable but male sterile, and more detailed analysis confirmed that it is required during terminal differentiation of spermatids, which correlates with its expression. In this case, the reason for alternative subunits is not clear, since Alpha6 can compensate for Alpha6T loss, but the strong phenotype suggests that this specialized proteasome is specifically

needed, and that the two types of proteasomes are somehow different.

1.3.4 Proteasome-associated proteins

Detailed analysis and more sensitive isolation methods have uncovered loosely associated proteasomal proteins (Schmidt et al., 2005b). These proteins are present on proteasome at sub-stoichiometric levels, and are therefore not considered subunits. Several E3 ubiquitin ligases are found on proteasomes, and in some cases it was demonstrated that this interaction is important for E3 ligase activity (Chuang and Madura, 2005; Farras et al., 2001; Xie and Varshavsky, 2002) (Sakata et al., 2003; Seeger et al., 2003). Furthermore, some proteasome-associated proteins have similar roles to those of intrinsic subunits, like ubiquitin-binding, deubiquitination and unfolding (Demartino and Gillette, 2007). This means that the function of some proteasomal subunits is supplemented by other proteins. For instance, deletion of the ubiquitin receptor Rpn10 subunit does not affect global protein degradation in yeast, but the additional removal of Rad23, an associated proteins that contains a ubiquitin-binding (UBA) domain results in marked impairment of protein degradation (Demartino and Gillette, 2007). Similar UBA proteins also contain a UBL domain that confers binding to Rpn subunits. These proteins, such as Dsk2, ddi1, p97/cdc48 and p62, are thought to shuttle substrate proteins to the proteasome, thus controlling rates of degradation (Demartino and Gillette, 2007) (Finley, 2009). Although the complexity of such regulation is not well understood, it might also represent an important element of proteasomal function.

Resident or associated deubiquitinases also regulate the proteasome to some degree, as is the case of Uch37 and Ubp6 in yeast. In the former case, Uch37, a proteasomal subunit does not remove ubiquitin chains in one group, but rather shortens them (Lam et al., 1997). This shortening function might reduce the affinity of the substrate to the proteasome, or alternatively, function as an editing molecule that prevents the degradation of lightly ubiquitinated substrates (Lam et al., 1997; Thrower et al., 2000). Similarly, Ubp6 (Usp14 in mammals) also cleaves the ubiquitin chain progressively, and could act as a way to remove supernumerary chains (Guterman and Glickman, 2004; Hanna et al., 2006). The removal of Ubp6 cause a decrease in cellular ubiquitin, and Ubp6 is upregulated in response to reduced levels of ubiquitin (Anderson et al., 2005; Hanna et al., 2007). Moreover, inactivated Ubp6 cause an increase of cellular proteasome levels, suggesting that Ubp6 regulates both ubiquitin and proteasome function (Hanna et al., 2007). The fact that cells can sense the amount of free ubiquitin and adjust proteasome levels is an example of proteasome activity that is also regulated on the transcriptional level.

1.3.5 Transcriptional regulation

Proteasome subunit composition in cells is stoichometric, suggesting that some control over proteasome function is governed by transcription (Glickman and Raveh, 2005). In budding yeast, Rpn4 is a general transcription factor that recognizes PACE sequences on proteasome subunit promoters, as well as its own (Mannhaupt et al., 1999; Xie and Varshavsky, 2001). Rpn4 is a short-lived protein, but when proteasome function is altered, Rpn4 levels are consequently elevated, resulting in upregulation of proteasomal

subunits. The enhanced proteasome activity results in Rpn4 degradation. This negative feedback loop allows for a rapid cellular response in cases such as mild stress, but prevents the negative effect of over-expressed proteasomes (Ju et al., 2004; Ju and Xie, 2004; London et al., 2004).

1.3.6 Post-translational modifications

Post-translational modifications are another way proteasomes are regulated (Glickman and Raveh, 2005). Several proteasomal subunits in various organisms are found in both phosphorylated and unphosphorylated states, and phosphorylation is correlated with enhanced proteasome activity (Fernandez Murray et al., 2002; Iwafune et al., 2004). It is thought that phosphorylation controls the assembly into a stable 26S proteasome (Satoh et al., 2001). During IFN-gamma induction, for instance, decreased phosphorylation results in the disassociation of 19S and 20S, possibly to allow the assembly of the specialized immunoproteasome (Rivett et al., 2001) (Bose et al., 2004). Still, to what extent this modification affects proteasome function is not completely clear, but has recently been implicated in proteasome localization (see below).

Other modifications, such as O-glycosylation and caspase cleavage, were also demonstrated as affecting proteasome function under certain circumstances. In the former case, glycosylation inhibits proteasome activity, which might contribute to the cellular glucose-sensing pathway (Sumegi et al., 2003). Proteasomal subunits have also been demonstrated to be caspase substrates in both *Drosophila* and human cells (Adrain et al., 2004). During apoptosis, caspase cleavage of proteasomal subunits may lead to inactivated proteasomes and the accumulation of pro-apoptotic proteins (Sun et al.,

2004). Interestingly, REGγ is also a caspase substrate, suggesting another level of proteasomal regulation, one that controls the stability of alternative proteasomal activators (Adrain et al., 2004).

1.3.7 Subcellular localization

Proteasome density in a particular subcellular space or organelle has been observed in various systems (Wojcik and DeMartino, 2003). During the cell cycle and oocyte development, proteasome distribution shifts between cytoplasm and nucleus (Kawahara and Yokosawa, 1992; Lafarga et al., 2002). In yeast, GFP-tagged proteasomal subunits are found on the nuclear envelope, in the rough endoplasmic reticulum and in association with cytoskeletal networks (Bingol and Schuman, 2005; Wojcik and DeMartino, 2003). During DNA breaks, proteasomes have been associated with DNA and DNA damage proteins (Krogan et al., 2004). Most recently, proteasome localization and re-distribution was shown to have an active role in cellular function. During neuronal excitation, GFP-tagged proteasomes translocate on actin networks to synaptic spines, which contributes to the change of the protein profile at synapses (Bingol and Schuman, 2006). Furthermore, it appears that the phosphorylation activity and distribution of CaMKIIα, a proteasome-assosicated kinase, regulates this movement to the synapse (Bingol et al.). Thus, the fact that proteasome localization is regulated suggests that its preferential distribution is another layer of proteasomal regulation. As in neurons, proteasomes display movement from one cellular area to another during *Drosophila* spermatogenesis. At the individualization stage of terminal spermatid differentiation, proteasomes are detected in the nucleus, but redistribute to the cytoplasm

in a punctate pattern. As the IC moves down the length of the axoneme (see Chapter 2), proteasomes move with the complex within the CB (Zhong and Belote, 2007). This unique distribution suggests that the localized activity might have a role during this cellular remodeling process.

This thesis

My thesis concentrates on the role and regulation of non-apoptotic caspase activation during terminal spermatid differentiation, a process known as individualization. As mentioned in this introduction, I used individualization to study caspase regulation by conducting a genetic screen for mutants with abrogated caspase activation during this stage of sperm differentiation. The screen is described in Chapter 2. This screen uncovered several mutants, among them members of a Cullin-3 based ubiquitin ligase, as described in Chapter 3, and a novel F-box protein I termed Nutcracker, as described in Chapter 4. The fact that the screen isolated members of the UPS is in line with the known role it plays in regulating caspases and apoptosis. It also revealed a novel link to proteasome regulation, and its role in cellular processes. By conducting a proteomics-based screen for Nutcracker physical interactors, I isolated a proteasome activator, DmPI31, which I show has a role in both caspase activation and individualization. The characterization of PI31 and its interaction with Nutcracker is described in Chapter 5.

2. A male sterile screen for regulators of caspase activation[1]

2.1 Summary

Terminal differentiation of male germ cells in both *Drosophila* and mammals requires extensive cytoarchitectural remodeling, elimination of many organelles, and a large reduction in cell volume. The associated process, termed spermatid individualization, is facilitated by the apoptotic machinery, including caspases, but does not result in cell death. From a collection of more than 1000 male sterile lines previously described as individualization-defective, we conducted a screen for genes that, when mutated, cause the abrogation of caspase activation in this system,. This screen resulted in the isolation of 33 mutants that complemented into 22 genetic groups. The mutants were further characterized into subgroups based on secondary markers and morphology. The screen resulted in the isolation of a point mutation in *cytochrome-c-d*, an apoptosis regulator, previously described as a key player in this system as well. This chapter summarizes the key steps of the screen and initial mutant characterization.

2.2 Introduction

Spermatogenesis in *Drosophila melanogaster* takes place within individual units known as cysts. A single testis contains cysts at different stages of development, which are laid out in chronological order from the tip to the base (Wakimoto et al., 2004). Each cyst contains 64 spermatids, a result of four mitotic divisions followed by a meiotic

[1] Maya Bader wrote this chapter. Eli Arama conceived the genetic screen described in this chapter. Maya Bader and Eli Arama conducted the screen and characterized the isolated mutants.

division, which differentiate synchronously and remain initially connected via cytoplasmic bridges (Figure 2.1A) (Tates 1971; Tokuyasu 1974a,b, 1975a,b; Tokuyasu et al. 1972, 1977; Lindsley and Tokuyasu1980; Fuller 1993)(Fuller, 1993). During terminal differentiation, the spermatid nuclei condense and transform into the shape of a needle, and their mitochondria fuse into two unevenly sized elongated mitochondria (major and minor mitochondrial derivatives), that elongate beside the growing flagellar axoneme (Hales and Fuller, 1997). In the final step of differentiation, termed "individualization", the cytoplasmic bridges are disconnected and most of the cytoplasm is expelled, leading to individual sperm.

The individualization process involves the assembly of a cytoskeletal-membrane complex, referred to as the individualization complex (IC), which contains actin as its major cytoskeletal component (Figure 2.2A) (Fabrizio et al., 1998) (Noguchi and Miller, 2003). This complex is formed in cone-like structures around the elongated nuclei, and then descends caudally along the length of the spermatid bundle, expelling most of the cytoplasm in the process. The expelled cytoplasm accumulates around the IC, eventually turning into a membrane-enclosed structure termed the waste bag (WB) (Tokuyasu et al., 1972), which ultimately undergoes degradation.

It was recently demonstrated that an apoptosis-like mechanism is involved in the spermatid individualization process (Arama et al., 2003) (Huh et al., 2004). Specifically, it was shown that *Drosophila* caspases are activated at the onset of this stage (Figure 2.2B). Caspase activity is absolutely needed for spermatid differentiation because their inhibition by the broad-spectrum caspase inhibitor p35 or the *Drosophila* caspase inhibitor DIAP1 disrupts individualization (Arama et al., 2003) (Huh et al., 2004).

Furthermore, acridine orange (AO) staining was detected within the waste-bags, resembling apoptotic corpses (Arama et al., 2003).

Figure 2.1: Spermatogenesis in *Drosophila*

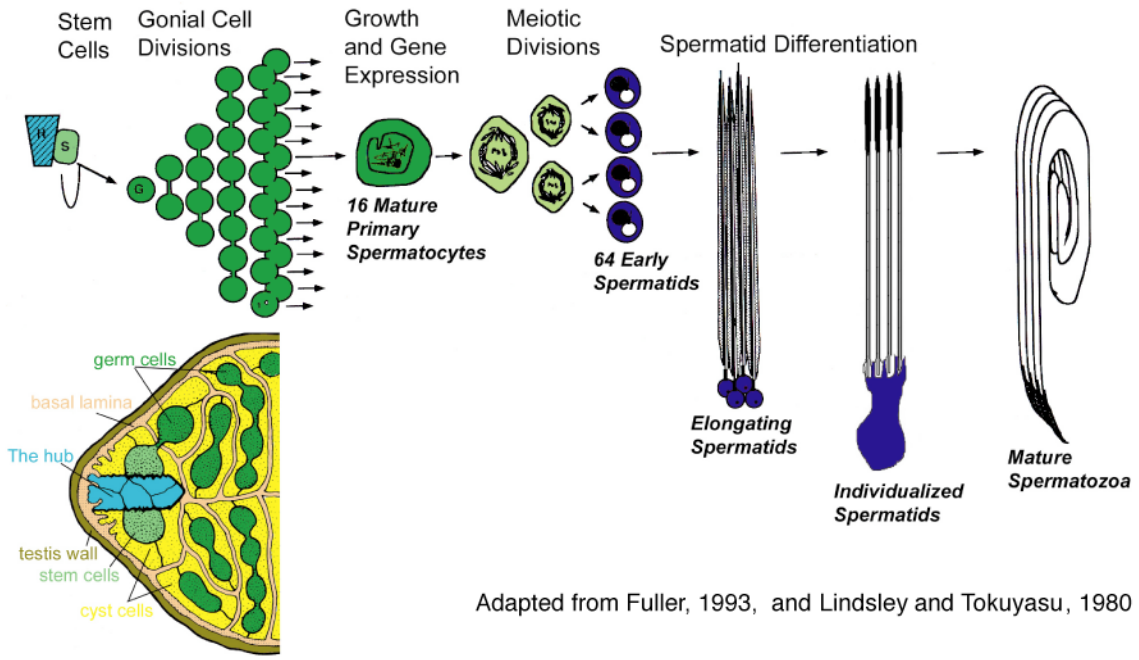

Figure 2.1 Spermatogenesis in *Drosophila* initiates when a germ-line stem cell, engulfed by two somatic cyst cells, undergoes four rounds of synchronous mitosis. The 16 resulting cells grow to about 25 times their original size, at which point they are considered primary spermatocytes. The cells then undergo an incomplete meiotic division to create 64 haploid spermatids. Because cytokinises is incomplete, the spermatids share their cytoplasm. As the spermatids differentiate, they undergo major morphological changes. Their nuclei condense and reshape into a needle-like structure, they develop an elongated ciliaic axeoneme and their mitochondria fuse and elongate alongside the axenome. At the final stage of differentiation, termed individualization, each spermatid is engulfed in its own membrane, creating individual sperm.

Traditional apoptotic regulators are also involved in activating caspases in this system. Mutations in one of the two *Drosophila* isoforms of cytochrome-c, *cytochrome-c-d*, completely eliminates caspase activity and causes male-sterility (Arama et al., 2003) (Arama et al., 2006). In addition, *Drosophila* apoptosome components are also required for proper individualization. Mutations in or the expression of a dominant negative form of the initiator caspase *dronc,* as well as mutations in or RNAi elimination of the Apaf-1 homologue *dark*, cause an aberrant individualization phenotype and disrupt active-caspase staining which lead to sterility (Arama et al., 2006; Huh et al., 2004). Furthermore, it was shown that the IAP antagonist Hid is needed for proper Dronc activation, and the lack of Hid results in the failure to individualize (Huh et al., 2004).

These data indicate that while the death machinery is used during individualization, these cells somehow avoid death, possibly by the spatio-temporal regulation of caspase activation or activity. It is therefore likely that caspase activation is controlled by a variety of other known or unknown proteins. In this chapter, I describe a screen for genes involved in caspase activation and regulation during spermatid differentiation.

Figure 2.2: Caspase activity is detected at the onset of spermatid individualization

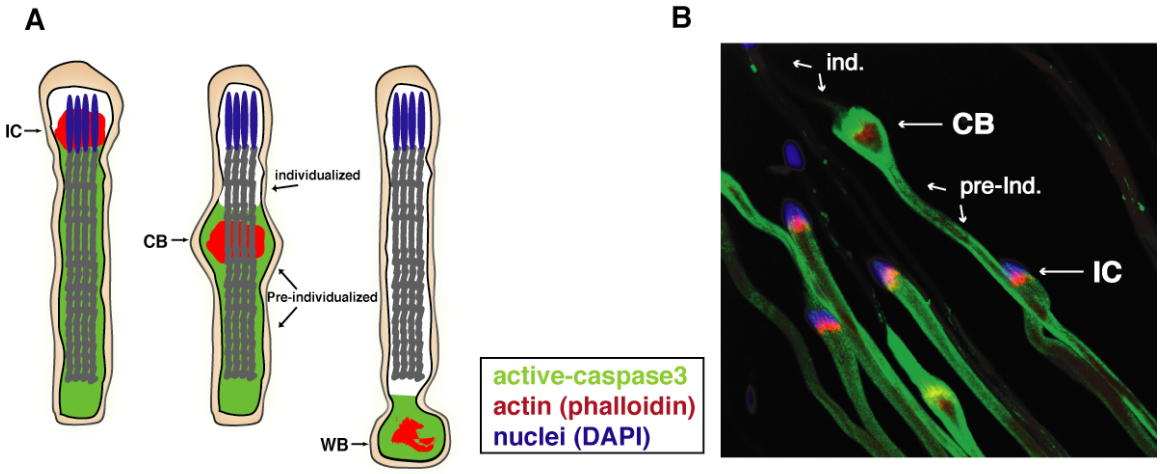

Figure 2.2 **[A]** A schematic diagram of spermatid individualization. At the final stage of differentiation, an actin based individualization complex (IC) is formed around the elongated nuclei of 64 spermatids that are connected by cytoplasmic bridges. As the IC transcends the length of the spermatids, it expels the excess cytoplasm and unneeded organelles, leaving each spermatid engulfed in its own membrane. During this movement, the excess material accumulates around the IC to create the cystic bulge (CB). When the complex reaches the end of the tails, the CB turns into the waste bag (WB), which eventually degrades. **[B]** Wild-type (*yw*) cysts were stained with DAPI (nuclei, blue), phalloidin (IC, red) and caspase-3 (cytoplasm, green). Active-caspase3 staining is detected as the IC forms around the nuclei. Staining is no longer detected in the post-individualized portion of the cyst, but accumulates in the CB.

2.3 Results

2.3.1 A screen for genes that regulate caspase activity during individualization

To learn more about the role and regulation of caspase activity during spermatid individualization, a screen was designed for mutants that lack caspase activity during this process. This screen employed an existing collection of more than 1000 male-sterile mutant lines that had been previously identified as having an individualization defect, among a collection of about 12,000 viable recessive mutations generated in the laboratory of Dr. Charles Zuker (Koundakjian et al., 2004) (Wakimoto et al., 2004). The Wakimoto et. al. study uncovered mutations in the vast majority of second and third chromosome genes involved in male fertility. The testicular phenotypes of the male-sterile mutants were classified by their appearance using phase-contrast microscopy. The mutant lines were then divided into groups, ranging from the partial elimination of the gonad (agametic) to late stage differentiation defects (classic). The latter group includes mutations that cause individualization failures, and appeared to consist of most of the male sterile lines (1138 out of 2131). Because active-caspase staining is normally detected at the onset of individualization, lines from this group were used to screen for mutants defective for capsae activation.

The testes of homozygote males from each line were dissected and stained with the cleaved caspase3 antibody (Figure 2.3A) (Arama et al., 2003) (Fan and Bergmann, 2009). 33 caspase-negative lines were identified (Table 2.1). It is important to note that the vast majority of male-sterile lines retained cleaved-caspase staining (> 97%), even though many displayed severe defects in spermatid individualization (Figure 2.3B). Therefore, consistent with earlier observations (Arama et al., 2003), caspase activation at

the onset of spermatid individualization appears to be independent of other aspects of sperm differentiation.

Table 2.1 Summary of male sterile mutants isolated from the caspase-deficeint screen

class	mutant #	gene name	group	viability	male	female	casp3	AXO49	mitochondria	IC	nuclei	category	Wakimoto/Fuller/Lindsey comments
i	ms961	*klhl10*	*1*	Good	Sterile	Sterile	negative	positive			fully elongated		Classic
i	ms61	*klhl10*	*1*	Good	Sterile	Fertile	negative	positive		scattered cones	scattered		Classic
i	ms462	*klhl10*	*1*	Good	Sterile	Sterile	negative	positive			scattered	Individualization failure	Classic
i	ms396	*klhl10*	*1*	Good	Sterile	Sterile	negative	positive			fully developed	Individualization failure	Classic
i	ms374	*klhl10*	*1*	Good	Sterile	Fertile	negative	positive			mostly developed	Individualization failure	Classic
i	ms311	*klhl10*	*1*	Good	Sterile	Fertile	negative	positive			fully developed	Individualization failure	Classic
i	ms266	*klhl10*	*1*	Good	Sterile	Sterile	negative	positive		scattered cones	scattered	Individualization failure	Classic
i	ms667		2	Good	Sterile	Fertile	negative	negative	fragmented		scattered/round	Individualization failure	Classic
i	ms389		2	Good	Sterile	Fertile	negative	negative	scattered		scattered	Individualization failure	Classic
i	ms444		3	Good	Sterile	Fertile	negative	positive	intact			Individualization failure	Classic
i	ms330		4	Good	Sterile	Fertile	negative	positive			scattered	Individualization failure	Classic. Degenerating spermatocyte clusters
i	ms72		4	Good	Sterile	Fertile	negative	positive				Individualization failure	
i	ms101		5	Good	Sterile	Fertile	negative	negative	scattered/dotted		scattered	Individualization failure	Rotated external genitalia in males. No individualization
i	ms734		6	Good	Sterile	Sterile	negative	positive				Individualization failure	Classic
i	ms282	*gft/mds*	7	Good	Sterile	Fertile	negative	positive		forms	fully developed		Classic
i	ms312	*cyt-c-d*	8	Good	Sterile	Sterile	negative	negative		forms		Individualization failure	Classic
i	ms547		9		Sterile	Fertile	negative	negative	fragmented		not fully developed	Individualization failure	Classic . DanÕs mapping has this in the th102 region
i	ms949		9		Sterile	Sterile	negative	negative	scattered			Individualization failure	females laid eggs classic
i	ms823		9	Good	Sterile	Sterile	negative	negative				Individualization failure	Classic. DanÕs data shows failure to complement Df th102
i	ms594		10		Sterile	Sterile	negative	positive			scattered/round		No eggs (McKeown) Classic
i	ms1056		10		Sterile	Sterile	negative		intact		scattered/round	Individualization failure	Few eggs classic, all three males
i	ms646		11		Sterile	Sterile	negative	positive			scattered/round	Individualization failure	Females no eggs or dead Leaky, some males fertile
i	ms1100		11	Good	Sterile	Fertile	negative		defect (?)		scattered/deformed	Individualization failure	Classic
i	ms761		12	Good	Sterile	Fertile	negative	positive			not fully developed/scattered	Individualization failure	Excessive debris along elongating bundles
i	ms579		12		Sterile	Fertile	negative	positive			not fully developed/scattered	Individualization failure	Classic
i	ms771	*nutcracker*	*13*	Good	Sterile	Fertile	negative	positive		does not form	almost fully developed		Classic. Male sterile Extremely low fertility in females
i	ms893		14	Good	Sterile	Fertile	negative	negative			scattered/defective	Individualization failure	Classic. Check with Dan on update for Df th 102 comps
i	ms549		15		Sterile	Fertile	negative	positive			scattered		Classic. Female weakly fertile.
i	ms731		16		Sterile	Fertile	negative	negative	scattered		not fully developed/scattered		Females weakly fertile. Testis with numerous all dark spheres within and without elongating bundles;
i	ms695		17		Sterile	Fertile	negative	negative	not fused		developed	Individualization failure	1. classic 2. classic, but no onions seen
i	ms702		18	Good	Sterile	Fertile	negative	negative	not elongated			Individualization failure	Classic
i	ms970		19	Good	Sterile	Sterile	negative	positive			a little scattered	Individualization failure	Classic
i	ms1040		20		Sterile	Sterile	negative	positive			not fully developed/scattered	Individualization failure	Classic. Females laid eggs
i	ms736		21		Sterile	Sterile	negative	positive	not fused		scattered	Individualization failure	Classic. No eggs (McKeown).

Table 2.1 All the male sterile mutants that were received from the Zucker collection were annotated ms1-1119. Listed are only those that display complete abrogation of caspase staining. This table incorporates information received from Barbara Wakimoto and Margaret Fuller (personal communication), including class, viability, male and female sterility, category and comments. The rest of the data was collected during the screen. The main text includes more detailed information on the phenotypes.

Figure 2.3: A screen for genes that regulate caspase activity during individualization

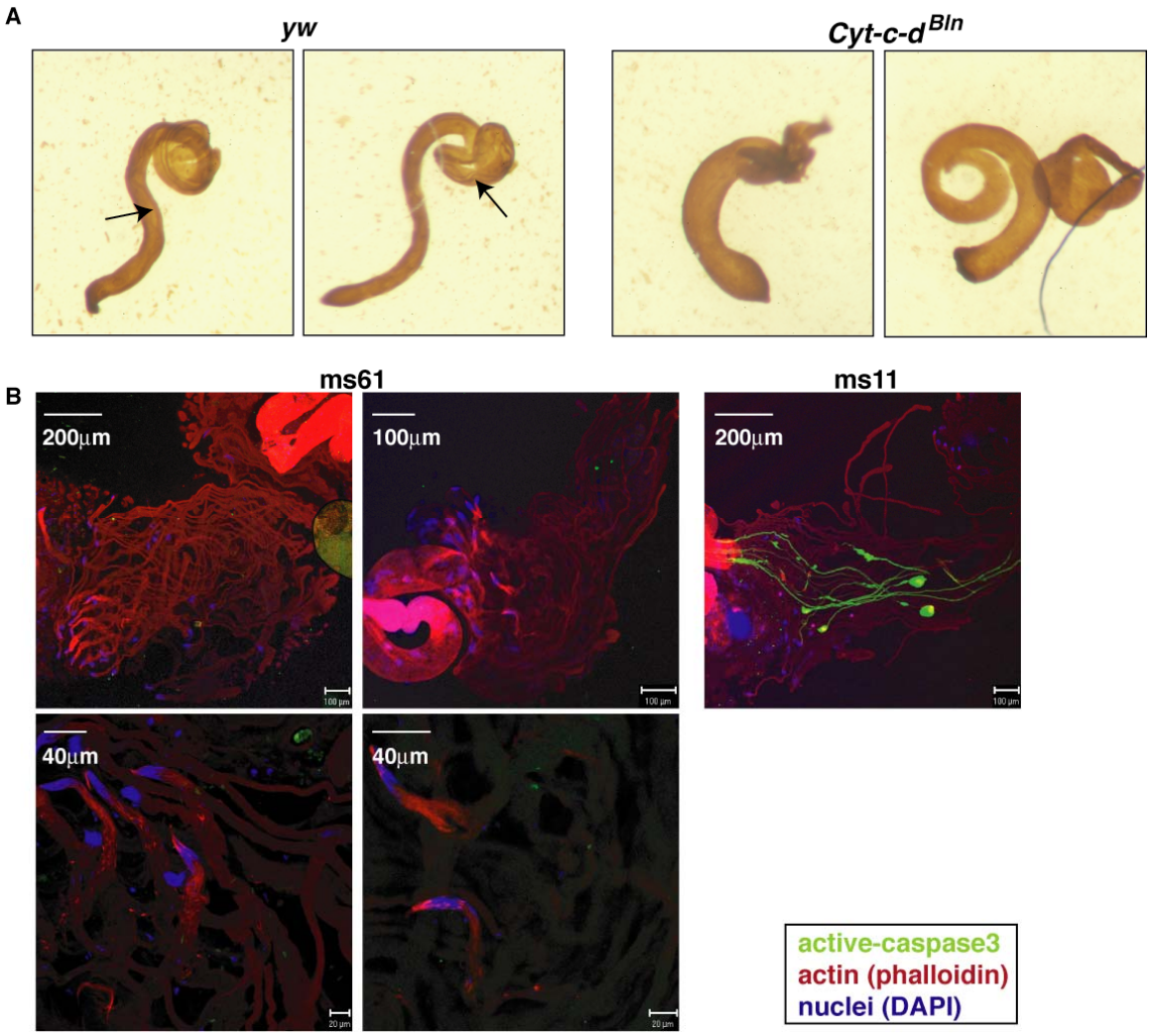

Figure 2.3 **[A]** Whole-mount testes immunocytochemically stained with the active-caspase3 antibody. This method was used to stain and screen roughly 850 individualization-defective lines for lack of caspase staining. In *yw* (wild-type) testes, caspase staining is detected as darker strands within elongated cysts. This staining is no longer detected in *cyt-c-d*^{bln} mutant testes. **[B]** Immunostaining of a caspase-negative mutant isolated in the screen, *ms61*. Compared to most individualization mutants (*ms11* in this example), only a small portion of mutants fail to activate caspases. Cysts were stained with DAPI (nuclei, blue), phalloidin (IC, red) and caspase-3 (cytoplasm, green)

2.3.2 Complementation analysis

The 33 mutant lines identified were subjected to complementation analysis. Each mutant line was crossed with all the other caspase-negative lines and the trans-hetrozygots were scored for sterility. Trans-hetrozygote males that failed to complement the sterility phenotype were assembled into an allelic group. This analysis revealed that the 33 mutant lines represent 22 allelic groups, or genes (Table 2.2).

Table 2.2: Complementation analysis

2nd chromosome

	ms61	ms72	ms330	ms101	ms282	ms311	ms266	ms312	ms389	ms462	ms444	ms374	ms396	ms961	ms667	ms734
ms61	N/A															
ms72	Y	N/A														
ms330	Y		N/A													
ms101	Y	Y	Y	N/A												
ms282	Y	Y	Y	Y	N/A											
ms311	N	CG	CG	Y	Y	N/A										
ms266	N	CG	CG	Y	Y	N	N/A									
ms312	Y	Y	Y	Y	Y	CG	Y	N/A								
ms389	Y	Y	Y	Y	Y	CG	CG	Y	N/A							
ms462	N	CG	CG	Y	Y	N	N	CG	CG	N/A						
ms444	Y		Y	Y	Y	CG	Y	Y	Y	CG	N/A					
ms374	N	CG	CG	Y	Y	N	N	CG	CG	N	CG	N/A				
ms396	N	CG	CG	Y	Y	G	G	CG	CG	G	CG	G	N/A			
ms961	N	Y	Y	Y	Y	N	N	Y	Y	N	Y	N	N	N/A		
ms667	CG	Y	Y	Y	Y	Y	Y	Y	N?	CG	Y	CG	CG	CG	N/A	
ms734	Y	Y	Y	Y	Y	CG	CG	Y	Y	CG	Y	Y	CG	CG		N/A
bln1	Y	Y	Y	Y	Y	CG	CG	N	Y	CG	Y	CG	CG	CG	CG	CG

3rd chromosome

	594	771	761	702	695	731	579	547	1056	1100	646	823	949	970	893	736	1040	549
594	N/A																	
771	Y	N/A																
761	Y	Y	N/A															
702	Y	Y	Y	N/A														
695	Y	Y	Y	Y	N/A													
731	Y	Y	Y	Y	Y	N/A												
579	Y	Y	N	Y	Y	Y	N/A											
547	Y	Y	Y	Y	Y	Y	Y	N/A										
1056	N	Y	Y	Y	Y	Y	Y	Y	N/A									
1100	Y	Y	Y	Y	Y	Y	Y	Y	Y	N/A								
646	Y	Y	Y	Y	Y	Y	Y	Y	Y	N	N/A							
823	Y	Y	Y	Y	Y	Y	Y	N	Y	Y	Y	N/A						
949	Y	Y	Y	Y	Y	Y	Y	N	Y	Y	Y	N	N/A					
970	Y	Y	Y	Y	Y	Y	Y	Y	Y	Y	Y	Y	Y	N/A				
893	Y	Y	Y	Y	Y	Y	Y	Y	Y	Y	Y	Y	Y	Y	N/A			
736		Y	Y	Y						Y		Y		Y	Y	N/A		
1040	Y	Y	Y	Y	Y	Y	Y	Y	Y	Y	Y	Y	Y	Y	Y		N/A	
549	Y		Y	Y	Y	Y	Y	Y	Y	Y	Y	Y	Y	Y	Y		Y	N/A
decay	Y	Y	Y	Y	Y	Y	Y	Y	Y	Y	Y	Y	Y	Y	Y			

Table 2.2 Each mutant line was crossed to the others and the trans-hetrozygot was subject to sterility testing. N = did not complement, Y = Complemented, CG = complemented with group member, G= group

2.3.3 Phenotypic Classification – AXO49 staining

Next, we wanted to distinguish between the active-caspase negative mutants that are specifically responsible for caspase activation and the mutants that affect the more upstream signaling pathways for the initiation of spermatid individualization. We used an additional antibody marker, AXO49, which stains axonemal-tubulin polyglycylation. This posttranslational modification was previously shown to occur at the final stages of spermatid maturation in a variety of organisms, including *Drosophila* (Bre et al., 1996) (Bre et al., 1998) (Rogowski et al., 2009). Although it takes place at a different cellular compartment to caspase activation, their staining patterns are identical, suggesting the presence of a "master" signal that coordinates the initiation of different processes at the onset of spermatid individualization (Figure 2.4). Thus, mutants that stain negatively for both antibodies must affect a more general individualization signal, whereas mutants that are cleaved-caspase negative but AXO49 positive more directly affect caspase activity. Out of the 33 mutant lines, 14 genes were found to be AXO49 positive (Table 2.1). In this experiment, the *Cytochrome-c-d Bln* allele (Arama et al., 2003) does not display AXO49 staining, which suggests that the mutants that are AXO49 positive might regulate caspases downstream of the mitochondria (data not shown).

Figure 2.4: Poly-glycylated axonal tubulin (AXO49) staining: an individualization marker

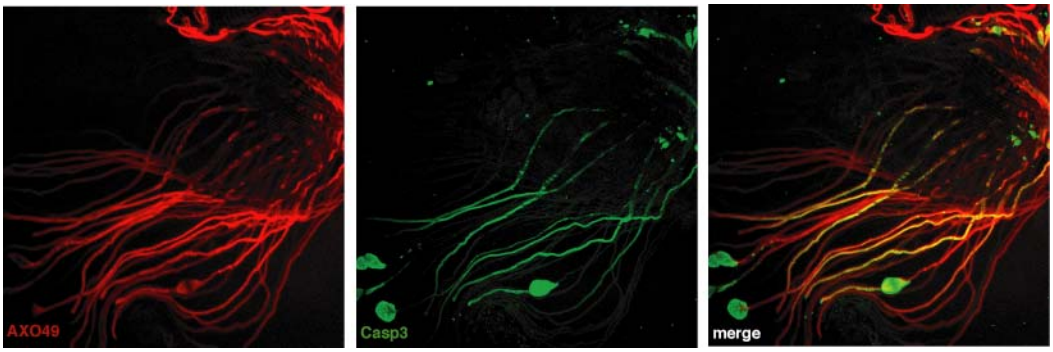

Figure 2.4 Poly-glycylated axonal tubulin staining is detected at the onset of individualization, and co-localizes with active-caspase staining. A *wild-type* (*yw*) testis was co-stained with both the AXO49 antibody (red) and the anti-cleaved-caspase3 antibody (green). Whereas caspase staining is detected in the CB and the pre-individualized portion of the cyst, AXO49 staining is detected along the entire length of the cyts.

2.3.4 Phenotypic Classification – morphological analysis

We further sub-grouped the isolated mutants by a more refined morphological characterization. Subcelluar and organelle abnormalities were visualized by staining mutant testes with specific markers. IC formation and movement were followed by staining testes with the actin marker phalloidin, while mitochondria and nuclei morphology and localization were examined by DAPI staining (Table 2.1).

While the majority of the mutants displayed normally fused and elongated mitochondria, a few mutants showed distinct abnormalities. Mitochondrial abnormalities included either mitochondria that failed to fuse properly, or those that fused but failed to elongate. Some mitochondria appeared fragmented, which could be a result of not

fusing. Although this analysis was not carried out for all the mutants, an interesting correlation emerged by which the mutants that display mitochondrial defects are also poly-glycylation (AXO49) negative.

Nuclear morphology also ranged in severity. Some mutants displayed fully developed, elongated nuclear-bundles. Most mutants displayed some degree of abnormality, the most common being nuclei that are developed and elongated, but are no longer bundled and scattered down the cyst. Other defects include nuclei that are not fully developed, either elongated but not properly shaped, or still round.

A detailed analysis of IC structure, formation and movement was conducted for a small number of mutants. The mutants examined also exhibited a range of abnormalities. In some cases the IC does not form at all, while in others the IC forms but does not transcend or the actin cones are scattered (example is *ms61* in Figure 2.3B). The morphological abnormalities found in these caspase-negative mutants suggest that proteins that control caspase activity also control other aspects of individualization, or that caspase activation is necessary for proper individualization morphology.

2.3.5 Isolation of an EMS derived allele of *cyt-c-d, ms312*

Cytochrome-c-d is absolutely required for caspase activation during individualization. Testes derived from the *cytochrome-c-d* p-element bln^1 mutant lack active-caspase staining and display individualization defects, resulting in sterility (Figure 2.3A) (Arama et al., 2003). To determine whether we isolated other alleles of *cytochrome-c-d* in our screen we checked if any of the 2nd chromosome mutants complement the Bln^1 allele (Table 2.2). Out of the 8 allelic groups, only one of the

mutants, *ms312*, failed to complement the sterility of Bln^1. Furthermore, *ms312* placed in trans to a deficiency that removes the *cytochrome-c-d* locus, Df(2L)Exel6039, is sterile and displays no caspase activation (Figure 2.5). Genomic sequence analyses of the transcription units of *cyt-c-d* in *ms312* flies revealed a point mutation of TGG-TGA at codon 62 in *cyt-c-d*, causing a change of Trp62 into a stop codon that results in a truncation of almost half of the protein. These results demonstrate the isolation of a new EMS derived allele of *cytochrome-c-d*, further affirming the involvement of this gene in caspase activation (Arama et al., 2006) (Mendes et al., 2006).

Figure 2.5: Isolation of an EMS derived allele of *cytochrome-c-d*

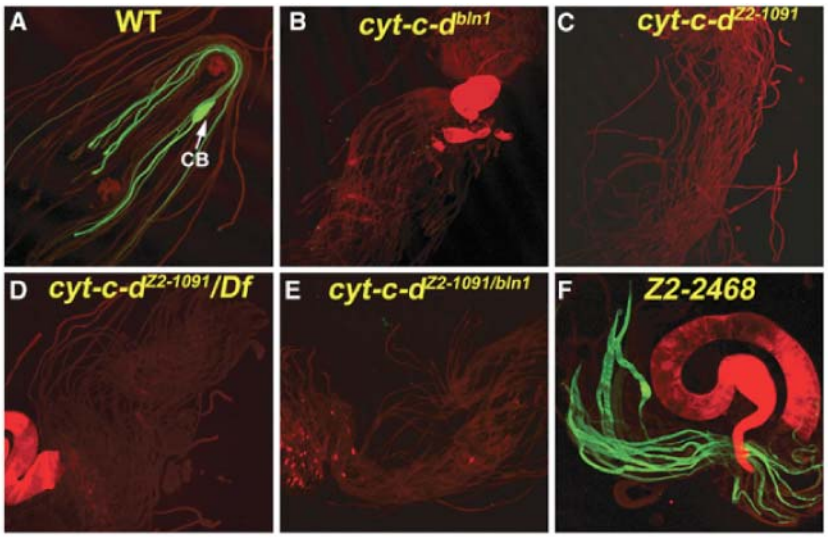

The EMBO Journal (2006) 25, 232 - 243

Figure 2.5 **[A–F]** Mutations in *cytochrome-c-d* block caspase activation and spermatid individualization. Visualization of active caspases with anti-cleaved caspase-3 antibody (green) in **[A]** wild-type **[B]** *cyt-c-d*^{bln1} **[C]** *cyt-c-d*$^{Z2\text{-}1091}$ **[D]** *cyt-c-d*$^{ms312/DF(2L)Exel6039}$ **[E]** *cyt-c-d*$^{ms312/cyt\text{-}c\text{-}dbln1}$ **[F]** *Z2-2468*. Whereas caspase-positive elongated spermatid cysts at different individualization stages can be readily seen in wild-type testes [A] (white arrow pointing at a CB), no caspase staining was detected in spermatids of flies homozygous for the P-element allele, *bln1* [B] and the point mutation allele, *ms312* [C]. Similarly, spermatids of *ms312* flies either trans-heterozygous to the small deficiency Df(2L)Exel6039 [D] or to the *bln1* allele [E] also displayed no caspase staining. In contrast, the vast majority of male-sterile mutants with spermatid individualization defects display strong caspase-positive cysts (*Z2-2468* [F]). To visualize all the spermatids, the testes were counter-stained with phalloidin that binds F-actin (red).

2.4 Materials and Methods

Fly stocks

Maureen Cahill and Charles Zucker kindly shipped the male-sterile Zucker collection. *ms312* is the mutant allele *Z2-1091* and *ms61* is *Z2-1827*. The p-element *blanks* (bln^1) mutant was procured from the Bloomington stock center and Df(2L)Exel6039 from Exelixis.

Screening the male sterile lines for caspase-deficiency by immunohistochemistry

The testes of at least three homozygous males from each sterile-line were dissected in testis buffer (10mM Tris-Hcl [pH 6.8], 183 mM KCl, 47 mM NaCl, 1 mM EDTA, and 1 mM PMSF) and placed in fixative made of 4% formaldehyde in PBX (PBS + 0.1% Triton X- 100) in a MultiScreen 96 well filter plates (MADVN6510, Millipore), standing on ice. After dissections, the plate was rocked for 20 min at RT. Solutions in all the wells were changed simultaneously using vacuum filtration (Millipore). Testes were washed three times in PBX for 10 min, blocked with PBS/BSA (1% BSA in PBS) for 45 min, incubated with 100 µl of the cleaved-caspase3 antibody (diluted 1:75 in PBS/BSA) overnight at 4°C, and washed three times with PBX for 10 min. Testes were incubated with 100 µl of the secondary antibody (biotinylated universal antibody diluted 1:50 in PBS/BSA, Vectastain, Vector) for 1 hr, washed three times in PBX for 10 min, and the colorimetric assay was developed using the Vectastain kit (Vector) according to manufacture's recommendations and DAB (Fast DAB tablet set, Sigma). The reaction was stopped by washing twice with 120 mM Tris-HCl.

Antibody staining

Young (0-2 day old) adult testes were dissected in testis buffer (TB; 10 mM Tris-HCl [pH 6.8], 183 mM KCl, 47 mM NaCl, 1 mM EDTA, and 1 mM PMSF), transferred to a 2.5 µl drop of TB on a siliconized coverslip (GOLD SEAL), opened using thin forceps, and sandwiched between a cover-slip and a poly-L-lysine-coated slide. The sandwich was frozen in liquid nitrogen, the coverslip was removed with a razor blade, and the slide was placed in ice-cold absolute ethanol. The slides were drained and a hydrophobic ring surrounding the opaque tissue was drawn using a PAP PEN (Zymed Laboratories). The tissue was fixed in 4% formaldehyde in PBS for 20 min, rinsed twice with PBS for 5 min, incubated in PBT (PBS + 0.1% Triton X-100) for 30 min, and rinsed twice again. The fixed testes were then blocked with PBS/BSA (1% BSA in PBS) for 45 min, incubated with primary antibody (diluted in PBS/BSA) within the hydrophobic ring overnight at 4°C inside a humid chamber, and rinsed twice for 5 min in PBS. Testes were incubated with the secondary antibody (diluted in PBS) for 1 hr at room temperature, together with with 1 ng/µl TRITC-phalloidin (Sigma), rinsed once for 15 min at room temperature, and mounted in Vectashield mounting medium with DAPI (Vector Laboratories). Cleaved-caspase3 antibody staining was carried out using a rabbit polyclonal anti-Cleaved Caspase-3 (Asp175) antibody (Cell Signaling Technology) diluted 1:75. Axonemal tubulin polyglycylation antibody staining was carried out using the mouse monoclonal antibody AXO 49 (Marie-Helene Bre, University of Paris-Sud, France) diluted 1:5,000**.** Secondary anti- rabbit antibodies were purchased from Jackson ImmunoResearch Laboratories. All pictures were taken with a Zeiss confocal microscope.

Sterility testing

0-2 day old individual males (20-30) were crossed to 2-3 virgin females and the emergence of living progeny was assed every 2-3 days for two weeks. Males were rendered sterile if no progeny was detected after this time period.

Isolation of genomic DNA and PCR

Genomic DNA was isolated from 25-50 adult flies using the High Pure PCR Template Preparation Kit (Roche). 2μg of genomic DNA were used to amplify the *cyt-c-* coding regions from wild-type or *cyt-c-d*^{ms312} homozygotes in a PCR reaction. PCR reactions were carried out using DyNAzyme EXT DNA polymerase (Finnzymes), according to the manufacturer instructions. The products were purified using the High Pure PCR Product Purification Kit (Roche), concentrated by evaporation, and sequenced (Genewiz).

3. A Ubiquitin Ligase Complex Regulates Caspase Activation During Sperm Differentiation in *Drosophila**[2]

Summary

In this chapter, I describe the identification and characterization of a testis-specific Cullin-3-dependent ubiquitin ligase complex that is required for caspase activation in spermatids. Mutations in either a testis specific isoform of Cullin-3, $Cul3_{Testis}$, the small RING protein Roc1b, or a *Drosophila* orthologue of the mammalian BTB-Kelch protein Klhl10 all reduce or eliminate effector caspase activation in spermatids. Significantly, all three genes encode proteins that can physically interact to form a ubiquitin ligase complex. Roc1b binds to the catalytic core of Cullin-3, and Klhl10 binds specifically to a unique testis-specific N-terminal Cul3 (TeNC) domain of $Cul3_{Testis}$ that is required for activation of effector caspase in spermatids. These findings reveal a novel role of Cullin-based ubiquitin ligases in caspase regulation.

3.2 Introduction

Ubiquitin-mediated protein degradation is a tightly regulated process, in which proteins are tagged with ubiquitin moieties through a series of enzymatic reactions involving an E1-activating enzyme, E2-conjugating enzyme, and E3 ubiquitin ligase that

[2] This chapter was co-written with Dr. Eli Arama and published in (Arama et. al., 2007). Eli Arama conceived of most of the experiments in this chapter, which were executed by Eli Arama and Maya Bader.

determine substrate specificity. Tagged proteins are then degraded by the 26S proteasome (Ardley and Robinson, 2005; Glickman and Ciechanover, 2002; Hershko and Ciechanover, 1998). Cullins are major components of specific types of multi-complex E3-ubiquitin ligases, which serve as scaffolds for two functional modules: a catalytic module, comprised of a small RING domain protein that recruits the ubiquitin-conjugating enzyme, and a substrate recognition module that binds to the substrate and brings it within proximity to the catalytic module (Petroski and Deshaies, 2005; Willems et al., 2004). The human genome encodes seven different Cullins: Cullin-1, 2, 3, 4A, 4B, 5, and 7. The SCF (Skp1-Cullin-1-F-box) complexes are so far the best-characterized Cullin-dependent E3 ligases. More recently, the molecular composition and function of the Cullin-3-dependent E3 ligase complex has also been described (Figueroa et al., 2005; Furukawa et al., 2003; Geyer et al., 2003; Pintard et al., 2003; Wilkins et al., 2004; Xu et al., 2003). In this complex, Broad-complex, Tramtrack and Bric-a-Brac (BTB) domain-containing proteins mediate binding of the Cullin to the substrate whereas the Skp1/F-box heterodimer fulfill this function in the SCF complex (Petroski and Deshaies, 2005; Pintard et al., 2004; Willems et al., 2004). In the past decade, Cullins have been implicated in a variety of cellular activities (Willems et al., 2004). However, very little is known about their involvement in the regulation of caspase activation and apoptosis. Here, I describe the identification of *cullin-3* mutants from a genetic screen for mutants that abrogate effector caspase activation during terminal differentiation of *Drosophila* spermatids (see Chapter 2). We isolated several *cullin-3* alleles with mutations in a testis-specific N-terminal Cullin-3 (TeNC) domain. We show that the small RING domain protein, Roc1b, interacts with Cullin-3 in spermatids to promote effector caspase

activation. We also identified a BTB-domain protein, Klhl10, that selectively binds to the testis-specific form of Cullin-3, but not to somatic Cullin-3. Finally, mutant alleles of *klhl10* were isolated that block effector caspase activation and cause male sterility. Together, these results define a novel Cullin-3-dependent E3 ubiquitin ligase complex that regulates effector caspase activation in *Drosophila* spermatids. Given the conserved nature of these proteins, these findings may have important implications for caspase regulation in other systems.

3.3 Results

3.3.1 *ms282* is a male sterile mutant defective in caspase activation during sperm individualization

A mutant isolated in the screen, *ms282*, belongs to a previously analyzed complementation group from the original male-sterility screen (B. Wakimoto, personal communication). We termed this complementation group "*medusa*" (*mds*; in Greek mythology Medusa represents both life and death). *ms282*, hence *mds1,* is AXO49-positive but completely negative for cleaved-caspase3 as a homozygote or in trans to deficiencies that cover the corresponding region (Figures 3.1B-D and Figure 3.1S1). The remaining four *mds* alleles retained various levels of cleaved-caspase3 staining but failed to complement the sterility of *mds1*, suggesting that they are hypomorphic alleles. All these mutations were later mapped to the *Drosophila cullin-3* gene and were thus designated $cul3^{mds1\text{-}5}$ (Zuker lines # *Z2-1089*, *Z2-4870*, *Z2-4061*, *Z2-1270*, and *Z2-1062*, respectively; Figures 3.1E-G). $cul3^{mds2}$ contains an unrelated lethal mutation in the

background and therefore was analyzed in trans to the other alleles or deficiencies in the region.

Figure 3.1 **[A-H]** Visualization of active caspases with anti-cleaved caspase-3 antibody (green) and axonemal tubulin polyglycylation with anti-glycylated tubulin monoclonal antibody (AXO 49; red). These figures are composed of a green layer only in the left panel, and green and red layers combined in the right panel. **[A]** Wild-type individualizing spermatids stain positively for active effector caspase and polyglycylated axonemal tubulin (white arrows pointing at cystic bulges -CBs - and red arrow pointing at a waste bag - WB). Elongated spermatids from **[B]** homozygotes for the null $cul3^{mds1}$ allele or **[C and D]** transheterozygotes for $cul3^{mds1}$ and two different deficiencies that cover the *cullin-3* gene, *DF*(2L)ED3 and *DF*(2L)Exel8034, respectively, stain for polyglycylation but not for active effector caspase. **[E-G]** Homozygote mutants for three hypomorphic $cul3_{Testis}$ alleles, $cul3^{mds5}$, $cul3^{mds3}$ and $cul3^{mds4}$, respectively, have spermatid individualization defects but still display some levels of active effector caspase expression. **[H]** However, the level of active effector caspase expression was dramatically reduced in spermatids from transheterozygote mutants for the null $cul3^{mds1}$ and either of the hypomorphic alleles, such as $cul3^{mds4}$. All the figures are in the same magnification; scale bar 200 μm. **[I]** The diagram depicts a DEVDase activity assay for $cul3^{mds1}$ mutant testes. Caspase-3-like (DEVDase) activity is detected in wild-type testes, and is blocked either after treatment with the caspase-3 inhibitor Z-VAD.fmk or in $cul3^{mds1}$ mutant testes. DEVDase activity, presented as relative luminescence units (RLU), was determined on Ac-DEVD-pNA substrate in testis extracts made of 180 wild-type (*yw*) or $cul3^{mds1}$ mutant testes treated with Z-VAD or left untreated (DMSO). Readings were obtained every 2 min, and each time interval represents an average (mean ± s.e.m.) of five readings. Note that the level of DEVDase activity in $cul3^{mds1}$ mutant testes is similar to the corresponding level in wild-type testes that were treated with Z-VAD. **[J]** A Western blot analysis for the assessment of the relative protein amounts used in (I). A portion of the testis extracts in (I) were used as controls to determine the relative amounts of total protein in each extract using the anti-β-Tubulin antibody.

Figure 3.1 Mutations in Cullin3T block caspase activation and spermatid individualization, but not axonemal tubulin polyglycylation

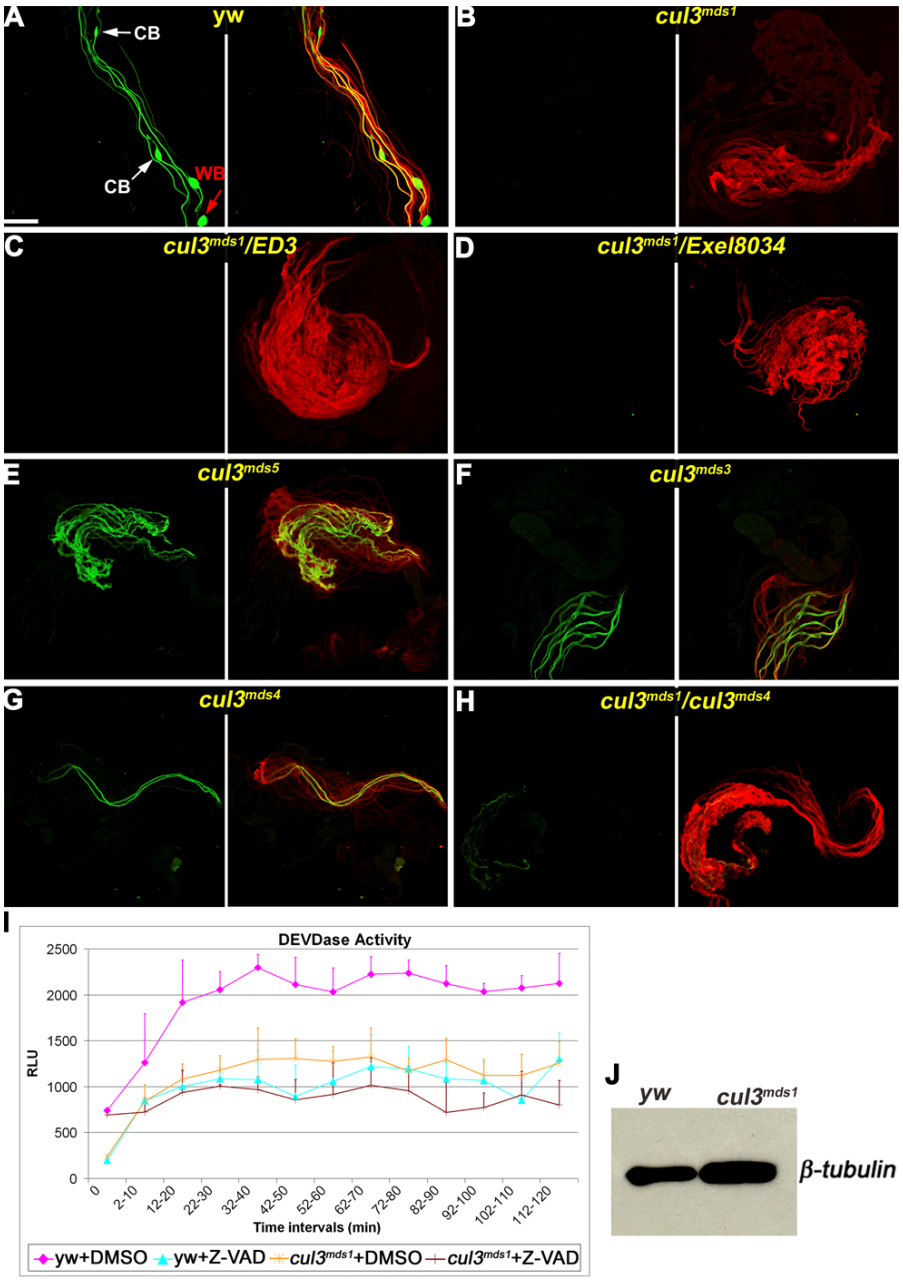

Drosophila apoptotic effector caspases, such as drICE and Dcp-1, can display DEVD cleaving activity (Fraser et al., 1997; Song et al., 2000; Song et al., 1997). We have previously shown that wild type adult testes also contain DEVDase activity and that this activity is reduced in *cyt-c-d* mutant testes (Arama et al., 2006). To provide independent evidence for a requirement of Cullin-3 in caspase activation, we measured DEVDase activity in $cul3^{mds1}$ mutant testes. Whereas lysates of wild type testes displayed significant levels of DEVDase activity, activity in $cul3^{mds1}$ mutant testes was reduced to background levels, comparable to the reduction achieved with the potent caspase inhibitor Z-VAD.fmk (Figures 3.1I and 3.1J). These results confirm that *cullin-3* is required for the activation of effector caspases in spermatids.

3.3.2 Genetic and molecular characterizations of the *Cullin-3* locus

To map the *mds* alleles, we first searched for genomic deletions that failed to complement the sterility of the *mds* males. Utilizing the "deficiency kit" from FlyBase, the male-sterility was mapped to genomic segment 35C1-35D1 on the left arm of the second chromosome (Figure 3.1S1). We then performed similar complementation tests with available mutants in this region and found that lethal *cullin-3* mutants (Ashburner et al., 1990; Mistry et al., 2004) failed to complement the sterility of *mds* mutant males, suggesting that the *mds* alleles may represent a unique class of mutations in the *cullin-3* gene (Table 3.1). Since the *Drosophila cullin-3* gene was previously termed *gft* (Mistry et al., 2004), we will henceforth refer to the lethal *cullin-3* alleles as $cul3^{gft}$. To determine the molecular nature of the *mds* mutations, we analyzed first the *cullin-3* genomic organization. The *cullin-3* gene consists of 14 exons, 11 of which contain coding

sequences (Figure 3.2A; a partial genomic map was provided in (Mistry et al., 2004)). Our genetic and molecular analyses identified a new exon, 1D, and suggested that the *cullin-3* gene codes for two major isoforms that are somatic and testis specific (Figures 3.2A and 3.2B). A lethal *P*-element insertion in the 5' UTR of the *cullin-3* gene, $cul3^{gft[06430],}$ which fail to complement the lethality of other *gft* alleles, complemented the sterility of the *mds* alleles, suggesting that these noncoding sequences are only required for the somatic function of *cullin-3* (Figure 3.2A, Table 3.1). Additionally, genomic PCR followed by sequencing analysis revealed that the *mds1* mutant contains a deletion in the intron that is flanked by exon 2 and exon 3, suggesting that this intron contains sequences that are only required for the function of *cullin-3* in spermatids (Figures 3.2A and 3.2C). Finally, RT-PCR as well as sequence analyses of several independent clones from adult testis and somatic cDNA libraries confirmed the presence of two major *cullin-3* mRNA isoforms, $cul3_{Soma}$ and $cul3_{Testis}$ (Figures 3.2A and 3.2B). While both isoforms share extensive similarity (exons 3-11), $cul3_{Soma}$ contains a unique, 20 amino-acid long N-terminal polypeptide (encoded by exon 2), and $cul3_{Testis}$ contains a unique, 181 amino-acid long Testis-specific N-terminal Cul3 (TeNC) domain encoded by exon 1D (Figures 3.2A and 3.2B; part of exon 1D is incorrectly annotated in FlyBase as an independent gene, CG31829). We also identified three different mRNA isoforms of $cul3_{Soma}$ but these only differ in their 5' UTRs (encoded by exons 1A, 1B, and 1C, Figure 3.2A). Cullins were previously thought to be universally expressed.

Figure 3.1S1 Mapping of the *mds1* Mutation

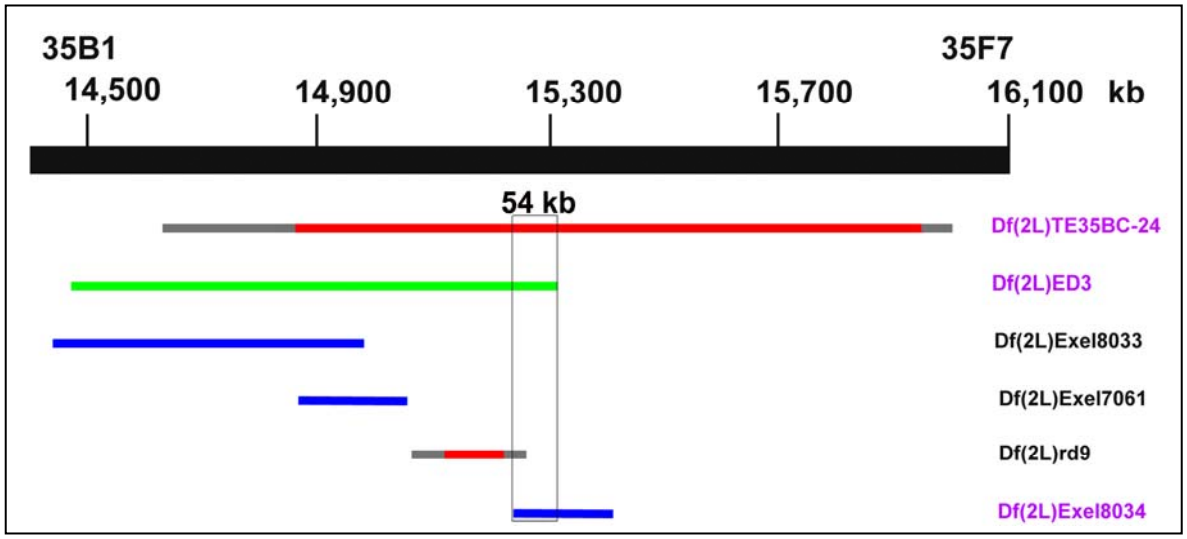

Figure 3.1S1 The thick bar represents the cytological region between 35B1 and 35F7. The relative nucleotide positions of this region within the second chromosome are indicated above the bar. Thin bars depict available deficiencies in this region (red flanked by gray, Bloomington's deficiencies; green, DrosDel's deficiency; blue, Exelixis' deficiencies). The *mds1* mutants were crossed to all the deficiency lines from FlyBase's second chromosome "kit" and the trans-heterozygotes were tested for male fertility. The deficiency line *Df*(2L)*TE35BC-24,* which contains a large chromosomal deletion (cytological region 35B4/6–35E1/2) failed to complement the sterility of *mds1* males, suggesting that this region covers the *mds1* mutation. Additional smaller deletion lines in this region were subsequently analyzed. The deficiencies shown in purple, *Df*(2L)ED3 and *Df*(2L)Exel8034, failed to complement, whereas the deficiencies shown in black complemented the *mds1* sterility. This genetic analysis restricted the *mds1* mutation to a 54-kb genomic interval comprising nine genes (from the *gft* gene in 35C1 to the *nht* gene in 35D1).

Table 3.1. *cullin3*^{gft} lethal mutants failed to complement the sterility of *cullin3*^{mds} mutant males

Allelic type	*cul3*^{gft1}	*cul3*^{gft2}	*cul3*$^{gft[gr18]}$	*cul3*$^{gft[d577]}$	*cul3*^{gft4}	*cul3*^{gft3}	*cul3*$^{gft[06430]}$
cul3^{mds1}	0	0	0	0	0	0	100
cul3^{mds2}	0	0	0	0	0	0	100
cul3^{mds3}	0	0	0	0	10.2±11.5	98.4±4.5	100
cul3^{mds4}	0	0	0	0	0.9±0.9	92.5±5	100
cul3^{mds5}	0	0	0	0	74±23	92.4±4.2	100

Table 3.1 Males with transheterozygous allelic combinations of each of the indicated *cul3*^{gft} alleles (upper row) in trans to each of the indicated *cul3*^{mds} alleles (lefties column) were analyzed for fertility. Ten males from every transheterozygote line were allowed to mate separately with three wild-type virgin females for seven days at 25^{0}C. After the parents were removed, the number of offspring was counted for 19 days. The averages and standard deviations of the total offspring numbers were calculated for each of the semi- or barely- fertile lines, and the values are presented as "percentage of fertility", when the average fertility of wild-type males was considered as 100%. When the lines were completely sterile the value "0" was entered, whereas "100" was entered when the offspring numbers were comparable to wild-type.

Figure 3.2S1 The TeNC Domain Has Been Highly Conserved Throughout *Drosophila* Phylogeny

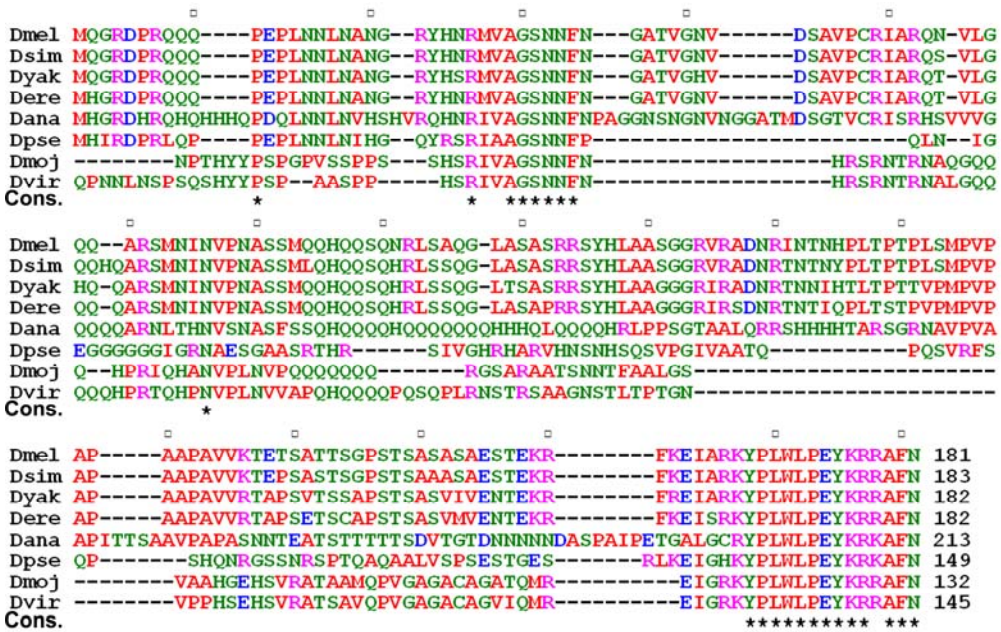

Figure 3.2S1 The TeNC domains of $Cul3_{Testis}$ from eight *Drosophila* species were aligned using the ClustalW program (Dmel, *melanogaster;* Dsim, *simulans;* Dyak, *yakuba;* Dere, *erecta;* Dana, *ananassae;* Dpse, *pseudoobscura;* Dmoj, *mojavensis;* Dvir, *virilis*). Identical or similar amino acids are depicted by the same color. In the consensus (cons.) lines, asterisks represent residues that are identical in all the species. Square dots appear above every tenth residue, and the total numbers of amino acid in each domain appear on the right of every line in the final block. Although conservation appears throughout the domain, two regions of high conservation in the beginning and in the very end of the domain are revealed. Note that the divergence time distance between *D. melanogaster* and *D. mojavensis* or *D. virilis* is 40 million years.

To determine the molecular nature of the *mds* alleles, we sequenced PCR-amplified genomic fragments of the *cullin-3* locus from these mutants. As expected from the genetic analysis, all *mds* alleles contained mutations in or near exon 1D and hence affect only the testis-specific isoform: $cul3^{mds1}$ has a 181 bp deletion that eliminates part of 5' UTR of $cul3_{Testis}$ (orange brackets in Figure 3.2A and 3.2C). The two hypomorphic alleles, $cul3^{mds3}$ and $cul3^{mds4}$ contain a C to T transversion at positions 341 and 347, which convert glutamine to stop codons at amino acids 8 and 10, respectively. As a result, translation may initiate downstream of the normal translation initiation site (orange stars in Figure 3.2A and Figure 3.2S1). $cul3^{mds2}$ contains a G to A transversion of a splice donor site in the intron that is flanked by exons 1D and 3; this presumably abrogates splicing between these exons (Figure 3.2A). $cul3^{mds5}$ has a G114 to A transversion within the 5' UTR of $cul3_{Testis}$ (Figure 3.2A). In contrast, three of the lethal *gft* alleles that failed to complement the sterility of *mds* mutant males, $cul3^{gft[GR18]}$, $cul3^{gft4}$, and $cul3^{gft2}$, contain mutations in exons 4, 10 and 11, respectively, that are shared by both isoforms of *cullin*-3 (purple stars in Figure 3.1A;(Mistry et al., 2004)).

Transheterozygous combinations between $cul3^{mds1}$ and four strong *gft* alleles, $cul3^{gft2}$, $cul3^{gft[GR18]}$, $cul3^{gft1}$, and $cul3^{gft[d577]}$, were sterile and their elongated spermatids were cleaved-caspase3-negative but AXO 49-positive (Figures 3.2E, 3.2G, 3.2H, Table 3.1). Other *mds*/*gft* combinations with weaker alleles produced reduced levels of cleaved caspase-3 staining, wild type levels of axonemal tubulin polyglycylation, and decreased fertility (Figures 3.1H, 3.2I, Table 3.1, Figure 3.2S2). Collectively, these results suggest that a testis-specific isoform of *cullin-3* is required for effector caspase activation and spermatid individualization.

Figure 3.2 **[A]** Genomic organization of the *cullin-3* locus. Thick bars indicate exons and dotted lines indicate introns. Solid bars indicate coding sequences, while open bars indicate UTRs. The *Drosophila cullin-3* gene contains 14 exons, nine of which encode the bulk of the protein (exons 3-11) and are shared by both the somatic and testis-specific isoforms. While the three somatic isoforms ($cul3_{Soma}$) differ in their 5' UTRs, each beginning with a unique first exon (exons 1A, 1B, and 1C), they share a second, somatic-only exon that contains a start codon (exon 2, green bar). The testis isoform, $cul3_{Testis}$, begins with a unique first exon (1D, blue bar) that includes both 5' UTR and coding sequences, including a start codon. The relative locations of the molecular lesions in $cul3_{Testis}$ (orange, $cul3^{mds1-5}$ alleles) and $cul3_{Soma}$ (purple, $cul3^{gft2,\ 4,\ GR18}$ alleles) are shown with stars (see the main text for more details on the precise molecular lesions of the $cul3^{mds1-5}$ alleles). The molecular alterations of the $cul3^{gft}$ alleles were reported in (Mistry et al., 2004; Sulston, 1983): $cul3^{gft06430}$ contains a *PZ* element insertion 228 nucleotides from exon 2 (the insertion is indicated by a purple triangle), $cul3^{gft[GR18]}$ is missing a single nucleotide causing a premature stop codon at amino acid 167; $cul3^{gft4}$ bears a C to T transversion, which results in an A710 to V conversion, and $cul3^{gft2}$ contains a 5 nucleotide deletion that results in a premature stop codon at amino acid 748 that removes half of the C-terminal Cullin Homology Domain (CHD). **[B]** A scheme of the two major mRNA isoforms of *cullin-3*, $cul3_{Testis}$ and $cul3_{Soma}$. **[C]** Genomic PCR and sequencing analyses of the *cullin-3* locus revealed a 181 bp deletion in $cul3^{mds1}$ (the arrows in A depict the relative locations of the primers used in this gPCR; *yw* and *Canton S* strains were used as wild-type controls). **[D]** For a positive control, wild-type spermatids were stained for cleaved caspase-3 expression (green). **[E]** Consistent with the idea that both the *mds* and *gft* alleles affect the same gene, *cullin-3*, $cul3^{mds1}/cul3^{gft2}$ transheterozygote mutant spermatids displayed defects in individualization and negatively stained for cleaved caspase-3 (left panel). Spermatids were counter-stained with phalloidin that binds to F-actin in the spermatids' tail (right panel, red; the strong red staining at the bottom corresponds to remnants of the testis sheath).

Figure 3.2. The *cul3*$^{mds1-5}$ alleles contain mutations in a new exon of the *cullin-3* gene

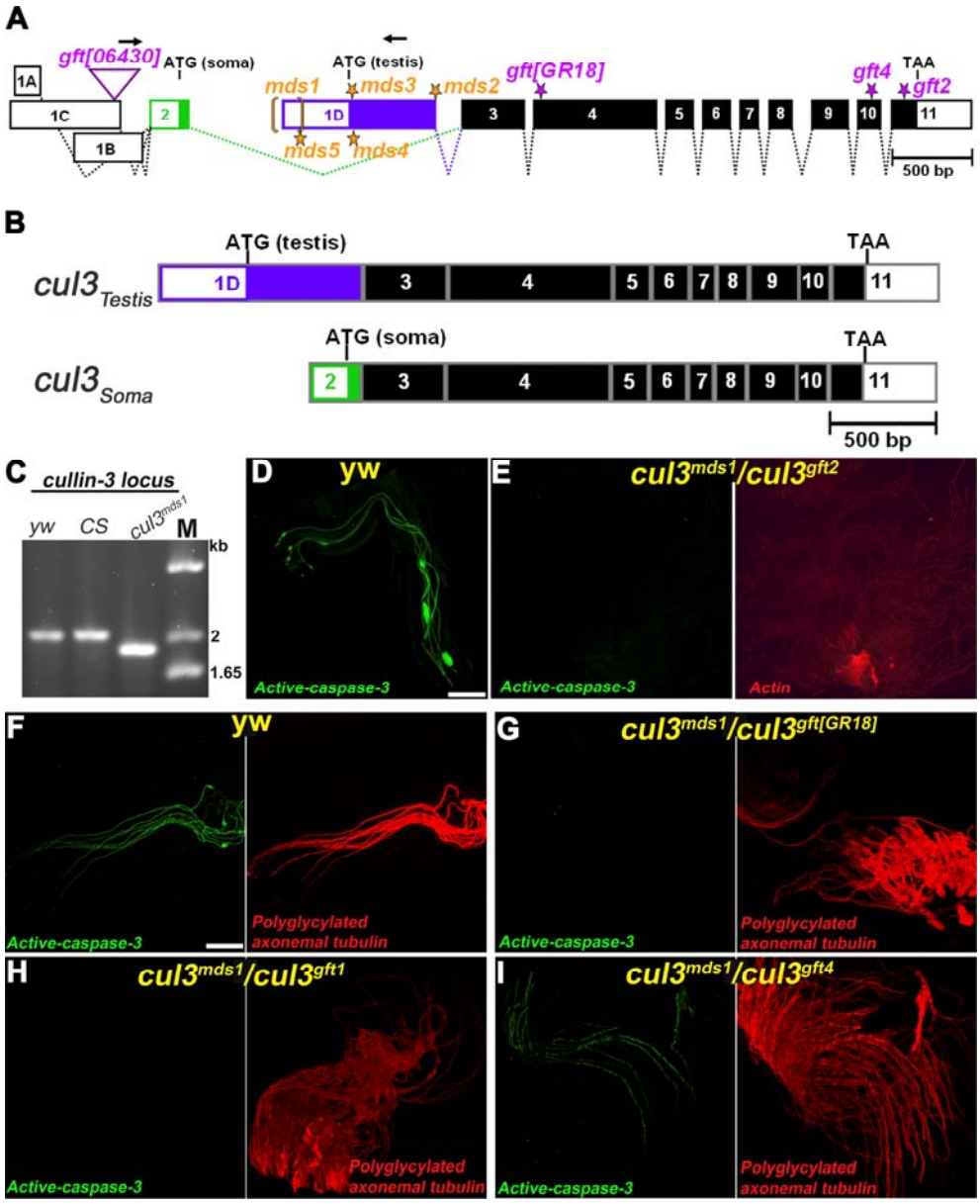

Figure 3.2S2 The Expression Level of Cleaved Effector Caspase is *Cullin3T* Dose-Dependent

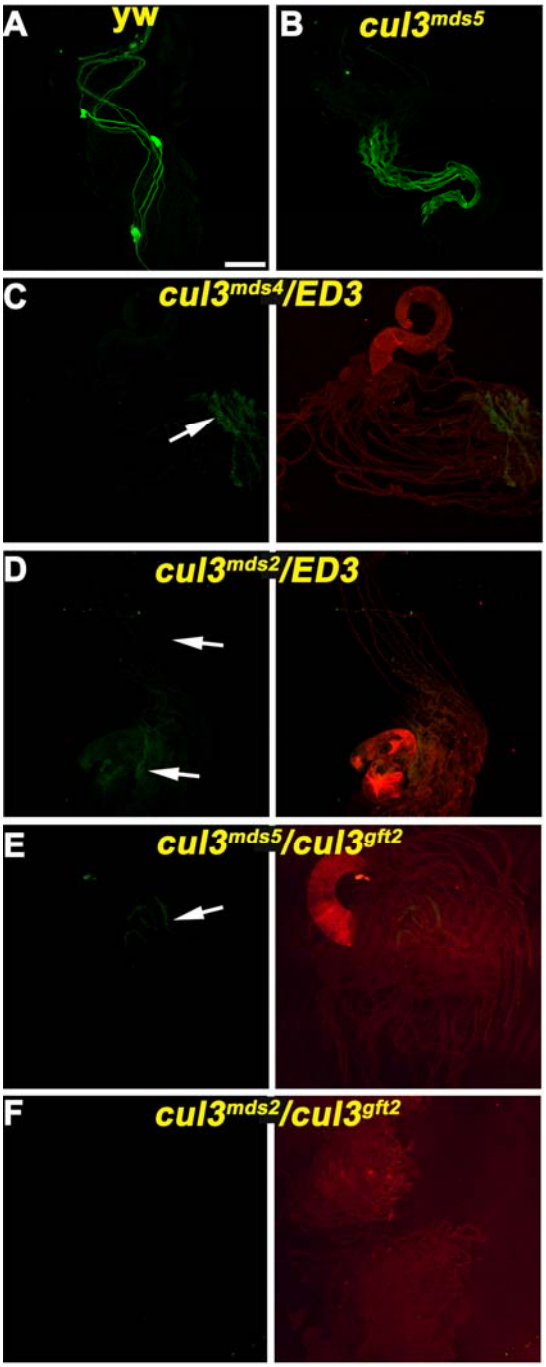

Figure 3.2S2 **[A-F]** Cleaved caspase-3 is visualized by cleaved-caspase3 antibody (green). In **[C–F]**, the spermatids were also counter-stained with phalloidin, which detects F-actin (red). **[C-F]** Each figure is composed of a green layer alone (left panels) and combined green and red layers (right panels). **[A]** Wild-type control spermatids display cleaved caspase-3 expression. **[B]** Spermatids from the hypomorphic *cul3*^{mds} mutants, such as *cul3*^{mds5}, also display readable levels of cleaved caspase-3 expression. **[C-F]** However, a dramatic decrease in the level of cleaved caspase-3 expression is observed upon reduction of *cullin-3* gene copy or functionality by **[C-D]** crossing the hypomorphic *cul3*^{mds} mutants, such as *cul3*^{mds2}, *cul3*^{mds4}, or *cul3*^{mds5}, to deficiencies that cover the *cullin-3* locus, such as *DF*(2L)ED3, or to **[E-F]** the strong *cul3*$^{-/-}$ alleles, such as *cul3*^{gft2}, respectively. All figures were taken at the same magnification. Scale bar, 200 μm.

3.3.3 Expression of cul3$_{Testis}$ is restricted to the male germ-line

Our genetic analyses suggested the existence of two functionally distinct isoforms of *cullin-3*, *cul3*$_{Testis}$ and *cul3*$_{Soma}$. One possible explanation for this is that the two isoforms are differentially expressed. To test this idea, we examined the distribution of *cullin-3* transcripts in the testis and the soma. Comparative RT-PCR experiments were performed using specific primers in the unique 5' UTRs of *cul3*$_{Soma}$ and *cul3*$_{Testis}$ and a reverse primer in their common 3'UTR (black arrows in Figure 3.3A). *cul3*$_{Soma}$ was the only isoform detectable in the soma of adult females (which lack testes), and *cul3*$_{Testis}$ was the major isoform in testes (Figure 3.3B). Dissected testes contain both germ cells and somatic cells, such as the testicular wall, muscles cells, and cyst cells. To determine whether *cul3*$_{Testis}$ is germ cell specific, we also analyzed RNA from a mutant lacking germ cells. Both the somatic and testis forms of *cullin-3* were expressed in wild type, but only *cul3*$_{Soma}$ was detected in the germ-cell-less reproductive tracts of adult males derived from *oskar* mutant mothers (Figure 3.3C). Since *cul3*$_{Testis}$ is not detectable in adult females, this indicates that *cul3*$_{Testis}$ expression is restricted to male germ cells, and that *cul3*$_{Soma}$ expression is mainly, if not exclusively restricted to somatic cells (Figures 3.3B and 3.3C). Finally, consistent with the idea that promoter and 5' UTR sequences of *cul3*$_{Testis}$ are absent in *cul3*^{mds1} mutants (Figure 3.2A), neither *cul3*$_{Testis}$ transcripts nor protein were detected in *cul3*^{mds1} mutant testes. Therefore, *cul3*^{mds1} has both the genetic and molecular properties of a *cul3*$_{Testis}$ null allele (Figures 3.3B and 3.3D). These results suggest that differential expression of *cul3*$_{Testis}$ in the male germ-line and *cul3*$_{Soma}$ in somatic tissues accounts for the distinct phenotypes (male sterility versus lethality) of the different classes of *cullin-3* mutations.

Figure 3.3 **[A]** Schematic structures of the *Drosophila cullin-3* gene (I) and of *cullin3*$_{Testis}$ (II) and *cullin3*$_{Soma}$ (III) mRNAs. Exons and introns are indicated by thick and thin bars, respectively. Thick black bars indicate coding sequences, while open bars indicate UTRs. The locations of the primers used in the comparative RT–PCR experiments in **[B -C]** are indicated by arrows, and the expected length sizes of the amplified fragments are indicated above each scheme. **[B]** Analysis of *cullin3*$_{Testis}$ versus *cullin3*$_{Soma}$ expression in the testis and the soma. The above primers (arrows in A) to amplify either a 2997-bp *cullin3*$_{Testis}$ or a 2642-bp *cullin3*$_{Soma}$ cDNA fragment were added to one reaction master-mix. The reaction was stopped at different cycle points to identify the linear amplification phase (30 and 35 cycles are indicated). The "RT" columns represent reverse transcriptase followed by PCR reactions, and the "Taq" are the control, PCR-only, reactions. Note that the *cullin3*$_{Testis}$ expression levels were much higher in the wild-type testes than these of *cullin3*$_{Soma}$. On the other hand, only *cullin3*$_{Soma}$ transcripts were detected in somatic tissues, which are represented by adult female flies. In addition, no *cullin3*$_{Testis}$ transcripts were detected in *cullin3*^{mds1} mutant testes, confirming that this is a null *cullin3*$_{Testis}$ allele. **[C]** The expression of *cullin3*$_{Testis}$ is restricted to the male germ-cells. While the expression of *cullin3*$_{Soma}$ was not affected in sons of *oskar* agametic testes, no *cullin3*$_{Testis}$ expression was detected. **[D]** Consistent with the RT-PCR analysis, no Cullin3$_{Testis}$ protein was detected in *cullin3*^{mds1} mutant testes on Western blot. Note, however, that expression of the Cullin3$_{Soma}$ protein in *cullin3*^{mds1} mutant testes was unaffected.

Figure 3.3 The expression of *cullin3*$_{Testis}$ is restricted to male germ-cells

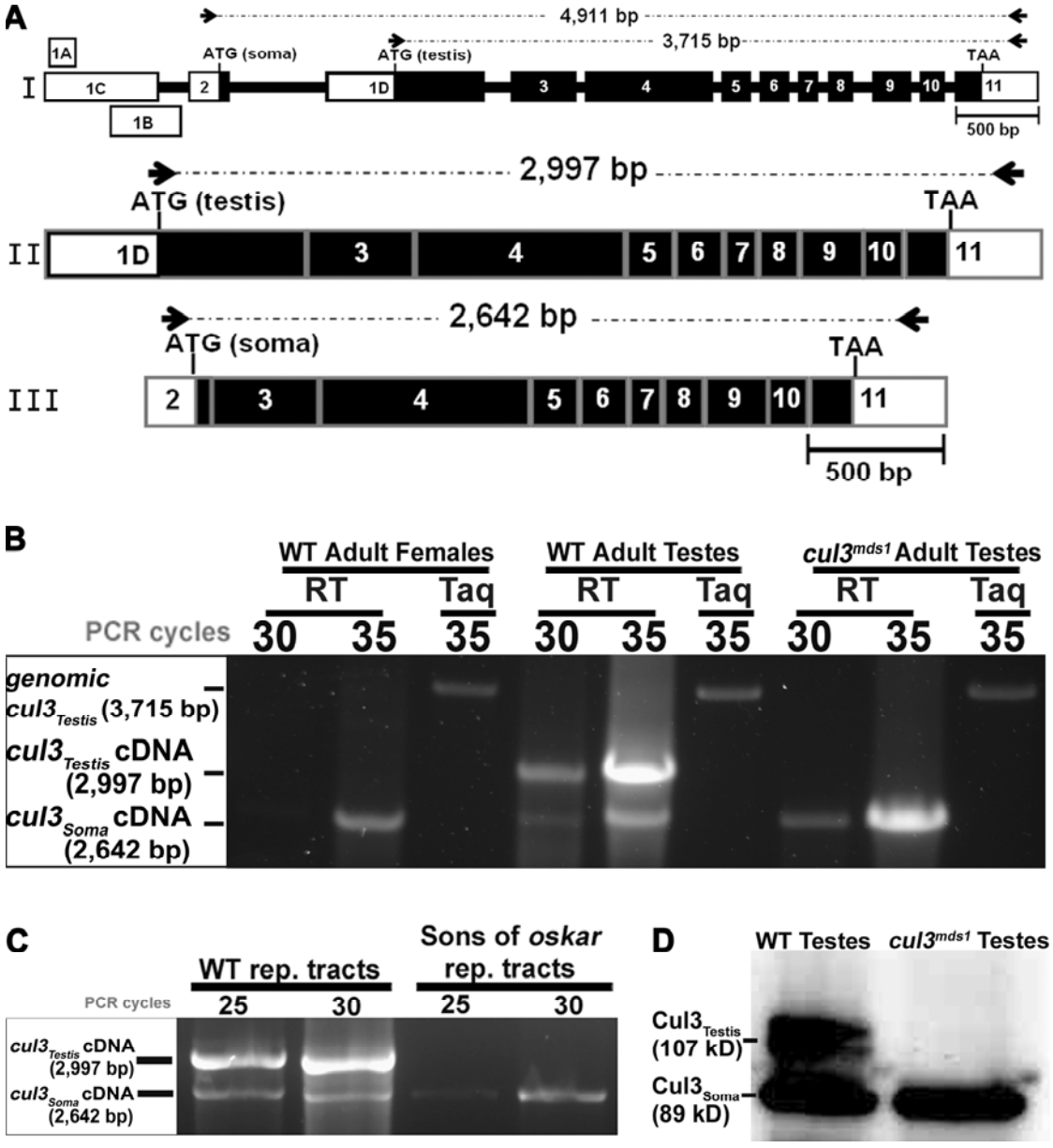

3.3.4 The TeNC domain in $Cul3_{Testis}$ is required for caspase activation and male fertility

The N-terminal region of Cullins is thought to mediate binding to a specific substrate recognition module ((Willems et al., 2004){Petroski, 2005 #59; Figure 6.1A). To test whether the unique testis-specific N-terminal Cul3 (TeNC) domain is required for the function of $Cul3_{Testis}$, we tested whether expression of $Cul3_{Soma}$, which lacks a TeNC domain, was able to functionally substitute for the loss of $Cul3_{Testis}$ in developing spermatids. For this purpose, we generated transgenic flies that express the coding regions of either $cul3_{Testis}$ (Figure 3.4A-I) or $cul3_{Soma}$ (Figure 3.4A-II) under the control of the $cul3_{Testis}$ promoter and 5' and 3' UTRs. At least three independent transgenic lines for each of these constructs were crossed to $cul3^{mds1}$ flies, and proper expression of the transgenes was confirmed by RT–PCR analysis (Figures 3.4B and 3.4C). We examined the ability of these transgenes to rescue caspase activation, spermatid individualization and male sterility of $cul3^{mds1}$ flies. As expected, transgenes with either one or two copies of the $cul3_{Testis}$ open reading frame (ORF) fully rescued cleaved-caspase3 staining, spermatid individualization, and male fertility (Figures 3.4E and 3.4F; note the reappearance of cystic bulges and waste bags). This proves that both the caspase and sterility phenotypes seen in $cul3^{mds1}$ mutant flies are due to the loss of *cullin-3* function. We next tested the ability of $cul3_{Soma}$ to functionally substitute for the loss of $cul3_{Testis}$. Neither one nor two copies of $cul3_{Soma}$ rescued spermatid individualization or male fertility, although we observed a very low levels of cleaved-caspase3 staining (Figures 3.4H and 3.4I). Since the $cul3_{Soma}$ and $cul3_{Testis}$ ORF transgenes were expressed under

the same promoter and at comparable levels, we conclude that the TeNC domain is necessary for efficient caspase activation and spermatid individualization.

Figure 3.4 **[A]** Schematic structure of the rescue constructs for *cul3*$_{Testis}$ mutant male sterile flies. The constructs, *tr-cul3*$_{Testis}$ and *tr-cul3*$_{Soma}$ are composed of the *cullin3*$_{Testis}$ isoform's promoter region (dark blue, consists of the intronic sequences flanked by exons 2 and 1D) and 5' UTR (light blue) that were fused upstream of the coding regions (ORFs) of either *cullin3*$_{Testis}$ or *cullin3*$_{Soma}$ followed by the 3' UTR of *cullin3*$_{Testis}$. **[B-C]** Transcriptional expression from the transgenes was confirmed by RT–PCR analyses on RNA from testes of the indicated genotypes. The relative locations of the primers are indicated with black arrows in (A). 'RT+Taq' and 'Taq' indicate reactions with reverse transcriptase or without it, respectively, to control for possible genomic DNA contamination. **[B]** To differentiate between the *cullin3*$_{Testis}$ endogenous (endog.) and transgenic (transg.) cDNAs, we cleaved the RT-PCR fragments with XhoI, a unique restriction site in the transgene. Note that the RT-PCR product from *cullin3*^{mds1}; *tr-cullin3*$_{Testis}$ but not from wild-type testes was cleaved by XhoI, confirming its transgenic source. **[C]** Transgenic expression of *cullin3*$_{Soma}$ (*tr-cul3*$_{Soma}$) in adult testes. Note the absence of the endogenous *cullin3*$_{Testis}$ cDNA band and in contrast, the presence of the transgenic *cullin3*$_{Soma}$ band in *cullin3*^{mds1}; *tr-cul3*$_{Soma}$/+ testes. **[D-I]** Testes stained for cleaved caspase-3 (green) and ICs (Phalloidin, red). **[D]** Mutant spermatids for *cullin3*$_{Testis}$ manifest a block in caspase activation and spermatid individualization. **[E]** Either one or **[F]** two copies of transgenic *cullin3*$_{Testis}$ (*tr-cul3*$_{Testis}$) restored caspase activation, spermatid individualization, and fertility of *cul3*^{mds1} mutant male flies. **[G]** Wild-type control testes. Note the CBs and WBs (green oval structures). **[H-I]** In contrast, dramatically reduced cleaved-caspase3-positive cysts were found in *cullin3*^{mds1} mutants which ectopically express **[H]** one or **[I]** two copies of the *cullin3*$_{Soma}$ transgene (*tr-cul3*$_{Soma}$). These spermatids failed to individualize, no CBs and WBs were detected and the males were sterile. Scale bars 200 μm.

Figure 3.4 *cullin3*$_{Testis}$ but not *cullin3*$_{Soma}$ can restore caspase activation and spermatid individualization to *cullin3*$_{Testis}$ null mutants

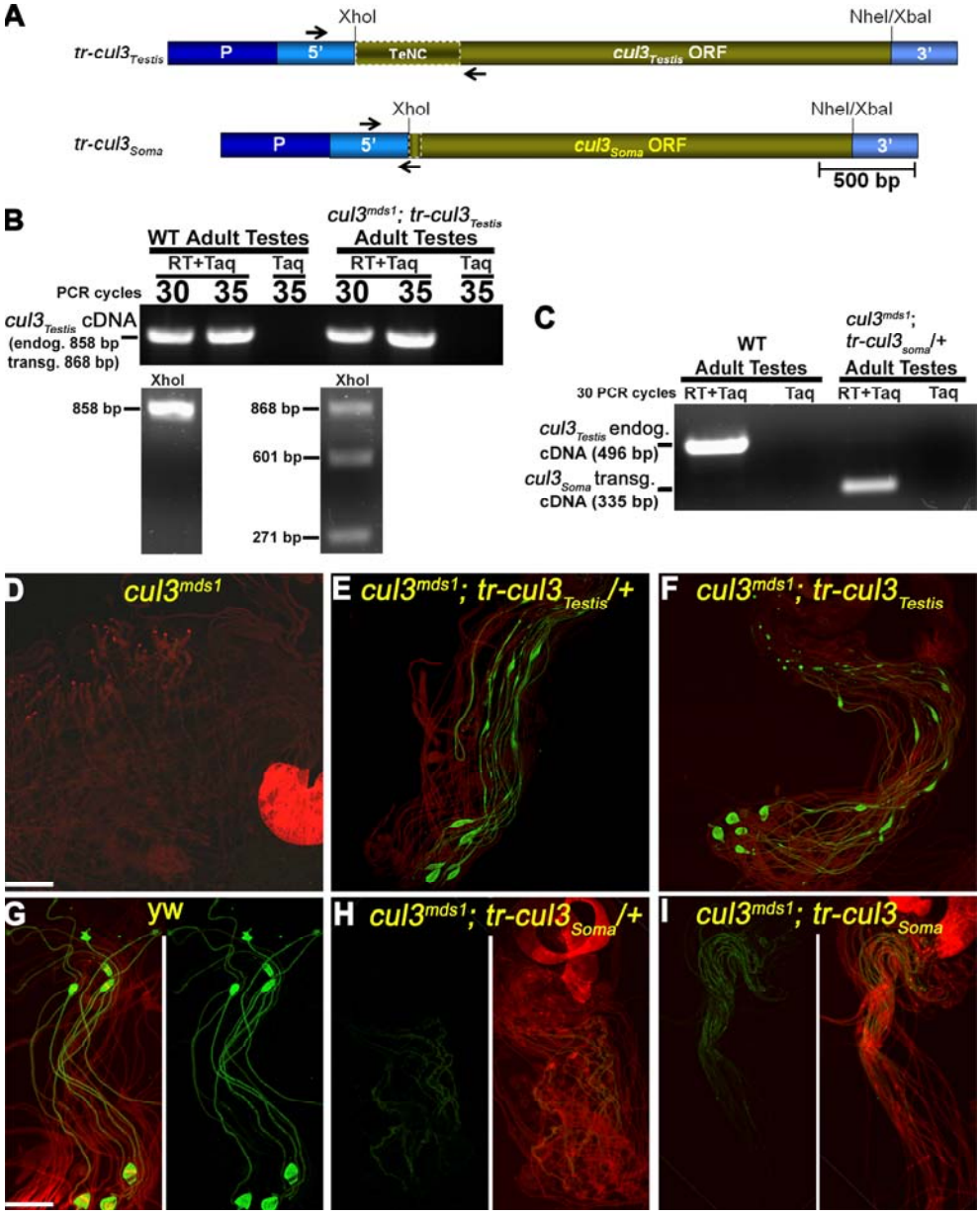

3.3.5 *roc1b* genetically interacts with c*ul3*$_{Testis}$ to facilitate effector caspase activation

Cullins contain a C-terminal cullin homology domain (CHD) that can bind small RING domain proteins, which in turn recruit a ubiquitin-conjugating enzyme (E2) to generate the catalytic module {Petroski, 2005 #220}(Cardozo and Pagano, 2004; Pintard et al., 2004). The *Drosophila* genome contains three small RING domain proteins, Roc1a, Roc1b, and Roc2, all of which are capable of activating ubiquitin conjugation *in vitro* (Noureddine et al., 2002). Loss of Roc1a function causes lethality, and targeted disruption of *roc1b* was previously reported to cause male sterility (Donaldson et al., 2004; Noureddine et al., 2002). Furthermore, Cullin-3 preferentially co-immunoprecipitates with Roc1b, indicating that both proteins form a complex (Donaldson et al., 2004). We therefore examined whether loss of *roc1b* function affects caspase activation and individualization of spermatids. We found that *roc1b*^{dc3} mutant spermatids displayed reduced levels of cleaved-caspase3 staining and failed to individualize (Figure 3.5A). To test whether *roc1b* genetically interacts with *cul3*$_{Testis}$, we generated double mutants between *roc1b*^{dc3} and the hypomorphic *cul3*^{mds} alleles. Homozygous mutants for either *cul3*^{mds} or *roc1b*^{dc3} showed moderate levels of cleaved-caspase3 staining (Figures 3.1E-G and Figure 3.5B). In contrast, cleaved-caspase3 staining was completely abolished in spermatids of the double mutants, demonstrating that *cul3*$_{Testis}$ genetically interacts with *roc1b* to promote caspase activation in spermatids (Figure 3.5C). These results support the idea that Roc1b is a functionally relevant partner of Cullin-3 *in vivo*.

Figure 3.5 Double mutants for *cullin3*$_{Testis}$ and *roc1b* block caspase activation during spermatid differentiation

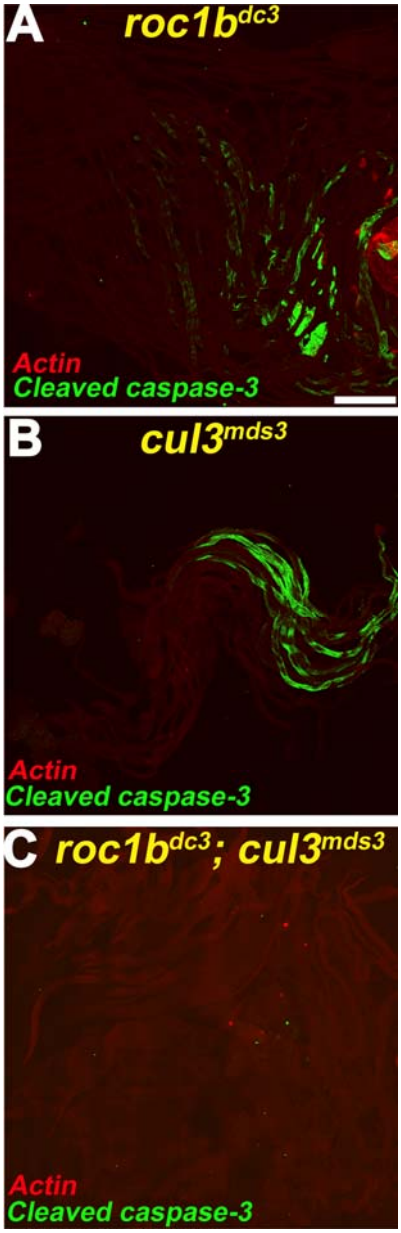

Figure 3.5 **[A-C]** Testes stained for cleaved caspase-3 (green) and spermatid's tail (Phalloidin, red). **[A]** Spermatids in *roc1b* mutant flies display severe individualization defects and still display some levels of cleaved-caspase3 staining. **[B]** Similarly, spermatids in flies homozygous for weak *cullin3*$_{Testis}$ alleles, such as *cullin3*^{mds3}, also display some level of cleaved-caspase3 staining. **[C]** However, spermatids mutants for both *roc1b* and *cullin3*$_{Testis}$ manifest a complete block in caspase activation during individualization.

3.3.6 $Cul3_{Testis}$ preferentially interacts with the BTB-domain protein Klhl10 in yeast

Cullin-3-dependent E3 ligases use BTB domain containing proteins for substrate recognition (Geyer et al., 2003; Pintard et al., 2004; Xu et al., 2003). The number of genes encoding BTB domain containing proteins is very large, with an estimated 140-250 proteins in *Drosophila* (Petroski and Deshaies, 2005; Pintard et al., 2004). We performed a yeast two hybrid (Y2H) screen using the coding region of $Cul3_{Testis}$ as bait to identify potential protein partners for $Cul3_{Testis}$ in a library of adult *Drosophila* cDNAs (Figure 3.6). Several cDNA clones which encode for *Drosophila* orthologues of three BTB domain containing proteins, Spop (CG9924), Ipp (CG9426), and Klhl10 (CG12423) were isolated in this screen (Figure 3.6). Notably, both mouse Klhl10, which shares 46% identity with its *Drosophila* counterpart, and mouse Spop as well as *Drosophila* Spop were previously shown to interact with Cullin-3 (Hernandez-Munoz et al., 2005; Kwon et al., 2006; Wang et al., 2006; Xu et al., 2003). Given our previous results implicating the TeNC domain in $Cul3_{Testis}$ function, we asked whether any of these proteins bind preferentially to this domain. For this, we examined interactions between these BTB domain containing proteins and $Cul3_{Testis}$, $Cul3_{Soma}$ or the TeNC domain alone in two different yeast strains. Whereas Spop and Ipp interacted with either $Cul3_{Testis}$ or $Cul3_{Soma}$, Klhl10 interacted with $Cul3_{Testis}$ only (Figures 3.6A and 3.6B). However, the TeNC domain alone was not able to bind to any of the BTB domain containing proteins in this assay. We conclude that the TeNC domain is required but not sufficient for BTB protein binding. These results identify Klhl10 as a potential partner of $Cul3_{Testis}$ in spermatids.

Figure 3.6 Klhl10, a BTB and Kelch domains protein, preferentially interacts with Cullin3$_{Testis}$ and not with Cullin3$_{Soma}$

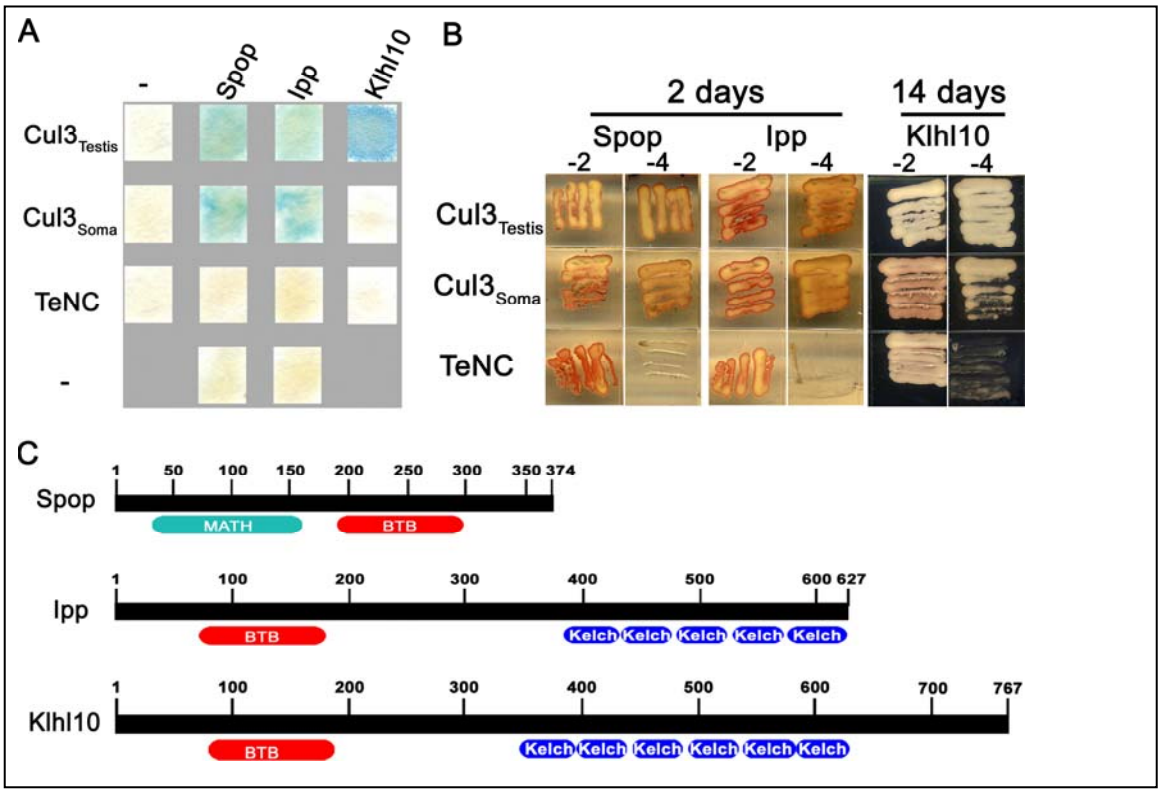

Figure 3.6 **[A]** Three BTB-domain proteins, the *Drosophila* orthologues of Spop, Ipp, and Klhl10, were found to interact with Cullin3$_{Testis}$ in a yeast-two-hybrid screen. β-galactosidase filter assay demonstrates that whereas Spop and Ipp can also interact with Cullin3$_{Soma}$, Klhl10 only interacts with Cullin3$_{Testis}$. While the TeNC domain of Cullin3$_{Testis}$ is required for this interaction, it is not sufficient to mediate the interaction with Klhl10. **[B]** Similarly, in a nutrient-omitted medium assay, yeasts with both Cullin3$_{Testis}$ and Klhl10 grew rapidly (2 days) on plates that lacked, in addition to leucine and tryptophan (-2), also histidine and adenine (-4 plates). However, yeast with Klhl10 and Cullin3$_{Soma}$ grew very poorly on -4 plates. Even after two weeks of incubation the colony is only partially established. Note that the results for the auxotrophy rescue of Klhl10 are shown not after 2 days but rather after 14 days in order to reflect the weak interaction between Klhl10 and Cullin3$_{Soma}$. **[C]** Schematic representations of Spop, Ipp and Klhl10, and the relative locations of their major domains. The BTB-domains of all these proteins are sufficient for binding to Cullin-3.

3.3.7 Mutations in *klhl10* abrogate effector caspase activation during spermatid individualization

If Klhl10 is indeed a physiologically relevant Cullin-3 binding-partner *in vivo*, mutations in *klhl10* should affect the function of this E3 complex and thus block caspase activation. To test this hypothesis, we searched for loss-of-function mutations in this gene. Genetic analysis of the *klhl10* gene is complicated due to its position within a heterochromatic, cytologically unmapped portion on the 2nd chromosome. However, we were able to identify seven *klhl10* alleles (*klhl10*$^{1\text{-}7}$) in our collection of cleaved-caspase3-defective mutants. All alleles were defective in spermatid individualization and recessive male-sterile, failed to complement each other, lacked cleaved-caspase3 staining but were AXO 49-positive (Figures 3.7A-F, see chapter 2). This phenotype is virtually identical to the loss of Cul3$_{Testis}$ function. By using RT-PCR and sequence analyses we identified mutations in six of these *klhl10* alleles (Figures 3.7I and 3.7J). Five of these alleles, *klhl10*$^{2\text{-}6}$ (Zuker lines # *Z2-1331 (ms266)*, *Z2-0960 (ms311)*, *Z2-2739 (ms374)*, *Z2-3284 (ms396)*, *Z2-4385 (ms462)*) have mutations in highly conserved amino acids of the Kelch repeats, a domain that mediates interaction with the substrate (colored stars and amino-acid residues in Figures 3.7I and 3.7J, respectively) A sixth mutation, *klhl10*^{7} (*Z2-3353, ms961*) contains a G508 to A transversion that converts a highly conserved alanine (A170) to threonine in the BTB domain (grey star in Figure 3.7I). No mutations were identified in the ORF of *klhl10*^{1} (*Z2-1827, ms61*), suggesting that this allele carries a mutation in a regulatory region. To prove that these mutations are indeed responsible for the observed phenotypes, we conducted transgenic rescue experiments. Expression of the *klhl10* coding region under the control of the *cul3*$_{Testis}$ promoter (together with *cul3*$_{Testis}$ 5'

and 3' UTRs, see Materials and Methods) completely restored cleaved-caspase3 staining and rescued all the sterility phenotypes associated with *klhl10* mutant alleles (Figures 3.7G and 3.7H). Collectively, these results suggest that $Cul3_{Testis}$ interacts functionally and physically with Roc1b and Klhl10 to promote caspase activation and spermatid individualization in *Drosophila*.

Figure 3.7 **[A-H]** Visualization of active effector caspase with anti-cleaved caspase-3 antibody (green) and (A-F) axonemal tubulin polyglycylation with anti-glycylated tubulin monoclonal antibody (AXO 49; red) or (G-H) F-actin, which stains the ICs and the spermatids' tails (phalloidin; red). These figures are composed of combined green and red layers. **[A]** Wild-type individualizing spermatids positively stain for cleaved caspase-3 and polyglycylated axonemal tubulin. **[B-F]** In a variety of *klhl10* alleles, elongated spermatids stain for polyglycylation but not for cleaved caspase-3. **[G-H]** Transgenic *klhl10* construct (*tr-klhl10*, composed of $cullin3_{Testis}$ promoter and 5' UTR, *klhl10* coding region, and $cullin3_{Testis}$ 3' UTR) restores caspase activation, spermatid individualization, and fertility to *klhl10* mutant male flies. **[I]** Schematic representation of the Klhl10 protein. The relative locations of the BTB, BACK and Kelch domains are depicted by thick bars. Different colored stars depict the locations of the different mutations, and the colors correspond to the colored amino-acids in **[J]**. The molecular nature of the mutations and their color code are as follows: $klhl10^{2}$ (*Z2-1331*) carries a G1801 to A transversion that converts glutamic acid (E601, red) to lysine at repeat VI, $klhl10^{3}$ (*Z2-0960*) carries a G1119 to A transversion that converts tryptophan (W373, purple) to stop codon, resulting in a deletion of most of the Kelch domain, $klhl10^{4}$ (*Z2-2739*) carries a C1237 to T transversion that converts arginine (R413, yellow) to stop codon, which also deletes most of the Kelch repeats, $klhl10^{5}$ (*Z2-3284*) carries a G1486 to A transversion that converts glycine (G496, blue) to arginine at repeat IV, and $klhl10^{6}$ (*Z2-4385*) carries a C1439 to T transversion that converts serine (S480, green) to phenylalanine at repeat IV. On the other hand, $klhl10^{7}$ (*Z2-3353*) carries a G508 to A transversion that converts a highly conserved alanine (A170) to threonine in the BTB domain (grey star). **[J]** Alignment of the six Kelch repeats of Klhl10. The alignment is based on the crystal structure of the Keap1 Kelch domain which folds into a β-propeller structure with six blades. The residue range for each blade is indicated at the left. The four conserved β-strands in each blade are indicated above the sequences by arrows. Residues conserved in all six blades are highlighted with dark grey and appear in upper case in the consensus line, while residues that are conserved in at least three blades appear in lower case. Any two and above conserved residues are highlighted with light grey. Color highlighted residues are mutated in the various *klhl10* alleles and correspond to the stars in (I).

Figure 3.7 Mutations in *klhl10* block caspase activation and spermatid individualization, but not axonemal tubulin polyglycylation

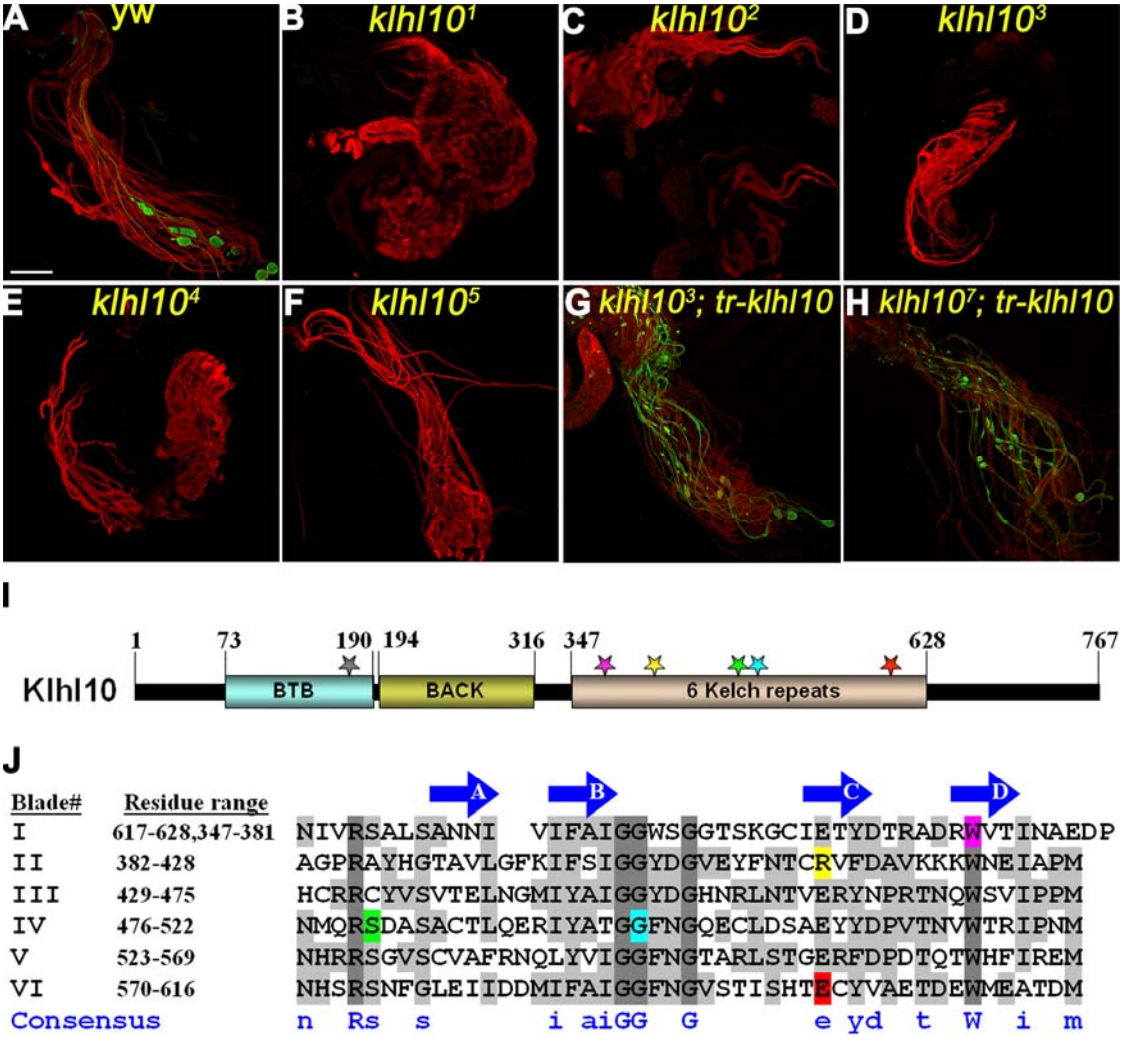

3.3.8 Elevated level of ubiquitinated protein expression in individualizing spermatids requires an intact Cul3-Roc1b-Klhl10 complex

Our results suggest that a Cul3-Roc1b-Klhl10 E3 ubiquitin ligase complex functions at the onset of spermatid individualization. To explore this further, we investigated the level and spatio-termporal distribution of ubiquitinated proteins during spermatid individualization, and the consequences of loss of Cul3 and Klhl10 function on this pattern. For this purpose, we stained wild-type testes with the FK2 monoclonal antibody, which specifically detects ubiquitin conjugated proteins but not free ubiquitin. At the onset of individualization, a steep gradient of ubiquitinated protein expression is detected from the nuclear heads of the spermatids to the tips of their tails (yellow arrows in Figure 3.8A). During the caudal translocation of the IC, ubiquitinated proteins became completely depleted from the newly individualized portion of the spermatids (the region that is flanked by a white arrowhead and a white arrow in Figure 3.8A). The staining remained abundant, however, in the pre-individualized portion of the spermatids, with the highest levels seen in the cystic bulge (CB; Figures 3.8A-C). At the end of individualization, the newly formed waste bag (WB) contained high levels of ubiquitinated proteins (Figure 3.8D). This spatiotemporal pattern of protein ubiquitination is very similar to the distribution of active effector caspase. This striking correlation supports the idea that protein ubiquitination facilitates effector caspase activation in individualizing spermatids. Next, to test whether the observed ubiquitination process depends on an intact Cul3-Klhl10 complex, we stained $cul3_{Testis}$ and *klhl10* mutant spermatids with the FK2 antibody. The overall level of protein ubiquitination was dramatically decreased in elongated spermatids from both mutants

(Figures 3.8E and 3.8F). Furthermore, this reduction was specific to late elongated spermatids, because protein ubiquitination during early stages of spermatid maturation was not significantly affected in *cul3*$_{Testis}$ mutant and *klhl10* mutant flies (Figures 3.8G-I). These results show that protein ubiquitination during spermatid individualization is largely mediated by the Cul3-Klhl10 complex. Therefore, we conclude that the Cul3-Roc1b-Klhl10 complex is functionally active as an E3 ubiquitin ligase to promote protein ubiquitination during spermatid individualization.

Figure 3.8 The Cullin3-Roc1b-Klhl10 complex promotes protein ubiquitination during spermatid individualization

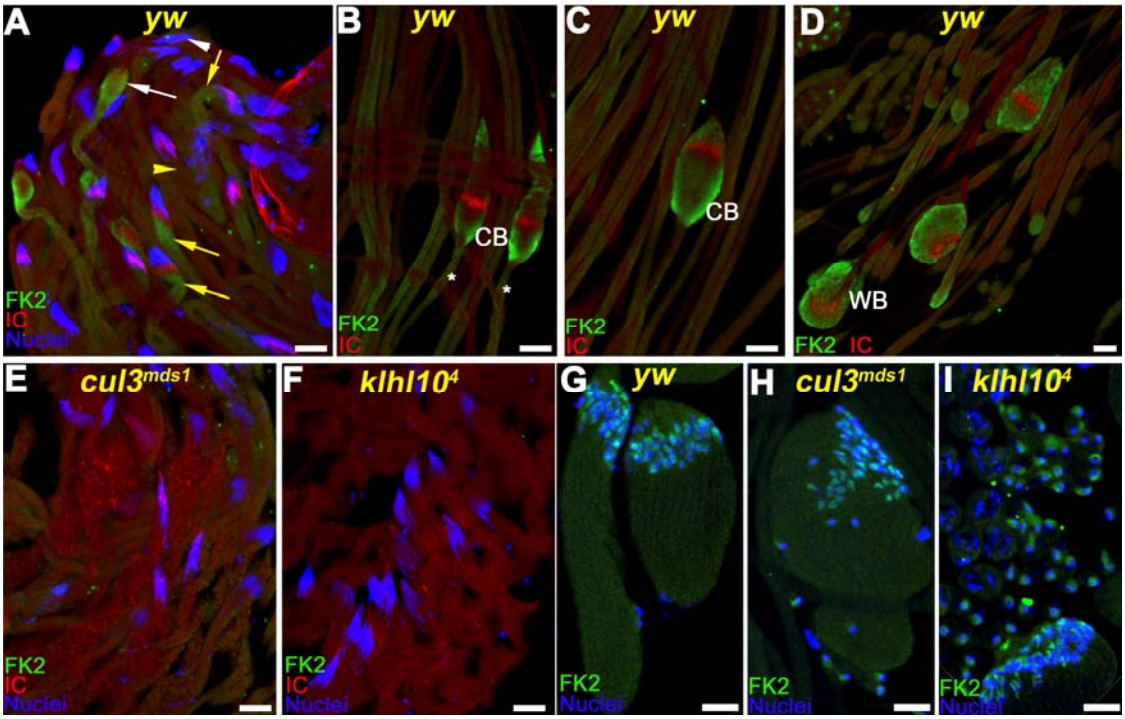

Figure 3.8 Testes were stained with the anti-multi ubiquitin monoclonal antibody (FK2) that detects ubiquitinated proteins (green), phalloidin which marks the individualization complex (IC, red), and DAPI to visualize the nuclei (blue). **[A]** Before the formation of an IC, very low levels of ubiquitinated proteins are detected (yellow arrowhead). Once a mature IC is assembled in the vicinity of the nuclei, a steep gradient of ubiquitinated protein staining is detected from the very bottom of the nuclei to the tip of the spermatids' tails (yellow arrows). After the caudal translocation of the IC, ubiquitinated proteins are no longer detectable in the post-individualized portion of the spermatids (the region between the nuclei, indicated by a white arrowhead, and an early CB, indicated by a white arrow). **[B-C]** When the bulk cytoplasm of the spermatids accumulates in a cystic bulge (CB), ubiquitinated proteins are prominent within the CB and the pre-individualized region (white asterisks). **[D]** Once all the cytoplasm is stripped away, ubiquitinated proteins are detectable only in the waste bag (WB). **[E]** and **[F]** Elongated spermatids from either *cullin3*^{mds1} or *klhl10*^{4} mutants, respectively, did not stain for ubiquitinated proteins. **[G]** Protein ubiquitination is detected in nuclei of early elongating spermatids. **[H]** and **[I]** The pattern of protein ubiquitination at earlier stages of spermatid maturation is not affected in *cullin3*^{mds1} and *klhl10*^{4} mutants. Scale bars 100 μm.

3.3.9 dBruce, a Giant IAP-like protein, can bind the substrate-recognition protein Klhl10

Our results suggest a simple working model in which the Cul3-Roc1b-Klhl10 complex promotes caspase activation via ubiquitination and degradation of a caspase inhibitor (Figure 6.1A). The best-characterized family of endogenous caspase inhibitors is the IAP family (Salvesen and Duckett, 2002; Singer et al., 1999). Diap1 is essential for the survival of most, if not all somatic cells (Steller, 2008) (Bader and Steller, 2009). However, it appears that Diap1 is not the major caspase inhibitor in this context. If Diap1 was a substrate for Cullin-3–mediated protein degradation, we would have expected to see an increase of this protein in cul3 mutants. However, no significant differences in Diap1 protein levels between wild-type and $cul3_{Testis}$ and *klhl10* mutant testes were detected (Figure 3.9A). Another candidate is the giant, 4852 amino acid-long, IAP-like protein, dBruce. dBruce function is necessary to protect sperm against unwanted caspase activity, because loss of *dbruce* function causes degeneration of spermatid nuclei and male sterility (Arama et al., 2003; Goyal et al., 2000). To further investigate possible interactions between dBruce and the Cul3-Roc1b-Klhl10 complex, we tested whether the substrate recruitment protein Klhl10 can bind to dBruce. For this purpose, we expressed tagged versions of Klhl10 and portions of dBruce in S2 cells and performed co-immunoprecipitation (co-IP) experiments (Figure 3.9B and 3.9C). In this system, Klhl10 efficiently immunoprecipitated both a dBruce ‘‘mini gene’’ (consisting of the first N-terminal 1,622 amino acids, including the BIR domain, and the last C’ terminal 446 amino acids that contain the UBC domain; Figure 3.9B). Furthermore, a tagged peptide with the first N-terminal 387 amino acids of dBruce that includes the BIR domain (amino

acids 251–321) is sufficient to bind to Klhl10 in this assay (Figure 3.9C). These data are consistent with the idea that dBruce is a substrate for the Cullin-3-based E3-ligase complex.

Figure 3.9. Diap1 levels are not affected in the absence of the functional Cullin3-Roc1b-Klhl10 complex, but dBruce can interact with the substrate recruitment protein Klhl10 in S2 cells

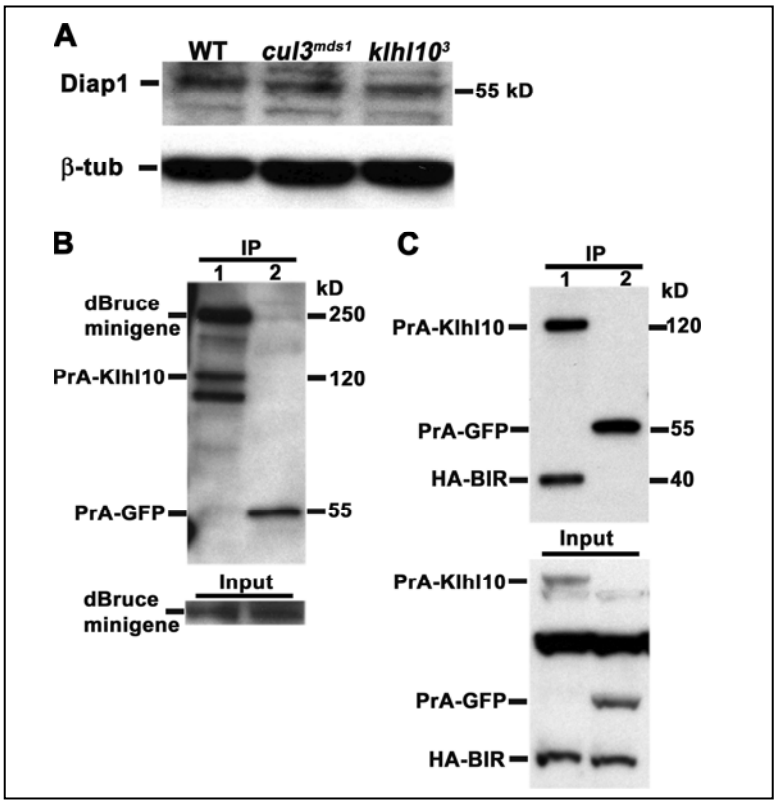

Figure 3.9 **[A]** Diap1 protein levels were not affected in *cul3*^{mds1} and *klhl*^{103} mutant testes, as assessed by Western blotting of protein extracts from dissected testes. Therefore, Diap1 does not appear to be a major target for the Cullin3-based E3-ligase complex. β-tubulin protein levels served as loading control. **[B-C]** Co-IP experiment in S2 cells indicate that Klhl10 can bind to the BIR domain of dBruce. The immunoprecipitate (IP) is shown at the top, and pre-incubation of whole lysates are shown at the bottom (Input). Cell lysates were incubated with IgG beads which bind to Protein A (PrA). For Western blotting of IPs, **[B]** anti-dBruce antibody or **[C]** anti-HA antibody were used. **[B]** Cells were co-transfected with a *dBruce* ‘‘mini gene’’ (consisting of the first N-terminal 1,622 amino acids, including the BIR domain, and the last C-terminal 446 amino acids that contain the UBC domain) and (lane 1) PrA-klhl10 or (lane 2) PrA-GFP **[C]** Cells were co-transfected with HA-tagged dBruce-BIR peptide containing the first N-terminal 387 amino acids of dBruce that includes the BIR domain region (amino acids 251–321). This motif is sufficient to bind to Klhl10 in S2 cells.

3.4 Materials and Methods

Fly Strains and Expression Vectors

yw flies were used as wild-type controls. The Zuker mutants *Z2-1089* (*ms282, cul3*^{mds1}), *Z2-4870* (*cul3*^{mds2}), *Z2-4061* (*cul3*^{mds3}), *Z2-1270* (*cul3*^{mds4}), *Z2-1062* (*cul3*^{mds5}), *Z2-1827* (*ms61, klhl10*^{1}), *Z2-1331* (*ms266, klhl10*^{2}), *Z2-0960* (*ms311, klhl10*^{3}), *Z2-2739* (*ms374, klhl10*^{4}), *Z2-3284* (*ms396, klhl10*^{5}), *Z2-4385* (*ms462, klhl10*^{6}), and *Z2-3353* (*ms961, klhl10*^{7}) were obtained from C.S. Zuker (University of California at San Diego), the *gft* mutants *cul3*^{gft1}, *cul3*^{gft2}, *cul3*^{gft3}, *cul3*^{gft4}, *cul3*^{gftGR18}, and *cul3*^{gftd577} from M. Ashburner (University of Cambridge, UK), the *osk*$^{[301]}$/TM3 and *osk*$^{[CE4]/}$TM3 lines from R. Lehmann (Skirball Institute, NYU School of Medicine, NY), *roc1b*^{dc3} from R.J. Duronio (University of North Carolina at Chapel Hill, NC), the deficiency lines *DF*(2L)ED3 from the Bloomington Stock Center, and the deficiency line *DF*(2L)Exel8034 from Exelixis. The following BDGP's *cul3*$_{Testis}$ EST clones AT08710, AT10339, AT08501, AT07783, AT21182, AT19493, and AT03216 and the *cul3*$_{Soma}$ EST clones SD20020 and RE58323 were either completely or partially sequenced and some of them were used as templates in PCR reactions for subcloning.

The *tr-cul3*$_{Testis}$ and *tr-cul3*$_{Soma}$ rescue constructs were generated as follows: a 979 bp fragment of the presumed promoter region and 5' UTR and a 345 bp fragment from the 3' UTR of *cul3*$_{Testis}$ were PCR amplified from genomic DNA (forward primer CACATTGGAGCATCGTTAAA and reverse primer GAGATTGCTACGCTGGTCCA with added *Nsi*I and *Stu*I restriction sites, respectively) and the BDGP's EST clone AT07783 (forward primer GGCCCACAAAAAGTAGCA and reverse primer

AGAGAATATCAAGAAATATATTAGAGGG with added *Nhe*I and *Acc*65I restriction sites, respectively), were subcloned in a sequential order into the *Pst*I + *Stu*I and *Spe*I + *Acc*65I sites, respectively, of the CaSpeR-4 vector (from V. Pirrotta). Subsequently, the complete coding regions of $cul3_{Testis}$ (a 2817 bp fragment) and $cul3_{Soma}$ (a 2336 bp fragment) were PCR amplified from the BDGP's EST clones AT07783 (using the forward primer ATGCAAGGCCGCGATCCCCG and reverse primer TTAGGCCAAGTAGTTGTACA with added *Xho*I and *Nhe*I restriction sites, respectively) and SD20020 (using forward primer ATGAATCTGCGGGGAAATCC and reverse primer TTAGGCCAAGTAGTTGTACA with added *Xho*I and *Nhe*I restriction sites, respectively), and ligated into the *Xho*I and *Xba*I restrictions sites between the $cul3_{Testis}$ 5' and 3' UTRs within the CaSpeR-4 vector, to generate *tr-*$cul3_{Testis}$ and *tr-*$cul3_{Soma,}$ respectively.

To generate the *tr-klhl10* rescue construct, the ORF of *klhl10* (a 2320 bp fragment) was PCR amplified from the BDGP's EST clone AT19737 (using the forward primer ATGAGTCGTAATCAAAACG and reverse primer CTATGTACGACGACGAATTT with added *Sal*I and *Xba*I restriction sites, respectively), and ligated into the *Xho*I and *Xba*I restriction sites between the $cul3_{Testis}$ 5' and 3' UTRs within the above vector.

Standard *Drosophila* techniques were used to generate transgenic lines from these constructs.

Antibody Staining

Cleaved effector caspase antibody staining of young (0-2 day old) adult testes was carried out as described in chapter 2. The mouse anti-multi Ubiquitin monoclonal antibody (FK2, Stressgen) was used at a dilution of 1:100.

Isolation of Genomic DNA and Sequencing of the Mutant Alleles

Genomic DNA was isolated from 25-50 adult flies using the High Pure PCR Template Preparation Kit (Roche). Two µg of genomic DNA were used to amplify overlapping fragments from the *cullin-3* or *klhl10* loci in wild-type and homozygote mutant lines. PCR reactions were carried out using DyNAzyme EXT DNA polymerase (Finnzymes), according to the manufacturer instructions. The products were purified using the High Pure PCR Product Purification Kit (Roche), concentrated by evaporation, and sequenced in a GENEWIZ sequencing facility.

DEVDase Activity Assay

180 testes were dissected from newly eclosed wild-type or $cul3^{mds1}$ homozygote males, collected into 0.5 µl standard skirted tubes (Fisherbrand #05-669-25), standing on ice and containing 70 µl of testis buffer (10 mM Tris-HCl [pH 6.8], 183 mM KCl, 47 mM NaCl, 1mM EDTA, and 1mM PMSF), homogenized using a Pellet Pestle Motor (Kontes), and subsequently transferred into three new tubes (30:30:10 µl). The tubes with the 10 µl of the testes extracts were used for Western blot analysis to control for equal protein concentration by probing with anti-β-tubulin antibody (E7; 1:1000; Hybridoma Bank). Either Z-VAD (20 µM final concentration; Enzyme Systems Products) or DMSO was added to each of the 30 µl tubes, and the samples were transferred to a 96 well assay white plate (Costar #3610, Corning Inc), and allowed to incubate for 10 min at RT.

Caspase-Glo 3/7 reagent (Promega) was added to a final volume of 200 µl and the signal was detected with a multiwell plate reader (SPECTRA max M2, Molecular Devices). Luminescence readings were obtained every two minutes; therefore, each time interval in the figure represents an average of five readings. These experiments were repeated three times with similar results.

RNA isolation and RT–PCR

Total RNA was extracted by using the Micro-to-Midi Total RNA Purification System (Invitrogen) according to the manufacturer'srecommendations. 10–20 young adult testes or male reproductive tracts and 10 adult females were used to obtain enough RNA for 5–10 RT–PCR reactions. The samples were collected into 1.5 ml Eppendorf tubes, standing on ice and containing 300 µl of the Invitrogen kit's lysis buffer and 3 µl of 2-mercaptoethanol, homogenized using a Pellet Pestle Motor (Kontes), and subsequently purified using the same kit. In cases when the genomic DNA had to be removed, the 30 µl of the RNA was incubated with 4 µl of RQ1 DNase and 3.8 µl of appropriate buffer (Promega) for 1.5 h at 37°C, and subsequently purified again with the Invitrogen kit. The RNA was stored in -80°C or immediately utilized for RT–PCR reactions using the SuperScriptTM III One-Step RT–PCR System with Platinums Taq DNA polymerase (Invitrogen). The Mastercycler Gradient PCR machine (Eppendorf) was programmed as follows: 50°C for 30 min for the RT step followed by 94°C for 2 min, and the amplification steps of 94°C for 30 s, 60°C for 30 s, 68°C for 1 min. A master-mix was prepared and aliquoted to five tubes, each of which was amplified for 17, 20, 25, 30, or 35 cycles. Absence of genomic DNA in RNA preparations was verified by replacing the RT/Taq mix with only Taq DNA polymerase (Invitrogen). The comparative RT–PCR

reactions in Figure 3 were performed using two pairs of primers in a same reaction mix: For cul3Testis, the forward primer TCTCATGCAAGGCCGCGATC and the reverse primer CGGGTTATTGGCTGGCGGTC amplified a 2997 bp cDNA fragment (and a 3715 bp genomic fragment), while for cul3Soma, the forward primer CATTGATTGCCGCCGAGGAA and the reverse primer CGGGTTATTGGCTGGCGGTC amplified a 2642 bp cDNA fragment (and a 4911 bp genomic fragment).

For amplification of the 868 bp fragment of the transgenic tr-cul3Testis (and the 858 bp endogenous fragment) in Figure 4B, the forward primer GAGACCCGAATCGCGAGTAG and the reverse primer GCATTCTTTAAGCTGGCCCA were used. For amplification of the 335 bp fragment of the transgenic *tr-cul3*$_{Soma}$ in Figure 4C, the forward primer GAGACCCGAATCGCGAGTAG (specific for *cul3*$_{Testis}$ promoter) and the reverse primer CATTTTGCCCTCCTTCTTGG (specific for *cul3*$_{Soma}$) were used. To simultaneously amplify a 496 bp fragment of the endogenous *cul3*$_{Testis}$ the reverse primer GGAGGCGTTGGGCACATTGA was also used in the same reaction.

For amplification of the 538 bp fragment from *drice* mRNA in figure S5A, the forward primer GCCCACCTTGAAGTCTCGCG and the reverse primer CAGGATGTCCAGCCGCTTGC were used. For amplification of the 527 bp fragment from *dronc* mRNA in Figure S5B, the forward primer CCACCGCCTATAACCTGCTG and the reverse primer CTGCACATACGACGAGGAGG were used.

Plasmid Construction, Yeast Strains and cDNA Library Screening

The $Cul3_{Testis}$ and $Cul3_{Soma}$ "bait" constructs were generated as follows: a 2817 bp fragment containing the entire $Cul3_{Testis}$ coding region was PCR amplified from the BDGP's EST clone AT19493 (forward primer CAAGGCCGCGATCCCCG and reverse primer TTAGGCCAAGTAGTTGTACA with added *Eco*RI and *Pst*I restriction sites, respectively), and a 2336 bp fragment containing the entire $Cul3_{Soma}$ coding region was PCR amplified from the BDGP's EST clone SD20020 (forward primer AATCTGCGGGGAAATCCTC and reverse primer TTAGGCCAAGTAGTTGTACA with added *Eco*RI and *Pst*I restriction sites, respectively), and were both subcloned in frame to the GAL4 DNA binding domain using the *Eco*RI and *Pst*I sites of the pGBKT7 vector (Matchmaker, Clontech). For the TeNC domain "bait" construct, a 600 bp fragment containing the entire TeNC ORF was PCR amplified from wild-type genomic DNA (forward primer CAAGGCCGCGATCCCCG and reverse primer GGGATATTAAGACTTTCGCT with added *Eco*RI and *Bgl*II restriction sites, respectively), and subcloned in frame to the GAL4 DNA binding domain using the *Eco*RI and *Bam*HI sites of the pGBKT7 vector (Matchmaker, Clontech).

Two-hybrid screen was performed using *Saccharomyces cerevisiae* strain AH109 and an adult *Drosophila* cDNA library (Matchmaker, Clontech). Selection was accomplished on synthetic complete medium lacking tryptophan, leucine and adenine for 3-7 days at 30°C. To test for LacZ activity, positive "prey" cDNA clones were isolated and transformed into the Y187 yeast strain, which was pre-transformed with the appropriate "bait" constructs.

The UAS-*dbruce* "mini gene" was generated as follows: a 5022 bp fragment encoding the N-terminal 1622 a.a. of dBruce (including the BIR domain) was cleaved by *Eco*RI and *Xho*I from the BDGP's EST clone LD31268 and subcloned into the *Eco*RI and *Xho*I sites of the pUASt vector to generate the UAS-*dbruce-5'* vector. Next, a 1990 bp fragment encoding the C-terminal 446 amino acids of dBruce (including the UBC domain) was cleaved with *Sal*I and *Xba*I from clone T1A-ClaI (originally identified as clone T1A in the T. Hazelrigg testis cDNA library by J. Agapite and was further cleaved with ClaI to remove the first 357 bp and then self ligated), and subcloned in frame into the XhoI and XbaI sites of the UAS-*dbruce-5'* vector to generate the UAS-*dbruce* "mini gene" plasmid.

Western Blotting of Adult Testis, Antibodies, and Immunoprecipitation

40-60 testes from wild-type and mutant adult males were used to prepare extracts in 30 µl of cell lysis buffer (20 mM HEPES–KOH [pH 7.6], 150 mM NaCl, 10% glycerol, 1% Triton X-100, 2 mM EDTA, 1× protease inhibitor cocktail, and 1 mM DTT). Total protein was used for Western blot analysis using either mouse anti-CUL-3 (1:1,000; BD Transduction Laboratories, cat #611848) [102] or rabbit anti-Diap1 antibody [30].

To generate the anti-dBruce antibody, sequence encoding the C-terminal 446 amino acids of dBruce was cleaved from the T1A-ClaI cDNA clone (see above) using *Sal*I and *Xma*I and then cloned into the *Xho*I and *Xma*I sites of a derivative plasmid of the pET14b (Novagen). The expression plasmid was then transformed into BL21/DE3/pLys, followed by 2 hr IPTG induction to express His_6-dBruce-C-term. This protein was purified by nickel affinity chromatography and used to raise rat polyclonal antibody

(Covance). This antibody recognizes the dBruce "mini gene" band on a Western blot (1:1,000).

For immunoprecipitation reactions, S2 cells were co-transfected with Actin-*Gal4*, UAS-*PrA-klhl10*, and either UAS-*dbruce* "mini gene" or UAS-*HA-(dbruce)BIR* plasmids. For negative controls, S2 cells were co-transfected as above but with UAS-*PrA-GFP* instead of UAS-*PrA-klhl10*. Cells were lysed 48 h post-transfection and the extracts were then incubated with Protein A/G-agarose (Roche) at 4°C for 1.5 h. Bound proteins were eluted by boiling in 3 x SDS loading buffer and detected with anti-dBruce antibody (for the presence of dBruce "mini gene") or anti-HA antibody (for the presence of HA-(dBruce)BIR

4. A novel F-box protein is required for caspase activation during cellular remodeling in *Drosophila*[3]

4.1 Summary

In this chapter, I describe the mapping and characterization of another mutants we isolated in the screen. I show that *ms771* maps to a novel F-box protein that we termed Nutcracker, which is strictly required for caspase activation and sperm differentiation. Nutcracker interacts through its F-box domain with members of a Cullin-1-based ubiquitin ligase complex (SCF), Cullin-1 and SkpA. This ubiquitin ligase does not regulate the stability of the caspase inhibitors DIAP1 and DIAP2, but physically binds dBruce, a BIR containing giant protein involved in apoptosis regulation. Furthermore, *nutcracker* mutants disrupt proteasome activity without affecting their distribution. These findings define a new SCF complex required for caspase activation during sperm differentiation and highlight the role of regulated proteolysis during this process.

4.2 Introduction

The ability to rapidly degrade specific proteins as a way to control their function within larger protein networks is the primary advantage of the E3 ubiquitin ligase, and is thus a central participant in many cellular pathways (Broemer and Meier, 2009; Jesenberger and Jentsch, 2002; Nakayama and Nakayama, 2006) (Cardozo and Pagano, 2004; Hershko, 1997; Isaksson et al., 1996; Kipreos and Pagano, 2000). E3 ligases are

[3] Maya Bader wrote, conceived of and conducted the experiments in this chapter. Dr. Sigi Benjamin provided the Alpha6T-GFP immunoflourcense images in Figure 4.6.

classified into three types: the single-subunit RING containing protein (like Diap1 and XIAP), the multi-subunit RING containing, and the HECT-domain type (Cardozo and Pagano, 2004). Most of the multi-subunit RING ligases contain a cullin protein, as described in the previous chapter. The best characterized is the SCF (Skp-Cullin-F-box) ligase. In this complex, the cullin scaffolding subunit Cullin-1 simultaneously interacts at the amino terminus with the adaptor subunit Skp1 (S-phase-kinase-associated protein- 1) and at the carboxyl terminus with a RING protein (such as Roc1, Roc2, or Rbx1) and a specific E2-conjugase. Skp1, in turn, binds to one of many F-box proteins (Petroski and Deshaies, 2005; Willems et al., 2004). F-box proteins are the substrate binding proteins in this complex, and appear to associate with a discrete number of specific substrates through a protein–protein interaction domain (Kipreos and Pagano, 2000).

The protein-protein interaction domain has been used to further classify F-box proteins; those that contain a Leucine-Rich Repeat (LRR) are sometimes called FBLs (**F**-**B**ox-**L**RR), those that contains WD-40 domains, FBW (**F**-**B**ox-**W**D-40), and those that contain another or an unknown interaction domain, FBX or FBXO (for **F**-**B**oX **O**nly) (Cardozo and Pagano, 2004). F-box proteins are found in most eukaryotes, 11 in *S. cerevisiae*, 326 predicted in *C. elegans,* 22 in *Drosophila*, and at least 38 in humans, but the function of most is yet unknown (Kipreos and Pagano, 2000).

The abundance of these proteins in many genomes indicates that they participate in many cellular pathways. The best known function is in cell-cycle regulation, but F-box proteins have also been shown to play roles in cytoskeletal dynamics, as well as the degradation of cell-surface receptors, transcription-factor inhibitors, and non-cell-cycle transcription factors. In contrast, and although there is much evidence for the role of E3

ligases in apoptosis regulation (see chapter 1), there are not many examples of F-box proteins being involved in cell-death and caspase regulation. In *Drosophila*, mutations in the F-box protein Morgue have been shown to suppress Reaper and Grim induced cell death in the eye, and might mediate the degradation of Diap1 (Hays et al., 2002; Schreader et al., 2003; Wing et al., 2002). However, a direct role for Morgue in caspase regulation has not been shown, and it still not known whether it acts as an E3 or E2 in this system (this protein also contains a UBC domain that mediates E2-like activity).

Here, I describe a new ubiqutin-ligase complex that regulates caspase activity during sperm individualization. From the genetic screen, I isolated an F-box protein we called Nutcracker, which shares some sequence similarity with the mammalian FBXO7 protein. Flies mutant for *nutcracker* are viable but male sterile, displaying elongated spermatids with no activated caspases and severe individualization defects. I further show that Nutcracker physically interacts with SkpA and Cullin-1, two main components of an SCF ubiquitin ligase complex, and that the Nutcracker's F-box domain is important for both complex binding and caspase activation. Nutcracker can also associate with dBruce, a giant BIR and UBC domains containing IAP-like protein, indicating a direct link between this SCF complex and the apoptotic machinery. Finally, I show that loss of *nutcracker* function causes reduced proteasome activity without affecting proteasome distribution or numbers. These findings demonstrate the first role of an SCF ubiquitin-ligase complex in caspase activation and proteasome regulation, and they suggest that the involvement of controlled proteolysis in caspase activation is broader than has been previously appreciated.

4.3 Results

4.3.1 *ms771* is a male sterile mutant defective in caspase activation during sperm individualization.

We sought to characterize another mutant from our caspase activation screen. The mutant *ms771* is cleaved-caspase negative and polyglycylation positive, and is represented in our screen by a single allele. *ms771* is homozygote viable with no gross defects apart from male sterility (Figure 4.1A). Consistent with the idea that this mutant is specific for caspase activation, ultrastructural analysis portrayed morphologically intact mitochondria and axoneme, albeit some vacuolar structures are detected, indicating individualization defects (Figure 4.1B).

Figure 4.1: *ms771* is a male sterile mutant defective in caspase activity during sperm differentiation

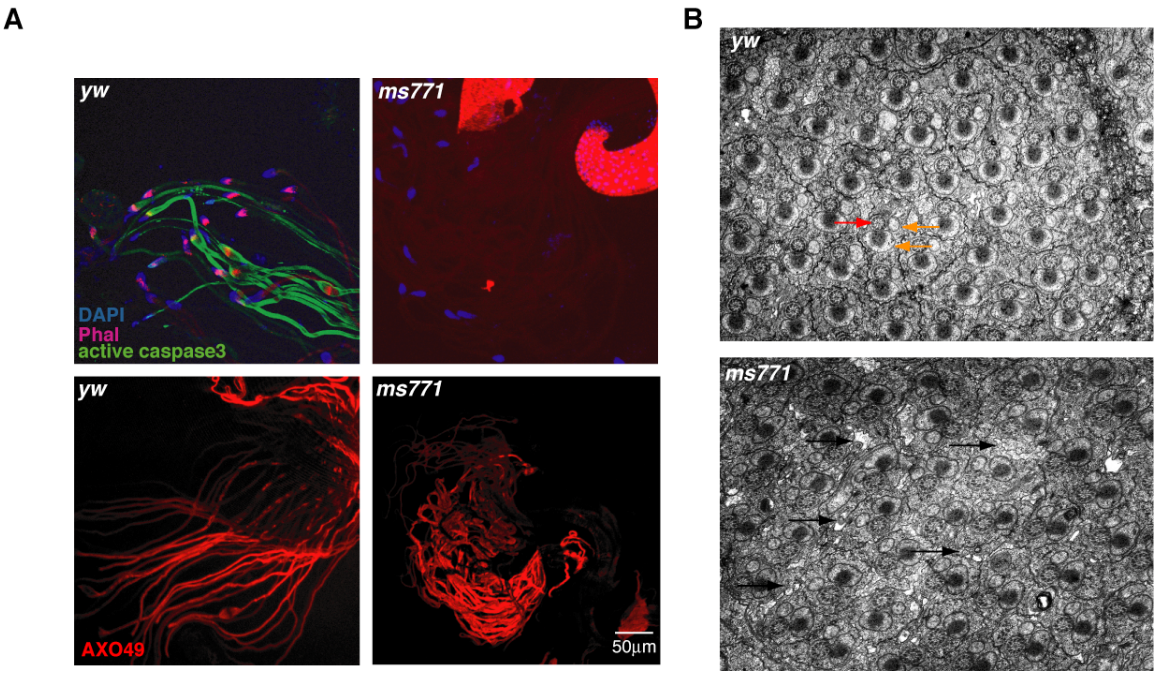

Figure 4.1 **[A]** *ms771* mutant testes fail to stain for active-caspases-3 (green). As opposed to cysts from *yw* testes, cysts from *ms771* homozygote males do not stain for cleaved-caspase3. The mutant nuclei elongate, but the IC does not form. Like the wild-type, *ms771* cysts stain positively for AXO49 (red), a late differentiation marker, indicating that these deficiencies are not caused by a global differentiation defect. **[B]** Electron micrograph (EM) images of cysts during individualization. Each spermatid within the cyst contains an axoneme (red arrow) and two mitochondrial derivatives (smaller and larger round structures, orange arrows). The *ms771* mutant displays normal formation of these structures, but the space between the spermatids indicates that individualization is not proceeding normally (black arrows).

4.3.2 The *ms771* mutant maps to an uncharacterized F-box protein, Nutcracker

To genetically map *ms771*, the deficiency "kit" of large genomic deletion lines was screened for deletions that fail to complement its sterility. Two overlapping lines, Df(3L)HR119 and Df(3L)GN34, corresponding to regions 63C2;63F7 and 63E8-9;64A8-9 respectively, failed to complement the sterility phenotype of *ms771*, and the transheterozygotes stained negative for active caspase-3. A smaller deficiency in the overlapping region, Exel6097 (Figure 4.2A), also failed to complement sterility and caspase staining (Figure 4.2B). This deficiency deletes 15 genes and the coding regions of several of them were PCR amplified from *ms771* mutants and sequenced. A premature stop-codon mutation was identified in a novel gene (*CG10855*), which encodes a putative F-box protein. We termed this gene *nutcracker* for novel ubiquitin targeting complex responsible for activating caspases.

We next looked for possible transposon-drived mutations in *nutcracker* and identified a *piggyBac* insertion in the intron of *nutcracker* (*nutcracker*^{07259}), which was obtained from the Bloomington Stock Center (Figure 4.2A). Complementation analysis with the *nutcracker*^{ms771} mutant resulted in a failure of *nutcracker*^{07259} to complement the male sterility of the former, indicating that *nutcracker*^{07259} is indeed an allele of *nutcracker*. Staining of testes from the *nutcracker*^{07259} mutants displayed individualization defects, although they still exhibited some level of active caspases, suggesting that it is a weak allele of *nutcracker* (Figure 4.2B). Finally, transgenic expression of an intact *nutcracker* gene using the testis specific promoter of the *hsp83* gene restores proper caspase activation, spermatid individualization and fertility in both

nutcracker mutants, indicating that all the male sterility associated phenotypes are due to mutations in *nutcracker* (Figure 4.2B).

To further characterize *nutcracker* expression, we first examined its mRNA distribution. We extracted mRNA from either wild-type or *son-of-oskar* males, which lack germ-cells and functioning testes, and compared *nutcracker* levels by semi-quantitative RT-PCR. This analysis revealed that more mRNA is found in the wild-type animal (cycle 25, Figure 4.2C), indicating that *nutcracker* mRNA is preferentially expressed in testes.

We also generated an antibody to full-length Nutcracker. A band of about 35kd, corresponding to the predicted size of Nutcracker, is detected in testes lysates by Western blotting (Figure 4.3A). By contrast, a smaller band is detected in lysates from *nutcracker*^{ms771} testes, consistent with the finding that this allele contains a premature stop-codon that deletes the entire F-box domain (Figure 4.3A). The fact that this stable but truncated protein still displays the mutant phenotypes suggests that the F-box domain is important for Nutcracker's physiological role in sperm differentiation.

Analysis of *nutcracker*^{07259} mRNA using RT-PCR revealed a 600 bp insertion that causes a frame-shift, likely a result of failed splicing due to the transposon insertion (Figure 4.2A and Figure 3B). This mutation results in a complete elimination of the Nutcracker protein as detected by Western analysis (Figure 4.3A). However, because this allele behaves as a genetic hypomorph, it is likely that a small amount of wild-type protein is still produced, but at levels below Western-blot detection.

Figure 4.2: *ms771* maps to *nutcracker*, an uncharacterized F-box protein expressed in testes

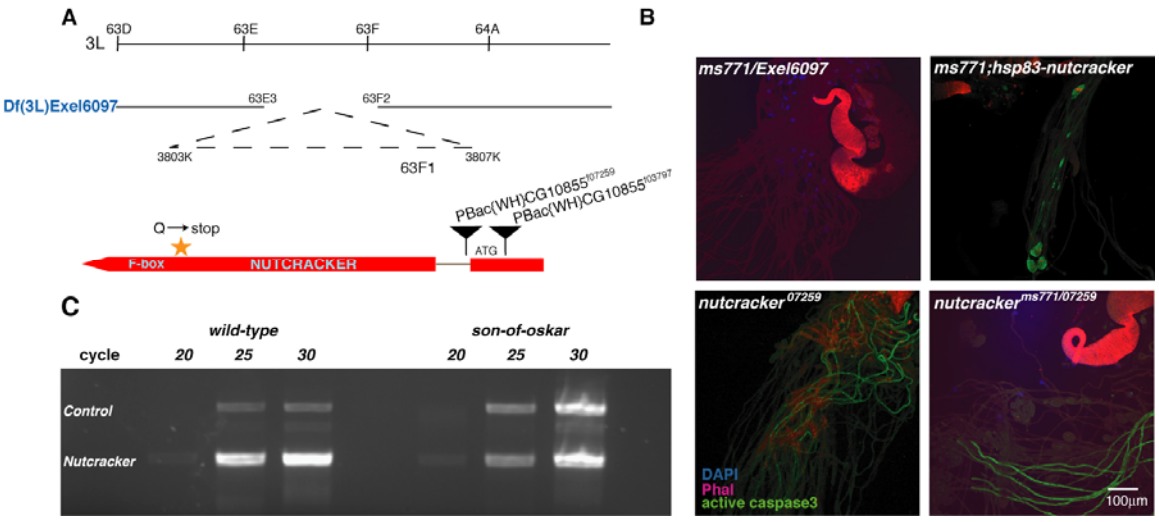

Figure 4.2 **[A]** Nutcracker genomic region. *nutcracker* is located at position 63F1, within the region removed by the deficiency Exel6097. Two piggyback insertions (inverted triangles) are annotated for *nutcracker*: *Pbac(WH)CG10855*^{f03797} is inserted upstream of the ATG start site, and *Pbac(WH)CG10855*^{07259} *(nutcracker*^{07259}*)*, inserted in the intronic region. An orange star indicates the location of the premature stop-codon mutation in *nutcracker*^{ms771} that results in the truncation of the F-box domain. **[B]** The *ms771* mutation maps to *nutcracker*. The deficiency Exel6097 fails to complement *ms771* sterility and staining, and both these defects are rescued by reintroducing *nutcracker* ORF. *nutcracker*^{07259}, also has individualization defects and is hypomorphic for caspase-3 staining. The staining is slightly reduced, but not eliminated, in the trans-hetrozygote *nutcracker*$^{ms771/07259}$. **[C]** *nutcracker* is expressed in the germ-line. Semi-quantitative RT-PCR of *nutcracker* mRNA, using total mRNA taken from either wild-type or *son-of-oskar* males. More transcripts were detected in the wild-type, indicating that it is preferentially expressed in testes.

Figure 4.3: *ms771* harbors a truncated Nutcracker protein

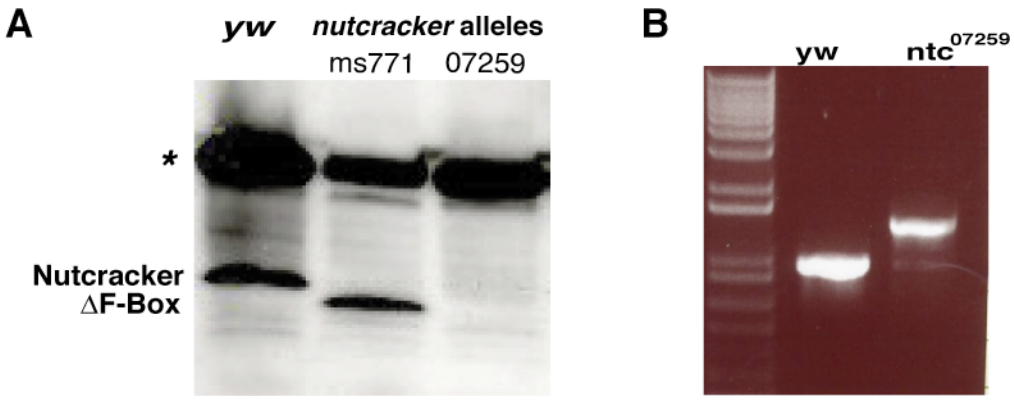

Figure 4.3 **[A]** Western blot of testes lysates using the Nutcracker antibody displays a ~35kd band corresponding to the predicated size. Analysis on testes lysates taken from the mutant flies indicate that while *nutcracker*^{ms771} (ms771) harbors a truncated form of Nutcracker protein, *nutcracker*^{07259} (07259) mutant is a protein null. The star indicates a non-specific band that serves as a loading control. **[B]** RT-PCR analysis of *nutcracker* mRNA transcripts collected from *wild-type* (*yw*) or *nutcracker*^{07259} (ntc^{07259}) adult testes. Compared to the predicted transcript size found in wild-type testis mRNA, *nutcracker*^{07259} transcript contains a ~600 base-pair insertion. Sequencing analysis of the corresponding band revealed that this insertion is located in the middle of the transcript, resulting in a frame-shift of the ORF.

4.3.3 Nutcracker is part of an SCF ubiquitin ligase complex

To examine whether Nutcracker is in complex with other SCF members in the testis, we tagged Nutcracker with ProteinA (PrA) and placed it downstream to the DJ promoter and 5'UTR, and upstream to the *cyt-c-d* 3'UTR (DJ-PrA-ntc), which are specifically and highly expressed in spermatids (Arama et al., 2006; Santel et al., 1998; Santel et al., 1997). Transgenic fly lines were generated and checked for expression by Western-blotting (not shown). These transgenes restored caspase staining, but failed to

rescue the sterility phenotype of the *nutcracker* mutants due to the possible misexpression of this construct, or domain obstruction by the PrA tag. Co-immunoprecipitation (co-IP) experiments using lysates of testes from these transgenic flies showed that PrA-ntc specifically binds both endogenous SkpA and Cullin1, suggesting that Nutcracker functions in an SCF complex (Figure 4.4A). To investigate the role of the F-box domain in mediating this interaction, we also constructed a truncated form of PrA-tagged Nutcracker, deleting the F-box domain, similar to the stop-codon mutation in *nutcracker*^{ms771} (PrA-ntcΔF). Unlike full-length Nutcracker, PrA-ntcΔF was unable to enrich either Cullin1 or SkpA in co-IP experiments (Figure 4.4A). These results confirm that Nutcracker forms an SCF complex, mediated through its F-box domain, and puts forth the possibility that the phenotypes observed in *nutcracker*^{ms771} are caused by the inability to form this complex.

4.3.4 Nutcracker and Cullin1 co-localize with actin cones at the individualization complex

We wanted to visualize Nutcracker localization in context of the morphological events during individualization. For immuno-staining, we affinity purified Nutcracker serum and used it to stain testes (Figure 4.4B). Nutcracker partially co-localizes with the forming individualization complex, although they do not completely overlap. As the complex moves, Nutcracker staining is detected within the CB, but the most prominent staining is observed around the outer layer of the IC itself, at the base of the cones. Various focal planes of the CB show that the majority of the protein accumulates around the outer borders of the IC, and only slightly intertwines between the cones. This

indicates that the protein may be anchored in the vicinity where the cones attach to the outer membrane. We also stained testes from *nutcracker*^{07279} flies, which failed to display a protein band by Western-blot. Similarly, we were unable to detect protein by immunostaining (Figure 4.4B), demonstrating the specificity of the antibody in detecting Nutcracker staining pattern.

We wanted to know whether this localization of Nutcracker corresponded to the localization of the SCF complex. The pattern of Cullin1 staining at ICs in *yw* testes is similar to that of Nutcracker (Figure 4.4C), placing these proteins in the same vicinity in the IC. Together with the biochemical data, this strongly supports their physical interaction *in vivo* and their combined role in individualization.

4.3.5 Nutcracker mutants display defects in individualization complex formation

nutcracker^{ms771} mutant testes are defective in IC formation as no actin cone formation is observed around the elongated nuclei (Figure 4.1A). When Nutcracker is misexpressed in this background, as in the DJ-PrA-ntc transgene, these phenotypes are partially rescued; cysts display cleaved-caspase3 staining, and some cysts form ICs at the tip of the cyst (Figure 4.4D). However, these ICs appear irregular, mostly scattered, and in some cases individual actin cones can be observed scattered along the length of the cyst. This may explain why sterility is not rescued, and indicates that the timing and level of Nutcracker expression are important for IC integrity. Furthermore, in the testes of the hypomorphic allele *nutcracker*^{07259}, which stain positive for cleaved-caspase3, some irregular ICs are observed (Figure 4.4B), further suggesting that actin filament

formation and organization, as well as caspase activation are sensitive to the levels of Nutcracker.

Figure 4.4 **[A]** The F-box protein Nutcracker co-IPs with members of the SCF complex. ProteinA (PrA)-tagged Nutcracker (PrA-ntc) was expressed in testes and its endogenous interacting partners were identified by Western Blot. Co-IP followed by western-blot analysis using either Cullin1 or SkpA antibodies demonstrate that Nutcracker binds both Cullin1 and SkpA, both part of the SCF ubiquitin ligase (middle lane of the co-IP). The interaction is hindered by the removal of the F-box domain (PrA-ntcΔF), suggesting that Nutcracker is part of this complex (right lane of the co-IP). The input panel indicates that equal amounts of either SkpA or Cullin1 were present in the lysate at the beginning of the experiment. **[B]** Nutcracker antibody staining (green). As the IC forms around the elongated nuclei, Nutcracker protein accumulates around it (upper left panel). After the IC begins movement, Nutcracker localizes around the bulge, intertwined within the complex, as can be viewed by the two planes shown (lower left panel). The staining completely disappears in *nutcracker*^{07259}, which occasionally displays formed, yet defective, ICs (upper and lower right panels). The ICs are stained with phalloidin (red), and the nuclei are stained with DAPI (blue). **[C]** Cullin1 staining (green) of *yw* testes showing similar staining pattern to Nutcracker (arrows point to the staining around the nuclei in the left panel, and to the staining around the IC in the right panel). **[D]** Nutcracker misexpression affects IC integrity. DJ-PrA-ntc was expressed in *nutcracker*^{ms771} background. The DJ promoter drives high levels of expression at later stages of differentiation, so Nutcracker is over-expressed and mistimed. This misexpression does not rescue sterility, but does restore some cleaved-caspase3 staining (not shown). The IC, which does not form in *nutcracker*^{ms771}, does form in this background (Phalloidin, red), but its formation is altered, and the actin cones are scattered (white arrows).

Figure 4.4: Nutcracker and Cullin1 form an SCF complex and co-localize with Actin at the individualization complex

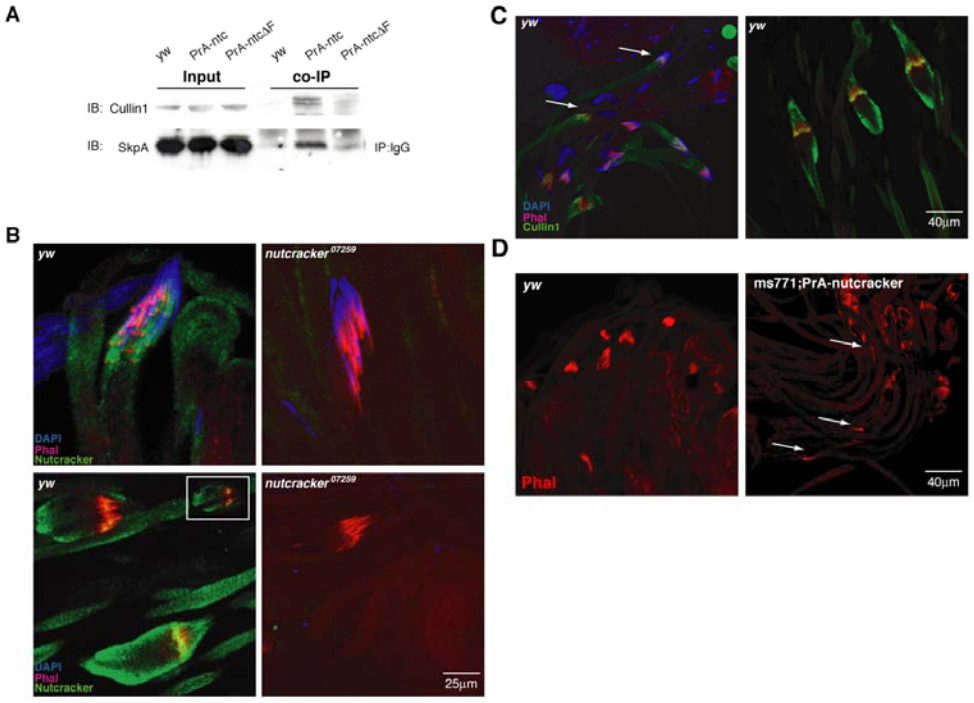

4.3.6 Nutcracker physically interacts with dBruce, a giant IAP-like protein

In *Drosophila*, two IAPs have been shown to directly inhibit active caspases, DIAP1 and DIAP2 (Hay et al., 1995), but only DIAP1 is strictly needed for controlling caspases *in vivo* (Goyal et al., 2000; Lisi et al., 2000). IAPs are regulated by ubiquitin-mediated degradation, which removes them from caspases thus allowing proteolysis (Ryoo et al., 2002; Wilson et al., 2002). Therefore, we wanted to know if a Nutcracker-containing SCF ubiquitin-ligase mediates the degradation of these proteins. We checked steady-state levels of DIAP1 protein in *nutcracker*^{ms771} mutants by Western blot and found no difference compared to *wild-type*, suggesting that Nutcracker does not regulate its stability (Figure 4.5A). Furthermore, co-IP experiments using testes lysates, and those conducted by co-expressing tagged DIAP1 and Nutcracker proteins in S2 cells, failed to detect an interaction between these proteins (data not shown). We also checked another IAP, DIAP2, which is able to inhibit caspases *in vitro* (Ribeiro et al., 2007) and has a role in *Drosophila* immunity (Kleino et al., 2005). The levels of this inhibitor are also unchanged in *nutcracker*^{ms771} mutants (Figure 4.5A). These suggest that Nutcracker regulates caspase activation independently of the known direct inhibitors of caspases.

Next, we investigated another IAP, dBruce, which has a known role in spermatogenesis (Arama et al., 2003) and was shown to inhibit apoptosis induced by Reaper (Vernooy et al., 2002). dBruce is a large (~500kd) protein that contains both a BIR domain, and a UBC domain, found in E2 conjugating enzymes. Mutations in this gene are male sterile, and cause nuclear degeneration, presumably by excess caspase activation (Arama et al., 2003). To check whether this protein is a potential substrate of Nutcracker, we conducted co-IP experiments by co-expressing PrA-ntc and a shorter

version of dBruce (one consisting of about half of the protein, including the BIR and UBC domains, since the entire gene is yet to be cloned) in S2 cells. In this experiment, the dBruce 'mini gene' physically interacts with both the full-length and truncated forms of Nutcracker (Figure 4.5B).

In order to define the genetic interaction between *nutcracker* and *dBruce* we generated double mutants, by recombining *dBruce* mutants onto the *nutcracker*^{07259} chromosome. We rationalized that if dBruce is the substrate of Nutcracker, then the reduction of caspase staining in this hypomorphic *nutcracker* mutant may be further decreased in double mutants. We used two *dBruce* mutants previously isolated in our lab (J. Agapite, K. McCall and H.S, unpublished, and (Arama et al., 2003)). One mutant, *8-1e*, was characterized as harboring a deletion that deletes the BIR domain of dBruce, while the other, 10-1e, contains a deletion that deletes almost the entire protein, including the UBC domain (but still contains the N' terminal BIR domain). When we stained the double mutants *dBruce*$^{8\text{-}1e}$, *nutcracker*^{07259} or *dBruce*$^{10\text{-}1e}$, *nutcracker*^{07259} we saw no change of caspase staining (Figure 4.5C) compared to the *nutcracker* single mutant. Furthermore, morphological analysis of either double mutant did not reveal more severe individualization defects compared to single mutants. These data argue against a simple, linear pathway in which Nutcracker activates caspases by inhibiting dBruce.

Figure 4.5: Nutcracker physically interacts with dBruce, a giant IAP-like protein

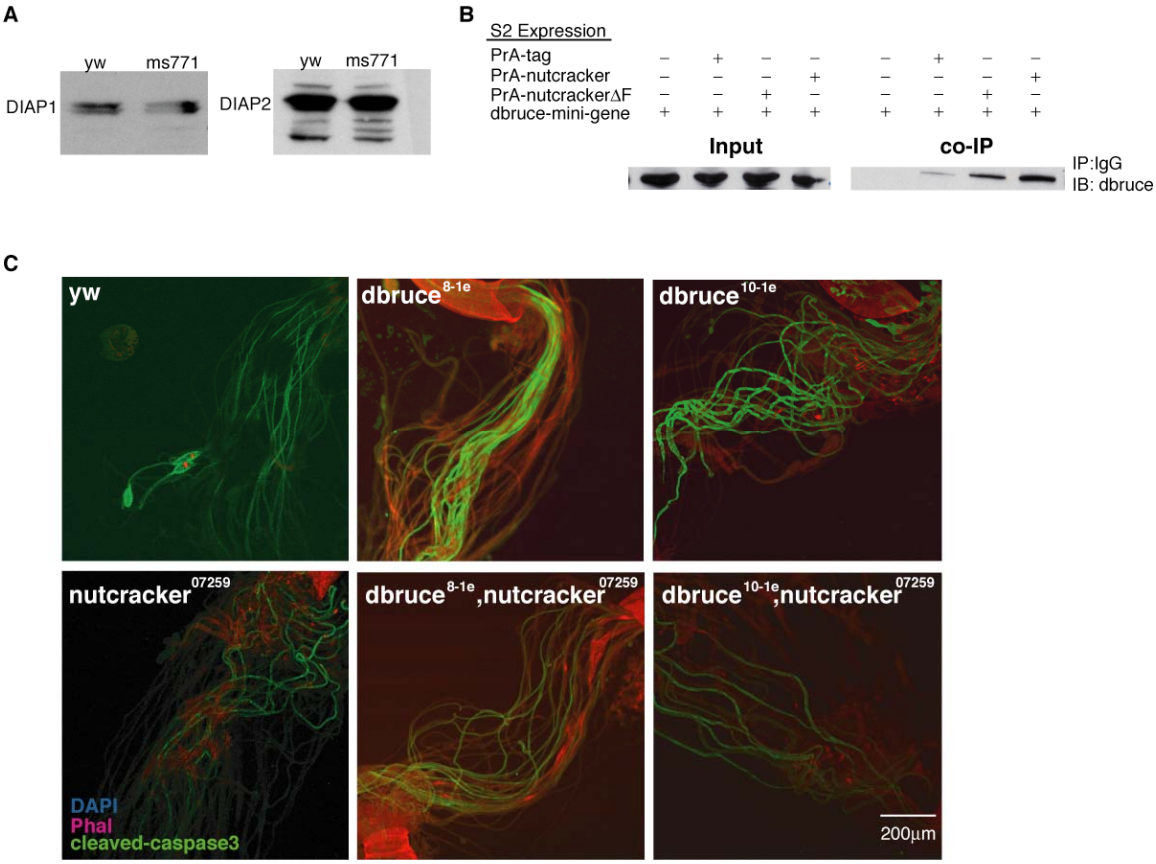

Figure 4.5 **[A]** Western blots of total protein lysates from *yw* or *nutcracker*^{ms771} testes using either DIAP1 or DIAP2 antibodies indicate that Nutcracker does not effect the levels of these direct caspase inhibitors. **[B]** The F-box protein Nutcracker physically binds dBruce. PrA, PrA-ntc or PrA-ntcΔF were expressed in S2 cells together with the dBruce 'mini-gene' construct. Western blot analysis of this co-IP experiment revealed that dBruce binds both full length and truncated Nutcracker, suggesting that dBruce is an interacting protein but its interaction to Nutcracker is independent of the SCF complex. **[C]** Genetic interaction between *dBruce* and *nutcracker*. Caspase staining (green) of *nutcracker* hypomorphic allele *nutcracker*^{07259} is unchanged in the double mutants with dBruce$^{8\text{-}1e}$ or dBruce$^{10\text{-}1e}$.

4.3.7 Proteasome activity is reduced in *nutcracker* mutants

Proteasome activity is important for spermatid individualization (Zhong and Belote, 2007). In particular, IC movement and caspase activation are abnormal in a mutant for a testis-specific proteasome subunit, *alpha6T*. Given that some aspects of the *nutcracker* mutant phenotypes resemble the loss of *alpha6T* function, we wanted to explore whether *nutcracker* has an effect on proteasomes.

We utilized a GFP-tagged Alpha6T protein (Zhong and Belote, 2007) to ask whether proteasome distribution or numbers are altered in *nutcracker* mutant background. Alpha6T-GFP is a faithful reporter of proteasome localization, since it can rescue *alpha6T* mutant phenotypes and is fully incorporated into proteasomes (Zhong and Belote, 2007). Alpha6T is co-localized with the elongated nuclei just before IC formation (Figure 4.6A, top right panel) but moves in front of the actin cones after the IC forms (Figure 4.6A, bottom right panel). In $nutcracker^{ms771}$, where no ICs form, Alpha6T persists in the nuclei (Figure 4.6A, top left panel). In contrast, in the hypomorphic $nutcracker^{07259}$, where occasional ICs form, Alpha6T-GFP is detected at its normal location in front of the actin cones (Figure 4.6A, bottom left panel). These data indicates that the movement and overall distribution of proteasomes does not depend on *nutcracker* function, but on IC formation.

We next asked if *nutcracker* influences proteasome activity directly. For this purpose, we assayed the proteasome activity in wild-type, $nutcracker^{ms771}$ *or* $nutcracker^{ms771}$ flies that are expressing a *nutcracker* rescue construct. Testes from these genotypes were lysed and differences in proteasome activity were detected by measuring the hydrolysis of a fluorogenic peptide. Compared to wild-type testes, proteasome

activity is reduced in *nutcracker*^{ms771} mutants (Figure 4.6B). This activity is restored by reintroducing *nutcracker* into the mutant background, indicating that the decreased activity is indeed caused by reduced *nutcracker* function. In order to investigate if this reduced activity is caused by a reduction in proteasome numbers in the mutant, we looked at levels of three different proteasome subunits. Assaying individual subunit proteins is a good indicator of proteasome number because the majority of proteasome subunits in the cell are incorporated into the proteasome complex (Glickman and Raveh, 2005). Compared to the wild-type, we found the levels of Alpha7, Rpn3 and Rpt4 proteins unchanged in *nutcracker*^{ms771} mutant testes (Alpha7 in Figure 4.6C and not shown). We also checked total cellular proteasome levels by purifying endogenous proteasomes from either wild-type or *nutcracker*^{ms771} (Figure 4.6D). We found that proteasome levels in the mutant are virtually identical to the wild-type, as detected by their commassie staining pattern on an SDS blot. These data demonstrate that equal amounts of proteasomes are formed in the mutant, suggesting that *nutcracker* acts directly on proteasome activity. Taken together, these results indicate that *nutcracker* controls caspase activation and spermatid individualization by regulating proteasome activity.

Figure 4.6 **[A]** Proteasome distribution during individualization. GFP-tagged-Alpha6T is a marker for proteasome localization (Zhong and Belote, 2007). Alpha6T is detected in elongated nuclei before the IC forms (top left panel), and after IC formation moves basely to it (bottom left panel). Testes of *nutcracker*^{ms771} display no Alpha6T outside the nuclei (top right panel). In contrast, in the *nutcracker*^{07259} hypomorphic allele, where occasional ICs are formed, Alpha6T is detected at its normal location in front of the IC (bottom right panel). **[B]** Testes from *nutcracker*^{ms771} display decreased proteasome activity. Total protein was extracted from the indicated genotype and proteasome activity was detected by measuring fluorogenic-peptide hydrolysis after 10 minutes. Measurements are plotted as relative luminescence units (RLU). Each genotype sample was split, and a proteasome-inhibitor (MG-132) was added to half the sample to confirm the specificity of the read-out. *yw*=Wild-type, ms771=*nutcracker*^{ms771}, ms771-rescue=*nutcracker*^{ms771};hsp83-nutcracker. **[C]** The levels of the proteasome subunit Alpha7 are unchanged in the *nutcracker*^{ms771} mutant. Total protein was extracted from either *wild-type* (yw) or *nutcracker*^{ms771} (ms771) testes and the amount of the indicated proteins were detected by western-blot analysis. Amounts of other SCF members (Cullin1 and SkpA) were also assayed and used as loading controls. **[D]** wild-type and *ms771* mutants have equal proteasomes levels. Endogenous proteasomes were purified from wild-type (*yw*) or mutant (*ms771*) testes and ran on an SDS-gel followed by Comassie staining. The comassie staining pattern is similar to that of other proteasome purification blots, as in (Holzl et al., 2000). The identical staining pattern between the wild-type and mutant testes indicates that proteasomes are not down-regulated in the mutant. A wild-type sample without UBL (-UBL) was used as negative control for unspecific binding to beads (see Materials and Methods).

Figure 4.6: Nutcracker affects proteasome activity, but not their distribution or numbers

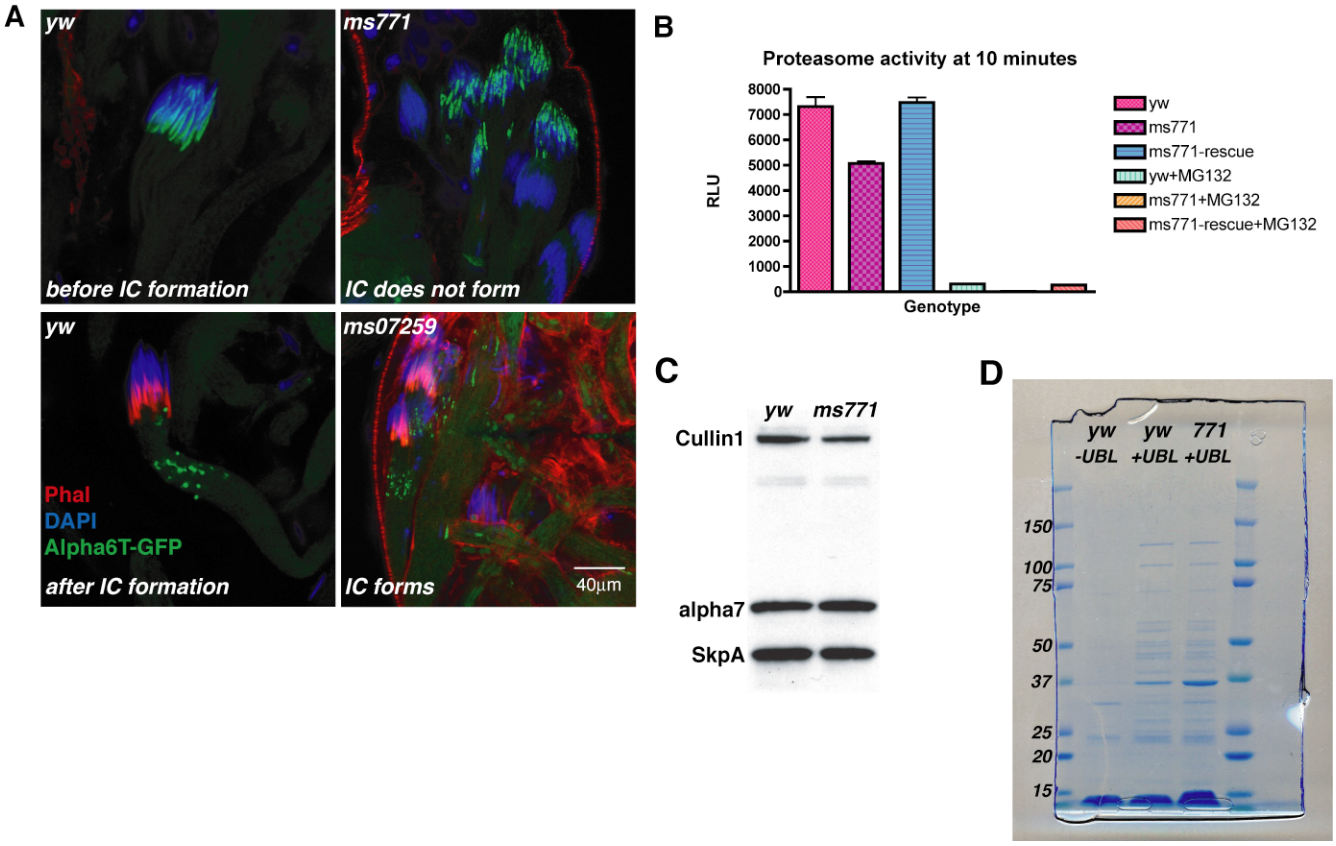

4.4. Materials and Methods

Fly strains. *yw* flies were used as wild-type controls. The Zuker mutant Z3-4692 (ms771) was obtained from C.S. Zuker (UCSD); alpha6T; Alpha6T-GFP was obtained from John Belote (Syracuse University); the deficiency lines Df(3L)HR119 and Df(3L)GN34 and the PBac insertion PBac(A et al.)CG10855^{f07259} from the Bloomington Stock Center, and DF(3L)Exel6097 from Exelixis.

Electron Microscopy

Wild-type and *bln* mutant testes were dissected in chilled glutaraldehyde (2.5% in 0.1 M cacodylic buffer, pH 7.4) and fixed on ice. The testes were post-fixed in 1% osmium tetroxide in the same buffer on ice, dehydrated in graded concentrations of ethanol, stained *en* bloc with uranyl acetate, and embedded in Epon. For the transmission electron microscopy (TEM), ultra-thin sections were cut on a Reichert-Jung Ultracut E microtome and poststained with uranyl acetate and lead citrate. Sections were examined and photographed on a JEOL100CXII at 80 kV.

Molecular Biology

DGRC clone LD12948 was used to amplify CG10855. For rescuing the *nutcracker*^{ms771} mutant phenotypes, CG10855 ORF was amplified by PCR (primers 1+2) and cloned into pHSP83(5'-3'UTRs) (Arama et al., 2006), which contained the 5' and 3' UTRs of Cytochrome-c-d. For antibody generation, CG10855 ORF was amplified by PCR (primers 3+4) and cloned into pET41a(+) (Novagen), which contains an N' terminal GST-tag. For antibody affinity purification, CG10855 ORFs was also cloned into pET101/D-TOPO (Invitrogen) (primers 5+6), which contains a C' terminal His-tag. For testes expression of tagged proteins, a ProteinA (PrA) tag was cloned into Casper-4

containing the Don-Juan promotor (primers 7+8), and full-length CG10855 was cloned in frame to it (primers 9+10). ΔFbox was created by PCR amplification of CG10855 with out the last 174 nucleotides, and this product was also cloned in frame into Casper-4-DJ-PrA (primers 9+11). The construction of the dBruce 'mini-gene' was is detailed in (Arama et al., 2007). See table below for primer sequence and restriction sites.

Antibody generation and tissue staining.

Cleaved effector caspase antibody staining of young (0–2 day old) adult testes was carried out as described in (Arama et al., 2007) using a rabbit polyclonal anti-cleaved Caspase-3 (Asp175) antibody (Cell Signaling Technology) diluted 1:75. The only changes are that the subsequent TRITC phalloidin (Sigma) incubation for staining of actin filaments was carried out during incubation with the secondary antibody and the slides were subsequently rinsed twice for 10 min in PBS. Axonemal tubulin polyglycylation antibody staining was carried out using the mouse ponoclonal antibody Axo 49 (a kind gift from Marie-Helene Bre, University of Paris-Sud, France) diluted 1:5000. Anti-CG10855 was created by injecting guinea-pig with full-length recombinant CG10855 (Cocalico Biologicals, Inc.), and the staining was carried out as described in (Hime et al., 1996), with a 1:100 dilution of affinity purified serum. The serum was purified by expressing a C' terminal His tagged-CG10855 in BL21 *E.Coli* (expressed for 1.5 hours at 37°C), the bacterial lysate was run on SDS-PAGE, transferred onto an immobilon-P membrane (Milipore) and blocked in 5% milk in PBST (0.1% Triton-X in PBS). 500uL of serum was pipetted onto the membrane and incubated for 3 hrs, and once removed, the purified antibody was eluted by 50mM glycine [pH2.5]. The antibody was then neutralized with 0.1M Tris [pH 9.0].

Genomic DNA Isolation and sequencing of the mutant alleles.

Genomic DNA was isolated as in chapter 3. This DNA (20 ng) was used to amplify CG10855 with primers corresponding to its 5' and 3' UTRs (primers 12-15). PCR reactions were carried out using DyNAzyme EXT DNA polymerase (NEB) according to the manufacturer's protocol. The products were purified using the High Pure PCR Product Purification Kit (Roche), concentrated by evaporation, and sequenced in a GENEWIZ sequencing facility. See table bellow for primer sequences.

RNA isolation and RT-PCR

Total RNA isolation and RT-PCR were conducted as in chapter 3. Primers corresponding to the 5' and 3' UTRs were used to amplify CG10855 mRNA (primers 12+13). See table bellow for primer sequence.

Western Blot

To create testes lysate, testes were dissected in lysis buffer (20mM Hepes pH7.6, 150mM NaCl, 10% glycerol, 1% TritonX100, 2mM EDTA, 1mM DTT), homogenized and spun at 14,000 rpm for 15 minutes at 4°C. Protein concentration was determined by Bradford assay (Biorad), and 30-50ug total-protein, dissolved in SDS loading buffer, was separated by SDS-PAGE. After transfer, the immobilon-P membrane (Milipore) was blocked with 5% milk in TBST (0.1% tween20 in PBS) for 1 hour, and incubated with primery antibody overnight at 4°C. The membrane was then washed 3 times in TBST, incubated in HRP-conjugated secondary antibody for 1 hour, and washed 3 more times with TBST before developing with ECL reagents (Amersham) and Kodak Biomax MR film. The following antibodies were used in a 1:1000 dilution: anti-nutcracker(sera), anti-Cul1(Zymed), anti-SkpA (a kind gift from T. Murphy), anti-DIAP1 (a kind gift from HD.

Ryoo), anti-DIAP2 (a kind gift from P. Meier) and anti-dBruce (Arama et al., 2007). Anti-Alpha7 (Biomol) was used at 1:200.

Immunoprecipitations

For testes-IP, testes were dissected in IP buffer (50mM Hepes pH7.5, 150mM NaCl, 15mM MgCl2, 10% glycerol, 1% TritonX100, 1mM EDTA, 1mM DTT), lysed (as in Western blot), and equal amounts of protein were incubated for 2 hrs at 4°C with Dynabeads (Invitrogen) that were conjugated to rabbit IgG according to the manufacture's protocol. The beads were washed 5 times in lysis buffer (except that detergent was reduced to 0.1%), and eluted in SDS loading buffer by boiling.

Proteasome activity assay

Testes were lysed as in Western-blot. Protein concentration was measured and equal amounts of lysates were added at a 1:1 volume ratio to the Proteasome-Glo proteasome activity detection kit (Promega). The assay was carried out according to the manufacturers protocol. All reactions were conducted in a 96-well plate and read on a SpectraMax M2 micro-plate reader (Molecular Devices).

Endogenous proteasome purification from tissue (testes)

This protocol was adapted from Besche HC and Goldberg AL, unpublished.

400 testes from each genotype were dissected into proteasome purification buffer (25mM HEPES, 5mM $MgCl_2$, 10% glycerol) and frozen over night at -20°C. Samples were thawed on ice, and 1mM DTT, 1mM ATP was added to them. The samples were homogenized, left on ice for 20 minutes, and spun at 14,000 rpm for 15 minutes at 4°C. The supernatant was collected, and protein concentration was determined by Bradford assay (Biorad). Meanwhile, for each sample, 150µl gluthation-sepahrose bead slurry (GE

Healthcare) was added to dolphin tubes (Sigma), washed in 1ml cold buffer, and resuspended in 200µl cold buffer (50% slurry). The supernatants were then added to each dolphin tube, together with 150-200µg GST-UBL (see purification protocol bellow). These samples were rocked at 4°C for 2 hours. After incubation, the beads were washed 4 times in cold buffer (the wash was collected by spinning at 500g for 5 minutes at 4°C). Proteasomes were eluted by incubating the beads with 50µl His-UIM (~ 2µg/µl) (see purification protocol bellow) for 40 minutes at RT, and collected by spinning the mixture at 500g for 5 minutes at 4°C. The result is purified non-denatured endogenous proteasomes.

In figure 4.6D, the samples were boiled for 5 minutes after addition of SDS loading buffer and run on SDS-PAGE (4-12% Biorad Criterion gels). The gel was incubated with boiled commassie (Pierce) for 1 hour at RT, and washing with H_2O for 1 hour.

Purification of GST-UBL:

The expression plasmid pDEST15-UBL-HHR23B was obtained from Besche HC and Goldberg AL, unpublished. The plasmid was transformed into BL21 cells (Invitrogen), and grown on Ampicillin. Expression was induced according to standard procedures with 0.1% L-arabinose (1g/L) (Sigma) for 3 hours at 37°C to O.D 0.6. A 2 Liter culture was spun down and resuspended with 100 ml Lysis buffer (10 mM $MgCl_2$ 1mM DTT, 2mM ATP, DNAse I in PBS) on ice, sonicated extensively, and spun at maximum speed. The supernatant was loaded onto a GSTtrap FPLC column (GE Healthcare). The column was washed with binding buffer (10 mM $MgCl_2$ 1mM DTT, in PBS) and eluted with elution buffer (binding buffer + 100 M Tris pH 8.0, 100mM NaCl, 1mM DTT and 20mM reduced GSH). The samples were desalted on a NAP^{25} column (Amersham) with HEPES

buffer (25 mM HEPES pH 7.2, 10% glycerol, 5mM $MgCl_2$, 1mM DTT) according column manufacturers' protocol. The samples were stored at -80°C. This protein is 38kd.

Purification of His-UIM:

The expression plasmid pET26bHis10-UIM2-S5a was obtained from Besche HC and Goldberg AL, unpublished, who received it from (Young et al., 1998). The plasmid was transformed into BL21 (DE3) cells (Invitrogen), and grown on Kanamycin. Expression was induced in a 2 liter culture according to standard procedures with 0.5mM IPTG (Sigma) for 2 hours at 30°C to O.D 0.6. The culture was spun down and resuspended with 100 ml Lysis buffer (25mM HEPES pH 7.5, 500mM NaCl, 1mM DTT, 0.025% NP-40, 20mM Imidazole) on ice, sonicated for 20 minutes (30 sec X40, 1 minute break), and spun at maximum speed. The supernatant was loaded onto a 3ml HisPur Cobalt Spin Columns (Pierce), according to the manufacturers' protocol, using the lysis buffer as wash. The protein was eluted with elution buffer (25mM HEPES pH 7.5, 500mM NaCl, 1mM DTT, 0.025% NP-40, 500mM Imidazole). The samples were desalted on a NAP^{25} column (Amersham) with HEPES buffer (25 mM HEPES pH 7.2, 10% glycerol, 5mM $MgCl_2$, 1mM DTT) according column manufacturers' protocol. The sample was concentrated with ultra15 column (Amicon, Millipore) with a 3KD cutoff and stored at -80°C. This protein is 7.5kd.

Table 4.1 – Primer list

	Primer name	Sequence	Forward res. site	Reverse res. site	Into plasmid
1	CG10855-coding-forward-MfeI	GCCCAATTGATGTCAGACACTAAATCCGA	MfeI		pHSP83 (5'3'-UTRs) (cut with EcoRI)
2	CG10855-coding-reverese-BamHI	GATGGATCCTTAGCTTCTGCCGCCCTTTA		BamHI	pHSP83 (5'3'-UTRs)
3	CG10855-coding-forward-SpeI	GACACTAGTTCAGACACTAAATCCGAAATT	SpeI		pET41a(+)
4	CG10855-coding-reverese-NcoI	TTTCCATGGTTAGCTTCTGCCGCCCTTTAGCC		NcoI	pET41a(+)
5	CG10855-coding-forward-TOPO	CACCATGTCAGACACTAAATCCGA			pET101/D-TOPO
6	CG10855-reverse-(no_stop) TOPO	GCTTCTGCCGCCCTTTAGCC			pET101/D-TOPO

7	PrA-into-DJ-for-salI	CAGTCGACATGGGTGAAGCTCAAAAACTTAAT	SalI		Casper4-DJ (cut with XhoI)
8	PrA-into-DJ-rev-BamHI	CAGGATCCCCTCCGCCTCCCGGCATCGTCTTTAAGGCT-		BamHI	Casper4-DJ
9	CG10855-into PrA-DJ-for-BamHI	CAGGATCCTCAGACACTAAATCCGAAAT	BamHI		Casper4-PrA-DJ
10	CG10855-into PrA-DJ-rev- NotI	CAGCGGCCGCTTAGCTTCTGCCGCCCTTTA		NotI	Casper4-PrA-DJ
11	CG10855 ΔF-into PrA-DJ-rev- NotI	CAGCGGCCGCTTACATTAGTTGCTGCGATC			Casper4-PrA-DJ
12	5’ CG10855-main	GTGCCACAGCTTATCAACGA			Sequencing from CG10855 5’ UTR
13	3’ CG10855-main	CCCGAGAATCTTTATGCACC			Sequencing from CG10855 3’ UTR
14	5’ CG10855	CCGAAATCCGCACATAGCAGGT			Sequencing from CG10855

	-mid				mid gene forward
15	3’ CG10855 -mid	GGCACCCATTCCAGAGTAGC			Sequencing from CG10855 mid gene reverse

5. A conserved F-box–regulatory complex controls proteasome activity in *Drosophila*[4]

5.1 Summary

The Ubiquitin-Proteasome System catalyzes the degradation of most intracellular proteins. Although ubiquitination of proteins is the primary determinant of their stability, there is growing evidence that proteasome function is also regulated. In this chapter, I describe the functional characterization of a conserved proteasomal regulatory complex. We identify DmPI31 as a binding partner of the F-box protein Nutcracker, a component of an SCF ubiquitin ligase (E3) required for caspase activation during sperm differentiation in *Drosophila*. DmPI31 and Nutcracker bind by a mechanism that is conserved with mammalian FBXO7 and PI31. Nutcracker promotes DmPI31 stability, which is necessary for caspase activation, proteasome function and proper sperm differentiation. DmPI31 can activate 26S proteasomes *in vitro*, and loss of *dmPI31* function causes cell-cycle abnormalities and defects in protein degradation, suggesting that DmPI31 promotes proteasome activity *in vivo*. These findings demonstrate a role for controlled proteolysis during cellular remodeling and represent a new mode of proteasomal regulation.

[4] Maya Bader wrote, conceived of and conducted most of the experiments in this chapter. David Smith (Goldberg lab at Harvard Medical school) and Sigi Benjamin contributed to Figure 5.5. Orly Wapinski aided in the generation of PI31 homologous recombination mutants.

5.2 Introduction

In the introduction chapter of this thesis, I described the variety of ways the proteasome, a large protease that executes the degradation of most cellular proteins, is regulated. The degradation of individual proteins is mostly controlled by their modification with the small protein Ubiquitin (Ub), mediated by E1, E2 and E3 enzymes. Nonetheless, it is becoming increasingly clear that the proteasome itself, traditionally thought to be a passive "garbage disposal", has an active role in many cellular processes, and thus its regulation is an integral part of cellular function. In this chapter, I describe the identification and the functional characterization of a novel proteasome regulatory complex that controls caspase activation and spermatogenesis in *Drosophila*. This complex is comprised of Nutcracker, an F-box protein (Chapter 4), and the proteasome regulator DmPI31.

Proteasome activity can be modulated in many ways, including the binding of alternative activators, the replacement of catalytic subunits with tissue and context specific paralogs, post-translational modifications of its subunits, transcriptional control and the binding of a variety of enzymes, that have active and regulatory roles (see Figure 1.3 of this thesis). For instance, several E3 ubiquitin ligases, among them F-box proteins, are found on proteasomes, and in some cases it was demonstrated that this interaction is important for the ligase activity (Chuang and Madura, 2005; Farras et al., 2001; Xie and Varshavsky, 2002) (Sakata et al., 2003; Seeger et al., 2003). However, the exact requirement for E3 ligases at the proteasome has not been fully explained (Demartino and Gillette, 2007).

The mammalian PI31 (**P**roteasome **I**nhibitor **31**kd), was originally identified in an *in vitro* based screen for proteasome regulators (Chu-Ping et al., 1992), and was labeled a proteasome inhibitor because its addition inhibited the hydrolysis of small synthetic substrates and large unfolded proteins by the 20S proteasome (CP) (McCutchen-Maloney et al., 2000; Zaiss et al., 1999). Because this protein competes with the RP (PA700) and PA28 for binding the proteasome, it was suggested that it disrupts the formation of an intact proteasome (McCutchen-Maloney et al., 2000; Zaiss et al., 1999). PI31 harbors a proline-rich domain, which encompasses a third of the protein at its C' terminus and is important for its inhibitory activity (McCutchen-Maloney et al., 2000). Interestingly, similar to the Rpt subunits of the RP base, PI31 proteins contain a HYbX motif, suggesting it is acts by threading its unfolded C' terminus into the CP channel. When over-expressed in cell culture, PI31 has no indirect effect on proteasome function, but was found to disrupt the formation of the immunoproteasome under immunological conditions (Zaiss et al., 2002). However, conclusions on the function of PI31 are based on experiments using *in vitro* systems or on its over-expression in cell culture, and so the functional role of this protein is largely unknown.

In this study, I conducted a tissue-specific proteomic screen for Nutcracker interactors, and identified the *Drosophila* homologue of PI31, DmPI31 as a Nutcracker-binding partner. I characterize the physical interaction between these proteins, and demonstrated that their interaction is conserved with mammalian FBXO7 and PI31. DmPI31 stability is promoted by Nutcracker, and they functionally cooperate to activate caspases and drive sperm differentiation. Furthermore, DmPI31 can activate purified proteasomes *in vitro* and *in vivo*, a novel activity for this protein. I also show that loss of

dmPI31 function causes the accumulation of poly-ubiquitinated proteins and leads to meiotic defects and male sterility, demonstrating that *dmPI31* is required for proper proteasome activity *in vivo*. These findings define a new mechanism for the regulation of proteasome function.

5.3 Results

5.3.1 Proteomic screen to identify Nutcracker interacting proteins

Nutcracker is a *Drosophila* F-box protein that we previously identified and described in a screen for mutants that fail to activate caspases during spermatid differentiation (Chapter 4). To further understand its role in caspase activation and spermatogenesis, we first sought to identify interacting partners. We devised a proteomics screen, which involved co-immunoprecipitation (co-IP) of Nutcracker followed by identification of associated proteins using mass-spectrometry (Figure 5.1A).

A protein-A (PrA) tagged version of full-length Nutcracker (PrA-ntc) was expressed in S2 cells. After co-IP, the interacting proteins were then identified by mass using MS/MS mass-spectrometry (Figure 5.1S1). This analysis revealed a group of proteins belonging to the UPS, primarily proteasome subunits (alpha1 and alpha7) and a putative proteasome inhibitor, DmPI31 (CG8979) (Figure 5.1S1).

In order to confirm that these interactions occur in *Drosophila* spermatids, we generated flies that express PrA-ntc in the testes of adult males under the control of the Don-Juan promoter (Santel et al., 1997; White-Cooper et al., 1998). Subsequent co-IP was used to identify proteins that are expressed where Nutcracker actually functions (Chapter 4). DmPI31 was again identified as a Nutcracker interactor (Figure 5.1B).

Thus, these two proteins appear to physically interact in the testis. Next, we generated an antibody against endogenous DmPI31 and confirmed this interaction (Figure 5.3A), as well as the association of Nutcracker and the proteasome subunit alpha7 (Figure 5.1S1) by Western blot analysis. We chose to focus on DmPI31 because of its potential role in regulating the proteasome.

Figure 5.1: Proteomic screen to identify Nutcracker interacting proteins

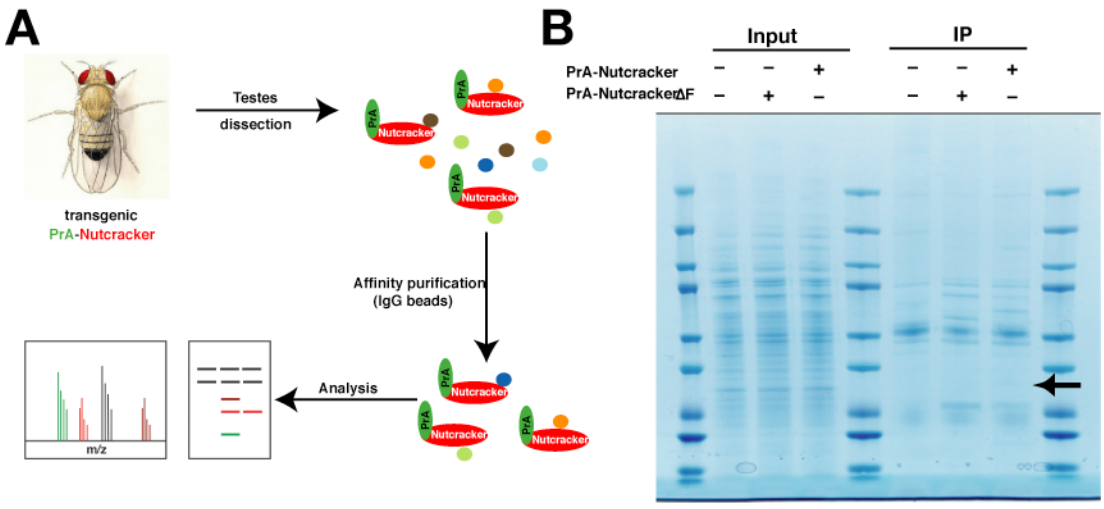

Figure 5.1 **[A]** Scheme for testis specific interactors of Nutcracker; PrA-nutcracker was specifically expressed in testes under the control of the Don-Juan (DJ) promoter. Testes from these lines were dissected, lysed, and incubated with IgG beads. Interacting complexes were eluted off the beads, and identified by either mass-spectrometry or Western-blot analysis. **[B]** SDS-PAGE commassie blots of Nutcracker interactors from testes lysate. An arrow marks the DmPI31 band.

Figure 5.1S1: Nutcracker co-IPs with DmPI31 and the proteasome subunit alpha7

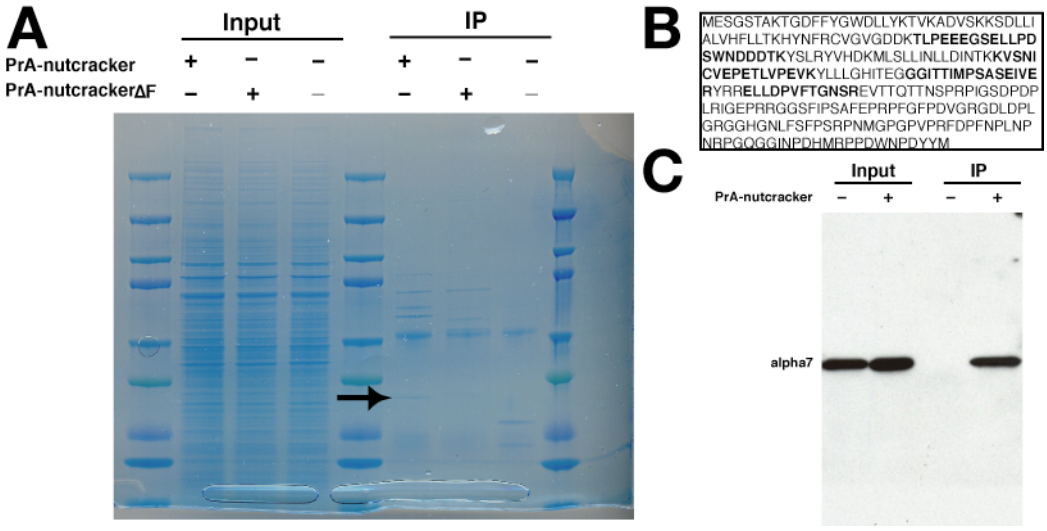

Figure 5.1S1 **[A]** SDS-PAGE commassie blots of Nutcracker interactors from S2 cell lysate. An arrow marks the DmPI31 band **[B]** The trypsin-digested band from (A) revealed 4 peptides corresponding to DmPI31. **[C]** PrA-nutcracker was expressed in testes and used to make lysates for co-immunoprecipitation (IP) assays. Interaction with proteasome subunit alpha7 was detected using an antibody against the mammalian alpha7 protein, which detects the *Drosophila* form.

5.3.2 DmPI31 is highly expressed in the testes and is localized to Individualization Complexes

DmPI31 is the *Drosophila* homologue of mammalian PI31 proteins. The *Drosophila* homologue shares over 45% homology with these proteins (Figure 5.2A). *dmPI31* mRNA profiling suggests that it is expressed throughout the *Drosophila* life cycle, but drops substantially in the adult female (Arbeitman et al., 2002). These data

were further corroborated by semi-quantitative RT-PCR experiments, which demonstrated that mRNA levels in adult females are equivalent to those of *son-of-oskar* males, which lack germ cells and functioning testes. This result also suggests that the majority of the mRNA originates in testes (Figure 5.2B).

In order to follow the expression of DmPI31 protein and to define its intracellular localization during sperm differentiation, testes were stained with the DmPI31 antibody. We previously showed that Nutcracker protein is in the CB, located around the IC's actin cones (Chapter 4). DmPI31 is present at the IC when it is forming around the nuclei (Figure 5.2C, middle panel), and in "speckles" along the entire length of the cyst (Figure 5.2C, left panel). Staining was also detected in the CB, and like Nutcracker, DmPI31 is located at the IC (Figure 5.2C, right panel). These findings suggest that DmPI31 and Nutcracker localize to the same cellular compartment during individualization, further supporting their likely physical interaction.

Figure 5.2: DmPI31 is highly expressed in the testis, and is localized to Individualization Complexes

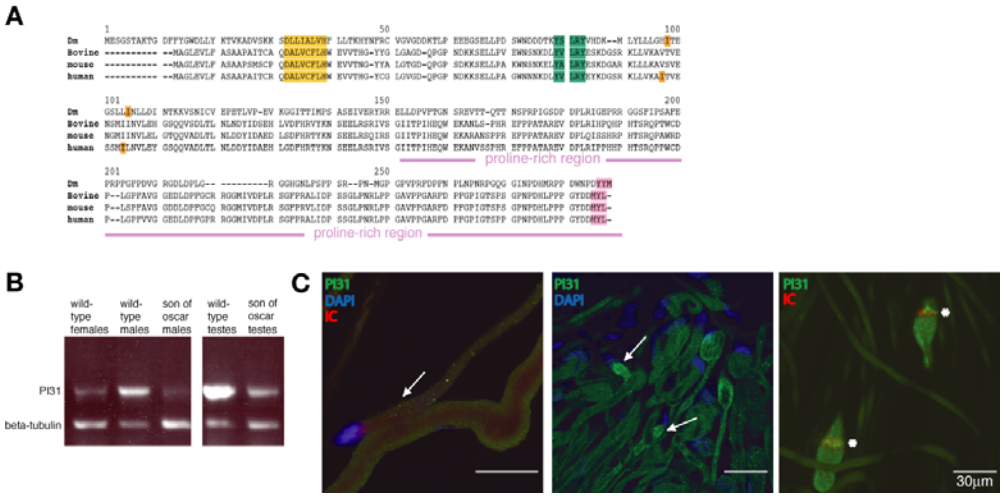

Figure 5.2 **[A]** Multiple alignment *DmPI31* compared to 3 mammalian homologues (Dm-*Drosophila melanogaster*, accession no. NP_7250931.1), Bovine (accession no. NP_001069946), mouse (accession no. NP_997611.1), and human (accession no. AAI26463.1). DmPI31 shares an overall 45% homology with the mammalian proteins, corresponding to 29% identity and 16% similarity as predicted by the ClustalW program (http://www.ebi.ac.uk/Tools/clustalw2). Highlighted in yellow and green (DX_7H and YXLXY motifs, respectively, are identical or similar amino-acids important for PI31 secondary fold. Highlighted in blue are amino acids found to mediate PI31-FBXO7 binding (Kirk et al., 2008). **[B]** DmPI31 mRNA is highly concentrated in adult testes. Semi-quantitative RT-PCR of DmPI31 mRNA transcripts taken from whole-body adult females, wild-type males or *son-of-oskar* males, which lack germ-cells and functional testes. These are also compared to mRNA transcripts from wild-type testes or *son-of-oskar* testes. *β-tubulin* primers were used as control for total mRNA concentrations. Shown is cycle 25, 5 cycles before saturation. **[C]** DmPI31 localization during individualization; DmPI31 protein is detected at the base of the elongated nuclei (arrows), and in a speckle pattern down the length of the cyst (arrow). Similarly to nutcracker, DmPI31 is detected within the CB, located at the IC (asterisks).

5.3.3 DmPI31-Nutcracker interaction is dependent on the conserved FP domain

We wanted to determine whether DmPI31 is associated with a Nutcracker-based SCF Ub-ligase, and if so, how it binds to this complex. We previously showed that the F-box domain of Nutcracker is important for binding Cullin1 and SkpA, since removal of this domain abolishes binding (Chapter 4). Therefore, to check if the F-box domain is crucial for Nutcracker-DmPI31 binding, we performed co-IP experiments using either the original PrA-ntc expressing testes or those expressing a truncated version that is missing the F-box domain (PrA-ntcΔF). As shown in Figure 5.3A, IP of both PrA-ntc and PrA-ntcΔF resulted in enrichment of DmPI31. This suggests that the interaction between Nutcracker and DmPI31 is independent of the F-box domain.

To further investigate the nature of Nutcracker-DmPI31 interaction, we looked at a related, structurally defined association between the mammalian F-box protein FBXO7 and PI31 (Kirk et al., 2007). Nutcracker has some homology with FBXO7 and they share a critical conserved valine (Figure 5.3S1) that is required for FBXO7-PI31 binding (Kirk et al., 2007). We mutated this valine in Nutcracker (V>E) to examine its significance in the Nutcracker-DmPI31 interaction. We expressed either PrA-ntc or PrA-ntc-V-E in S2 cells and repeated the co-IP experiment. As demonstrated in Figure 5.3B, significantly less endogenous DmPI31 was bound to the mutant Nutcracker than the wild type form. These results further define a conserved domain within Nutcracker that is essential for the interaction with DmPI31.

We also investigated whether the domain used by PI31 to bind FBXO7 is also conserved in DmPI31. Two isoleucines in positions 83 and 90 in human PI31 are required for binding to FBXO7, and define a domain called the FP domain Kirk et al.,

2007). DmPI31 also contains a FP domain (Figure 5.2A), and mutating the corresponding isoleucines (I96>E,I103>E) greatly reduced binding to Nutcracker (Figure 5.3C). Therefore, binding of DmPI31 to Nutcracker occurs via a conserved globular FP domain.

Figure 5.3S1: The F-box protein Nutcracker shares sequence homology with the F-box-only protein FBXO7

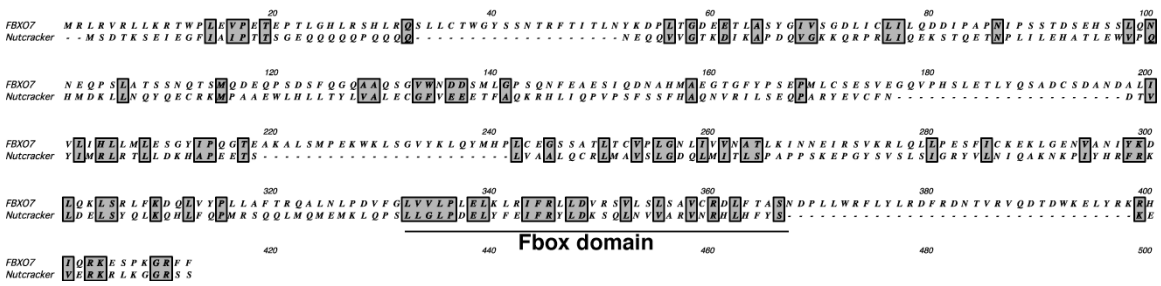

Alignment of the *Drosophila* Nutcracker protein against human FBXO7 (accession number CAG30377). The proteins have the highest similarity between their F-box domains. Overall, they share 17 identical amino-acids (5% of Nutcracker, 2% of FBXO7), and 36 similar amino acids (11% of Nutcracker, 7% of FBXO7). Not shown are the last ~100 amino acids of FBXO7, as it is a longer protein.

Figure 5.3 **[A]** Nutcracker-DmPI31 interaction is not dependant on the F-box domain. PrA-ntc or PrA-ntcΔF were expressed in testes and used to make lysates for (co-IP) assays. Non-PrA expressing wild-type testes (*yw*) were used as a negative control. In all experiments but [C], DmPI31 binding was detected by Western-blot analysis using DmPI31 antibody. In [C], HA-PI31 is detected with the HA antibody. **[B**] Nutcracker-DmPI31 binding is mediated by a specialized domain. A conserved valine that mediates the interaction between the human PI31 and the F-box protein FBXO7 was mutated to check for its importance in mediating DmPI31-nutcracker binding. PrA-ntc or PrA-ntcV-E were expressed in S2 cells and used as lysates for co-IP. Non-PrA expressing cells were used as a negative control. **[C]** Two conserved Isoluecines in PI31 that mediate the interaction between the human PI31 and the F-box protein FBXO7 were mutated in DmPI31 to check for their importance in mediating DmPI31-Nutcracker binding. PrA-ntc and either HA-PI31 or HA-PI31I96E,I103E were expressed in S2 cells and used as lysates for co-IP. Cells expressing HA-PI31 alone were used as a negative control. **[D]** Mutations in *nutcracker* affect DmPI31 stability. Total lysates from testes of the indicated genotypes were used to detect steady-state DmPI31 protein levels. The cleaved form of DmPI31 found in *nutcracker* mutants is indicated by an arrow. The lowest molecular weight band is unspecific and serves as a loading control. Lanes are marked *yw (*wild-type), ms771$^{(+/-)}$ (*nutcracker*^{ms771} heterozygote), ms771$^{(-/-)}$ (*nutcracker*^{ms771} homozygote), ms771$^{(-/-)}$ Rescue *(nutcracker*^{ms771};hsp83-nutcracker), ms07259 (*nutcracker*^{07259} homozygote). **[E]** The cleaved form of DmPI31 can physically associate with Nutcracker. PrA-ntc was expressed in testes of either *nutcracker*$^{ms771/+}$ (heterozygote) or *nutcracker*$^{ms771/ms771}$ (homozygote) background and used to make lysates for co-IP. The cleaved form of DmPI31 found in *nutcracker* homozygote mutants is indicated by an arrow. Non-PrA expressing (*yw)* testes were used as a negative control.

Figure 5.3: Nutcracker is a positive regulator of DmPI31 and binds it through a conserved domain

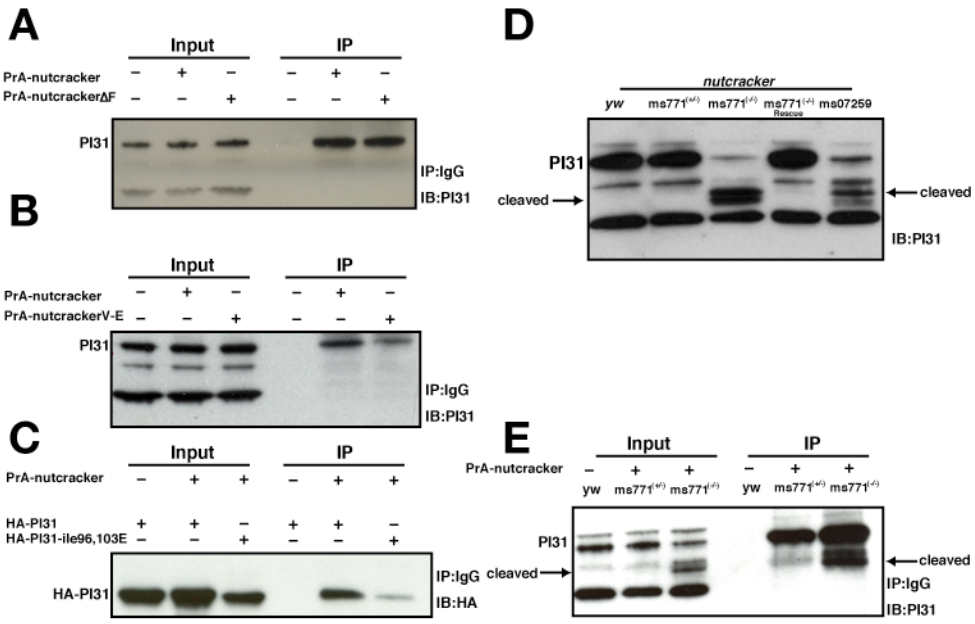

5.3.4 Nutcracker controls DmPI31 protein levels

Since the Nutcracker-DmPI31 interaction is independent of the F-box domain, we asked whether DmPI31 might be a substrate of the Nutcracker-containing SCF ubiquitin ligase. We prepared testes lysates from either wild-type or *nutcracker* mutant flies, and assayed DmPI31 protein levels by Western blot analysis. If DmPI31 was a substrate of Nutcracker, we would have expected DmPI31 to accumulate in the mutants. In contrast, DmPI31 levels were greatly reduced in testes of both Nutcracker-null (nutcracker^{07259}) or truncated F-box (*nutcracker*^{ms771}) mutants (Figure 5.3D) (Chapter 4). Instead, smaller molecular weight products were detected. The full-length DmPI31 band was fully restored in *nutcracker*^{ms771} flies that express wild-type Nutcracker (*nutcracker* "rescue" transgenes: hsp83-nutcracker). This indicates that DmPI31 is cleaved in *nutcracker* mutant background, suggesting that Nutcracker positively regulates DmPI31 protein levels and/or stability. Also, since a stable but F-box-truncated form of Nutcracker (*nutcracker*^{ms771}) still destabilizes DmPI31, it is likely that the F-box domain might also be important for stabilizing DmPI31, either directly through binding, or indirectly through other proteins.

The amino-terminal region of PI31 is structured and contains the FP domain, while the carboxy-terminal end, which contains proline rich sequences, is unstructured (Kirk et al., 2007; McCutchen-Maloney et al., 2000) (Figure 5.2A). We therefore wanted to investigate whether the cleaved form of DmPI31 detected in the total lysate of *nutcracker* mutants is the result of random proteolysis, or cleavage of a specific portion of the protein. Therefore, we determined if the interaction with Nutcracker is lost by the cleavage event. We repeated the co-IP experiment, but this time we expressed PrA-ntc in

the testes of the *nutcracker*^{ms771} mutant flies (Figure 5.3E). PrA-ntc was able to IP both the full length and cleaved forms of DmPI31, indicating that the cleaved form is still folded and that the interaction domain is not lost. Because we established that the interaction domain for binding Nutcracker is in the amino-terminus, it is likely that the carboxy-terminal region is the one lost in the *nutcracker* mutant background. This conclusion is particularly interesting since the carboxy-terminal end of the mammalian PI31 is sufficient to inhibit the proteasome, while a truncated protein without this domain cannot (McCutchen-Maloney et al., 2000). Furthermore, analysis of the C' terminal cleavage of HA-DmPI31 that occurs when this construct is expressed in S2 cells (Figure 5.3S2) revealed that this cleavage is proteasome dependent. In this system, DmPI31 cleavage is also protected by Nutcracker, because ectopic expression of increasing levels of Nutcracker inhibited the cleavage (Figure 5.3S2). These results further confirm Nutcracker's ability to promote DmPI31 stability, possibly by sheltering it from proteasome-mediated cleavage.

Figure 5.3S2: DmPI31 is cleaved in a proteasome-depandent manner but protected by Nutcracker

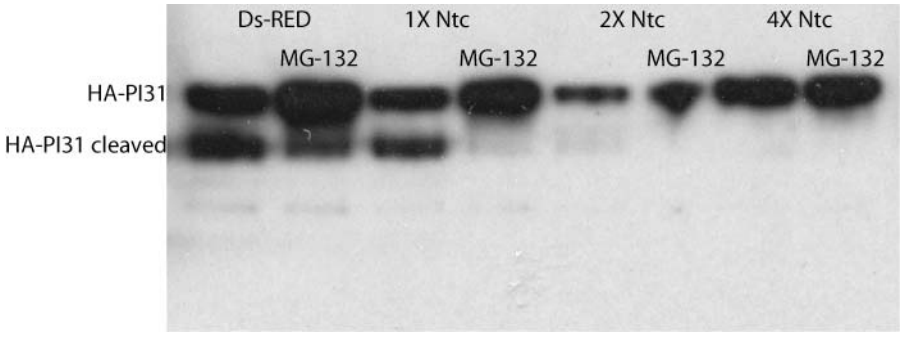

S2 cells expressing HA-DmPI31 were lysed and run on SDS-PAGE. A C' terminal cleavage was detected in cells that co-express a Ds-RED plasmid, but is protected in cells that are expressing increasing amounts of Nutcracker. This cleavage is eliminated by the addition of the proteasome inhibitor MG-132.

5.3.5 Nutcracker and DmPI31 act together to activate caspases and control sperm differentiation

We asked if the interaction between the two proteins is important for their biological activity *in vivo*. For this purpose, we mutated the FP domain and examined the functional consequences. We utilized the nutcrackerV-E mutation that abrogated binding in co-IP experiments and asked if *nutcracker*^{ms771} mutant phenotypes could still be rescued by a transgene carrying this mutation. When compared to the wild type version of the *nutcracker* rescue construct (hsp83-nutcracker), hsp83-nutcrackerV-E transgenic flies were unable to rescue the *nutcracker*^{ms771} sterility phenotype (0% of 5 fly lines examined, versus 100% of 5 wild-type rescue lines). When we stained testes from these

males with the caspase3 antibody, we noticed that some staining and morphology were restored (data not shown), demonstrating that the mutated construct was expressed and able to partially function. However, it appears that full Nutcracker activity requires binding to DmPI31 (Table 5.1).

Table 5.1

Genotype	Fertility	Caspase3 staining	DmPI31 cleavage	Morphology
Wild-type (*yw*)	100%	yes	no	normal
ntc$^{-/-}$	0%	no	yes	no IC formed, failure to individualize
ntc$^{-/-}$ + nutcracker-wt	100%	yes	no	normal
ntc$^{-/-}$ + nutcracker-V-E	0%	yes	partial	incomplete individualization
ntc$^{-/-}$ + PI31	0%	yes		no IC formed failure to individualize

Table 5.1 Summary of *nutcracker*^{ms771} (ntc$^{-/-}$) phenotypes rescued by the ectopic expression of either wild-type *nutcracker* construct (nutcracker-wt), a *nutcracker* construct containing a mutation that prevents binding to DmPI31 (nutcrackerV-E) or a DmPI31 construct (PI31).

We then investigated if the inability of the mutated rescue construct to restore fertility is caused by persistent DmPI31 cleavage. We prepared total lysates from the partially rescued lines followed by Western blot analysis and found that hsp83-nutcrackerV-E;*nutcracker*$^{ms771/ms771}$ still displayed DmPI31 cleavage (Figure 5.4A), albeit less than in the original *nutcracker*^{ms771} mutant line. This indicates that the interaction between Nutcracker and DmPI31 is important for Nutcracker's role in stabilizing DmPI31, and that this stabilization is crucial for proper sperm differentiation.

If Nutcracker functions through DmPI31 stabilization to promote caspase activation and sperm differentiation, it may be possible to at least partially compensate for the loss of Nutcracker function by expressing DmPI31. We over-expressed DmPI31 in a *nutcracker*^{ms771} mutant background and observed partial restoration of caspase staining (Figure 5.4B). This suggests that Nutcracker activates caspases, at least in part, by stabilizing DmPI31. According to this interpretation, Nutcracker is dispensable for caspase activation if sufficient amounts of full-length DmPI31 are expressed in spermatids. Taken together, our results demonstrate that Nutcracker and DmPI31 need to physically interact for their full biological activities.

Figure 5.4: Nutcracker controls caspase activation and sperm individualization by promoting DmPI31 stability

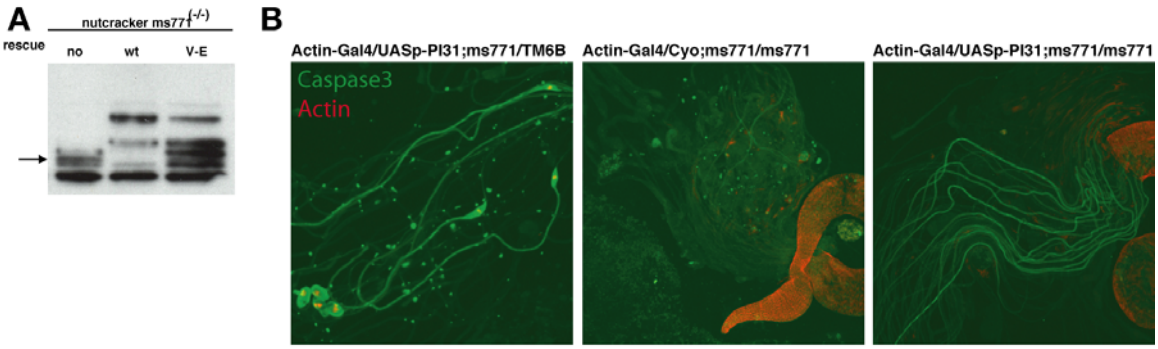

Figure 5.4 **[A]** DmPI31 stability is dependant on Nutcracker binding. Total testes lysates from *nutcracker*^{ms771} mutants expressing the indicated rescue constructs were used to detect steady-state DmPI31 protein levels. hsp83-nutcracker and hsp83-nutcrackerV-E rescue construct are labeled wt and V-E respectively. The cleaved form of DmPI31 found in nutcracker mutants is indicated by an arrow. The lowest molecular weight band is unspecific and serves as loading control. **[B]** Ectopic expression of DmPI31 rescues caspase3 staining in mutant *nutcracker* testes during individualization. Compared to non-PI31 expressing testes (middle panel), *nutcracker*^{ms771} homozygote mutant testes that are expressing DmPI31 (right panel) have activated caspases, as detected by the active-caspase3 antibody. Heterozygote *nutcracker*^{ms771} that are expressing DmPI31 (left panel) were used as a positive control to show no independent effects of DmPI31 expression. Cysts from the indicated genotypes were stained with DAPI (nuclei, blue), phalloidin (IC, red) and caspase-3 (cytoplasm, green).

5.3.6 DmPI31 can modulate 26S proteasomes *in vitro*

PI31 proteins were first identified as inhibitors of the catalytic particle of the proteasome based on the ability of recombinant bovine PI31 protein to inhibit purified 20S proteasomes (Chu-Ping et al., 1992; McCutchen-Maloney et al., 2000; Zaiss et al., 1999). Subsequent studies confirmed these results for mouse and human PI31 and also demonstrated PI31's ability to compete with 19S and 11S regulatory particles which resulted in a net inhibitory effect (McCutchen-Maloney et al., 2000).

In order to further understand the molecular role of *Drosophila* PI31 in regulating spermatogenesis, we investigated its effect on the proteasome's peptidase activity. We utilized the standard fluorogenic assay that measures the rate of hydrolysis of the peptide suc-LLVY-amc by the proteasome's chymotrypsin-like site. DmPI31 was expressed in *E. coli*, purified and added to purified mammalian 20S proteasomes. As expected, DmPI31 inhibited the activity of this enzyme, as has been found previously with the homologous mammalian PI31 proteins (Figure 5.5A). Surprisingly, when purified DmPI31 was added to mammalian 26S proteasomes, its peptidase activity was enhanced up to 3-fold (Figure 5.5A). Thus, when the 20S CP is associated with the 19S RP (and possibly various other interacting proteins), DmPI31 enhances proteasome function, in contrast to the inhibitory effect on purified 20S CP.

The capacity of 26S and 20S proteasomes to degrade these small peptides is determined by whether the gate for its substrate-entry channel is in its open conformation, and in the 26S particle, this entry is regulated by the ATPases in the 19S (Abdelwahid and Smith, 2007). Such an effect on gating could be mediated by DmPI31's C-terminus Hydrophobic-Tyrosin-X (HbYX) motif. Consistently, we found that mutant DmPI31

protein lacking the HbYX motif could still activate the 26S, but with a reduced efficiency (Figure 5.5B). Indeed, removing the HbYX motif results in a 60% decrease in affinity to the proteasome. These data indicate that DmPI31, despite its original designation as a proteasome inhibitor, can function as an activator of the 26S proteasome, which is the dominant form *in vivo* (Besche et al., 2009).

5.3.7 Ectopic expression of DmPI31 can increase proteasome activity *in vivo*

We conducted a series of genetic studies to determine whether DmPI31 can affect proteasome activity *in vivo.* For this purpose, we analyzed whether expression of DmPI31 had an effect on phenotypes caused by impaired proteasome function. Targeted expression of the dominant temperature sensitive proteasome alleles UAS-DTS5 and UAS-DTS7 with GMR-Gal4 causes a small, rough eye phenotype when raised at 29°C (Belote and Fortier, 2002) (Figure 5.5C and 5.5D). Co-expression of DmPI31 with these constructs suppressed this phenotype, resulting in increased eye size and restoration of ommatidial structure (Figure 5.5E). In this experiment, DmPI31 expression was able to override the inhibitory effect of mutations in the catalytic subunits of the proteasome. This result supports the conclusion that DmPI31 can increase proteasome activity *in vivo* and suggests that DmPI31 functions as a proteasome activator.

To further investigate the role of DmPI31 in regulating the proteasome in this assay, we checked if its carboxy terminal HbYX motif is important for this activity. We removed this motif from our DmPI31 expression construct and tested if it was still able to suppress proteasome mutant phenotypes. Compared to the full-length protein, the truncated construct was less efficient in suppressing the rough eye phenotypes, because

despite restoring eye size, more melanotic tissue was observed (Figure 5.5F). This indicates that the DmPI31 HbYX motif is necessary (but not sufficient) to modulate proteasome activity. Furthermore, our results suggest that DmPI31 is a proteasome activator and that its activity is inhibited in *nutcracker* mutants.

Figure 5.5: DmPI31 modulates proteasomes *in vitro* and *in vivo*

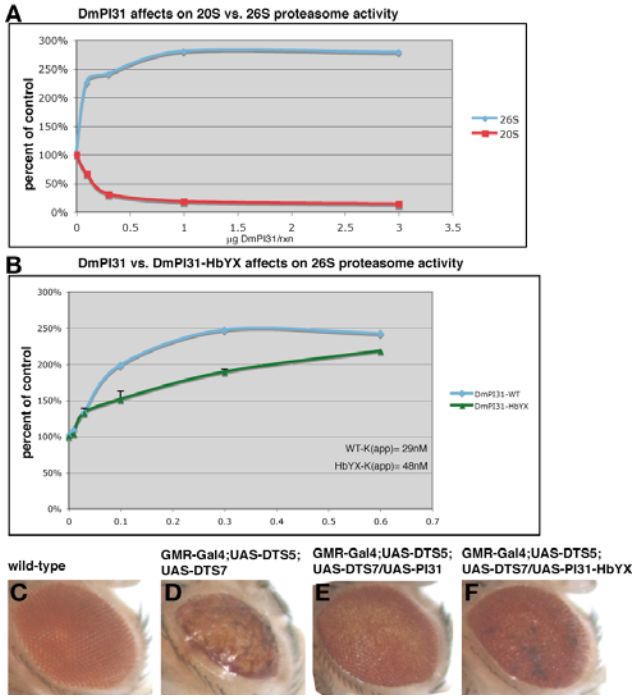

Figure 5.5 **[A-B]** *In vitro* proteasome activity assays using Suc-LLVY-AMC substrate. Rates are plotted relative to that of the control sample lacking DmPI31. For each concentration, the rates are calculated from three different readings within an experiment, and each experiment was repeated at least three times. **[A]** DmPI31 is an inhibitor of 20S but an activator of the 26S proteasomes. Increasing concentrations of purified DmPI31 were used and the effect on the activity of purified bovine 20S or 26S proteasomes was monitored by rate of fluorogenic substrate hydrolysis. 0.15μg 20S or 0.05μg 26S were used per reaction. **[B]** DmPI31 lacking the HbYX motif displays reduced ability to activate mammalian 26S proteasomes. These experiments were preformed as in [A] with 26S proteasomes. The K(app) was calculated by using the concentration of DmPI31 or DmPI31-HbYX at saturation. **[C-F]** DmPI31 expression suppresses proteasome mutant phenotypes in the adult eye. **[C]** Wild-type eye. **[D]** The dominant negative temperature sensitive mutants UAS-DTS5 and UAS-DTS7 cause a small rough eye phenotype when targeted to the eye with the GMR-Gal4 driver. **[E]** The rough eye phenotype is suppressed by co-expressing full-length DmPI31. **[F]** DmPI31 without its C' terminal HbYX motif is a less efficient suppressor, as more melanotic tissue is observed. For more details, see material and methods.

5.3.8 DmPI31 is required for proteasome function

In order to determine the physiological function of *dmPI31*, we generated loss-of-function mutations in this gene by homologous recombination (Figure 5.6S1)(Gong and Golic, 2003). *dmPI31* mutants are recessively lethal and die at the late third instar larval/early pupal transition, a developmental stage where many cell cycle mutants are lethal (Gatti and Baker, 1989) (Axton et al., 1994). Mutant larvae also develop melanotic tumors, are slower to develop and smaller (Figure 5.6S2). All these phenotypes can be rescued by transgenic expression of *dmPI31* (using UASt-HA-PI31 transgenic flies under the control of the tubulin-Gal4, tubulin Gal80^{ts} promoters at 23°C), demonstrating that the mutant phenotypes are caused by loss of *dmPI31* function. On the other hand, over-expression of DmPI31 caused lethality (data not shown). These findings indicate that cells are highly sensitive to the amounts of PI31, since both elimination of the gene or over-expression are detrimental and cause organismal lethality.

Amongst the many cellular processes regulated by the UPS is cell cycle progression. We therefore examined whether *dmPI31* mutants have cell cycle defects, focusing on the male germ line. By expressing *dmPI31* transgenically in somatic cells we were able to rescue lethality and generate viable "mosaic" adults that lack *dmPI31* function in germ cells because germ cells use a different *tubulin* promoter than somatic cells (Kemphues et al., 1980) (Hoyle et al., 1995). When the testes of these flies were dissected, they appeared irregular and exhibited a meiotic arrest phenotype (Bai et al., 1996). This phenotype is characterized by the abundance of underdeveloped 16 cell stage cysts, which fail to undergo proper meiosis. Antibody staining against DmPI31

confirmed the absence of protein in both the germ-line cells (GSCs) and primary spermatocytes (Figure 5.6A).

Next, we stained testes with cell cycle markers. BrdU staining at the tip of the testes closest to the hub was similar to the wild-type, indicating that mitosis of germ-line cells proceeded normally (Figure 5.6B). In contrast, when we stained with the phospho-histone3 (PH3) antibody, which labels dividing nuclei, we did not detect cysts in the 32-cell stage, suggesting that these cells are not undergoing meiosis (Figure 5.6C). Furthermore, staining with the Vasa antibody, which is specific for germ cell progenitors, showed that loss of *dmPI31* function prevents germ cell differentiation and leads to persistence of progenitor identity (Figure 5.6D) (Chang et al., 2005). Moreover, we saw that cyclin B, a protein important for both mitotic and meiotic cell cycles, which is degraded by the proteasome during the final stages of meiosis, also persisted in these cells (Figure 6E)(Fuller, 1998). These results are consistent with the idea that loss of *dmPI31* impairs proteasome function and that DmPI31 is a proteasome activator.

To further test whether *dmPI31* mutants have reduced proteasome activity, we stained testes with the FK2 antibody, which detects Ub-conjugated proteins and can therefore be used to visualize poly-ubiquitinated, non-degraded proteins that accumulate when 26S proteasome function is impaired (Fujimuro et al., 1997) (Haas et al., 2007). In wild type cells, FK2 staining was diffuse in the cytoplasm and strong in the nucleus of meiotic cells (Figure 5.6F). In contrast, in *dmPI31* mutant cells, punctate staining was seen in most cells, and in some cases in one or two nuclei of each cyst. This pattern of staining suggests that proteasome activity is defective, and that Ub-conjugates accumulate as intracellular aggregates. Taken together, our results show that *dmPI31* is

required for proper protein degradation and cell cycle progression, supporting a role of this protein as a proteasome activator.

Figure 5.6S1: *dmPI31* mutants generated by homologous recombination

Figure 5.6S1 **[A]** Genetic scheme for the generation *dmPI31* homologous recombination mutants. Flies carrying the genetic targeting construct (GTC) were generated (see Materials and Methods) and crossed to flies carrying 70Flp, 70I-SceI, which excise and linearize the construct. The resulting white eyed progeny (some containing germ-line integration of the targeting construct in the correct region) were crossed to 70Flp to remove residual GTC. Individual red-eye progeny of this cross was balanced and checked for absence of *dmPI31* genomic region. For more details, see Materials and Methods and (Gong and Golic, 2003; Gong and Golic, 2004). **[B]** DmPI31 RNA is eliminated in $dmPI31^{HR}$ mutants. RT-PCR analysis on mRNA taken from either $dmPI31^{HR}$ heterozygote or homozygote larvae (#11) (sorted by the presence or absence of GFP balancer chromosome) failed to detect mRNA amplification of dmPI31 transcript in the mutant. Tubulin primers were used as an internal control for total mRNA levels. **[C]** DmPI31 protein is eliminated in $dmPI31^{HR}$ mutants. Protein lystes from either wild-type (yw) or $dmPI31^{HR}$ (#10 and #11) homozygote mutant pupa was used to observe DmPI31 protein levels by western blot analysis. This analysis failed to detect DmP31 protein in the mutants. The additional non-specific bands are used as loading controls.

Figure 5.6S2: *dmPI31* mutants arrest at the late third instar larval/early pupal transition, and develop melanotic tumors

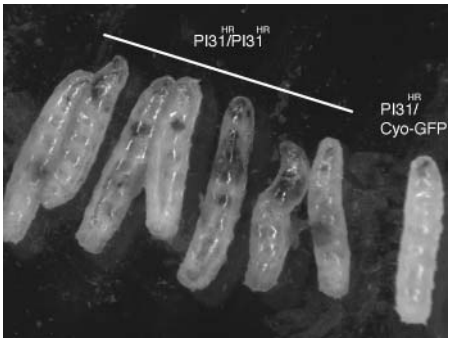

Figure 5.6S2 Light microscopy images of second-third instar *dmPI31*^{HR} mutants. At 25°C, the larva die as late instar larva after developing melanotic tumors (90%-100% of larva display varying amount of tumors). At room-temperature (23-24°C), most larva survive to pupation but arrest immediately thereafter, and display dark necrotic tissue throughout the pupal case. Mutants were sorted by the presence or absence of GFP balancer chromosome. A *dmPI31*^{HR} heterozygote (PI31^{HR}/CyO-GFP) larva is shown for comparison.

Figure 5.6S3: *dmPI31* mosiac testes display a 'meiotic arrest' phenotype

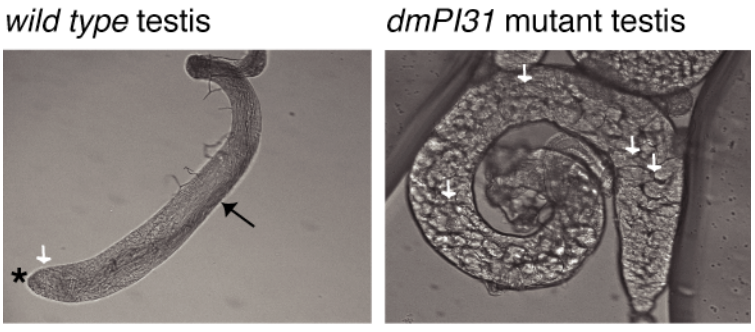

Figure 5.6S3 Light microscopy images of intact testes. The wild-type testis inhabits all stages of cyst differentiation, including GSCs (asterisks), primary spermatocytes (white arrow) and strands of elongated cysts (arrow). *dmPI31* mutant testes feature a "bag-of-marbles" phenotype, resulting from an abundance of undifferentiated 16-cell stage cysts (circular structures, some are marked by white arrow).

Figure 5.6 **[A-F]** *dmPI31* mutants display cell-cycle defects. The right panel depicts wild-type testes, while the left depicts DmPI31 mutants that have been rescued to adulthood. **[A-A`]** DmPI31 antibody staining (green). The wild type testis displays staining in germ-line stem cells (GSCs) and primary spermatocytes. This staining is lost in *dmPI31* mutant testes. The inset depicts a larger magnification of the apical tip, where these cells reside. **[B-B`]** BrdU incorporation assay to detect dividing GSCs. Anti-BrdU staining (green) after incorporation is detected at the epical tip of the wild type testis, marking mitotic divisions. Similar incorporation is detected in the *dmPI31* mutant testis, showing that mitotic divisions are undergoing normally. Nuclei are stained with DAPI (blue). **[C-C`]** Phospho-histone3 (PH3) antibody staining (green), which marks meiotic divisions. The PH3 antibody stains dividing nuclei, and therefore detects cells that are undergoing either mitosis or meiosis. Compared to wild-type testis, which displays staining in the nuclei of 32 cell cysts, no staining is detected in cysts of the *dmPI31* mutant testis, suggesting that meiosis is stunted. An arrow points to a 32-cell cyst (enlarged in inset) where PH3 staining is detected in wild type. **[D-D`]** Anti-Vasa antibody staining (green). This antibody is specific for germ cell progenitors. During normal differentiation, Vasa staining is strongest in GSCs and primary spermatocytes, and disappears when cells approach meiosis. By contrast, *dmPI31* mutant testes contain cyst with persistent Vasa staining, indicating that these cells maintain progenitor identity and fail to differentiate. **[E-E`]** CyclinB staining. CyclinB is normally detected in 16 cell stage cysts and disappears just before meiosis completes. In *dmPI31* mutant cells, CyclinB persists in 16-cell stage cysts, indicating that its degradation is misregulated. **[F-F`]** FK2 staining of ubiquitin-conjugated proteins. FK2 detects the abundance of poly-ubiquitnated proteins and is thus a detector of proteasome activity. In normal germ-line cells (a pre-meiotic cyst is circled), FK2 staining is diffuse, and prominent staining is detected in differentiating nuclei (asterisks in separate cyst). In contrast, most *dmPI31* mutant cells display punctate staining (arrows point to poly-ubiquitnated protein clusters), indicating accumulation of non-degraded poly-ubiquitinated proteins.

Figure 5.6: *dmPI31* is required for proteasome function *in vivo*

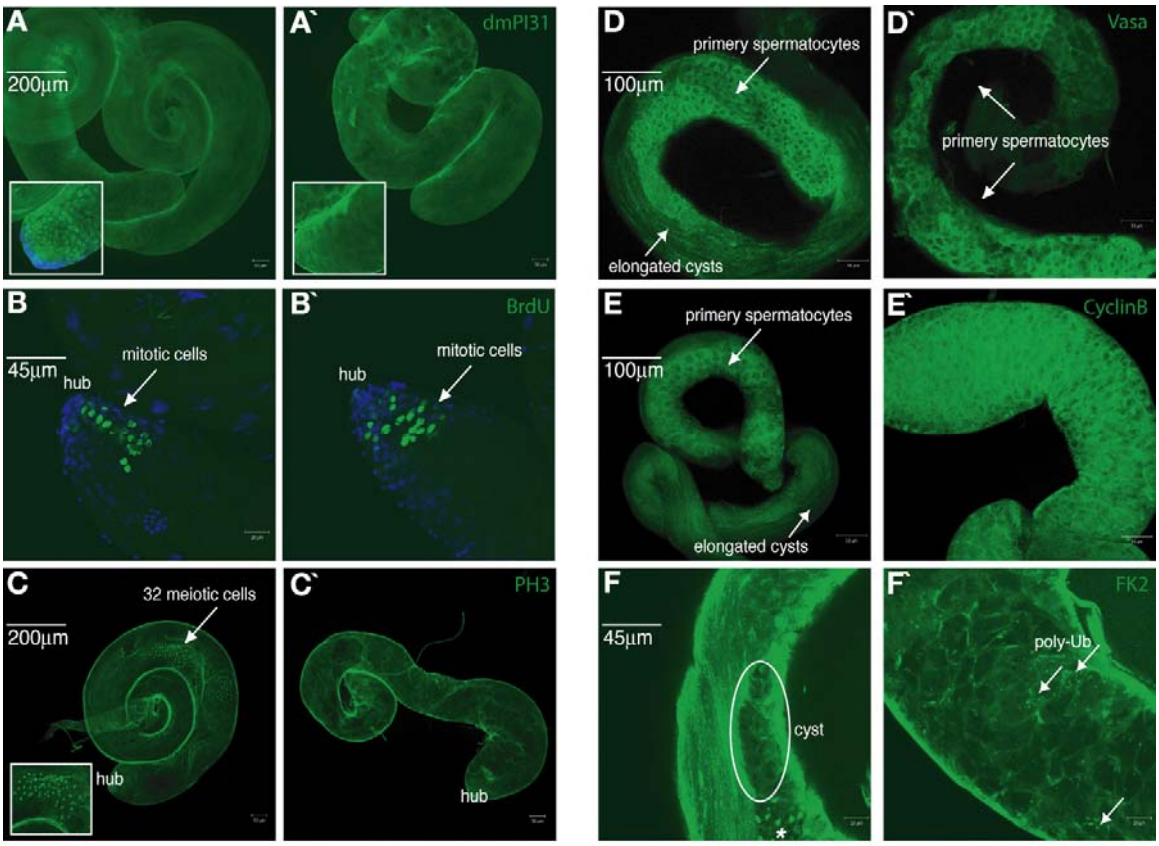

5.4 Materials and methods

Fly strains. *yw* flies were used as wild-type controls. The Zuker mutant Z3-4692 (ms771) was obtained from C.S. Zuker (UCSD); the osk[301]/TM3 and osk[CE4]/TM3 lines from R. Lehmann (NYU School of Medicine); w^{1118};70FLP,70ISceI and w^{1118};70FLP lines from L.B. Vosshall (The Rockefeller University); tubulin-Gal4 from HD. Ryoo; UAS-DTS5 and UAS-DTS7 were obtained from J. Belote (Syracuse University); the deficiency lines Df(2R)BSC199 and Df(2R)ED2247 and the PBac insertion PBac(A et al.)CG10855^{f07259} from the Bloomington Stock Center, as were tubulin-Gal80^{ts} and actin-Gal4.

Constructs and clones

DGRC clone LD12948 was used to amplify *nutcracker* ORF. For testes expression of tagged proteins, ProteinA (PrA) tag was cloned into CaSpeR-4 containing the Don-Juan promotor, and full-length *nutcracker* (ntc) was cloned in frame to it (DJ-PrA-ntc) (see Chapter 4). ΔFbox was created by PCR amplification of *Nutcracker* without the last 174 nucleotides, and this product was also cloned in frame into CaSpeR-4-DJ-PrA (DJ-PrA-ntcΔF) (see Chapter 4). Transgenic flies were created by injecting w^{1118} flies with these constructs. For cell culture experiments, the same inserts were amplified and cloned into a UAS_t plasmid containing the PrA tag at the N-terminus (UAS_t-PrA-ntc and UAS_t-PrA-ntcΔF) (primers 1+2 and 1+3 respectively). The V-E mutation in DJ-nutcracker was created with the Quick Change Site-Directed Mutagenesis Kit (Stratagene) (UAS_t-PrA-ntcV-E) (primers 4+5). For rescuing *nutcracker*^{ms771} mutant phenotypes, *nutcracker* ORF was amplified by PCR and cloned into pHSP83(5'-3'UTRs) (Arama et al., 2006), which contained the 5' and 3' UTRs of *Cytochrome-c-d* (hsp83-ntc) (see Chapter 4). The

V-E mutation in this construct was created with the Quick Change Site-Directed Mutagenesis Kit (Stratagene) (hsp83-ntc-V-E) (primers 4+5).

DGRC clone GH01278 was used to amplify *dmPI31* ORF. For cell culture IP experiments, *dmPI31* ORF was amplified and cloned into UAS_t that contained an HA tag at the N-terminus (UASt-HA-DmPI31) (primers 6+7). The I96E,I103E mutations were created with the Quick Change Site-Directed Mutagenesis Kit (Stratagene) (UASt-HA-DmPI31-I96E,I103E) (primers 8+9). For rescuing *dmPI31* mutant phenotypes and over-expression experiments, these constructs were injected into w^{1118} flies and transgenic fly lines were created. For rescuing of *nutcracker*^{ms771} caspase staining, HA-*dmPI31* was amplified and cloned into UASp (primers 10+11), which expresses better in the germ line (Rorth, 1998), and this construct was used to create transgenic fly lines. For antibody generation and recombinant protein purification, *dmPI31* ORF was amplified and cloned into pET101/D-TOPO (Invitrogen) (primers 11+12), which contains a C' terminal His-tag or into pET28a(+) (Novagen), which contains an N' His-tag. Elimination of the HbYX motif was achieved by introducing a premature stop codon with the Quick Change Site-Directed Mutagenesis Kit (Stratagene) (primers 13+14).

For homologous recombination, BACPAC clone BACR14L19 (Children's Hospital Oakland Research Institute) was used to amplify 5' and 3' ~5 kb homology fragments flanking *DmPI31* (primers 16-19). These were cloned into CMC105 (a gift from L. Vosshall).

Immunoprecipitations

For testes-IP, testes were dissected in IP buffer (50mM Hepes pH7.5, 150mM NaCl, 15mM MgCl2, 10% glycerol, 1% TritonX100, 1mM EDTA, 1mM DTT), homogenized

and spun at 14,000 rpm for 15 minutes at 4°C. Equal amounts of protein were assessed by Bradford assay (Biorad) and incubated for 2 hrs at 4°C with Dynabeads (Invitrogen) that were conjugated to rabbit IgG according to the manufacture's protocol. The beads were washed five times in lysis buffer (except that detergent was reduced to 0.1%), and eluted in SDS loading buffer by boiling. For the S2 cell IP, cells were transfected (Fugene6, Roche), and left to express for 36-48 hrs. The cells were washed twice in ice-cold PBS, lysed in 200µl ice-cold 1% NP-40 in PBS, left on ice for 15 minutes, then spun at 14,000 rpm for 15 minutes at 4°C. The IP was then conducted similarly to the testes IP, except the washes were done with ice-cold PBS. 0.5-1mg of total-protein was used for IP-Western, and 7-10mg for mass-spectrometry identification.

Mass spectrometry analysis

After co-immunoprecipitation, the isolated proteins were resolved by SDS-PAGE (5%–15% gradient) and stained with Coomassie Blue (GelCode Blue; Pierce). The visible bands were excised and subjected to trypsin digestion. The resulting peptides were extracted, and proteins were identified by mass spectrometry at the Rockefeller University Proteomics Resource Center. Peptides sequences were analyzed using the MASCOT search engine (http://www.matrixscience.com/).

Western Blot Analysis

Testes that were dissected in lysis buffer (20mM Hepes pH7.6, 150mM NaCl, 10% glycerol, 1% TritonX100, 2mM EDTA, 1mM DTT) and lysed as in IP experiments. Protein concentration was determined by Bradford assay (Biorad), and 30-50µg total-protein, dissolved in SDS loading buffer, was separated by SDS-PAGE. After transfer, the immobilon-P membrane (Milipore) was blocked with 5% milk in TBST (0.1%

tween20 in PBS) for 1 hour, and incubated with primary antibody overnight at 4^{o} c. The membrane was then washed 3 times in TBST, incubated in HRP-conjugated secondary antibody for 1 hour, and washed 3 more times with TBST before developing with ECL reagents (Amersham) and Kodak Biomax MR film. The following antibodies and dilutions were used: anti-DmPI31[sera], 1:1000, anti-HA, 1:5000 (Roche), anti-alpha7, 1:200 (Biomol).

RNA extraction and RT-PCR

Total RNA extraction and RT-PCR was carried out as in Chapter 3. To amplify *DmPI31* RNA, primers corresponding to the ORF were used. Amplification after 25 cycles is shown, which is 5 cycles before saturation (data not shown). Amplification of *tubulin* RNA was used as a control, using primers corresponding to 500bp of the gene (primers 20+21).

Antibody generation and tissue staining Cleaved effector caspase antibody staining of young (0–2 day old) adult testes was carried out as described in (Arama et al., 2007) using a rabbit polyclonal anti-cleaved Caspase-3 (Asp175) antibody (Cell Signaling Technology) diluted 1:75. The only changes are that the subsequent TRITC-phalloidin (Sigma) incubation for staining of actin filaments was carried out during incubation with the secondary antibody and the slides were subsequently rinsed twice for 10 min in PBS. Anti-DmPI31 was created by injecting guinie-pigs with full-length recombinant DmPI31 (Cocalico Biologicals, Inc.) (see purification procedure bellow), and the staining was carried out as described in (Hime et al., 1996), with the generated serum diluted 1:250. Staining of unopened testes and BrdU incorporation was conducted as in (Beall et al., 2002), with the following antibodies and dilutions: mouse anti-BrdU-FITC (1:100, BD-

Pharmingen), rabbit anti-Vasa (1:100, a gift from R. Lehmann), mouse anti-CyclinB clone F2F4 (1:10, DSHB) and mouse FK2 (1:100, Stressgen).

Purification of recombinant DmPI31

A 1 liter culture of BL21 cells expressing TOPO-His-DmPI31 was grown at 37°C to O.D 0.6. Expression was then induced 0.5mM IPTG for 1.5 hours at 37°C. The cell were pelleted, frozen, and thawed on ice for 20 minutes. The pellet was resuspended with 30ml Lysis buffer (50 mM NaH_2PO_4, 300mM NaCl, 10mM Immidizole, 0.05% Tween pH 7.0), on ice for an additional 20 minutes. The mixture was then sonicated for 20 minutes (10X 30 seconds + 1 minutes break). After centrifugation (14,000 rpm for 30 minutes at 4°C), the supernatant was loaded onto a 3ml HisPur Cobalt Spin Columns (Pierce), according to the manufacturers' protocol – using the lysis buffer as wash. The protein was eluted with elution buffer (50 mM NaH_2PO_4, 300mM NaCl, 250mM Immidizole, 0.05% Tween pH 7.0).

For proteasome activity assay, the protein was eluted with elution buffer (50mM Tris pH 7.5 300mM Immidizole 300mM NaCl), it was then dialyzed in 50mM Tris pH7.5 and 5% glycerol.

Sterility testing

0-2 day old individual males (20-30) were crossed to 2-3 virgin females and the emergence of living progeny was assed every 2-3 days for two weeks. Males were rendered sterile if no progeny was detected after this time period.

Proteasome activity assay

To measure proteasome activity, the fluorogenic peptide substrate Suc-LLVY-amc (Enzo Life Sciences, maintained in DMSO) was used at a final concentration of 100 μM in

reaction buffer (50mM Tris, 5% glycerol). Hydrolysis of suc-LLVY-amc was monitored at λ_{ex} 380 nm and λ_{em} 440 nm. All reactions were conducted in a 96-well plate and read on a SpectraMax M2 micro-plate reader (Molecular Devices). For experiments on 20S proteasomes, 0.05-0.15µg of purified Bovine 20S was used per 100µl reaction, at 37°C. For experiments on 26S proteasomes, 0.05µg of purified Bovine 26S was used per 100 µl reaction, in the same buffer plus 10mM mgCl and 100µM ATP, at 37ºC. K(apparent) was calculated with the standard ligand binding equation using sigmaplot (www.sigmaplot.com) using DmPI31 concentration at saturation as maximal affinity.

DTS5-DTS7 disruption of eye development

UAS-DTS5/CyO;UAS-DTS7/TM6B, UAS-DTS5/CyO;UAS-DTS7/UAS-HA-PI31, UAS-DTS5/UAS-PI31;UAS-DTS7/TM6B (not shown) or UAS-DTS5/CyO;UAS-DTS7/UAS-HA-PI31-HbYX were grown at 29°C throughout their lifecycle, and the affects on eye development were monitored after enclosure. UAS-DTS5/UAS-GFP;UAS-DTS7/TM6B or UAS-DTS5/CyO;UAS-DTS7/UAS-GFP (not shown) were used as negative controls to show that the affects were not due to UAS copy number.

Homologous Recombination

5′ and 3′ homology regions were amplified by Expand High Fidelity PCR (Roche) from BACPAC clone BACR14L19 (GenBank entry AC007474, Children's Hospital Oakland Research Institute) with primers corresponding to nucleotides 81,075–81,098/85,257–81,098 (5′arm = 4.201 kb fragment) and 86,124–86,144/90,179–90,200 (3′arm = 4.076 kb fragment) of this BAC clone. These primers contained AvrII and AscI sites flanking the 5'arm fragment and NotI and NheI flanking the 3'arm fragment, which were cloned into these sites in CMC105 (a gift from L. Vosshall, see scanned plasmid map). This

vector contains two polylinkers flanking the mini-white gene with a unique I-SceI site 5′ of the *white* gene, flanked by FRT sites and conventional P element repeats. This construct was designed to delete the whole ORF of *dmPI31* replacing it with the eye color marker, *white*.

Virgin female flies carrying one of three independently generated targeting construct insertions on the third chromosome were crossed to w^{1118};70FLP, 70I-SceI, Sco/CyO. To expand the progeny from each cross, each vial contained 10-15 females and 5-10 males, and the flies were transferred to a new vial every 2-3 days for ~10 days. 3-day-old progeny from each vial were heat shocked at 37°C for 1 hour. Approximately 30,000 progeny were screened for white-eyed adult virgin females, which were crossed to w^{1118};70FLP males. The cross scheme and heat shock of progeny was conducted as described above. ~200,000 resulting adult progeny was screened for the reappearance of red-eyed flies, which were individually balanced to establish stable lines (Figure 5.6S1A). Of 20 mutant alleles obtained, 13 were gene replacements, as detected by complementation analysis of these recessively lethal lines. The deficiency lines Df(2R)BSC199 and Df(2R)ED2247, corresponding to regions 48C5-48E4 and 48A3-48D5 respectively, which contain the *DmPI31* genomic region, failed to complement this lethality. The deletion of *DmPI31* was confirmed in three lines by RT-PCR and Western-blot analysis of second instar larve lysates (Figure 5.6S1B+C). As indicated in the main text, the recessive lethality in these lines was rescued by reintroducing a transgenic insertion of *DmPI31* ORF.

Table 5.2 – Primer list

	Primer name	Sequence	Forward res. site	Reverse res. site	Into plasmid
1	PrA-CG10855 Forward EcoRI	CGAGAATTCATGGGTGAAGCTCAAAAACT	EcoRI		UASt
2	CG10855 -coding-reverse-XbaI	CGATCTAGAAGCTTCTGCCGCCCTTTAGC		XbaI	UASt
3	CG10855 ΔF-coding-reverse-XbaI	CGATCTAGAGTTGCTGCGATCGCATGGGC		XbaI	UASt
4	CG10855 -rescue-QC-V-E -F	GTGCCGGCTGATGGCCGAGAGCCTGGGGGA TCAGC			pHSP83 (5'3'-UTRs)
5	CG10855 -rescue-QC-V-E R	GCTGATCCCCCAGGCTCTCGGCCATCAGCCG GCAC			pHSP83 (5'3'-UTRs)
6	DmPI31-Forward-NotI	AAATATGCGGCCGCCATGGAAAGTGGGTCG ACTGC	NotI		UASt
7	DmPI31-	CCGCTCGAGTTACATGTAGTAATCGGGAT		XhoI	UASt

	reverse-Xho				
8	DmPI31 QC-Ile96-103 F	GTCCAACAGGTTTTCCAGCAGGGAGCCCTCG GTTTCGTGGCCCAGC			UASt
9	DmPI31 QC-Ile96-103 R	GCTGGGCCACGAAACCGAGGGCTCCCTGCT GGAAAACCTGTTGGAC			UASt
10	HA-DmPI31-forward-NotI	AAATATGCGGCCGCCATGTACCCGTACGAC GTCCC	NotI		UASp
11	DmPI31-reverse-SpeI	GACTAGTTTACATGTAGTAATCGGGAT		SpeI	UASp
12	DmPI31-TOPO-Forward	CACCATGGAAAGTGGGTCGACTGC			pET101/D-TOPO
13	DmPI31-TOPO-Reverse	CATGTAGTAATCGGGATTCC			pET101/D-TOPO
14	DmPI31 QC-HbYX F	CTTGGCAGTCGACCCACTTTCCATGGCGGCC GCGCCAGCATAGTC			pET28a(+)/ UASt-HA-PI31/UASp-HA-PI31

15	DmPI31 QC-HbYXF	GACTATGCTGGCGCGGCCGCCATGGAAAGTGGGTCGACTGCCAAG			pET28a(+)/UASt-HA-PI31/UASp-HA-PI31
16	HR-5'-arm-Forward	ATGGCGCGCCTTAGAAGCAACCGAAGTGTGGG	AscI		CMC105
17	HR-5'-arm-Reverse	ATCCTAGGACCAGATTGGAATCCCGATTACTAC		AvrII	CMC105
18	HR-3'-arm-Forward	AGCAGCGCGGCCGCCCCAACCGTAAAAGAAATCGC	NotI		CMC105
19	HR-3'-arm-Reverse	GCTGCTCCGCGGGAGGAACGACCAAAGCAGGCGG		NheI	CMC105
20	Beta_tub (56D) Forward (490 from end)	CAGATGTTCGATGCCAAGAA			For RT-PCR
21	Beta_tub (56D) Rev(stop)	TTAGTTCTCGTCGACCTCAG			For RT-PCR

6. Discussion

6.1 A male sterile screen for regulators of caspase activation

The work described in this thesis originated in a screen for mutants that are defective in activating caspases, potent proteases, at the onset of spermatid terminal differentiation. The screen utilized a collection of more than 1000 male sterile lines that were previously described as having morphological defects at the final stage of the differentiation process, termed individualization. During this stage, the bulk cytoplasm and excess organelles are removed to create highly motile sperm. I hypothesize that caspases are aiding the elimination process by either partially degrading sub-cellular compartments, or by cleaving cytoplasmic substrates that lead to partial degeneration. In either case, caspase activation is necessary for proper differentiation, as all but one of caspase-negative mutants isolated from this screen or by others are male sterile (Huh et al., 2004) (Muro et al., 2006).

Given the potency of these caspases, it is likely that their regulation is tightly controlled to prevent the degeneration of the entire cell. Initial work uncovered the role of known caspase regulators in this process, such as Dark and Hid (Arama et al., 2003), (Arama et al., 2006; Huh et al., 2004), but since mutations in these genes only resulted in a partial caspase activation deficiency, it appeared plausible that other regulators in this process have yet to be discovered. Mutations in only one known caspase regulator, *cytochrome-c-d*, displayed completely abrogated caspase staining. The screen was thus based on finding other genes that are completely caspase deficient, in order to find new caspase regulators and to understand how the cells avoid overall death.

The screen uncovered 33 mutant lines that fell into 22 genetic complementation groups. These displayed a range of other morphological phenotypes, from mitochondrial defects, to improper bundling of the nuclei to defective IC formation. Nonetheless, since all the individualization mutants that we screened displayed morphological defects but only a small subset were caspase-deficient (< 3%), I believe that caspase activation in this system is governed by specific regulators or processes immediately associated with caspase regulation. In this regard, the isolation of caspase-activation mutants that also display mitochondrial defects implies that, as in normal apoptosis, signaling through this organelle is important for activating caspases. A plausible hypothesis is that the degeneration of the minor mitochondrial lobe during the individualization process facilitates the release of caspase activators, such as Cytochrome-c. Indeed, Cytochome-c-d is localized to mitochondrial 'whorls' as the IC moves down the length of the spermatids (Arama et al., 2006). A more careful analysis of mitochondrial morphology in the caspase negative mutants, or probing the mitochondrial localization of the genes important for caspase activation in this system, would shed light on this interesting connection.

One of the mutants that we isolated in our screen is a point mutation in *cytochrome-c-d*. This not only emphasized the role this protein plays in caspase activation, but also validated the screen as a successful tool for the isolation of specific caspase regulators. The success of the screen was further affirmed by mapping other mutants that were isolated. Two of the complementation groups mapped to components of the same protein complex – a Cullin-3 Ub-ligase. The isolation of proteins from the same complex demonstrates that the screen was sensitive and specific.

The fruitfulness of this screen in producing relevant mutants demonstrates yet again that the Zucker male sterile collection is a valuable resource for not only understanding the complexity of sperm differentiation, but also as a way of approaching cell biological problems. In this case, non-apoptotic caspase activation is a phenomenon not limited to *Drosophila* spermatids, and this system provides a tractable means of studying it *in vivo*. Moreover, some aspects of spermatid differentiation are reminiscent of other partial degeneration processes in similar looking cells, such as pruning of axons and dendrites, and genes important during spermatogenesis are also required in other processes. One such example is the RNA binding protein, Boule. Boule was originally discovered for its role in spermatocyte differentiation (Castrillon et al., 1993; Haynes et al., 1997), but has been recently implicated in dendritic pruning during metamorphosis (Hoopfer et al., 2008). Another example is *purity-of-essence* (*poe*), mutations which cause individualization defects, but also motor neuron problems (Castrillon et al., 1993) (Fabrizio et al., 1998; Richards et al., 1996). These examples demonstrate that unraveling the genes that regulate spermatogenesis, with the help of the Zucker collection, might help answer questions in other systems as well.

6.2 A new role of the ubiquitin-proteasome system (UPS) in caspase regulation

Ubiquitin pathway proteins have well-established roles in the regulation of the cell cycle, DNA damage checkpoint, signal transduction and in the regulation of apoptosis (Broemer and Meier, 2009; Jesenberger and Jentsch, 2002; Nakayama and Nakayama, 2006) (Hershko, 1997; Isaksson et al., 1996; Pagano, 1997). Although ubiquitination was originally described as a degradation signal, ubiquitin modification

has since been characterized to lead to other outcomes besides degradation. The diversity of these ubiquitin-type modifications places ubiquitin or ubiquitin-like (UBLs) ligases as major players in complex regulatory networks, much like kinases and phosphotases.

The E3 ligases described in this thesis, a Cullin-3-based complex and an SCF E3 ubiquitin ligase complex have not been previously shown to have direct roles in caspase activation. It is unlikely that these E3 ligases regulates caspases at the mRNA level, since transcripts of effector caspase *drice* and initiator caspase *dronc* are present in $cul3^{mds1}$ or $nutcracker^{ms771}$ mutant testes (data not shown). A more likely model is that they promote degradation of a caspase inhibitor (Figure 6.1A). According to this model, the ubiquitination and degradation of this hypothetical caspase inhibitor at the onset of spermatid individualization would de-repress effector caspases and promote sperm differentiation. The best characterized family of endogenous caspase inhibitors is the Inhibitor of Apoptosis Protein (IAP) family (Bader and Steller, 2009; Bergmann et al., 2003. Diap1 is essential for the survival of most, if not all somatic cells {Goyal, 2000 #29; Ditzel and Meier, 2005; Hays et al., 2002; Kuranaga et al., 2006; Ryoo et al., 2002; Salvesen and Duckett, 2002; Wang et al., 1999; Wilson et al., 2002). Still, it appears that Diap1 is not the relevant caspase inhibitor in this context. If Diap1 was a major substrate for Cullin-3- or Nutcracker- mediated protein degradation, we would have expected to see a marked increase of this protein in the isolated mutants. However, no significant differences in Diap1 protein levels were detected between wild type and *cullin3T*, *klhl10* or $nutcracker^{ms771}$ mutant testes.

A more likely candidate is the giant, IAP-like protein dBruce. *dBruce* function is necessary to protect sperm against unwanted caspase activity since loss of *dbruce*

function causes degeneration of spermatid nuclei and male sterility (Agapite, 2002; Arama et al., 2003; Goyal et al., 2000). To further investigate possible interactions between dBruce and the Cullin3-Roc1b-Klhl10 complex, we showed that the substrate recruitment protein, Klhl10, can bind to dBruce, and that its BIR domain is sufficient for this interaction. dBruce can also physically bind Nutcracker, in an interaction that is independent of the F-box domain. These data are consistent with the idea that dBruce could be a common substrate for the Cullin-3-based and SCF E3-ligase complexes isolated in our screen. However, we were unable to determine the steady state levels of dBruce in the mutants, due to the inability of the generated antibody to detect endogenous protein, so it is yet unclear whether it is indeed a substrate or a complex partner.

The isolation of two different ubiquitin ligases from the screen indicates that caspase activation in this system is tightly controlled by ubiquitin modifications. These two complexes could regulate the stability of the same substrate, as is the case for regulation of *Cubitus interruptus* (*Ci*) stability in *hedgehog* signaling by both Cullin-1 and Cullin-3 based complexes (Jiang, 2006; Ou et al., 2002), or target multiple important substrates. Alternatively, they may play non-degradative roles in controlling caspase activity. For instance, mono-ubiquitination affects the targeted localization of proteins (Haglund and Dikic, 2005). Another possibility is that these E3-ligases mediate the non-classical Lys-63 ubiquitin chain addition that is important for protein-protein interaction. Therefore, these ubiquitin-ligases may control the proper localization of or control interactions between caspase regulators.

6.3 Molecular similarities between *Drosophila* and mammalian spermatogenesis

A recent report suggested that mammalian Klhl10 and Cullin-3 can interact *in vitro,* and that Cullin-3 is highly expressed during late murine spermatogenesis (Wang et al., 2006). In addition, Klhl10 was shown to be exclusively expressed in the cytoplasm of developmentally advanced murine spermatids, and mice carrying a null *klhl10* allele are infertile due to defects during late spermatid maturation (Yan et al., 2004b). These data suggest that a similar E3 complex may function in late mammalian spermatogenesis, and that the defects in *klhl10* mutant mice may be due to lack of caspase-3 activity. Despite apparent anatomical differences between insect and mammalian spermiogenesis, there are similarities in the removal of bulk spermatid cytoplasm. As occurs in insects, intracellular bridges between spermatids and the bulk of the cytoplasm are eliminated during mammalian spermatogenesis. In addition, residual bodies, which contain the extruded cytoplasm of the mammalian spermatids, show high levels of active caspase-3 expression and may be homologous to the insect "waste bag" (Blanco-Rodriguez and Martinez-Garcia, 1999; Kissel et al., 2005). Furthermore, targeted deletion of the mouse *Sept4* locus, which encodes the pro-apoptotic protein ARTS, causes defects in the elimination of residual cytoplasm during sperm maturation (Kissel et al., 2005). Finally, a recent study reported a high frequency of mutations in *klhl10* from infertile oligozoospermic men (Yatsenko et al., 2006). These intriguing anatomical and molecular similarities between spermatid individualization processes in *Drosophila* and mammals suggest that further studies on the link between the UPS and apoptotic proteins during sperm differentiation in *Drosophila* may provide new insights into the etiology of some forms of human infertilities.

6.4 The isolation of a conserved proteasome regulatory complex

In this study, I also identified and characterized a proteasome regulatory complex that combines two distinct components of the UPS – an F-box protein (Nutcracker), which usually catalyzes ubiquitin conjugation to a set of substrates, and a proteasome regulator (DmPI31), which directly controls substrate hydrolysis by the proteasome. Although several studies have reported the physical association between certain Ub-ligases and the 26S proteasome, I now demonstrate a clear functional significance of this interaction *in vivo* (Demartino and Gillette, 2007; Finley, 2009). I show that the F-box protein Nutcracker and the proteasome regulator DmPI31 function together as a complex to control non-apoptotic caspase activation and sperm differentiation. Furthermore, their interaction is mediated through their FP domain, a conserved domain found in mammalian homologues {Kirk, 2008 #330}. I therefore propose that this complex represents a new and conserved mode of proteasomal regulation.

6.4.1 Nutcracker and DmPI31 interact through a conserved FP domain

DmPI31 was discovered in a screen for physical interactors of the F-box protein Nutcracker, but unlike the typical subunits of an SCF ubiquitin ligase complex (Bader et al., 2010; Bader, 2010; Kipreos and Pagano, 2000), DmPI31's interaction with Nutcracker does not require the F-box domain. Instead, it utilizes another domain, the FP domain of both Nutcracker and DmPI31. This interaction is structurally conserved with the mammalian F-box protein FBXO7 and PI31 (Kirk et al., 2008). FBXO7 has a unique role of regulating both the cell cycle (by binding CDK6 (Laman et al., 2005)) and

apoptosis (by mediating the ubiquitination of cIAP1 (A et al., 2006)). The interaction described here might help explain this dual role, as the Nutcracker-DmPI31 complex regulates both cell-cycle progression and caspase activation. In this respect, given that Nutcracker functions predominantly in testes, while DmPI31 has a more general developmental role, it is possible that PI31 pairs with different F-box proteins in other settings.

6.4.2 Nutcracker controls caspase activation and sperm individualization by promoting DmPI31 stability

I initially considered that DmPI31 might be a substrate of the Nutcracker-containing SCF E3-ligase complex. However, I found that DmPI31 protein did not accumulate in *nutcracker* mutants, as would be expected if it were a substrate. Instead, a *nutcracker* mutant that carries a stable but truncated F-box domain (*nutcracker*^{ms771}) resulted in the cleavage and truncation of DmPI31. Hence, the Nutcracker F-box domain is important for the stability of full-length DmPI31 (Figure 6.1B). This stabilization has a functional role in caspase activation and sperm differentiation, because a *nutcracker* transgene with reduced ability to bind DmPI31 showed persistent DmPI31 cleavage and did not fully rescue *nutcracker* mutant phenotypes. Additionally, over-expression of DmPI31 in a *nutcracker* mutant background resulted in partial restoration of caspase activation. This suggests that physical interaction with DmPI31 is important for Nutcracker activity, that Nutcracker acts upstream of DmPI31 to control its stability, and that the levels of active (full-length) DmPI31 need to be carefully regulated to mediate proper caspase activation and spermatid remodeling.

It is still unclear whether Nutcracker and PI31 forms a complex that regulate proteasome activity, or if Nutcracker is an actual PI31 regulator. PI31 mutant germ cells arrest at an earlier developmental stage than do Nutcracker mutants that arrest at the onset of individualization. Because Nutcracker is only required later suggests that it may be necessary at a certain time point to change PI31 dynamics or stability as its regulator. Another possibility is that Nutcracker is needed to regulate PI31 sub-cellular localization at this stage. Examining DmPI31 localization at the different stages of spermatid differentiation, its co-localization with Nutcracker and the proteasome, and how these are affected in *nutcracker* mutant background would further expand our understanding on the relationship between DmPI31 and Nutcracker. Furthermore, if Nutcracker mediates the ubiquitination of DmPI31, it is more likely that Nutcracker is a DmPI31 regulator. Figuring whether Nutcracker ubiquitinates DmPI31, and the type of ubiquitination (mono-, Lys-63 or Lys-48) would demonstarte such an interaction.

If Nutcracker is not a regulator of PI31, it could be that the two form a complex to control caspase activation and other aspects of differentiation by directly modulating proteasome activity. An alternative model proposes that Nutcracker sequesters DmPI31 onto the proteasome, possibly to couple ubiquination and proteasome activation in order to facilitate local degradation (Figure 6.1B). By virtue of binding DmPI31, or by an F-box mediated protection, Nutcracker prevents proteasome-dependant cleavage of DmPI31 activity domain. Thus, when *nutcracker* is mutated, DmPI31's functional domain is cleaved, causing the observed defects. The careful examination of binding dynamics between PI31, Nutcracker and the proteasome would distinguish the different possibilities (see below).

6.4.3 DmPI31 is a proteasome activator

Despite its original identification as a proteasome inhibitor (PI), DmPI31 can activate purified 26S proteasomes. The ability of DmPI31 to enhance the degradation of standard tetrapeptide substrates implies a role in promoting the opening of the substrate-entry channel, a property exhibited by other proteasome activating complexes (Abdelwahid and Smith, 2007; Al-Said et al., 2008). In line with this, DmPI31's C-terminal HbYX motif, which resembles the proteasome-interacting, gate-opening domains on the proteasome-regulatory ATPases, is also important for DmPI31's *in vivo* effects (Abdelwahid and Smith, 2007; Al-Said et al., 2008). Furthermore, transgenes without this motif can no longer rescue *dmPI31* lethality (data not shown).

Activation of the 26S particle by DmPI31 is consistent with the phenotypes of *dmPI31* mutants. Loss of *dmPI31* function causes lethality, indicating that this gene has a vital function, presumably by regulating proteasome activity in the soma. Germ-line cells lacking *dmPI31* fail to undergo meiosis and maintain stem cell identity. These phenotypes are consistent with defects in protein degradation (Alessandrini et al., 1997; Fuller, 1998). Accordingly, we observed that poly-ubiquitinated proteins accumulate in *dmPI31* mutant germ-cells, proving strong evidence for insufficient proteasome activity. Furthermore, expressing DmPI31 was able to suppress the phenotypes of proteasome mutants. This indicates that elevated levels of DmPI31 can boost the reduced proteasome activity in these mutants. Taken together, all these results argue that DmPI31 is a proteasome activator. Nonetheless, more can be learnt by studying the somatic phenotypes of *dmPI31* mutants. Does abnormal proteasome activity results in the lethal phenotypes, which lead to cell-cycle abnormalities?

Another interesting question that arises from these results is the mechanism by which PI31 activate the proteasome. Does PI31 form an alternative cap or does it enhance the housekeeping (26S) proteasome? Alternately, does it stabilize the 26S proteasome? These could be addressed by conducting careful PI31-proteasome binding assays to understand the mechanism and stoichometry of this interaction. If PI31 requires Nutcracker to bind, or if it associates with the 19S particle rather than 20S, a reasonable model is that the Nutcracker-PI31 interaction stabilizes the 26S proteasome by docking both particles together. Another outcome could be if multiple PI31 molecules are found on a single proteasome (as could be asserted by determining stoichometry), which would suggest that PI31 forms an alternative cap. In this scenario, Nutcracker (or other F-box proteins) could target specific substrates to this alternative proteasome. Some of these questions could also be answered by conducting Electron microscopy on purified *Drosophila* proteasomes and PI31 (as in (Smith et al., 2005)). These types of experiments could show how the addition of PI31 affects the proteasome; does it increase binding between the 19S and 20S particles? Do new types of proteasomes form? How are the outcomes changed by the addition of truncated or HbYX mutants?

6.5 Controlled proteolysis during cellular remodeling

Our findings may have important implications not only on the study of caspase regulation, but also on the role of regulated proteolysis during cellular remodeling and transformation. An interesting question raised by our results is how spermatids can survive high levels of apoptotic effector caspase activity. Since transgenic ectopic expression of the effector caspase drICE leads to spermatid death (data not shown), we

propose that caspase activity in spermatids is restricted to specific sub-cellular compartments. A related phenomenon has been observed during the caspase-dependent pruning of neurites (Kuo et al., 2006; Williams et al., 2006). This process is similar to spermatid individualization in that it uses the apoptotic machinery for the destruction of parts of a cell (Awasaki et al., 2006; Kuo et al., 2006; Watts et al., 2003; Williams et al., 2006). Interestingly, a requirement for the Ubiquitin-Proteasome-System in the process of axon pruning was also reported (Watts et al., 2003). These similarities suggest that the processes of axon pruning and spermatid individualization may use similar mechanisms to restrain the activity of apoptotic proteins for cellular remodeling. In neurons, synaptic activity can lead to proteasome re-distribution and local degradation of synaptic proteins (Bingol and Schuman, 2005; Bingol and Schuman, 2006; Bingol et al.). Likewise, it is possible that the proposed caspase inhibitor is only locally degraded, which would allow for localized caspase activity in developing spermatids.

During individualization, the majority of proteasomes are also located in a distinct sub-cellular pattern in spermatids, near the minor mitochondrial lobes and sites of membrane rearrangements (Arama et al., 2006; Zhong and Belote, 2007) (Alenina et al., 2009) (Sigalit Benjamin and Hermann Steller unpublished). It is possible that local proteasome activity facilitates mitochondrial degradation, or local degradation of mitochondrial proteins that lead to caspase activation.

Sperm differentiation involves a major reduction in cell volume and can be viewed, from a cell biological standpoint, as ‘programmed cell atrophy’. Like in neuronal pruning and individualization, intracellular proteolysis mediated by both proteasomes and caspases is associated with various pathologies that involve cell and

tissue wasting, such as myopathies (Lecker et al., 2006) (Luo and O'Leary, 2005; Raff et al., 2002; Ventadour and Attaix, 2006), but also as facilitators of cellular and tissue wasting during disease (Lecker et al.) (Saxena and Caroni, 2007). Our results reveal an unexpected new link in the regulation of both capases and proteasomes. Therefore, it is possible that the protein complexes isolated in this study play a role in diseases that are associated with excessive protein turnover.

Figure 6.1 **[A]** A genetic screen for genes that promote caspase activation uncovered two E3 ubiquitin- ligase complexes. The first, a Cullin-3 based complex, contains the substrate binding protein Klhl10. Klhl10 utilizes the BTB domain to bind Cullin-3 and a Kelch domain to bind substrates. In this study, it was shown that a testis specific TeNC domain in Cullin-3 is used to bind Klhl10. Mutations in the TeNC, BTB or Kelch domains resulted in complete loss of caspase staining, indicating that the formation of this complex, and the ability to bind substrates is crucial for caspase activation. The second complex, an SCF (Skp-Cullin-F-box), contains Cullin-1 as its scaffolding protein, the F-box protein Nutcracker as its substrate binding module, and SkpA to attach them. F-box proteins use their F-box domain to bind the SCF complex. In the *nutcracker* mutant, a truncation of this domain results in complete lack of caspase staining, indicating that caspase activation is dependant on SCF complex formation. Our model proposes that these ligase complexes promote the degradation of a caspase inhibitor, possibly dBruce, which accumulates in the mutants. The lingering inhibitor prevents the activation of caspases. Furthermore, the decreased proteasome activity in *nutcracker* mutants suggests that Nutcracker, independently or as part of the SCF complex, is promoting caspase activation through its action on the proteasome. This complex can modify proteins that activate the proteasome, which could include, for example, DmPI31 (PI31). Caspase activation could then be facilitated by ubiquitin-mediated regulation. **[B]** A model for Nutcracker-DmPI31 proteasome regulation complex. Our model suggests that Nutcracker and DmPI31 form a complex during sperm-cell differentiation that regulates proteasome activity and subsequent caspase activation. Nutcracker binds DmPI31 through an amino terminal FP domain, and protects DmPI31 proline-rich carboxy terminal region through its F-box domain. The protection could be mediated through Nutcrackers Ub-ligase activity, or through direct binding. The carboxy-terminal region contains the HbYX motif and other sequences important for DmPI31 activity on proteasomes. Thus, when *Nutcracker* is mutated, DmPI31's functional domain is cleaved, causing defects in proteasome and caspase activation. A possible mode of action could be that Nutcracker sequesters DmPI31 onto the proteasome, possibly to couple ubiquination and proteasome activation in order to facilitate local degradation.

Figure 6.1 Model

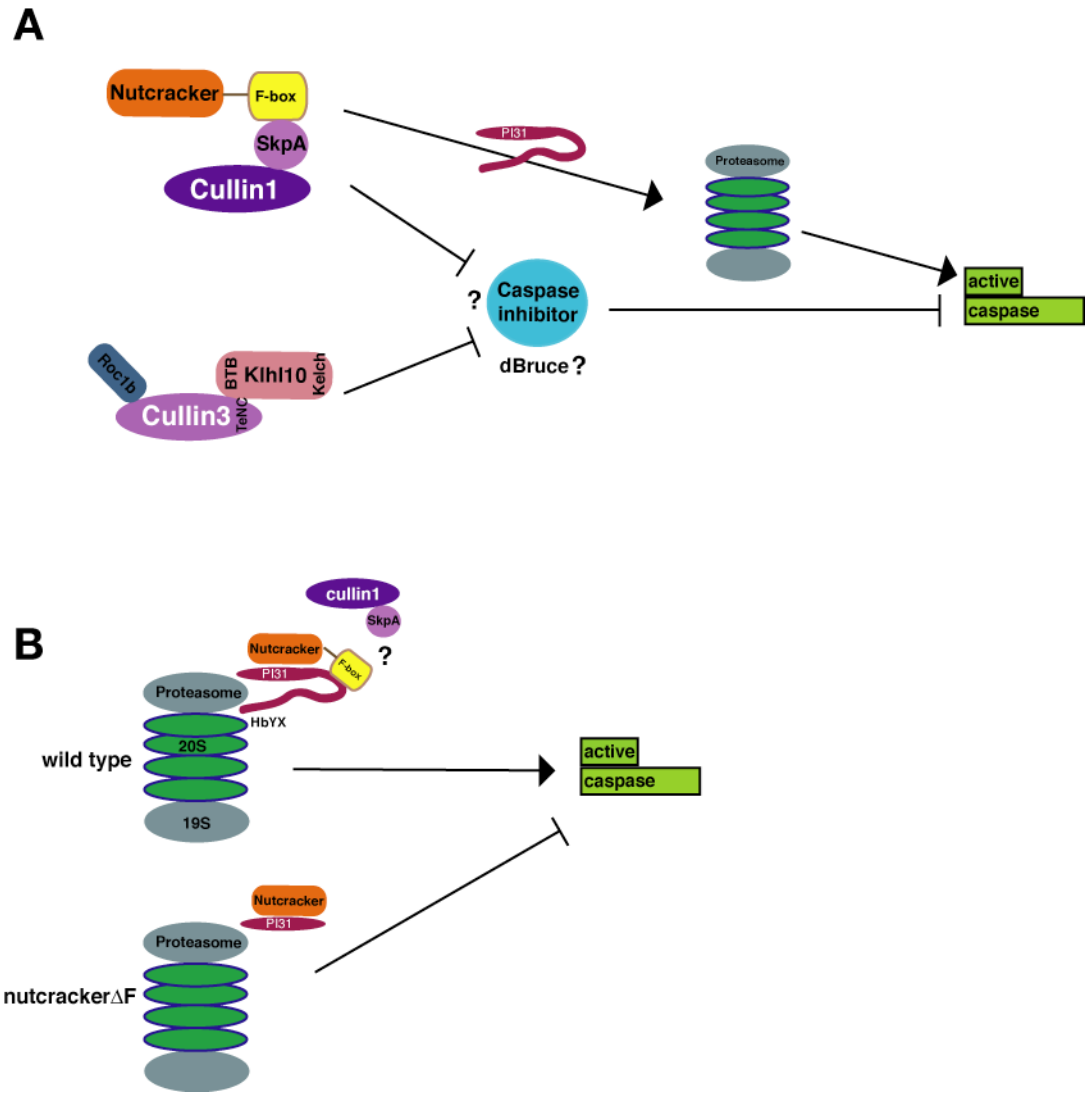

7. References

A, B., A, S., A, D. and V, G. (2006). Cardiorespiratory compromise under conscious sedation during upper gastrointestinal endoscopy. *J Coll Physicians Surg Pak* **16**, 585-9.

Abdelwahid, E. and Smith, G. (2007). Apoptosis in chronic heart failure. *Int J Cardiol* **114**, 375.

Abdelwahid, E., Yokokura, T., Krieser, R. J., Balasundaram, S., Fowle, W. H. and White, K. (2007). Mitochondrial disruption in Drosophila apoptosis. *Dev Cell* **12**, 793-806.

Abraham, M. C. and Shaham, S. (2004). Death without caspases, caspases without death. *Trends Cell Biol* **14**, 184-93.

Adrain, C., Creagh, E. M., Cullen, S. P. and Martin, S. J. (2004). Caspase-dependent inactivation of proteasome function during programmed cell death in Drosophila and man. *J Biol Chem* **279**, 36923-30.

Agapite, J. (2002). Genetic analysis of programmed cell death on Drosophila melanogaster. . *Ph.D. thesis, Department of Biology, Massachusetts Institute of Technology*.

Al-Said, S., Al-Naimi, A., Al-Ansari, A., Younis, N., Shamsodini, A., K, A. s. and Shokeir, A. A. (2008). Varicocelectomy for male infertility: a comparative study of open, laparoscopic and microsurgical approaches. *J Urol* **180**, 266-70.

Alenina, N., Kikic, D., Todiras, M., Mosienko, V., Qadri, F., Plehm, R., Boye, P., Vilianovitch, L., Sohr, R., Tenner, K. et al. (2009). Growth retardation and altered autonomic control in mice lacking brain serotonin. *Proc Natl Acad Sci U S A* **106**, 10332-7.

Alessandrini, A., Chiaur, D. S. and Pagano, M. (1997). Regulation of the cyclin-dependent kinase inhibitor p27 by degradation and phosphorylation. *Leukemia* **11**, 342-5.

Anderson, C., Crimmins, S., Wilson, J. A., Korbel, G. A., Ploegh, H. L. and Wilson, S. M. (2005). Loss of Usp14 results in reduced levels of ubiquitin in ataxia mice. *J Neurochem* **95**, 724-31.

Appleby, D. W. and Modak, S. P. (1977). DNA degradation in terminally differentiating lens fiber cells from chick embryos. *Proc Natl Acad Sci U S A* **74**, 5579-83.

Arama, E., Agapite, J. and Steller, H. (2003). Caspase activity and a specific cytochrome C are required for sperm differentiation in Drosophila. *Dev. Cell* **4**, 687-97.

Arama, E., Bader, M., Rieckhof, G. E. and Steller, H. (2007). A ubiquitin ligase complex regulates caspase activation during sperm differentiation in Drosophila. *PLoS Biol* **5**, e251.

Arama, E., Bader, M., Srivastava, M., Bergmann, A. and Steller, H. (2006). The two Drosophila cytochrome C proteins can function in both respiration and caspase activation. *Embo J.* **25**, 232-43.

Arbeitman, M. N., Furlong, E. E., Imam, F., Johnson, E., Null, B. H., Baker, B. S., Krasnow, M. A., Scott, M. P., Davis, R. W. and White, K. P. (2002). Gene expression during the life cycle of Drosophila melanogaster. *Science* **297**, 2270-5.

Ardley, H. C. and Robinson, P. A. (2005). E3 ubiquitin ligases. *Essays Biochem* **41**, 15-30.

Ashburner, M., Thompson, P., Roote, J., Lasko, P. F., Grau, Y., el Messal, M., Roth, S. and Simpson, P. (1990). The genetics of a small autosomal region of Drosophila melanogaster containing the structural gene for alcohol dehydrogenase. VII. Characterization of the region around the snail and cactus loci. *Genetics* **126**, 679-94.

Awasaki, T. and Ito, K. (2004). Engulfing action of glial cells is required for programmed axon pruning during Drosophila metamorphosis. *Curr Biol* **14**, 668-77.

Awasaki, T., Tatsumi, R., Takahashi, K., Arai, K., Nakanishi, Y., Ueda, R. and Ito, K. (2006). Essential role of the apoptotic cell engulfment genes draper and ced-6 in programmed axon pruning during Drosophila metamorphosis. *Neuron* **50**, 855-67.

Axton, J. M., Shamanski, F. L., Young, L. M., Henderson, D. S., Boyd, J. B. and Orr-Weaver, T. L. (1994). The inhibitor of DNA replication encoded by the Drosophila gene plutonium is a small, ankyrin repeat protein. *Embo J* **13**, 462-70.

Bader, M., Benjamin, S., Wapinski, O., Smilth, D., Goldberg, A. and Steller, H. (2010). A F-box–modulator complex controls proteasome activity

in Drosophila

. *submitted*.

Bader, M. and Steller, H. (2009). Regulation of cell death by the ubiquitin-proteasome system. *Curr Opin Cell Biol*.

Bader, M. A. E. S. H. (2010). A novel F-box protein is required for caspase activation during cellular remodeling in Drosophila

. *Development* **accepted**.

Bai, C., Sen, P., Hofmann, K., Ma, L., Goebl, M., Harper, J. W. and Elledge, S. J. (1996). SKP1 connects cell cycle regulators to the ubiquitin proteolysis machinery through a novel motif, the F-box. *Cell* **86**, 263-74.

Bartke, T., Pohl, C., Pyrowolakis, G. and Jentsch, S. (2004). Dual role of BRUCE as an antiapoptotic IAP and a chimeric E2/E3 ubiquitin ligase. *Mol Cell* **14**, 801-11.

Bassnett, S. (1992). Mitochondrial dynamics in differentiating fiber cells of the mammalian lens. *Curr Eye Res* **11**, 1227-32.

Bassnett, S. (1995). The fate of the Golgi apparatus and the endoplasmic reticulum during lens fiber cell differentiation. *Invest Ophthalmol Vis Sci* **36**, 1793-803.

Bassnett, S. (2002). Lens organelle degradation. *Exp Eye Res* **74**, 1-6.

Bassnett, S. and Beebe, D. C. (1992). Coincident loss of mitochondria and nuclei during lens fiber cell differentiation. *Dev Dyn* **194**, 85-93.

Bassnett, S. and Mataic, D. (1997). Chromatin degradation in differentiating fiber cells of the eye lens. *J Cell Biol* **137**, 37-49.

Beall, E. L., Manak, J. R., Zhou, S., Bell, M., Lipsick, J. S. and Botchan, M. R. (2002). Role for a Drosophila Myb-containing protein complex in site-specific DNA replication. *Nature* **420**, 833-7.

Belote, J. M. and Fortier, E. (2002). Targeted expression of dominant negative proteasome mutants in Drosophila melanogaster. *Genesis* **34**, 80-2.

Belote, J. M., Miller, M. and Smyth, K. A. (1998). Evolutionary conservation of a testes-specific proteasome subunit gene in Drosophila. *Gene* **215**, 93-100.

Benaroudj, N., Zwickl, P., Seemuller, E., Baumeister, W. and Goldberg, A. L. (2003). ATP hydrolysis by the proteasome regulatory complex PAN serves multiple functions in protein degradation. *Mol Cell* **11**, 69-78.

Bergmann, A., Yang, A. Y. and Srivastava, M. (2003). Regulators of IAP function: coming to grips with the grim reaper. *Curr Opin Cell Biol* **15**, 717-24.

Besche, H., Haas, W., Gygi, S. and Goldberg, A. (2009). Isolation of mammalian 26S proteasomes and p97/VCP complexes using the ubiquitin-like domain from HHR23B reveals novel proteasome-associated proteins. *Biochemistry*.

Bingol, B. and Schuman, E. M. (2005). Synaptic protein degradation by the ubiquitin proteasome system. *Curr Opin Neurobiol* **15**, 536-41.

Bingol, B. and Schuman, E. M. (2006). Activity-dependent dynamics and sequestration of proteasomes in dendritic spines. *Nature* **441**, 1144-8.

Bingol, B., Wang, C. F., Arnott, D., Cheng, D., Peng, J. and Sheng, M. Autophosphorylated CaMKIIalpha Acts as a Scaffold to Recruit Proteasomes to Dendritic Spines. *Cell* **140**, 567-578.

Blanco-Rodriguez, J. and Martinez-Garcia, C. (1999). Apoptosis is physiologically restricted to a specialized cytoplasmic compartment in rat spermatids. *Biol Reprod* **61**, 1541-7.

Blankenship, J. W., Varfolomeev, E., Goncharov, T., Fedorova, A. V., Kirkpatrick, D. S., Izrael-Tomasevic, A., Phu, L., Arnott, D., Aghajan, M., Zobel, K. et al. (2009). Ubiquitin binding modulates IAP antagonist-stimulated proteasomal degradation of c-IAP1 and c-IAP2(1). *Biochem J* **417**, 149-60.

Borissenko, L. and Groll, M. (2007). 20S proteasome and its inhibitors: crystallographic knowledge for drug development. *Chem Rev* **107**, 687-717.

Bose, S., Stratford, F. L., Broadfoot, K. I., Mason, G. G. and Rivett, A. J. (2004). Phosphorylation of 20S proteasome alpha subunit C8 (alpha7) stabilizes the 26S proteasome and plays a role in the regulation of proteasome complexes by gamma-interferon. *Biochem J* **378**, 177-84.

Bre, M. H., Redeker, V., Quibell, M., Darmanaden-Delorme, J., Bressac, C., Cosson, J., Huitorel, P., Schmitter, J. M., Rossler, J., Johnson, T. et al. (1996). Axonemal tubulin polyglycylation probed with two monoclonal antibodies: widespread evolutionary distribution, appearance during spermatozoan maturation and possible function in motility. *J Cell Sci* **109 (Pt 4)**, 727-38.

Bre, M. H., Redeker, V., Vinh, J., Rossier, J. and Levilliers, N. (1998). Tubulin polyglycylation: differential posttranslational modification of dynamic cytoplasmic and stable axonemal microtubules in paramecium. *Mol Biol Cell* **9**, 2655-65.

Broemer, M. and Meier, P. (2009). Ubiquitin-mediated regulation of apoptosis. *Trends Cell Biol* **19**, 130-40.

Cardozo, T. and Pagano, M. (2004). The SCF ubiquitin ligase: insights into a molecular machine. *Nat Rev Mol Cell Biol* **5**, 739-51.

Carlile, G. W., Smith, D. H. and Wiedmann, M. (2004). Caspase-3 has a nonapoptotic function in erythroid maturation. *Blood* **103**, 4310-6.

Cascio, P., Call, M., Petre, B. M., Walz, T. and Goldberg, A. L. (2002). Properties of the hybrid form of the 26S proteasome containing both 19S and PA28 complexes. *Embo J* **21**, 2636-45.

Castrillon, D. H., Gonczy, P., Alexander, S., Rawson, R., Eberhart, C. G., Viswanathan, S., DiNardo, S. and Wasserman, S. A. (1993). Toward a molecular genetic analysis of spermatogenesis in Drosophila melanogaster: characterization of male-sterile mutants generated by single P element mutagenesis. *Genetics* **135**, 489-505.

Cathelin, S., Rebe, C., Haddaoui, L., Simioni, N., Verdier, F., Fontenay, M., Launay, S., Mayeux, P. and Solary, E. (2006). Identification of proteins cleaved downstream of caspase activation in monocytes undergoing macrophage differentiation. *J Biol Chem* **281**, 17779-88.

Cerretti, D. P., Kozlosky, C. J., Mosley, B., Nelson, N., Van Ness, K., Greenstreet, T. A., March, C. J., Kronheim, S. R., Druck, T., Cannizzaro, L. A. et al. (1992). Molecular cloning of the interleukin-1 beta converting enzyme. *Science* **256**, 97-100.

Chai, J., Shiozaki, E., Srinivasula, S. M., Wu, Q., Datta, P., Alnemri, E. S. and Shi, Y. (2001). Structural basis of caspase-7 inhibition by XIAP. *Cell* **104**, 769-80.

Chai, J., Yan, N., Huh, J. R., Wu, J. W., Li, W., Hay, B. A. and Shi, Y. (2003). Molecular mechanism of Reaper-Grim-Hid-mediated suppression of DIAP1-dependent Dronc ubiquitination. *Nat Struct Biol* **10**, 892-8.

Chang, S. W., Lee, S. J. and Je, C. H. (2005). Phytoremediation of atrazine by poplar trees: toxicity, uptake, and transformation. *J Environ Sci Health B* **40**, 801-11.

Chen, F., Hersh, B. M., Conradt, B., Zhou, Z., Riemer, D., Gruenbaum, Y. and Horvitz, H. R. (2000). Translocation of C. elegans CED-4 to nuclear membranes during programmed cell death. *Science* **287**, 1485-9.

Chen, Z., Naito, M., Hori, S., Mashima, T., Yamori, T. and Tsuruo, T. (1999). A human IAP-family gene, apollon, expressed in human brain cancer cells. *Biochem Biophys Res Commun* **264**, 847-54.

Chew, S. K., Akdemir, F., Chen, P., Lu, W. J., Mills, K., Daish, T., Kumar, S., Rodriguez, A. and Abrams, J. M. (2004). The apical caspase dronc governs programmed and unprogrammed cell death in Drosophila. *Dev Cell* **7**, 897-907.

Chipuk, J. E., Fisher, J. C., Dillon, C. P., Kriwacki, R. W., Kuwana, T. and Green, D. R. (2008). Mechanism of apoptosis induction by inhibition of the anti-apoptotic BCL-2 proteins. *Proc Natl Acad Sci U S A* **105**, 20327-32.

Chu-Ping, M., Slaughter, C. A. and DeMartino, G. N. (1992). Purification and characterization of a protein inhibitor of the 20S proteasome (macropain). *Biochim Biophys Acta* **1119**, 303-11.

Chuang, S. M. and Madura, K. (2005). Saccharomyces cerevisiae Ub-conjugating enzyme Ubc4 binds the proteasome in the presence of translationally damaged proteins. *Genetics* **171**, 1477-84.

Clem, R. J. and Miller, L. K. (1994). Control of programmed cell death by the baculovirus genes p35 and iap. *Mol Cell Biol* **14**, 5212-22.

Conradt, B. and Horvitz, H. R. (1998). The C. elegans protein EGL-1 is required for programmed cell death and interacts with the Bcl-2-like protein CED-9. *Cell* **93**, 519-29.

Conte, D., Liston, P., Wong, J. W., Wright, K. E. and Korneluk, R. G. (2001). Thymocyte-targeted overexpression of xiap transgene disrupts T lymphoid apoptosis and maturation. *Proc Natl Acad Sci U S A* **98**, 5049-54.

Conze, D. B., Albert, L., Ferrick, D. A., Goeddel, D. V., Yeh, W. C., Mak, T. and Ashwell, J. D. (2005). Posttranscriptional downregulation of c-IAP2 by the ubiquitin protein ligase c-IAP1 in vivo. *Mol Cell Biol* **25**, 3348-56.

Coux, O., Tanaka, K. and Goldberg, A. L. (1996). Structure and functions of the 20S and 26S proteasomes. *Annu Rev Biochem* **65**, 801-47.

Crook, N. E., Clem, R. J. and Miller, L. K. (1993). An apoptosis-inhibiting baculovirus gene with a zinc finger-like motif. *J Virol* **67**, 2168-74.

Cullen, K. and McCall, K. (2004). Role of programmed cell death in patterning the Drosophila antennal arista. *Dev Biol* **275**, 82-92.

Dahm, R., Gribbon, C., Quinlan, R. A. and Prescott, A. R. (1998). Changes in the nucleolar and coiled body compartments precede lamina and chromatin reorganization during fibre cell denucleation in the bovine lens. *Eur J Cell Biol* **75**, 237-46.

Danial, N. N. and Korsmeyer, S. J. (2004). Cell death: critical control points. *Cell* **116**, 205-19.

De Botton, S., Sabri, S., Daugas, E., Zermati, Y., Guidotti, J. E., Hermine, O., Kroemer, G., Vainchenker, W. and Debili, N. (2002). Platelet formation is the consequence of caspase activation within megakaryocytes. *Blood* **100**, 1310-7.

De Maria, R., Zeuner, A., Eramo, A., Domenichelli, C., Bonci, D., Grignani, F., Srinivasula, S. M., Alnemri, E. S., Testa, U. and Peschle, C. (1999). Negative regulation of erythropoiesis by caspase-mediated cleavage of GATA-1. *Nature* **401**, 489-93.

Degterev, A., Boyce, M. and Yuan, J. (2003). A decade of caspases. *Oncogene* **22**, 8543-67.

del Peso, L., Gonzalez, V. M., Inohara, N., Ellis, R. E. and Nunez, G. (2000). Disruption of the CED-9.CED-4 complex by EGL-1 is a critical step for programmed cell death in Caenorhabditis elegans. *J Biol Chem* **275**, 27205-11.

del Peso, L., Gonzalez, V. M. and Nunez, G. (1998). Caenorhabditis elegans EGL-1 disrupts the interaction of CED-9 with CED-4 and promotes CED-3 activation. *J Biol Chem* **273**, 33495-500.

Demartino, G. N. and Gillette, T. G. (2007). Proteasomes: machines for all reasons. *Cell* **129**, 659-62.

DeMartino, G. N. and Slaughter, C. A. (1999). The proteasome, a novel protease regulated by multiple mechanisms. *J Biol Chem* **274**, 22123-6.

Denecker, G., Hoste, E., Gilbert, B., Hochepied, T., Ovaere, P., Lippens, S., Van den Broecke, C., Van Damme, P., D'Herde, K., Hachem, J. P. et al. (2007). Caspase-14 protects against epidermal UVB photodamage and water loss. *Nat Cell Biol* **9**, 666-74.

Deveraux, Q. L. and Reed, J. C. (1999). IAP family proteins--suppressors of apoptosis. *Genes Dev* **13**, 239-52.

Deveraux, Q. L., Takahashi, R., Salvesen, G. S. and Reed, J. C. (1997). X-linked IAP is a direct inhibitor of cell-death proteases. *Nature* **388**, 300-4.

Ditzel, M., Broemer, M., Tenev, T., Bolduc, C., Lee, T. V., Rigbolt, K. T., Elliott, R., Zvelebil, M., Blagoev, B., Bergmann, A. et al. (2008). Inactivation of effector caspases through nondegradative polyubiquitylation. *Mol Cell* **32**, 540-53.

Ditzel, M. and Meier, P. (2005). Ubiquitylation in apoptosis: DIAP1's (N-)en(d)igma. *Cell Death Differ* **12**, 1208-12.

Ditzel, M., Wilson, R., Tenev, T., Zachariou, A., Paul, A., Deas, E. and Meier, P. (2003). Degradation of DIAP1 by the N-end rule pathway is essential for regulating apoptosis. *Nat Cell Biol* **5**, 467-73.

Donaldson, T. D., Noureddine, M. A., Reynolds, P. J., Bradford, W. and Duronio, R. J. (2004). Targeted disruption of Drosophila Roc1b reveals functional differences in the Roc subunit of Cullin-dependent E3 ubiquitin ligases. *Mol Biol Cell* **15**, 4892-903.

Droin, N., Cathelin, S., Jacquel, A., Guery, L., Garrido, C., Fontenay, M., Hermine, O. and Solary, E. (2008). A role for caspases in the differentiation of erythroid cells and macrophages. *Biochimie* **90**, 416-22.

Eckelman, B. P., Salvesen, G. S. and Scott, F. L. (2006). Human inhibitor of apoptosis proteins: why XIAP is the black sheep of the family. *EMBO Rep* **7**, 988-94.

Ellis, H. M. and Horvitz, H. R. (1986). Genetic control of programmed cell death in the nematode C. elegans. *Cell* **44**, 817-29.

Fabrizio, J. J., Hime, G., Lemmon, S. K. and Bazinet, C. (1998). Genetic dissection of sperm individualization in Drosophila melanogaster. *Development* **125**, 1833-43.

Fan, Y. and Bergmann, A. (2009). The cleaved-Caspase-3 antibody is a marker of Caspase-9-like DRONC activity in Drosophila. *Cell Death Differ*.

Farras, R., Ferrando, A., Jasik, J., Kleinow, T., Okresz, L., Tiburcio, A., Salchert, K., del Pozo, C., Schell, J. and Koncz, C. (2001). SKP1-SnRK protein kinase interactions mediate proteasomal binding of a plant SCF ubiquitin ligase. *Embo J* **20**, 2742-56.

Feinstein-Rotkopf, Y. and Arama, E. (2009). Can't live without them, can live with them: roles of caspases during vital cellular processes. *Apoptosis*.

Fernandez Murray, P., Pardo, P. S., Zelada, A. M. and Passeron, S. (2002). In vivo and in vitro phosphorylation of Candida albicans 20S proteasome. *Arch Biochem Biophys* **404**, 116-25.

Fernando, P., Brunette, S. and Megeney, L. A. (2005). Neural stem cell differentiation is dependent upon endogenous caspase 3 activity. *Faseb J* **19**, 1671-3.

Fernando, P., Kelly, J. F., Balazsi, K., Slack, R. S. and Megeney, L. A. (2002). Caspase 3 activity is required for skeletal muscle differentiation. *Proc Natl Acad Sci U S A* **99**, 11025-30.

Figueroa, P., Gusmaroli, G., Serino, G., Habashi, J., Ma, L., Shen, Y., Feng, S., Bostick, M., Callis, J., Hellmann, H. et al. (2005). Arabidopsis has two redundant Cullin3 proteins that are essential for embryo development and that interact with RBX1 and BTB proteins to form multisubunit E3 ubiquitin ligase complexes in vivo. *Plant Cell* **17**, 1180-95.

Finley, D. (2009). Recognition and processing of ubiquitin-protein conjugates by the proteasome. *Annu Rev Biochem* **78**, 477-513.

Forster, A., Masters, E. I., Whitby, F. G., Robinson, H. and Hill, C. P. (2005). The 1.9 A structure of a proteasome-11S activator complex and implications for proteasome-PAN/PA700 interactions. *Mol Cell* **18**, 589-99.

Fraser, A. G., McCarthy, N. J. and Evan, G. I. (1997). drICE is an essential caspase required for apoptotic activity in Drosophila cells. *Embo J* **16**, 6192-9.

Freel, C. D., Richardson, D. A., Thomenius, M. J., Gan, E. C., Horn, S. R., Olson, M. R. and Kornbluth, S. (2008). Mitochondrial localization of Reaper to promote inhibitors of apoptosis protein degradation conferred by GH3 domain-lipid interactions. *J Biol Chem* **283**, 367-79.

Fujimuro, M., Sawada, H. and Yokosawa, H. (1997). Dynamics of ubiquitin conjugation during heat-shock response revealed by using a monoclonal antibody specific to multi-ubiquitin chains. *Eur J Biochem* **249**, 427-33.

Fujita, J., Crane, A. M., Souza, M. K., Dejosez, M., Kyba, M., Flavell, R. A., Thomson, J. A. and Zwaka, T. P. (2008). Caspase activity mediates the differentiation of embryonic stem cells. *Cell Stem Cell* **2**, 595-601.

Fuller, M. T. (1993). The Development of Drosophila melanogaster: Cold Spring Harbor, NY: Cold Spring Harbor Laboratory Press.

Fuller, M. T. (1998). Genetic control of cell proliferation and differentiation in Drosophila spermatogenesis. *Semin Cell Dev Biol* **9**, 433-44.

Furukawa, M., He, Y. J., Borchers, C. and Xiong, Y. (2003). Targeting of protein ubiquitination by BTB-Cullin 3-Roc1 ubiquitin ligases. *Nat Cell Biol* **5**, 1001-7.

Gatti, M. and Baker, B. S. (1989). Genes controlling essential cell-cycle functions in Drosophila melanogaster. *Genes Dev* **3**, 438-53.

Geisbrecht, E. R. and Montell, D. J. (2004). A role for Drosophila IAP1-mediated caspase inhibition in Rac-dependent cell migration. *Cell* **118**, 111-25.

Geyer, R., Wee, S., Anderson, S., Yates, J. and Wolf, D. A. (2003). BTB/POZ domain proteins are putative substrate adaptors for cullin 3 ubiquitin ligases. *Mol Cell* **12**, 783-90.

Glickman, M. H. and Ciechanover, A. (2002). The ubiquitin-proteasome proteolytic pathway: destruction for the sake of construction. *Physiol Rev* **82**, 373-428.

Glickman, M. H. and Raveh, D. (2005). Proteasome plasticity. *FEBS Lett* **579**, 3214-23.

Goldberg, A. L., Cascio, P., Saric, T. and Rock, K. L. (2002). The importance of the proteasome and subsequent proteolytic steps in the generation of antigenic peptides. *Mol Immunol* **39**, 147-64.

Gong, W. J. and Golic, K. G. (2003). Ends-out, or replacement, gene targeting in Drosophila. *Proc Natl Acad Sci U S A* **100**, 2556-61.

Gong, W. J. and Golic, K. G. (2004). Genomic deletions of the Drosophila melanogaster Hsp70 genes. *Genetics* **168**, 1467-76.

Gottfried, Y., Rotem, A., Lotan, R., Steller, H. and Larisch, S. (2004). The mitochondrial ARTS protein promotes apoptosis through targeting XIAP. *Embo J* **23**, 1627-35.

Goyal, L., McCall, K., Agapite, J., Hartwieg, E. and Steller, H. (2000). Induction of apoptosis by Drosophila reaper, hid and grim through inhibition of IAP function. *Embo J* **19**, 589-97.

Green, D. R. and Kroemer, G. (2004). The pathophysiology of mitochondrial cell death. *Science* **305**, 626-9.

Groettrup, M., Soza, A., Eggers, M., Kuehn, L., Dick, T. P., Schild, H., Rammensee, H. G., Koszinowski, U. H. and Kloetzel, P. M. (1996). A role for the proteasome regulator PA28alpha in antigen presentation. *Nature* **381**, 166-8.

Groll, M., Bajorek, M., Kohler, A., Moroder, L., Rubin, D. M., Huber, R., Glickman, M. H. and Finley, D. (2000). A gated channel into the proteasome core particle. *Nat Struct Biol* **7**, 1062-7.

Groll, M., Ditzel, L., Lowe, J., Stock, D., Bochtler, M., Bartunik, H. D. and Huber, R. (1997). Structure of 20S proteasome from yeast at 2.4 A resolution. *Nature* **386**, 463-71.

Grueber, W. B. and Jan, Y. N. (2004). Dendritic development: lessons from Drosophila and related branches. *Curr Opin Neurobiol* **14**, 74-82.

Guterman, A. and Glickman, M. H. (2004). Complementary roles for Rpn11 and Ubp6 in deubiquitination and proteolysis by the proteasome. *J Biol Chem* **279**, 1729-38.

Haas, K. F., Woodruff, E., 3rd and Broadie, K. (2007). Proteasome function is required to maintain muscle cellular architecture. *Biol Cell* **99**, 615-26.

Haglund, K. and Dikic, I. (2005). Ubiquitylation and cell signaling. *Embo J* **24**, 3353-9.

Haining, W. N., Carboy-Newcomb, C., Wei, C. L. and Steller, H. (1999). The proapoptotic function of Drosophila Hid is conserved in mammalian cells. *Proc Natl Acad Sci U S A* **96**, 4936-41.

Hales, K. G. and Fuller, M. T. (1997). Developmentally regulated mitochondrial fusion mediated by a conserved, novel, predicted GTPase. *Cell* **90**, 121-9.

Hanna, J., Hathaway, N. A., Tone, Y., Crosas, B., Elsasser, S., Kirkpatrick, D. S., Leggett, D. S., Gygi, S. P., King, R. W. and Finley, D. (2006). Deubiquitinating enzyme Ubp6 functions noncatalytically to delay proteasomal degradation. *Cell* **127**, 99-111.

Hanna, J., Meides, A., Zhang, D. P. and Finley, D. (2007). A ubiquitin stress response induces altered proteasome composition. *Cell* **129**, 747-59.

Hao, Y., Sekine, K., Kawabata, A., Nakamura, H., Ishioka, T., Ohata, H., Katayama, R., Hashimoto, C., Zhang, X., Noda, T. et al. (2004). Apollon ubiquitinates SMAC and caspase-9, and has an essential cytoprotection function. *Nat Cell Biol* **6**, 849-60.

Harlin, H., Reffey, S. B., Duckett, C. S., Lindsten, T. and Thompson, C. B. (2001). Characterization of XIAP-deficient mice. *Mol Cell Biol* **21**, 3604-8.

Hawkins, C. J., Wang, S. L. and Hay, B. A. (1999). A cloning method to identify caspases and their regulators in yeast: identification of Drosophila IAP1 as an inhibitor of the Drosophila caspase DCP-1. *Proc Natl Acad Sci U S A* **96**, 2885-90.

Hay, B. A. and Guo, M. (2006). Caspase-Dependent Cell Death in Drosophila. *Annu Rev Cell Dev Biol*.

Hay, B. A., Wassarman, D. A. and Rubin, G. M. (1995). Drosophila homologs of baculovirus inhibitor of apoptosis proteins function to block cell death. *Cell* **83**, 1253-62.

Haynes, S. R., Cooper, M. T., Pype, S. and Stolow, D. T. (1997). Involvement of a tissue-specific RNA recognition motif protein in Drosophila spermatogenesis. *Mol Cell Biol* **17**, 2708-15.

Hays, R., Wickline, L. and Cagan, R. (2002). Morgue mediates apoptosis in the Drosophila melanogaster retina by promoting degradation of DIAP1. *Nat. Cell Biol.* **4**, 425-31.

Helfer, B., Boswell, B. C., Finlay, D., Cipres, A., Vuori, K., Bong Kang, T., Wallach, D., Dorfleutner, A., Lahti, J. M., Flynn, D. C. et al. (2006). Caspase-8 promotes cell motility and calpain activity under nonapoptotic conditions. *Cancer Res* **66**, 4273-8.

Hengartner, M. O., Ellis, R. E. and Horvitz, H. R. (1992). Caenorhabditis elegans gene ced-9 protects cells from programmed cell death. *Nature* **356**, 494-9.

Hernandez-Munoz, I., Lund, A. H., van der Stoop, P., Boutsma, E., Muijrers, I., Verhoeven, E., Nusinow, D. A., Panning, B., Marahrens, Y. and van Lohuizen, M. (2005). Stable X chromosome inactivation involves the PRC1 Polycomb complex and requires histone MACROH2A1 and the CULLIN3/SPOP ubiquitin E3 ligase. *Proc Natl Acad Sci U S A* **102**, 7635-40.

Hershko, A. (1997). Roles of ubiquitin-mediated proteolysis in cell cycle control. *Curr Opin Cell Biol* **9**, 788-99.

Hershko, A. and Ciechanover, A. (1998). The ubiquitin system. *Annu Rev Biochem* **67**, 425-79.

Hime, G. R., Brill, J. A. and Fuller, M. T. (1996). Assembly of ring canals in the male germ line from structural components of the contractile ring. *J Cell Sci* **109 (Pt 12)**, 2779-88.

Hinds, M. G., Norton, R. S., Vaux, D. L. and Day, C. L. (1999). Solution structure of a baculoviral inhibitor of apoptosis (IAP) repeat. *Nat Struct Biol* **6**, 648-51.

Holzl, H., Kapelari, B., Kellermann, J., Seemuller, E., Sumegi, M., Udvardy, A., Medalia, O., Sperling, J., Muller, S. A., Engel, A. et al. (2000). The regulatory complex of Drosophila melanogaster 26S proteasomes. Subunit composition and localization of a deubiquitylating enzyme. *J Cell Biol* **150**, 119-30.

Hoopfer, E. D., Penton, A., Watts, R. J. and Luo, L. (2008). Genomic analysis of Drosophila neuronal remodeling: a role for the RNA-binding protein Boule as a negative regulator of axon pruning. *J Neurosci* **28**, 6092-103.

Hoyle, H. D., Hutchens, J. A., Turner, F. R. and Raff, E. C. (1995). Regulation of beta-tubulin function and expression in Drosophila spermatogenesis. *Dev Genet* **16**, 148-70.

Huang, Y., Park, Y. C., Rich, R. L., Segal, D., Myszka, D. G. and Wu, H. (2001). Structural basis of caspase inhibition by XIAP: differential roles of the linker versus the BIR domain. *Cell* **104**, 781-90.

Huh, J. R., Vernooy, S. Y., Yu, H., Yan, N., Shi, Y., Guo, M. and Hay, B. A. (2004). Multiple apoptotic caspase cascades are required in nonapoptotic roles for Drosophila spermatid individualization. *PLoS Biol* **2**, E15.

Isaksson, A., Musti, A. M. and Bohmann, D. (1996). Ubiquitin in signal transduction and cell transformation. *Biochim Biophys Acta* **1288**, F21-9.

Ishizaki, Y., Jacobson, M. D. and Raff, M. C. (1998). A role for caspases in lens fiber differentiation. *J Cell Biol* **140**, 153-8.

Iwafune, Y., Kawasaki, H. and Hirano, H. (2004). Identification of three phosphorylation sites in the alpha7 subunit of the yeast 20S proteasome in vivo using mass spectrometry. *Arch Biochem Biophys* **431**, 9-15.

Iwanczyk, J., Sadre-Bazzaz, K., Ferrell, K., Kondrashkina, E., Formosa, T., Hill, C. P. and Ortega, J. (2006). Structure of the Blm10-20 S proteasome complex by cryo-electron microscopy. Insights into the mechanism of activation of mature yeast proteasomes. *J Mol Biol* **363**, 648-59.

James, C. T., MacGregor, D., Lynch, A. S., Coates, D. and Isaac, R. E. (1997). The expression of a C. elegans neurotransmitter transporter gene (T25B6.7). *Biochem Soc Trans* **25**, 553S.

Janzen, V., Fleming, H. E., Riedt, T., Karlsson, G., Riese, M. J., Lo Celso, C., Reynolds, G., Milne, C. D., Paige, C. J., Karlsson, S. et al. (2008). Hematopoietic stem cell responsiveness to exogenous signals is limited by caspase-3. *Cell Stem Cell* **2**, 584-94.

Jesenberger, V. and Jentsch, S. (2002). Deadly encounter: ubiquitin meets apoptosis. *Nat Rev Mol Cell Biol* **3**, 112-21.

Jiang, J. (2006). Regulation of Hh/Gli Signaling by Dual Ubiquitin Pathways. *Cell Cycle* **5**.

Jin, Z., Li, Y., Pitti, R., Lawrence, D., Pham, V. C., Lill, J. R. and Ashkenazi, A. (2009). Cullin3-based polyubiquitination and p62-dependent aggregation of caspase-8 mediate extrinsic apoptosis signaling. *Cell* **137**, 721-35.

Joazeiro, C. A. and Weissman, A. M. (2000). RING finger proteins: mediators of ubiquitin ligase activity. *Cell* **102**, 549-52.

Jones, J. M., Datta, P., Srinivasula, S. M., Ji, W., Gupta, S., Zhang, Z., Davies, E., Hajnoczky, G., Saunders, T. L., Van Keuren, M. L. et al. (2003). Loss of Omi mitochondrial protease activity causes the neuromuscular disorder of mnd2 mutant mice. *Nature* **425**, 721-7.

Ju, D., Wang, L., Mao, X. and Xie, Y. (2004). Homeostatic regulation of the proteasome via an Rpn4-dependent feedback circuit. *Biochem Biophys Res Commun* **321**, 51-7.

Ju, D. and Xie, Y. (2004). Proteasomal degradation of RPN4 via two distinct mechanisms, ubiquitin-dependent and -independent. *J Biol Chem* **279**, 23851-4.

Kaiser, W. J., Vucic, D. and Miller, L. K. (1998). The Drosophila inhibitor of apoptosis D-IAP1 suppresses cell death induced by the caspase drICE. *FEBS Lett* **440**, 243-8.

Kang, T. B., Oh, G. S., Scandella, E., Bolinger, B., Ludewig, B., Kovalenko, A. and Wallach, D. (2008). Mutation of a self-processing site in caspase-8 compromises its apoptotic but not its nonapoptotic functions in bacterial artificial chromosome-transgenic mice. *J Immunol* **181**, 2522-32.

Kanuka, H., Kuranaga, E., Takemoto, K., Hiratou, T., Okano, H. and Miura, M. (2005). Drosophila caspase transduces Shaggy/GSK-3beta kinase activity in neural precursor development. *Embo J* **24**, 3793-806.

Kanuka, H., Sawamoto, K., Inohara, N., Matsuno, K., Okano, H. and Miura, M. (1999). Control of the cell death pathway by Dapaf-1, a Drosophila Apaf-1/CED-4-related caspase activator. *Mol Cell* **4**, 757-69.

Kawahara, H. and Yokosawa, H. (1992). Cell cycle-dependent change of proteasome distribution during embryonic development of the ascidian Halocynthia roretzi. *Dev Biol* **151**, 27-33.

Kemphues, K. J., Raff, E. C., Raff, R. A. and Kaufman, T. C. (1980). Mutation in a testis-specific beta-tubulin in Drosophila: analysis of its effects on meiosis and map location of the gene. *Cell* **21**, 445-51.

Khor, B., Bredemeyer, A. L., Huang, C. Y., Turnbull, I. R., Evans, R., Maggi, L. B., Jr., White, J. M., Walker, L. M., Carnes, K., Hess, R. A. et al. (2006). Proteasome activator PA200 is required for normal spermatogenesis. *Mol Cell Biol* **26**, 2999-3007.

Kipreos, E. T. and Pagano, M. (2000). The F-box protein family. *Genome Biol.* **1**, REVIEWS3002.

Kirk, R., Laman, H., Knowles, P. P., Murray-Rust, J., Lomonosov, M., Meziane el, K. and McDonald, N. Q. (2008). Structure of a conserved dimerization domain within the F-box protein Fbxo7 and the PI31 proteasome inhibitor. *J Biol Chem* **283**, 22325-35.

Kissel, H., Georgescu, M. M., Larisch, S., Manova, K., Hunnicutt, G. R. and Steller, H. (2005). The Sept4 septin locus is required for sperm terminal differentiation in mice. *Dev Cell* **8**, 353-64.

Kleijnen, M. F., Roelofs, J., Park, S., Hathaway, N. A., Glickman, M., King, R. W. and Finley, D. (2007). Stability of the proteasome can be regulated allosterically through engagement of its proteolytic active sites. *Nat Struct Mol Biol* **14**, 1180-8.

Kleino, A., Valanne, S., Ulvila, J., Kallio, J., Myllymäki, H., Enwald, H., Stöven, S., Poidevin, M., Ueda, R., Hultmark, D. et al. (2005). Inhibitor of apoptosis 2 and TAK1-binding protein are components of the Drosophila Imd pathway. *Embo J* **24**, 3423-34.

Kolbus, A., Pilat, S., Husak, Z., Deiner, E. M., Stengl, G., Beug, H. and Baccarini, M. (2002). Raf-1 antagonizes erythroid differentiation by restraining caspase activation. *J Exp Med* **196**, 1347-53.

Kornbluth, S. and White, K. (2005). Apoptosis in Drosophila: neither fish nor fowl (nor man, nor worm). *J Cell Sci* **118**, 1779-87.

Kothakota, S., Azuma, T., Reinhard, C., Klippel, A., Tang, J., Chu, K., McGarry, T. J., Kirschner, M. W., Koths, K., Kwiatkowski, D. J. et al. (1997). Caspase-3-generated fragment of gelsolin: effector of morphological change in apoptosis. *Science* **278**, 294-8.

Koundakjian, E. J., Cowan, D. M., Hardy, R. W. and Becker, A. H. (2004). The Zuker collection: a resource for the analysis of autosomal gene function in Drosophila melanogaster. *Genetics* **167**, 203-6.

Krogan, N. J., Lam, M. H., Fillingham, J., Keogh, M. C., Gebbia, M., Li, J., Datta, N., Cagney, G., Buratowski, S., Emili, A. et al. (2004). Proteasome involvement in the repair of DNA double-strand breaks. *Mol Cell* **16**, 1027-34.

Kuo, C. T., Jan, L. Y. and Jan, Y. N. (2005). Dendrite-specific remodeling of Drosophila sensory neurons requires matrix metalloproteases, ubiquitin-proteasome, and ecdysone signaling. *Proc Natl Acad Sci U S A* **102**, 15230-5.

Kuo, C. T., Zhu, S., Younger, S., Jan, L. Y. and Jan, Y. N. (2006). Identification of E2/E3 ubiquitinating enzymes and caspase activity regulating Drosophila sensory neuron dendrite pruning. *Neuron* **51**, 283-90.

Kuranaga, E., Kanuka, H., Tonoki, A., Takemoto, K., Tomioka, T., Kobayashi, M., Hayashi, S. and Miura, M. (2006). Drosophila IKK-related kinase regulates nonapoptotic function of caspases via degradation of IAPs. *Cell* **126**, 583-96.

Kuranaga, E. and Miura, M. (2007). Nonapoptotic functions of caspases: caspases as regulatory molecules for immunity and cell-fate determination. *Trends Cell Biol* **17**, 135-44.

Kwon, J. E., La, M., Oh, K. H., Oh, Y. M., Kim, G. R., Seol, J. H., Baek, S. H., Chiba, T., Tanaka, K., Bang, O. S. et al. (2006). BTB domain-containing speckle-type POZ protein (SPOP) serves as an adaptor of Daxx for ubiquitination by Cul3-based ubiquitin ligase. *J Biol Chem* **281**, 12664-72.

LaCasse, E. C., Mahoney, D. J., Cheung, H. H., Plenchette, S., Baird, S. and Korneluk, R. G. (2008). IAP-targeted therapies for cancer. *Oncogene* **27**, 6252-75.

Lafarga, M., Fernandez, R., Mayo, I., Berciano, M. T. and Castano, J. G. (2002). Proteasome dynamics during cell cycle in rat Schwann cells. *Glia* **38**, 313-28.

Lam, Y. A., Xu, W., DeMartino, G. N. and Cohen, R. E. (1997). Editing of ubiquitin conjugates by an isopeptidase in the 26S proteasome. *Nature* **385**, 737-40.

Laman, H., Funes, J. M., Ye, H., Henderson, S., Galinanes-Garcia, L., Hara, E., Knowles, P., McDonald, N. and Boshoff, C. (2005). Transforming activity of Fbxo7 is mediated specifically through regulation of cyclin D/cdk6. *Embo J* **24**, 3104-16.

Lamkanfi, M., Declercq, W., Kalai, M., Saelens, X. and Vandenabeele, P. (2002). Alice in caspase land. A phylogenetic analysis of caspases from worm to man. *Cell Death Differ* **9**, 358-61.

Larisch, S., Yi, Y., Lotan, R., Kerner, H., Eimerl, S., Tony Parks, W., Gottfried, Y., Birkey Reffey, S., de Caestecker, M. P., Danielpour, D. et al. (2000). A novel mitochondrial septin-like protein, ARTS, mediates apoptosis dependent on its P-loop motif. *Nat Cell Biol* **2**, 915-21.

Lecker, S. H., Goldberg, A. L. and Mitch, W. E. (2006). Protein degradation by the ubiquitin-proteasome pathway in normal and disease states. *J Am Soc Nephrol* **17**, 1807-19.

Lee, A., Morrow, J. S. and Fowler, V. M. (2001). Caspase remodeling of the spectrin membrane skeleton during lens development and aging. *J Biol Chem* **276**, 20735-42.

Lee, T. V., Ding, T., Chen, Z., Rajendran, V., Scherr, H., Lackey, M., Bolduc, C. and Bergmann, A. (2008). The E1 ubiquitin-activating enzyme Uba1 in Drosophila controls apoptosis autonomously and tissue growth non-autonomously. *Development* **135**, 43-52.

Lemmers, B., Salmena, L., Bidere, N., Su, H., Matysiak-Zablocki, E., Murakami, K., Ohashi, P. S., Jurisicova, A., Lenardo, M., Hakem, R. et al. (2007). Essential role for caspase-8 in Toll-like receptors and NFkappaB signaling. *J Biol Chem* **282**, 7416-23.

Leulier, F., Rodriguez, A., Khush, R. S., Abrams, J. M. and Lemaitre, B. (2000). The Drosophila caspase Dredd is required to resist gram-negative bacterial infection. *EMBO Rep* **1**, 353-8.

Li, J., Yin, H. L. and Yuan, J. (2008). Flightless-I regulates proinflammatory caspases by selectively modulating intracellular localization and caspase activity. *J Cell Biol* **181**, 321-33.

Li, P., Nijhawan, D., Budihardjo, I., Srinivasula, S. M., Ahmad, M., Alnemri, E. S. and Wang, X. (1997). Cytochrome c and dATP-dependent formation of Apaf-1/caspase-9 complex initiates an apoptotic protease cascade. *Cell* **91**, 479-89.

Li, X., Lonard, D. M., Jung, S. Y., Malovannaya, A., Feng, Q., Qin, J., Tsai, S. Y., Tsai, M. J. and O'Malley, B. W. (2006). The SRC-3/AIB1 coactivator is degraded in a ubiquitin- and ATP-independent manner by the REGgamma proteasome. *Cell* **124**, 381-92.

Lippens, S., Kockx, M., Knaapen, M., Mortier, L., Polakowska, R., Verheyen, A., Garmyn, M., Zwijsen, A., Formstecher, P., Huylebroeck, D. et al. (2000). Epidermal differentiation does not involve the pro-apoptotic executioner caspases, but is associated with caspase-14 induction and processing. *Cell Death Differ* **7**, 1218-24.

Lisi, S., Mazzon, I. and White, K. (2000). Diverse domains of THREAD/DIAP1 are required to inhibit apoptosis induced by REAPER and HID in Drosophila. *Genetics* **154**, 669-78.

Liu, C. W., Li, X., Thompson, D., Wooding, K., Chang, T. L., Tang, Z., Yu, H., Thomas, P. J. and DeMartino, G. N. (2006). ATP binding and ATP hydrolysis play distinct roles in the function of 26S proteasome. *Mol Cell* **24**, 39-50.

London, M. K., Keck, B. I., Ramos, P. C. and Dohmen, R. J. (2004). Regulatory mechanisms controlling biogenesis of ubiquitin and the proteasome. *FEBS Lett* **567**, 259-64.

Lotan, R., Rotem, A., Gonen, H., Finberg, J. P., Kemeny, S., Steller, H., Ciechanover, A. and Larisch, S. (2005). Regulation of the proapoptotic ARTS protein by ubiquitin-mediated degradation. *J Biol Chem* **280**, 25802-10.

Lotz, K., Pyrowolakis, G. and Jentsch, S. (2004). BRUCE, a giant E2/E3 ubiquitin ligase and inhibitor of apoptosis protein of the trans-Golgi network, is required for normal placenta development and mouse survival. *Mol Cell Biol* **24**, 9339-50.

Luo, L. and O'Leary, D. D. (2005). Axon retraction and degeneration in development and disease. *Annu Rev Neurosci* **28**, 127-56.

Ma, J., Katz, E. and Belote, J. M. (2002). Expression of proteasome subunit isoforms during spermatogenesis in Drosophila melanogaster. *Insect Mol Biol* **11**, 627-39.

MacDonald, J. M., Beach, M. G., Porpiglia, E., Sheehan, A. E., Watts, R. J. and Freeman, M. R. (2006). The Drosophila cell corpse engulfment receptor Draper mediates glial clearance of severed axons. *Neuron* **50**, 869-81.

Mannhaupt, G., Schnall, R., Karpov, V., Vetter, I. and Feldmann, H. (1999). Rpn4p acts as a transcription factor by binding to PACE, a nonamer box found upstream of 26S proteasomal and other genes in yeast. *FEBS Lett* **450**, 27-34.

Mariathasan, S., Newton, K., Monack, D. M., Vucic, D., French, D. M., Lee, W. P., Roose-Girma, M., Erickson, S. and Dixit, V. M. (2004). Differential activation of the inflammasome by caspase-1 adaptors ASC and Ipaf. *Nature* **430**, 213-8.

Mariathasan, S., Weiss, D. S., Newton, K., McBride, J., O'Rourke, K., Roose-Girma, M., Lee, W. P., Weinrauch, Y., Monack, D. M. and Dixit, V. M. (2006). Cryopyrin activates the inflammasome in response to toxins and ATP. *Nature* **440**, 228-32.

Martinon, F., Petrilli, V., Mayor, A., Tardivel, A. and Tschopp, J. (2006). Gout-associated uric acid crystals activate the NALP3 inflammasome. *Nature* **440**, 237-41.

Martins, L. M., Morrison, A., Klupsch, K., Fedele, V., Moisoi, N., Teismann, P., Abuin, A., Grau, E., Geppert, M., Livi, G. P. et al. (2004). Neuroprotective role of the Reaper-related serine protease HtrA2/Omi revealed by targeted deletion in mice. *Mol Cell Biol* **24**, 9848-62.

Masson, P., Andersson, O., Petersen, U. M. and Young, P. (2001). Identification and characterization of a Drosophila nuclear proteasome regulator. A homolog of human 11 S REGgamma (PA28gamma). *J Biol Chem* **276**, 1383-90.

McCutchen-Maloney, S. L., Matsuda, K., Shimbara, N., Binns, D. D., Tanaka, K., Slaughter, C. A. and DeMartino, G. N. (2000). cDNA cloning, expression, and functional characterization of PI31, a proline-rich inhibitor of the proteasome. *J Biol Chem* **275**, 18557-65.

McKearin, D. M. and Spradling, A. C. (1990). bag-of-marbles: a Drosophila gene required to initiate both male and female gametogenesis. *Genes Dev* **4**, 2242-51.

Meier, P., Silke, J., Leevers, S. J. and Evan, G. I. (2000). The Drosophila caspase DRONC is regulated by DIAP1. *Embo J* **19**, 598-611.

Mendes, C. S., Arama, E., Brown, S., Scherr, H., Srivastava, M., Bergmann, A., Steller, H. and Mollereau, B. (2006). Cytochrome c-d regulates developmental apoptosis in the Drosophila retina. *EMBO Rep*.

Mistry, H., Wilson, B. A., Roberts, I. J., O'Kane, C. J. and Skeath, J. B. (2004). Cullin-3 regulates pattern formation, external sensory organ development and cell survival during Drosophila development. *Mech Dev* **121**, 1495-507.

Miura, M., Chen, X. D., Allen, M. R., Bi, Y., Gronthos, S., Seo, B. M., Lakhani, S., Flavell, R. A., Feng, X. H., Robey, P. G. et al. (2004). A crucial role of caspase-3 in osteogenic differentiation of bone marrow stromal stem cells. *J Clin Invest* **114**, 1704-13.

Morioka, K., Tone, S., Mukaida, M. and Takano-Ohmuro, H. (1998). The apoptotic and nonapoptotic nature of the terminal differentiation of erythroid cells. *Exp Cell Res* **240**, 206-17.

Murata, S., Sasaki, K., Kishimoto, T., Niwa, S., Hayashi, H., Takahama, Y. and Tanaka, K. (2007). Regulation of CD8+ T cell development by thymus-specific proteasomes. *Science* **316**, 1349-53.

Muro, I., Berry, D. L., Huh, J. R., Chen, C. H., Huang, H., Yoo, S. J., Guo, M., Baehrecke, E. H. and Hay, B. A. (2006). The Drosophila caspase Ice is important for many apoptotic cell deaths and for spermatid individualization, a nonapoptotic process. *Development* **133**, 3305-15.

Nakayama, K. I. and Nakayama, K. (2006). Ubiquitin ligases: cell-cycle control and cancer. *Nat Rev Cancer* **6**, 369-81.

Netea, M. G., Lewis, E. C., Azam, T., Joosten, L. A., Jaekal, J., Bae, S. Y., Dinarello, C. A. and Kim, S. H. (2008). Interleukin-32 induces the differentiation of monocytes into macrophage-like cells. *Proc Natl Acad Sci U S A* **105**, 3515-20.

Nikolaev, A., McLaughlin, T., O'Leary, D. D. and Tessier-Lavigne, M. (2009). APP binds DR6 to trigger axon pruning and neuron death via distinct caspases. *Nature* **457**, 981-9.

Noguchi, T. and Miller, K. G. (2003). A role for actin dynamics in individualization during spermatogenesis in Drosophila melanogaster. *Development* **130**, 1805-16.

Noureddine, M. A., Donaldson, T. D., Thacker, S. A. and Duronio, R. J. (2002). Drosophila Roc1a encodes a RING-H2 protein with a unique function in processing the Hh signal transducer Ci by the SCF E3 ubiquitin ligase. *Dev Cell* **2**, 757-70.

Okada, H., Suh, W. K., Jin, J., Woo, M., Du, C., Elia, A., Duncan, G. S., Wakeham, A., Itie, A., Lowe, S. W. et al. (2002). Generation and characterization of Smac/DIABLO-deficient mice. *Mol Cell Biol* **22**, 3509-17.

Okuyama, R., Nguyen, B. C., Talora, C., Ogawa, E., Tommasi di Vignano, A., Lioumi, M., Chiorino, G., Tagami, H., Woo, M. and Dotto, G. P. (2004). High

commitment of embryonic keratinocytes to terminal differentiation through a Notch1-caspase 3 regulatory mechanism. *Dev Cell* **6**, 551-62.

Olson, M. R., Holley, C. L., Yoo, S. J., Huh, J. R., Hay, B. A. and Kornbluth, S. (2003). Reaper is regulated by IAP-mediated ubiquitination. *J Biol Chem* **278**, 4028-34.

Oomman, S., Strahlendorf, H., Dertien, J. and Strahlendorf, J. (2006). Bergmann glia utilize active caspase-3 for differentiation. *Brain Res* **1078**, 19-34.

Oshima, K., Takeda, M., Kuranaga, E., Ueda, R., Aigaki, T., Miura, M. and Hayashi, S. (2006). IKK epsilon regulates F actin assembly and interacts with Drosophila IAP1 in cellular morphogenesis. *Curr Biol* **16**, 1531-7.

Ou, C. Y., Lin, Y. F., Chen, Y. J. and Chien, C. T. (2002). Distinct protein degradation mechanisms mediated by Cul1 and Cul3 controlling Ci stability in Drosophila eye development. *Genes Dev* **16**, 2403-14.

Pagano, M. (1997). Cell cycle regulation by the ubiquitin pathway. *Faseb J* **11**, 1067-75.

Paquette, N., Broemer, M., Aggarwal, K., Chen, L., Husson, M., Erturk-Hasdemir, D., Reichhart, J. M., Meier, P. and Silverman, N. Caspase-mediated cleavage, IAP binding, and ubiquitination: linking three mechanisms crucial for Drosophila NF-kappaB signaling. *Mol Cell* **37**, 172-82.

Petroski, M. D. and Deshaies, R. J. (2005). Function and regulation of cullin-RING ubiquitin ligases. *Nat Rev Mol Cell Biol* **6**, 9-20.

Pintard, L., Willems, A. and Peter, M. (2004). Cullin-based ubiquitin ligases: Cul3-BTB complexes join the family. *Embo J* **23**, 1681-7.

Pintard, L., Willis, J. H., Willems, A., Johnson, J. L., Srayko, M., Kurz, T., Glaser, S., Mains, P. E., Tyers, M., Bowerman, B. et al. (2003). The BTB protein MEL-26 is a substrate-specific adaptor of the CUL-3 ubiquitin-ligase. *Nature* **425**, 311-6.

Potts, P. R., Singh, S., Knezek, M., Thompson, C. B. and Deshmukh, M. (2003). Critical function of endogenous XIAP in regulating caspase activation during sympathetic neuronal apoptosis. *J Cell Biol* **163**, 789-99.

Rabl, J., Smith, D. M., Yu, Y., Chang, S. C., Goldberg, A. L. and Cheng, Y. (2008). Mechanism of gate opening in the 20S proteasome by the proteasomal ATPases. *Mol Cell* **30**, 360-8.

Raff, M. C., Whitmore, A. V. and Finn, J. T. (2002). Axonal self-destruction and neurodegeneration. *Science* **296**, 868-71.

Ribaya, J. P., Ranmuthu, M., Copeland, J., Boyarskiy, S., Blair, A. P., Hay, B. and Laski, F. A. (2009). The deubiquitinase emperor's thumb is a regulator of apoptosis in Drosophila. *Dev Biol* **329**, 25-35.

Ribeil, J. A., Zermati, Y., Vandekerckhove, J., Cathelin, S., Kersual, J., Dussiot, M., Coulon, S., Moura, I. C., Zeuner, A., Kirkegaard-Sorensen, T. et al. (2007). Hsp70 regulates erythropoiesis by preventing caspase-3-mediated cleavage of GATA-1. *Nature* **445**, 102-5.

Ribeiro, P. S., Kuranaga, E., Tenev, T., Leulier, F., Miura, M. and Meier, P. (2007). DIAP2 functions as a mechanism-based regulator of drICE that contributes to the caspase activity threshold in living cells. *J Cell Biol* **179**, 1467-80.

Richards, S., Hillman, T. and Stern, M. (1996). Mutations in the Drosophila pushover gene confer increased neuronal excitability and spontaneous synaptic vesicle fusion. *Genetics* **142**, 1215-23.

Riedl, S. J., Renatus, M., Schwarzenbacher, R., Zhou, Q., Sun, C., Fesik, S. W., Liddington, R. C. and Salvesen, G. S. (2001). Structural basis for the inhibition of caspase-3 by XIAP. *Cell* **104**, 791-800.

Rivett, A. J., Bose, S., Brooks, P. and Broadfoot, K. I. (2001). Regulation of proteasome complexes by gamma-interferon and phosphorylation. *Biochimie* **83**, 363-6.

Rodriguez, A., Oliver, H., Zou, H., Chen, P., Wang, X. and Abrams, J. M. (1999). Dark is a Drosophila homologue of Apaf-1/CED-4 and functions in an evolutionarily conserved death pathway. *Nat Cell Biol* **1**, 272-9.

Rodriguez, J. and Lazebnik, Y. (1999). Caspase-9 and APAF-1 form an active holoenzyme. *Genes Dev* **13**, 3179-84.

Rogowski, K., Juge, F., van Dijk, J., Wloga, D., Strub, J. M., Levilliers, N., Thomas, D., Bre, M. H., Van Dorsselaer, A., Gaertig, J. et al. (2009). Evolutionary divergence of enzymatic mechanisms for posttranslational polyglycylation. *Cell* **137**, 1076-87.

Rorth, P. (1998). Gal4 in the Drosophila female germline. *Mech Dev* **78**, 113-8.

Roy, N., Deveraux, Q. L., Takahashi, R., Salvesen, G. S. and Reed, J. C. (1997). The c-IAP-1 and c-IAP-2 proteins are direct inhibitors of specific caspases. *Embo J* **16**, 6914-25.

Rubin, D. M., Glickman, M. H., Larsen, C. N., Dhruvakumar, S. and Finley, D. (1998). Active site mutants in the six regulatory particle ATPases reveal multiple roles for ATP in the proteasome. *Embo J* **17**, 4909-19.

Ryoo, H. D., Bergmann, A., Gonen, H., Ciechanover, A. and Steller, H. (2002). Regulation of Drosophila IAP1 degradation and apoptosis by reaper and ubcD1. *Nat. Cell Biol.* **4**, 432-8.

Ryoo, H. D., Gorenc, T. and Steller, H. (2004). Apoptotic cells can induce compensatory cell proliferation through the JNK and the Wingless signaling pathways. *Dev Cell* **7**, 491-501.

Sakata, E., Yamaguchi, Y., Kurimoto, E., Kikuchi, J., Yokoyama, S., Yamada, S., Kawahara, H., Yokosawa, H., Hattori, N., Mizuno, Y. et al. (2003). Parkin binds the Rpn10 subunit of 26S proteasomes through its ubiquitin-like domain. *EMBO Rep* **4**, 301-6.

Salvesen, G. S. and Duckett, C. S. (2002). IAP proteins: blocking the road to death's door. *Nat Rev Mol Cell Biol* **3**, 401-10.

Santel, A., Blumer, N., Kampfer, M. and Renkawitz-Pohl, R. (1998). Flagellar mitochondrial association of the male-specific Don Juan protein in Drosophila spermatozoa. *J Cell Sci* **111 (Pt 22)**, 3299-309.

Santel, A., Winhauer, T., Blümer, N. and Renkawitz-Pohl, R. (1997). The Drosophila don juan (dj) gene encodes a novel sperm specific protein component characterized by an unusual domain of a repetitive amino acid motif. *Mech Dev* **64**, 19-30.

Satoh, K., Sasajima, H., Nyoumura, K. I., Yokosawa, H. and Sawada, H. (2001). Assembly of the 26S proteasome is regulated by phosphorylation of the p45/Rpt6 ATPase subunit. *Biochemistry* **40**, 314-9.

Saxena, S. and Caroni, P. (2007). Mechanisms of axon degeneration: from development to disease. *Prog Neurobiol* **83**, 174-91.

Schile, A. J., Garcia-Fernandez, M. and Steller, H. (2008). Regulation of apoptosis by XIAP ubiquitin-ligase activity. *Genes Dev* **22**, 2256-66.

Schmidt, M., Haas, W., Crosas, B., Santamaria, P. G., Gygi, S. P., Walz, T. and Finley, D. (2005a). The HEAT repeat protein Blm10 regulates the yeast proteasome by capping the core particle. *Nat Struct Mol Biol* **12**, 294-303.

Schmidt, M., Hanna, J., Elsasser, S. and Finley, D. (2005b). Proteasome-associated proteins: regulation of a proteolytic machine. *Biol Chem* **386**, 725-37.

Schreader, B. A., Wang, Y. and Nambu, J. R. (2003). Drosophila morgue and the intersection between protein ubiquitination and programmed cell death. *Apoptosis* **8**, 129-39.

Scott, F. L., Denault, J. B., Riedl, S. J., Shin, H., Renatus, M. and Salvesen, G. S. (2005). XIAP inhibits caspase-3 and -7 using two binding sites: evolutionarily conserved mechanism of IAPs. *Embo J* **24**, 645-55.

Secchiero, P., Gonelli, A., Mirandola, P., Melloni, E., Zamai, L., Celeghini, C., Milani, D. and Zauli, G. (2002). Tumor necrosis factor-related apoptosis-inducing ligand induces monocytic maturation of leukemic and normal myeloid precursors through a caspase-dependent pathway. *Blood* **100**, 2421-9.

Seeger, M., Hartmann-Petersen, R., Wilkinson, C. R., Wallace, M., Samejima, I., Taylor, M. S. and Gordon, C. (2003). Interaction of the anaphase-promoting complex/cyclosome and proteasome protein complexes with multiubiquitin chain-binding proteins. *J Biol Chem* **278**, 16791-6.

Seshagiri, S. and Miller, L. K. (1997). Caenorhabditis elegans CED-4 stimulates CED-3 processing and CED-3-induced apoptosis. *Curr Biol* **7**, 455-60.

Shaham, S. (1998). Identification of multiple Caenorhabditis elegans caspases and their potential roles in proteolytic cascades. *J Biol Chem* **273**, 35109-17.

Shaham, S. and Horvitz, H. R. (1996). An alternatively spliced C. elegans ced-4 RNA encodes a novel cell death inhibitor. *Cell* **86**, 201-8.

Shapiro, P. J., Hsu, H. H., Jung, H., Robbins, E. S. and Ryoo, H. D. (2008). Regulation of the Drosophila apoptosome through feedback inhibition. *Nat Cell Biol* **10**, 1440-6.

Sharon, M., Taverner, T., Ambroggio, X. I., Deshaies, R. J. and Robinson, C. V. (2006). Structural organization of the 19S proteasome lid: insights from MS of intact complexes. *PLoS Biol* **4**, e267.

Shiozaki, E. N., Chai, J., Rigotti, D. J., Riedl, S. J., Li, P., Srinivasula, S. M., Alnemri, E. S., Fairman, R. and Shi, Y. (2003). Mechanism of XIAP-mediated inhibition of caspase-9. *Mol Cell* **11**, 519-27.

Singer, J. D., Gurian-West, M., Clurman, B. and Roberts, J. M. (1999). Cullin-3 targets cyclin E for ubiquitination and controls S phase in mammalian cells. *Genes Dev* **13**, 2375-87.

Smith, D. M., Chang, S. C., Park, S., Finley, D., Cheng, Y. and Goldberg, A. L. (2007). Docking of the proteasomal ATPases' carboxyl termini in the 20S proteasome's alpha ring opens the gate for substrate entry. *Mol Cell* **27**, 731-44.

Smith, D. M., Kafri, G., Cheng, Y., Ng, D., Walz, T. and Goldberg, A. L. (2005). ATP binding to PAN or the 26S ATPases causes association with the 20S proteasome, gate opening, and translocation of unfolded proteins. *Mol Cell* **20**, 687-98.

Song, Z., Guan, B., Bergman, A., Nicholson, D. W., Thornberry, N. A., Peterson, E. P. and Steller, H. (2000). Biochemical and genetic interactions between Drosophila caspases and the proapoptotic genes rpr, hid, and grim. *Mol Cell Biol* **20**, 2907-14.

Song, Z., McCall, K. and Steller, H. (1997). DCP-1, a Drosophila cell death protease essential for development. *Science* **275**, 536-40.

Sordet, O., Rebe, C., Plenchette, S., Zermati, Y., Hermine, O., Vainchenker, W., Garrido, C., Solary, E. and Dubrez-Daloz, L. (2002). Specific involvement of caspases in the differentiation of monocytes into macrophages. *Blood* **100**, 4446-53.

Spector, M. S., Desnoyers, S., Hoeppner, D. J. and Hengartner, M. O. (1997). Interaction between the C. elegans cell-death regulators CED-9 and CED-4. *Nature* **385**, 653-6.

Steller, H. (1995). Mechanisms and genes of cellular suicide. *Science* **267**, 1445-9.

Steller, H. (2008). Regulation of apoptosis in Drosophila. *Cell Death Differ* **15**, 1132-8.

Stoven, S., Silverman, N., Junell, A., Hedengren-Olcott, M., Erturk, D., Engstrom, Y., Maniatis, T. and Hultmark, D. (2003). Caspase-mediated processing of the Drosophila NF-kappaB factor Relish. *Proc Natl Acad Sci U S A* **100**, 5991-6.

Strehl, B., Seifert, U., Kruger, E., Heink, S., Kuckelkorn, U. and Kloetzel, P. M. (2005). Interferon-gamma, the functional plasticity of the ubiquitin-proteasome system, and MHC class I antigen processing. *Immunol Rev* **207**, 19-30.

Sulston, J. E. (1983). Neuronal cell lineages in the nematode Caenorhabditis elegans. *Cold Spring Harb Symp Quant Biol* **48 Pt 2**, 443-52.

Sulston, J. E. and Horvitz, H. R. (1977). Post-embryonic cell lineages of the nematode, Caenorhabditis elegans. *Dev Biol* **56**, 110-56.

Sumegi, M., Hunyadi-Gulyas, E., Medzihradszky, K. F. and Udvardy, A. (2003). 26S proteasome subunits are O-linked N-acetylglucosamine-modified in Drosophila melanogaster. *Biochem Biophys Res Commun* **312**, 1284-9.

Sun, C., Cai, M., Gunasekera, A. H., Meadows, R. P., Wang, H., Chen, J., Zhang, H., Wu, W., Xu, N., Ng, S. C. et al. (1999). NMR structure and mutagenesis of the inhibitor-of-apoptosis protein XIAP. *Nature* **401**, 818-22.

Sun, X. M., Butterworth, M., MacFarlane, M., Dubiel, W., Ciechanover, A. and Cohen, G. M. (2004). Caspase activation inhibits proteasome function during apoptosis. *Mol Cell* **14**, 81-93.

Sutterwala, F. S., Ogura, Y., Szczepanik, M., Lara-Tejero, M., Lichtenberger, G. S., Grant, E. P., Bertin, J., Coyle, A. J., Galan, J. E., Askenase, P. W. et al. (2006). Critical role for NALP3/CIAS1/Cryopyrin in innate and adaptive immunity through its regulation of caspase-1. *Immunity* **24**, 317-27.

Takahashi, R., Deveraux, Q., Tamm, I., Welsh, K., Assa-Munt, N., Salvesen, G. S. and Reed, J. C. (1998). A single BIR domain of XIAP sufficient for inhibiting caspases. *J Biol Chem* **273**, 7787-90.

Tanahashi, N., Yokota, K., Ahn, J. Y., Chung, C. H., Fujiwara, T., Takahashi, E., DeMartino, G. N., Slaughter, C. A., Toyonaga, T., Yamamura, K. et al. (1997). Molecular properties of the proteasome activator PA28 family proteins and gamma-interferon regulation. *Genes Cells* **2**, 195-211.

Tenev, T., Zachariou, A., Wilson, R., Ditzel, M. and Meier, P. (2005). IAPs are functionally non-equivalent and regulate effector caspases through distinct mechanisms. *Nat Cell Biol* **7**, 70-7.

Thornberry, N. A. and Lazebnik, Y. (1998). Caspases: enemies within. *Science* **281**, 1312-6.

Thrower, J. S., Hoffman, L., Rechsteiner, M. and Pickart, C. M. (2000). Recognition of the polyubiquitin proteolytic signal. *Embo J* **19**, 94-102.

Tokuyasu, K. T., Peacock, W. J. and Hardy, R. W. (1972). Dynamics of spermiogenesis in Drosophila melanogaster. I. Individualization process. *Z Zellforsch Mikrosk Anat* **124**, 479-506.

Ustrell, V., Hoffman, L., Pratt, G. and Rechsteiner, M. (2002). PA200, a nuclear proteasome activator involved in DNA repair. *Embo J* **21**, 3516-25.

Varfolomeev, E., Blankenship, J. W., Wayson, S. M., Fedorova, A. V., Kayagaki, N., Garg, P., Zobel, K., Dynek, J. N., Elliott, L. O., Wallweber, H. J. et al. (2007). IAP antagonists induce autoubiquitination of c-IAPs, NF-kappaB activation, and TNFalpha-dependent apoptosis. *Cell* **131**, 669-81.

Varkey, J., Chen, P., Jemmerson, R. and Abrams, J. M. (1999). Altered cytochrome c display precedes apoptotic cell death in Drosophila. *J Cell Biol* **144**, 701-10.

Vaux, D. L., Cory, S. and Adams, J. M. (1988). Bcl-2 gene promotes haemopoietic cell survival and cooperates with c-myc to immortalize pre-B cells. *Nature* **335**, 440-2.

Vaux, D. L. and Korsmeyer, S. J. (1999). Cell death in development. *Cell* **96**, 245-54.

Vaux, D. L. and Silke, J. (2005). IAPs, RINGs and ubiquitylation. *Nat Rev Mol Cell Biol* **6**, 287-97.

Ventadour, S. and Attaix, D. (2006). Mechanisms of skeletal muscle atrophy. *Curr Opin Rheumatol* **18**, 631-5.

Verma, R., Aravind, L., Oania, R., McDonald, W. H., Yates, J. R., 3rd, Koonin, E. V. and Deshaies, R. J. (2002). Role of Rpn11 metalloprotease in deubiquitination and degradation by the 26S proteasome. *Science* **298**, 611-5.

Vernooy, S. Y., Chow, V., Su, J., Verbrugghe, K., Yang, J., Cole, S., Olson, M. R. and Hay, B. A. (2002). Drosophila Bruce can potently suppress Rpr- and Grim-dependent but not Hid-dependent cell death. *Curr Biol* **12**, 1164-8.

Vince, J. E., Wong, W. W., Khan, N., Feltham, R., Chau, D., Ahmed, A. U., Benetatos, C. A., Chunduru, S. K., Condon, S. M., McKinlay, M. et al. (2007). IAP antagonists target cIAP1 to induce TNFalpha-dependent apoptosis. *Cell* **131**, 682-93.

Wakimoto, B. T., Lindsley, D. L. and Herrera, C. (2004). Toward a comprehensive genetic analysis of male fertility in Drosophila melanogaster. *Genetics* **167**, 207-16.

Wang, S., Zheng, H., Esaki, Y., Kelly, F. and Yan, W. (2006). Cullin3 is a KLHL10-interacting protein preferentially expressed during late spermiogenesis. *Biol Reprod* **74**, 102-8.

Wang, S. L., Hawkins, C. J., Yoo, S. J., Muller, H. A. and Hay, B. A. (1999). The Drosophila caspase inhibitor DIAP1 is essential for cell survival and is negatively regulated by HID. *Cell* **98**, 453-63.

Wang, X. (2001). The expanding role of mitochondria in apoptosis. *Genes Dev* **15**, 2922-33.

Watts, R. J., Hoopfer, E. D. and Luo, L. (2003). Axon pruning during Drosophila metamorphosis: evidence for local degeneration and requirement of the ubiquitin-proteasome system. *Neuron* **38**, 871-85.

Watts, R. J., Schuldiner, O., Perrino, J., Larsen, C. and Luo, L. (2004). Glia engulf degenerating axons during developmental axon pruning. *Curr Biol* **14**, 678-84.

Whitby, F. G., Masters, E. I., Kramer, L., Knowlton, J. R., Yao, Y., Wang, C. C. and Hill, C. P. (2000). Structural basis for the activation of 20S proteasomes by 11S regulators. *Nature* **408**, 115-20.

White, K., Grether, M. E., Abrams, J. M., Young, L., Farrell, K. and Steller, H. (1994). Genetic control of programmed cell death in Drosophila. *Science* **264**, 677-83.

White-Cooper, H., Schäfer, M. A., Alphey, L. S. and Fuller, M. T. (1998). Transcriptional and post-transcriptional control mechanisms coordinate the onset of spermatid differentiation with meiosis I in Drosophila. *Development* **125**, 125-34.

Wilkins, A., Ping, Q. and Carpenter, C. L. (2004). RhoBTB2 is a substrate of the mammalian Cul3 ubiquitin ligase complex. *Genes Dev* **18**, 856-61.

Willems, A. R., Schwab, M. and Tyers, M. (2004). A hitchhiker's guide to the cullin ubiquitin ligases: SCF and its kin. *Biochim Biophys Acta* **1695**, 133-70.

Williams, D. W., Kondo, S., Krzyzanowska, A., Hiromi, Y. and Truman, J. W. (2006). Local caspase activity directs engulfment of dendrites during pruning. *Nat Neurosci* **9**, 1234-6.

Williams, D. W. and Truman, J. W. (2005). Cellular mechanisms of dendrite pruning in Drosophila: insights from in vivo time-lapse of remodeling dendritic arborizing sensory neurons. *Development* **132**, 3631-42.

Wilson, R., Goyal, L., Ditzel, M., Zachariou, A., Baker, D. A., Agapite, J., Steller, H. and Meier, P. (2002). The DIAP1 RING finger mediates ubiquitination of Dronc and is indispensable for regulating apoptosis. *Nat Cell Biol* **4**, 445-50.

Wing, J. P., Schreader, B. A., Yokokura, T., Wang, Y., Andrews, P. S., Huseinovic, N., Dong, C. K., Ogdahl, J. L., Schwartz, L. M., White, K. et al. (2002). Drosophila

Morgue is an F box/ubiquitin conjugase domain protein important for grim-reaper mediated apoptosis. *Nat Cell Biol* **4**, 451-6.

Wojcik, C. and DeMartino, G. N. (2003). Intracellular localization of proteasomes. *Int J Biochem Cell Biol* **35**, 579-89.

Wride, M. A., Parker, E. and Sanders, E. J. (1999). Members of the bcl-2 and caspase families regulate nuclear degeneration during chick lens fibre differentiation. *Dev Biol* **213**, 142-56.

Wu, D., Wallen, H. D. and Nunez, G. (1997). Interaction and regulation of subcellular localization of CED-4 by CED-9. *Science* **275**, 1126-9.

Wu, G., Chai, J., Suber, T. L., Wu, J. W., Du, C., Wang, X. and Shi, Y. (2000). Structural basis of IAP recognition by Smac/DIABLO. *Nature* **408**, 1008-12.

Xie, Y. and Varshavsky, A. (2001). RPN4 is a ligand, substrate, and transcriptional regulator of the 26S proteasome: a negative feedback circuit. *Proc Natl Acad Sci U S A* **98**, 3056-61.

Xie, Y. and Varshavsky, A. (2002). UFD4 lacking the proteasome-binding region catalyses ubiquitination but is impaired in proteolysis. *Nat Cell Biol* **4**, 1003-7.

Xu, L., Wei, Y., Reboul, J., Vaglio, P., Shin, T. H., Vidal, M., Elledge, S. J. and Harper, J. W. (2003). BTB proteins are substrate-specific adaptors in an SCF-like modular ubiquitin ligase containing CUL-3. *Nature* **425**, 316-21.

Yan, N., Wu, J. W., Chai, J., Li, W. and Shi, Y. (2004a). Molecular mechanisms of DrICE inhibition by DIAP1 and removal of inhibition by Reaper, Hid and Grim. *Nat Struct Mol Biol* **11**, 420-8.

Yan, W., Ma, L., Burns, K. H. and Matzuk, M. M. (2004b). Haploinsufficiency of kelch-like protein homolog 10 causes infertility in male mice. *Proc Natl Acad Sci U S A* **101**, 7793-8.

Yang, X., Chang, H. Y. and Baltimore, D. (1998). Essential role of CED-4 oligomerization in CED-3 activation and apoptosis. *Science* **281**, 1355-7.

Yao, T. and Cohen, R. E. (2002). A cryptic protease couples deubiquitination and degradation by the proteasome. *Nature* **419**, 403-7.

Yatsenko, A. N., Roy, A., Chen, R., Ma, L., Murthy, L. J., Yan, W., Lamb, D. J. and Matzuk, M. M. (2006). Non-invasive genetic diagnosis of male infertility using spermatozoal RNA: KLHL10 mutations in oligozoospermic patients impair homodimerization. *Hum Mol Genet* **15**, 3411-9.

Yi, C. H. and Yuan, J. (2009). The Jekyll and Hyde functions of caspases. *Dev Cell* **16**, 21-34.

Young, P., Deveraux, Q., Beal, R. E., Pickart, C. M. and Rechsteiner, M. (1998). Characterization of two polyubiquitin binding sites in the 26 S protease subunit 5a. *J Biol Chem* **273**, 5461-7.

Yuan, J., Shaham, S., Ledoux, S., Ellis, H. M. and Horvitz, H. R. (1993). The C. elegans cell death gene ced-3 encodes a protein similar to mammalian interleukin-1 beta-converting enzyme. *Cell* **75**, 641-52.

Yuan, J. Y. and Horvitz, H. R. (1990). The Caenorhabditis elegans genes ced-3 and ced-4 act cell autonomously to cause programmed cell death. *Dev Biol* **138**, 33-41.

Zaiss, D. M., Standera, S., Holzhutter, H., Kloetzel, P. and Sijts, A. J. (1999). The proteasome inhibitor PI31 competes with PA28 for binding to 20S proteasomes. *FEBS Lett* **457**, 333-8.

Zaiss, D. M., Standera, S., Kloetzel, P. M. and Sijts, A. J. (2002). PI31 is a modulator of proteasome formation and antigen processing. *Proc Natl Acad Sci U S A* **99**, 14344-9.

Zandy, A. J., Lakhani, S., Zheng, T., Flavell, R. A. and Bassnett, S. (2005). Role of the executioner caspases during lens development. *J Biol Chem* **280**, 30263-72.

Zermati, Y., Garrido, C., Amsellem, S., Fishelson, S., Bouscary, D., Valensi, F., Varet, B., Solary, E. and Hermine, O. (2001). Caspase activation is required for terminal erythroid differentiation. *J Exp Med* **193**, 247-54.

Zhang, B., Zhang, Y. and Shacter, E. (2003). Caspase 3-mediated inactivation of rac GTPases promotes drug-induced apoptosis in human lymphoma cells. *Mol Cell Biol* **23**, 5716-25.

Zhong, L. and Belote, J. M. (2007). The testis-specific proteasome subunit Prosalpha6T of D. melanogaster is required for individualization and nuclear maturation during spermatogenesis. *Development* **134**, 3517-25.

Zhou, L., Song, Z., Tittel, J. and Steller, H. (1999). HAC-1, a Drosophila homolog of APAF-1 and CED-4 functions in developmental and radiation-induced apoptosis. *Mol Cell* **4**, 745-55.

Zimmermann, K. C., Waterhouse, N. J., Goldstein, J. C., Schuler, M. and Green, D. R. (2000). Aspirin induces apoptosis through release of cytochrome c from mitochondria. *Neoplasia* **2**, 505-13.

Zou, H., Henzel, W. J., Liu, X., Lutschg, A. and Wang, X. (1997). Apaf-1, a human protein homologous to C. elegans CED-4, participates in cytochrome c-dependent activation of caspase-3. *Cell* **90**, 405-13.

Zou, H., Li, Y., Liu, X. and Wang, X. (1999). An APAF-1.cytochrome c multimeric complex is a functional apoptosome that activates procaspase-9. *J Biol Chem* **274**, 11549-56.